TACKLING LYME DISEASE BY IDENTIFYING POTENTIAL SUBUNIT VACCINE CANDIDATES AND DEFINING THE MICROBIOTA OF *IXODES RICINUS* TICKS

A Dissertation

by

MALIHA BATOOL

Submitted to the Graduate and Professional School of Texas
A&M University
in partial fulfillment of the requirements for the degree of

DOCTOR OF PHILOSOPHY

Chair of Committee,	Artem Rogovskyy
Committee Members,	David Threadgill
	Jan Suchodolski
	Suryakant Waghela
Head of Department,	Ramesh Vemulapalli

May 2022

Major Subject: Biomedical Sciences

ABSTRACT

Lyme disease (LD), one of the most common tick-borne diseases in the Northern Hemisphere, is caused by *Borreliella* (*Borrelia*) *burgdorferi* (*B. burgdorferi*). The lack of vaccine, increases in LD cases, and wide distribution of *Ixodes* ticks necessitate the development of an LD vaccine for humans. Identification of protection-associated (PA) epitopes that could lead to the development of a second-generation vaccine against LD is, therefore, needed. Despite the presence of numerous antigenic proteins on the borrelial surface, VlsE is the only variable protein that undergoes rigorous antigenic variation. Although VlsE-mediated shielding of a surface antigen was recently demonstrated, it is unlikely that VlsE covers an entire surface of *B. burgdorferi*. Thus, it is hypothesized that only dominant epitopes are masked by VlsE, whereas subdominant epitopes remain exposed. Moreover, some exposed epitopes may induce protection when made dominant. The first study presented herein focused on the identification of surface epitopes that could provide protection despite VlsE. For that, immunocompetent mice were repeatedly immunized with VlsE-deficient *B. burgdorferi* and then challenged with wild-type (VlsE-expressing) *B. burgdorferi*. As a result, 50% of mice became protected due to the repeated exposure of surface epitopes in the absence of VlsE. Subsequently, antibody repertoires identified by random phage display libraries were defined and compared between protected and non-protected mice, which allowed us to pinpoint putative PA epitopes. The second study has examined a protective antibody response in the New Zealand White (NZW) rabbit model. In contrast to mice, NZW rabbits were previously shown to mount

a protective antibody response against wild-type *B. burgdorferi*. A series of passive immunization experiments demonstrated that anti-*B. burgdorferi* rabbit antibodies provided 100% protection in mice against VlsE-expressing wild type despite the fully functional VlsE system. In addition to protecting against homologous and heterologous challenges, anti-*B. burgdorferi* rabbit antibodies significantly reduced LD-induced arthritis in actively *B. burgdorferi*-infected mice. Lastly, the third study has analyzed of the metabiota of *Ixodes ricinus*, the tick species which is critical in maintaining the enzootic cycle of LD in Europe. The results demonstrated extensive sex-specific and regional-specific variations in the bacterial flora of adult ticks.

ACKNOWLEDGEMENTS

I would like to thank my committee chair and advisor, Dr. Artem S. Rogovskyy for mentoring me through each step of my doctoral program. I would like to thank my committee members, Dr. David W. Threadgill, Dr. Jan S. Suchodolski, and Dr. Suryakant D. Waghela for their guidance and support throughout the course of this program.

Importantly, I would like to thank each of the collaborators and my advisor for significantly contributing to the research projects described in this dissertation and our respective peer-reviewed publications. The latter also constitute chapters II-IV of this document. To properly acknowledge each of the contributor, detailed contribution statements are provided below.

Finally, I want to express my deep appreciation for all the emotional support by my friends and family.

CONTRIBUTORS AND FUNDING SOURCES

Contributors

This work was supervised by a thesis committee consisting of advisors Assistant Professor Artem S. Rogovskyy [Advisor] of the Department of Veterinary Pathobiology, Professor Jan S. Suchodolski of the Department of Small Animal Clinical Sciences, Clinical Assistant Professor Suryakant D. Waghela of the Department of Veterinary Pathobiology, and Professor David W. Threadgill of the Department of Biochemistry and Biophysics.

Indicated below are the task of each contributor for each publication/chapter. Of note, the abstract, the introduction (chapter 1), and conclusions (chapter 5) were written by Maliha Batool with very minor editing from her mentor.

Publication and chapter 2 titled "**Identification of surface epitopes associated with protection against highly immune-evasive VlsE-expressing Lyme disease spirochetes**": Maliha Batool: *western blot analysis, and generation of figures, an attempt to write an original draft and analyze data*. Salvador Eugenio C. Caoili: *bioinformatic analysis of conformational epitopes and generation of the respective figures, and writing the original draft*. Lawrence J. Dangott: *2-D gel electrophoresis, scaffold analysis, writing Materials and Methods (MM) sections of the original draft*. Ekaterina Gerasimov: *DNA read analysis, comparison of peptide profiles, and writing MM sections of the original draft*. Yurij Ionov: *phage display library and writing MM sections of the original draft*. Helen Piontkivska: *bioinformatic analyses of linear epitopes and writing MM sections of*

the original draft. Alex Zelikovsky: *DNA read analysis, comparison of peptide profiles, and writing MM sections of the original draft*. Suryakant D. Waghela: *conceptualization and review and editing of the original draft. David Chris Gillis: the mouse work and western blot analysis*. Artem S. Rogovskyy: *conceptualization, experimental design, data validation, data analysis, writing the original draft, generation of figures and tables, review and editing, supervision, and resources*.

Publication and chapter 3 titled "**New Zealand White rabbits effectively clear *Borrelia burgdorferi* B31 despite the bacteria's functional *vlsE* antigenic variation system**": Maliha Batool: *generation of in vitro-grown and host-adapted clones, western blot and ELISA analyses, conventional PCR and qRT-PCR analyses, data analysis, co-generation of figures and tables, and an attempt to write an original draft*. Andrew E. Hillhouse: *qRT-PCR analysis*. Yurij Ionov: *phage display library and writing MM section(s) of the original draft*. Kelli J. Kochan: *qRT-PCR analysis, and review and editing of the manuscript*. Fatemeh Mohebbi: *DNA read analysis, comparison of peptide profiles, prediction of anti-B31 reactivity to VlsE, and writing MM section(s) of the original draft*. George Stoica*: histopathology, writing MM section(s) of the original draft, and review and editing of the manuscript*. David W. Threadgill: *resources, and review and editing of the original draft*. Alex Zelikovsky: *DNA read analysis, comparison of peptide profiles, prediction of anti-B31 reactivity to VlsE, and writing MM section(s) of the original draft*. Suryakant D. Waghela: *data analysis, and review and editing of the manuscript*. Dominique J. Wiener: *histopathology, generation of figures, writing MM section(s) of the original draft, review and editing of the manuscript*. Artem S. Rogovskyy:

conceptualization, experimental design, all the rabbit work, immunization of mice, qRT-PCR analysis, data validation, data analysis, writing the original draft, review and editing of the manuscript, co-generation of figures and tables, review and editing of the manuscript, resources, supervision, resources. The other contributors are indicated in the acknowledgments of the publication.

Publication and chapter 4 titled "**Metagenomic analysis of individually analyzed ticks from Eastern Europe demonstrates regional and sex-dependent differences in the microbiota of *Ixodes ricinus***": Maliha Batool: *generation of controls (sample preparation, DNA extraction, PCR amplification of 16S rRNA targets), data analysis, data validation, data curation, generation of figures and tables, writing the original draft, review and editing of the manuscript*. John C. Blazier: *sequence processing, classification of amplicon sequence variants (ASVs), taxonomic classification, generation of alpha and beta diversity indices, and analysis of composition of microbiomes*. Yuliya V. Rogovska: *sample preparation, DNA extraction, and PCR amplification of 16S rRNA targets*. Jiangli Wang: *statistical analysis and writing MM section(s) of the original draft*. Shuling Liu: *statistical analysis and writing MM section(s) of the original draft*. Igor V. Nebogatkin: *tick collection and review and editing of the manuscript*. Artem S. Rogovskyy: *conceptualization, experimental design, tick collection, data validation, data analysis, writing the original draft, review and editing of the manuscript, supervision, resources*.

Funding sources

The work at Texas A&M University was supported by start-up funds provided by the Department of Veterinary Pathobiology, Texas A&M College of Veterinary Medicine

& Biomedical Sciences and Texas A&M AgriLife; by the Texas A&M AgriLife Vector-Borne Diseases Seed Grant; and partially supported by NIH Grant R03AI135159-02. The work at Roswell Park Cancer Institute was partially supported by the Phillip Hubbell Family Fund. The work at Kent State University was partially supported by Research Seed Award from Kent State University. The work at Georgia State University was partially supported by NSF Grant CCF-16119110, NSF Grant CCF-16119110, and NIH Grant 1R01EB025022-01.

TABLE OF CONTENTS

Page

LIST OF FIGURES

Page

Chapter 2

Chapter 3

Chapter 4

LIST OF TABLES

Page

Chapter 2

Chapter 3

Chapter 4

1. INTRODUCTION

Lyme disease (aka Lyme borreliosis; referred to here as LD) is the most commonly reported tick-borne infection in North America, Europe and parts of Asia (Mead, 2015). In the mid 1970's, LD was clinically misdiagnosed as a geographical clustering of juvenile rheumatoid arthritis in southeastern Connecticut, United States (Steere et al., 1977). Lyme arthritis was discovered to be a part of a complex multisystemic disorder recognized by a characteristic expanding annular skin lesion with a central zone of clearance, commonly known as erythema migrans (herein referred to as EM), acrodermatitis chronica atrophicans, and Bannwarth syndrome (Steere, 1989). In 1982, a spiral shaped bacterium, subsequently named *Borrelia burgdorferi* (*B. burgdorferi*) was identified as the causative agent of LD. *B. burgdorferi* was initially recovered from a species of the North American deer tick, *Ixodes scapularis*, also known as *Ixodes dammini* ticks (Burgdorfer et al., 1982). Subsequently, *B. burgdorferi* was isolated from those patients exhibiting clinical manifestations of LD infection, affecting the joints, skin, blood, heart and nervous system (Steere, 1989). It was soon discovered that the spirochete isolated from LD patients with EM were associated with those isolated from ticks. *B. burgdorferi* sensu lato is comprised of about 20 different genospecies, of which *B. burgdorferi* sensu stricto (ss), *B. garinii*, and *B. afzelii* are the three genospecies that are most commonly responsible for human infection. *B. burgdorferi* ss is responsible for LD in the United States, and *B. garinii* and *B. afzelii* cause LD in Europe and Asia (Mead, 2015).

Disease development is multisystemic and usually occurs in three stages: early localized, early disseminated, and late stages. At the early localized stage of infection, spirochetes are transmitted to the host via tick bite and cause EM. Within several days or up to several weeks postinfection, spirochetes spread hematogenous, and the infected host may present early-disseminated signs of disease. In addition to multiple skin lesions, the early disseminated stage is defined by cardiac, neurological, and rheumatologic involvement. Late-stage disease appears months to years after the original exposure and may present as arthritis, acrodermatitis chronica atrophicans, and late neuroborreliosis (Steere, 1989, 2001; Steere et al., 2004). As the infection advances, *B. burgdorferi* spirochetes disseminate into host tissue, where they encounter several levels of host defense (Embers et al., 2004). Despite development of an active immune response towards the pathogen, spirochetes can escape the clearance and persist for months to years in the mammalian host (Steere, 1989). For many, intravenous or oral antibiotic treatment is remedial. However, approximately 20% of individuals in the late stages of infection do not recover from their symptoms, despite several rounds of antibiotic therapy (Akin et al., 2001; Aucott, 2015).

B. burgdorferi spirochetes have developed several immune evasion tactics that render the host antibody response ineffective and support persistent infection, such as active immune suppression of innate and adaptive immunity, physical seclusion, and immune avoidance by antigenic variation (Embers et al., 2004). In addition, *B. burgdorferi* has approximately 150 lipoproteins (Casjens et al., 2000; Fraser et al., 1997a), and the rapid up- and down-regulation of several highly immunogenic proteins throughout

infection is documented (Kenedy et al., 2012b). Antigenic variation has been identified as an effective strategy developed by spirochetes to escape the immune response in mammals (Rogovskyy and Bankhead, 2013). The *vls* is an elaborate antigenic variation system in the *B. burgdorferi* B31 clone consisting of a *vls* expression site (VlsE) and 15 silent *vls* cassettes (Zhang et al., 1997). VlsE encodes a 34kDa surface-exposed lipoprotein that supports survival of *B. burgdorferi* in the mammalian host. The VlsE cassette region of the *B. burgdorferi* B31 strain has sequence homology with the 15 silent cassettes, allowing the sequence of surface-exposed lipoprotein VlsE to be repeatedly altered through segmental gene rearrangement events. The continuous changing of the VlsE sequence is a powerful diversity mechanism that allows *B. burgdorferi* spirochetes to remain one step ahead of the antibody-mediated immune response, establishing remarkable persistence (Zhang et al., 1997). Therefore VlsE, an antigenic protein, appears to be a key virulence factor of *B. burgdorferi* infection (Crother et al., 2004). In *B. burgdorferi* B31-infected mice, antigenic variation on the *vls* locus has been shown to occur as early as 4 days postinfection and to continue throughout the course of infection. This recombinational switching appears only during animal infection and has not been detected in either tick vectors or when spirochetes are grown *in vitro* (Indest et al., 2001; Zhang and Norris, 1998a, b). Although the surface of *B. burgdorferi* is densely populated with other surface-exposed proteins, none of these proteins undergo the protective vigorous antigenic variation like VlsE. Despite this, *B. burgdorferi* is still able to evade the host immune response. To explain this, there is a VlsE shielding mechanism showing that VlsE blocks antibody access to other epitopes of *B. burgdorferi*, thus avoiding the

host immune response (Lone and Bankhead, 2020). It is unlikely that VlsE molecules are able to cover the entire surface of *B. burgdorferi*. We hypothesized that despite the abundant presence of VlsE, some surface epitopes remain exposed, but because of their sub-dominant nature, antibodies produced against these epitopes are not sufficient to provide protection.

Chapter 1 and 2 of this dissertation focus on bacterial pathogenesis and anti-*Borrelia* antibodies in mouse and rabbit models of LD. We examined and compared anti-*Borrelia* antibodies in a repeated immunization study using mice in order to discover protection-associated peptides and identify promising candidates for a subunit vaccine against LD. We also examined and compared the protective efficacy of anti-*Borrelia* antibodies in the rabbit model at both early and late stages of *Borrelia* infection.

Chapter 3 of this dissertation focuses on the metagenomic analysis of *Ixodes ricnus* ticks, a principal vector, that maintains the enzootic spirochete cycle for LD in Europe and carry other medically relevant pathogens (Medlock et al., 2013; Parola and Raoult, 2001; Rizzoli et al., 2011b). The aim of this study was to compare microbiota of *Ixodes ricinus* ticks within regions and between regions collected from three administrative regions of Ukraine.

1.1. References

1. Mead PS. 2015. Epidemiology of Lyme disease. Infectious Disease Clinics 29:187-210.

2. Steere AC, Malawista SE, Snydman DR, Shope RE, Andiman WA, Ross MR, Steele FM. 1977. Lyme arthritis: an epidemic of oligoarticular arthritis in children and adults in three connecticut communities. Arthritis Rheum 20:7-17.

3. Steere AC. 1989. Lyme disease. N Engl J Med 321:586-96.

4. Burgdorfer W, Barbour AG, Hayes SF, Benach JL, Grunwaldt E, Davis JP. 1982. Lyme disease-a tick-borne spirochetosis? Science 216:1317-1319.

5. Steere AC. 2001. Lyme disease. N Engl J Med 345:115-25.

6. Steere AC, Coburn J, Glickstein L. 2004. The emergence of Lyme disease. J Clin Invest 113:1093-101.

7. Embers ME, Ramamoorthy R, Philipp MT. 2004. Survival strategies of *Borrelia burgdorferi*, the etiologic agent of Lyme disease. Microbes Infect 6:312-8.

8. Aucott JN. 2015. Posttreatment Lyme disease syndrome. Infect Dis Clin 29:309-323.

9. Akin E, Aversa J, Steere AC. 2001. Expression of adhesion molecules in synovia of patients with treatment-resistant Lyme arthritis. Infect immun 69:1774-1780.

10. Casjens S, Palmer N, van Vugt R, Huang WM, Stevenson B, Rosa P, Lathigra R, Sutton G, Peterson J, Dodson RJ, Haft D, Hickey E, Gwinn M, White O, Fraser CM. 2000. A bacterial genome in flux: the twelve linear and nine circular extrachromosomal DNAs in an infectious isolate of the Lyme disease spirochete *Borrelia burgdorferi*. Mol Microbiol 35:490-516.

11. Fraser CM, Casjens S, Huang WM, Sutton GG, Clayton R, Lathigra R, White O, Ketchum KA, Dodson R, Hickey EK, Gwinn M, Dougherty B, Tomb JF,

Fleischmann RD, Richardson D, Peterson J, Kerlavage AR, Quackenbush J, Salzberg S, Hanson M, van Vugt R, Palmer N, Adams MD, Gocayne J, Weidman J, Utterback T, Watthey L, McDonald L, Artiach P, Bowman C, Garland S, Fuji C, Cotton MD, Horst K, Roberts K, Hatch B, Smith HO, Venter JC. 1997. Genomic sequence of a Lyme disease spirochaete, *Borrelia burgdorferi*. Nature 390:580-6.

12. Kenedy MR, Lenhart TR, Akins DR. 2012. The role of *Borrelia burgdorferi* outer surface proteins. FEMS Immunol Med Microbiol 66:1-19.

13. Rogovskyy AS, Bankhead T. 2013. Variable VlsE is critical for host reinfection by the Lyme disease spirochete. PLoS One 8:e61226.

14. Zhang JR, Hardham JM, Barbour AG, Norris SJ. 1997. Antigenic variation in Lyme disease borreliae by promiscuous recombination of VMP-like sequence cassettes. Cell 89:275-85.

15. Crother TR, Champion CI, Whitelegge JP, Aguilera R, Wu XY, Blanco DR, Miller JN, Lovett MA. 2004. Temporal analysis of the antigenic composition of *Borrelia burgdorferi* during infection in rabbit skin. Infect Immun 72:5063-72.

16. Indest KJ, Howell JK, Jacobs MB, Scholl-Meeker D, Norris SJ, Philipp MT. 2001. Analysis of *Borrelia burgdorferi vlsE* gene expression and recombination in the tick vector. Infect Immun 69:7083-90.

17. Zhang JR, Norris SJ. 1998. Genetic variation of the *Borrelia burgdorferi* gene *vlsE* involves cassette-specific, segmental gene conversion. Infect Immun 66:3698-704.

18. Zhang JR, Norris SJ. 1998. Kinetics and in vivo induction of genetic variation of vlsE in *Borrelia burgdorferi*. Infect Immun 66:3689-97.

19. Lone AG, Bankhead T. 2020. The *borrelia burgdorferi* VlsE lipoprotein prevents antibody binding to arthritis-related surface antigen. Cell reports 30:3663-3670. e5.

20. Medlock JM, Hansford KM, Bormane A, Derdakova M, Estrada-Peña A, George J-C, Golovljova I, Jaenson TG, Jensen J-K, Jensen PM. 2013. Driving forces for changes in geographical distribution of *Ixodes ricinus* ticks in Europe. Parasit Vectors 6:1.

21. Parola P, Raoult D. 2001. Ticks and tickborne bacterial diseases in humans: an emerging infectious threat. Clin Infect Dis 32:897-928.

22. Rizzoli A, Hauffe HC, Carpi G, Vourc'h G, Neteler M, Rosa R. 2011. Lyme borreliosis in Europe. Euro Surveill 16:19906.

2. IDENTIFICATION OF SURFACE EPITOPES ASSOCIATED WITH PROTECTION AGAINST HIGHLY IMMUNE-EVASIVE VLSE-EXPRESSING LYME DISEASE SPIROCHETES[1*]

Maliha Batool[1], Salvador Eugenio C Caoili[2], Lawrence J Dangott[3], Ekaterina Gerasimov[4], Yurij Ionov[5], Halen Piontkivska[6], Alex Zelikovsky[7], Suryakant D Waghela[1], Artem S Rogovskyy[1]

1. Department of Veterinary Pathobiology, College of Veterinary Medicine and Biomedical Sciences, Texas A&M University, College Station, Texas, USA.
2. Department of Biochemistry and Molecular Biology, College of Medicine, University of the Philippines Manila, Manila, Philippines.
3. Department of Biochemistry and Biophysics, Texas A&M University, College Station, Texas, USA.
4. Department of Computer Science, Georgia State University, Atlanta, Georgia, USA.
5. Department of Cancer Genetics, Roswell Park Cancer Institute, Buffalo, New York, USA.
6. Department of Biological Sciences, Kent State University, Kent, Ohio, USA.

---

[1]*Reprinted with permission from "Identification of surface epitopes associated with protection against highly immune-evasive VlsE-expressing Lyme disease spirochetes" by Batool M., Caoili S.E.C., Dangott L.J., Gerasimov E., Ionov Y., Piontkivska H., Zelikovsky A., Waghela S.D., Rogovskyy A.S., 2018. *Infection Immunity*, 86, e00182-18, Copyright [2018] by ASM Journals.

7. Laboratory of Bioinformatics, I. M. Sechenov First Moscow State Medical University, Moscow, Russia.

2.1. Overview

The tick-borne pathogen, *B. burgdorferi*, is responsible for approximately 300,000 LD cases per year in the United States. Recent increases in the number of LD cases in addition to the spread of the tick vector and a lack of vaccine highlights an urgent need for designing and developing an efficacious LD vaccine. Identification of protective epitopes that could be used to develop a second-generation vaccine is therefore imperative. Despite the antigenicity of several lipoproteins and integral outer membrane proteins (OMPs) on *B. burgdorferi* surface, the spirochetes successfully evade antibodies primarily due to the VlsE-mediated antigenic variation. VlsE is thought to sterically block antibody access to protective epitopes of *B. burgdorferi*. However, it is highly unlikely that VlsE shields the entire surface epitome. Thus, identification of subdominant epitope targets that induce protection, when made dominant, is necessary to generate an efficacious vaccine. Towards the identification, we repeatedly immunized immunocompetent mice with live-attenuated VlsE-deleted *B. burgdorferi* and then challenged the animals with VlsE-expressing (host-adapted) wild type. Passive immunization and western blot data suggested that the protection of the 50% of repeatedly-immunized animals against the highly immune-evasive *B. burgdorferi* was antibody-mediated. Comparison of serum antibody repertoires identified in protected and non-protected animals permitted the identification of several putative epitopes significantly associated with the protection. Most linear putative epitopes were conserved between the main pathogenic *Borrelia* genospecies and found within known subdominant regions of OMPs. Currently, we are performing immunization studies to test whether the identified protection-associated epitopes are protective for mice.

2.2. Introduction

LD is the most prevalent arthropod-borne illness in the temperate regions of the northern hemisphere (Rizzoli et al., 2011a). In the United States alone, the tick-borne pathogen, *B. burgdorferi*, is responsible for approximately 300,000 LD cases per year (Hinckley et al., 2014). LD spirochetes are transmitted to humans via infected nymphs or adults of *Ixodes* spp. ticks. Early LD manifestation includes flu-like symptoms that may or may not be accompanied by a pathognomonic skin rash, erythrema migrans (Borchers et al., 2015). Later, however, approximately 80% of patients may develop arthritis (45-60%), neurological symptoms (11%), and/or carditis (4-8%). At present, a vaccine for humans is unavailable. Recent increases in the number of LD cases urge the need for generating an efficacious LD vaccine (Rizzoli et al., 2011a). Therefore, identification of protective epitopes for the development of a second-generation vaccine is imperative.

It is estimated that over 120 distinct potential lipoproteins are encoded by approximately 8% of *B. burgdorferi* B31 genome (Setubal et al., 2006). Recently, a comprehensive spatial assessment of the entire borrelial lipoproteome has identified 52 new surface lipoproteins (Dowdell et al., 2017). Thus, two thirds of lipoproteins are surface-exposed and most of these are encoded by *Borrelia* plasmids. The other 19% of surface lipoproteins are chromosomally encoded (Dowdell et al., 2017). The lipoproteins encoded by stable genetic elements most likely provide metabolic or housekeeping functions (Alva et al., 2016; Dowdell et al., 2017). In addition to lipoproteins, spirochetal membrane also contains integral outer membrane proteins (OMPs) that possess transmembrane-spanning domains. Unlike lipoproteins, OMPs do not contain N-terminal

lipid anchors (Kenedy et al., 2012a). *B. burgdorferi* OMPs play important physiological roles and, therefore expectedly, nearly all known OMPs (e.g., BamA, BesC, BB0405, P66, P13, Lmp1) are duly encoded by chromosomal loci (Fraser et al., 1997b). The integral OMPs are usually conserved among different *Borrelia* genospecies and are suggested to be good candidates for development of LD vaccine (Kenedy et al., 2012a).

The long-term immunoevasion of *Borrelia* spirochetes in the mammalian host is achieved via the *vls*-mediated locus (Norris, 2014). This antigenic variation system is located on a 28-kilobase linear plasmid (lp28-1) of *B. burgdorferi* B31 and comprises the *vlsE* expression site and 15 non-coding cassettes. Multiple variants of surface lipoprotein, VlsE (variable major protein-like sequence expressed) are constantly produced by homologous recombination between the *vlsE* gene and silent cassettes (Norris, 2006a; Zhang et al., 1997). This *vls*-mediated variation of VlsE is essential for the persistence of *B. burgdorferi* in immunocompetent mice (Bankhead and Chaconas, 2007; Iyer et al., 2003; Labandeira-Rey et al., 2003; Labandeira-Rey and Skare, 2001; Lawrenz et al., 2004; Purser and Norris, 2000; Rogovskyy and Bankhead, 2013). In contrast to VlsE-expressing wild type, mouse antibody efficiently clears the *vls*-depleted *B. burgdorferi* (ΔVlsE) as well as the isogenic clone with non-switchable VlsE (Rogovskyy and Bankhead, 2013).

There are at least two putative mechanisms that may explain how VlsE allows surface antigens to evade host antibodies (Labandeira-Rey et al., 2003; Liang et al., 2002; Palmer et al., 2016; Philipp et al., 2001; Rogovskyy and Bankhead, 2013). The first proposes that VlsE may sterically block antibody access to *B. burgdorferi* surface epitopes (VlsE-mediated masking). The second is VlsE-mediated suppression of host immune

response (Liang et al., 1999; Rogovskyy and Bankhead, 2013). Prior data suggest that, if VlsE is indeed involved, detectable immunosuppression is only transient and, practically, not sufficient for surface antigens to evade antibody-mediated clearance in the long run (Elsner et al., 2015; Rogovskyy et al., 2017). On the other hand, if the VlsE-mediated masking is at place, it is highly unlikely that VlsE molecules entirely shield surface antigens of *B. burgdorferi*. It is more plausible that surface (lipo)proteins contain epitopes that remain exposed despite the abundant VlsE presence. Moreover, some of these non-shielded epitopes (exposed, hereafter) may potentially be protective. Subdominant nature of exposed epitopes may supposedly account for their successful immune-evasion and, consequently, the lack of need for spirochetes to mask them. The present study has attempted to test the above assumptions using a repeated immunization assay in immunocompetent mice with a live-attenuated ΔVlsE clone. We observed that 50% of repeatedly-immunized mice were protected against challenge with a highly immune-evasive host-adapted wild-type *B. burgdorferi*. Application of random peptide phage display libraries (RPPDL) coupled with next generation sequencing (NGS) identified putative linear epitopes of surface antigens that were strongly associated with the observed protection. The corresponding protection-associated peptides should be tested as potential subunit vaccine candidates.

2.3. Materials and Methods

2.3.1. Ethics statement

The experimental procedures involving mice were carried out at Texas A&M University with an animal use protocol approved by the Institutional Animal Care and Use

Committee of Texas A&M University and was in full compliance with the United States Public Health Service guidelines on human care and laboratory animal use. The mice were maintained at Texas A&M University in an animal facility accredited by the American Association for Accreditation of Laboratory Animal Care (AAALAC).

2.3.2. Bacterial strains

Previously generated and characterized *B. burgdorferi* B31-A3 lp25::*kan* (WT) (Rogovskyy and Bankhead, 2014) and B31-A3 lp28-1Δvls lp25::*gent* (ΔVlsE) (Rogovskyy et al., 2017a) clones were used in the present study (Table 2.1). *Borrelia* spirochetes were grown in liquid Barbour-Stoenner-Kelly medium (BSK-II, hereafter) supplemented with 6% rabbit serum (Gemini Bio-Products, CA, USA) and incubated at 35°C under 2% CO2.

Table 2.1 *B. burgdorferi* B31 clones used in the study

***B. burgdorferi* clone**	**Missing plasmid(s)**	***vls*2-16 [a]**	***vlsE***	**Reference**
B31-A3 lp25::*kan* (WT)	cp9	+	+	(Rogovskyy and Bankhead, 2014)
B31-A3 lp28-1Δvls lp25::*gent* (ΔVlsE)	cp9	-	-	(Rogovskyy et al., 2017a)

[a] *vls2-16* denotes silent cassettes of the *vls* locus.

2.3.3. Generation of host-adapted *B. burgdorferi* clones

Male C3SnSmn.CB17-*Prkdc*^{scid}/J (referred to here as SCID) mice of 4-6 weeks of age were purchased from Jackson Laboratories (ME, USA). To generate host-adapted *B. burgdorferi*, SCID mice were subcutaneously inoculated, in the scapular region, with *in vitro*-grown WT or ΔVlsE at 1×10^4 spirochetes per animal. Mouse infection was confirmed by culturing approximately 50 µl of blood aseptically taken via cheek bleed at

day 7 post infection in 3 ml of BSK-II that contained an antibiotic cocktail (0.02 mg ml^{-1} phosphomycin, 0.05 mg ml^{-1} rifampicin and 2.5 mg ml^{-1} amphotericin B; the antibiotic cocktail hereafter). The presence of viable spirochetes in culture was confirmed by dark-field microscopy. Ear tissues were harvested at day 21 post infection and stored at -80°C until use.

2.3.4. Mouse immunization

A total of 18 male C3H/HeJ (C3H) of 4-6 weeks of age (Jackson Laboratories, ME, USA) were divided into three groups (6 animals per group) designated as 1X, 3X, and 4X (Fig. 2.1), and were immunized with host-adapted ΔVlsE (ha-ΔVlsE hereafter) as described (Rogovskyy et al., 2017a). Briefly, ear pinnae from each SCID mouse were excised into small circular pieces (approximately 2 mm in diameter). It was previously estimated that the number of spirochetes may vary from few to several hundred spirochetes in each full-thickness 1.5-mm-diameter ear biopsy (Barthold et al., 1995). Each mouse was subcutaneously transplanted in the lumbar region with a total of two ear pieces, one taken from the right and the other from the left ear of a SCID mouse. At day 21 post immunization, group 1X mice were challenged with host-adapted WT (ha-WT hereafter). Group 3X and 4X animals were immunized with ha-ΔVlsE at day 21 and 28. At day 35, group 3X mice were challenged with ha-WT and group 4X animals were immunized with ha-ΔVlsE. At day 42, the quadruplely-immunized mice (group 4X) were challenged with ha-WT. Blood was taken from each animal at day 7 post ha-WT challenge and was cultured (50 μl) in 3 ml of BSK-II containing the antibiotic cocktail and kanamycin (200 μg/mL). At day 21 post challenge, mice of each group were sacrificed

and bladder, heart, tibiotarsal joint, and ear tissues were cultured in 1 ml of BSK-II containing the antibiotic cocktail and kanamycin (200 µg/mL) at 35°C under 2% CO2. The cultures were maintained for 4 weeks and checked weekly for the presence of spirochetes by dark-field microscopy.

2.3.5. Passive immunization

In order to generate sufficient amount of immune sera, eight C3H mice were repeatedly immunized with ha-ΔVlsE at day 0, 21, 28, and 35 as detailed above. At day 42, blood was harvested from each immunized animal via cardiac punch. Approximately 450 µl of sera was ultimately obtained from each mouse and stored at -80^{o}C.

A total of 4 naïve C3H mice were challenged with ha-WT and retro-orbitally treated with 150 µl immune sera at day 0. At day 2 and 4 post challenge, the mice were retro-orbitally inoculated with 150 and 100 µl of immune sera, respectively. A biological replicate of this experiment included additional 4 C3H mice that were treated identically as described above. At day 7, 50 µl of blood was collected from each mouse and cultured in 3 ml of BSK-II. At day 14, the mice were sacrificed and bladder, heart, tibiotarsal joint, and ear tissues were cultured in BSK-II (heart tissue in 3 ml and the other tissues in 1 ml) at 35°C under 2% CO_2. The cultures were kept for 4 weeks and checked weekly for the presence of spirochetes by dark-field microscopy. In parallel, the control mice (6 and 5 animals per group for the first and second biological replicates, respectively) were also challenged with ha-WT derived from the same SCID mice to ensure host-adapted spirochetes were infectious.

2.3.6. 2-D Gel electrophoresis

Proteins were extracted from *in vitro*-grown WT using sodium dodecyl sulfate (SDS) sample buffer (Laemmli, 1970) in order to ensure complete protein solubilization. The protein solutions were extracted utilizing chloroform and methanol as described (Wessel and Flugge, 1984) in order to remove SDS and concentrate proteins. The precipitated proteins were dissolved in isoelectric focusing (IEF) sample buffer (7M urea, 2M thiourea, 4% CHAPS, 5 mM De Streak (GE Healthcare, MA, USA), and 0.5% Pharmalytes (pH 3-10; GE Healthcare, MA, USA) and then used to hydrate Immobiline pH gradient Drystrips (13 cm, pH 3-10NL, GE Healthcare, MA, USA). IEF was allowed to proceed for 65kVh when the Drystrips were sequentially treated with SDS-containing equilibration buffer that contained dithiorthreitol (Sigma, MO, USA) or iodoacetamide (Sigma, MO, USA). The treated strips were secured to SDS slab gels (12% acrylamide) and electrophoresed until the bromophenol blue dye front reached the bottom of the gels. The gels were subsequently subjected either to visual staining with InstantBlue™ protein stain (Expedeon, CA, USA) or to electrotransfer (Mozdzanowski et al., 1992) onto polyvinylidene fluoride (PVDF) membrane (EMD Millipore, MA, USA) prior to immune-interrogation. Informed by geographical correlation to the immunostained membranes, protein spots of interest were excised from the stained gels (see Fig. S1 in the supplemental material), subjected to in-gel digestion as described (Shevchenko et al., 2006) followed by nano-LCMSMS analysis using the LTQ Orbitrap XL instrument (Thermo Fisher Scientific, CA, USA).

2.3.7. Western blot analysis

The WT clone was grown in BSK-II to the late stationary phase. Spirochetes were counted, pelleted by centrifugation at 6,000xg for 10 min at 4°C, and washed two times with ice-cold phosphate-buffered saline (PBS). After PBS was removed, bacterial cells in the pellet were suspended in SDS-polyacrylamide gel electrophoresis (PAGE) sample buffer (100 mM Tris [pH 6.8], 2% SDS, 5% β-mercaptoethanol, 10% glycerol, 0.01% bromophenol blue) and then incubated at 95°C for 10 min. Approximately $1x10^6$ cells were loaded into 15% acrylamide minigel. Resolved proteins were transferred onto PVDF membrane with pore size of 0.45 um (Bio-Rad Laboratories, CA, USA). Each blot was blocked with 5% nonfat dry milk in PBS for 18 hr at 4°C and then incubated in the same solution supplemented with 1:500 diluted mouse anti-ΔVlsE immune or undiluted preimmune sera for 18 hr at 4°C. The preimmune sera were pooled from 3 naive C3H mice. All anti-ΔVlsE immune sera were collected from ΔVlsE-immunized mice immediately prior to ha-WT challenge. The immune sera were taken and pooled in equal volumes from individual mice. After 4 washes of 10 min each with PBS with Tween 20 (PBST), antigen bound antibodies were detected utilizing goat anti-mouse HorseRadish Peroxidase (HRP)-conjugated secondary antibody (Bio-Rad Laboratories, CA, USA) diluted to 1:5000 in 5% non-fat milk for 30 min. Finally, the blot was washed 3 times in Tris-buffered saline with Tween 20 (TBST) buffer for 10 min each and then once by nano-pure water. The blots were visualized using enhanced chemiLuminescence development.

2.3.8. Scaffold analysis

Scaffold Version 4 (Proteome Software, Inc., OR, USA) was used to probabilistically validate protein identifications derived from MS/MS sequencing results utilizing the X!Tandem (Craig and Beavis, 2003) and ProteinProphet algorithms (Nesvizhskii et al., 2003). Scaffold was first used to validate protein identifications derived from MS/MS sequencing results. Peptide identifications were assigned by SEQUEST and Mascot search engines using the X!Tandem database searching program (Craig and Beavis, 2003; Searle et al., 2008). Peptide identifications were then verified via PeptideProphet algorithms (Keller et al., 2002; Nesvizhskii et al., 2003; Searle, 2010).

2.3.9. Mapping of protection-associated peptides onto *B. burgdorferi* surface proteins identified by the 2D-gel analysis

The identity of proteins derived from the MS/MS sequencing (Scaffold analysis section) was ascertained by using BLASTP of 2-D gel-identified protein sequences against the reference genome of *B. burgdorferi* B31, with the relatively stringent cut-off E-value of 10^{-20}, resulting in a set of 33 *B. burgdorferi* B31 surface proteins. Then, 400 protection-associated peptides were mapped to these 33 proteins with BLASTP. Hits of 5 or more amino acids in length without gaps were only considered.

2.3.10. Phage display (Ph.D.) library

Approximately 20 µl of mouse serum and 10 µl of random peptide library Ph.D.-7 (NEB, MA, USA) diluted in 200 µl of TBST buffer containing 0.1% Tween 20 and 1% bovine serum albumin (BSA) were incubated at 25^{o}C for 18 hr (Liu et al., 2013). Antibody-bound phages were isolated by the addition of 20 µl of protein G-agarose beads

(Santa Cruz Biotechnology, Inc., TX, USA) to the phage-antibody mixture for 1 hr. To remove unbound phages, the bead mixture was transferred to a 96-well MultiScreen-Mesh filter plate (EMD Millipore, MA, USA) that contained a 20-μm-pore-size nylon mesh on the bottom. Vacuum was applied to the exterior of the nylon mesh for the removal of unbound phages. The beads were washed four times with 100 μl of TBST buffer per well. Then, antibody-bound phages were eluted with 100 μl of 100 mM Tris-glycine buffer (pH 2.2). The buffer was subsequently replaced with 20 μl of 1 M Tris buffer (pH 9.1). Amplification of eluted phages was performed by infecting bacteria according to the manufacturer's instructions. Amplified phages were subjected to two rounds of biopanning. Antibody-bound phages were isolated utilizing protein G-agarose beads. DNA was isolated by phenol-chloroform extraction and ethanol precipitation. Finally, 21 nucleotides (nt) long DNA fragments encoding random peptides were amplified by PCR utilizing the following forward and reverse primers, respectively:

5′AATGATACGGCGACCACCGAGATCTACACTCTTTCCCTACACGACGCTCTT CCGATCT(INDEX)TGGTACCTTTCTATTCTCACTCT-3′and5′ CAAGCAGAAGAGGGCATACGAGCTCTTCCGATCTAACAGTTTCGGCCGAAC CTCCACC-3′. The INDEX in the forward primer sequence indicated a six-nt bar code. For each serum sample, a different forward primer was used with a unique index sequence (Liu et al., 2013). The multiplex PCR-amplified DNA library was then purified on agarose gel and sequenced via Illumina HiSeq 2500 platform.

2.3.11. DNA reads analysis

As a result of the sequencing, a total of approximately 116 million DNA reads were generated. Reads were de-multiplexed based on bar codes. Each read contained a unique index sequence, 6-nt in length, and a 21-nt sequence encoding a random peptide: 5 '- (INDEX) GTGGTACCTTTCTATTCTCACTCT (21-nt sequence) G-3'. The 21-nt sequences of each read were then extracted between positions 30 and 50 and translated into 7-mer peptides in the first frame. After exclusion of peptides containing stop codons the mean number of peptides per serum sample was approximately ~1 x 10^7, of which about ~1.4 x 10^5 peptides per sample were non-redundant. A total of 761 unique peptides were statistically associated with sera from protected mice (p<0.05). The data were analyzed using a code written in Python (https://www.python.org).

2.3.12. Comparison of peptide profiles of sera from protected and non-protected mice

The strength of association between a peptide and a serum sample was measured as follows: a peptide, P, was associated with sera from protected mice if X(P), the lowest frequency of P among protected mice samples, was higher than Y(P), the highest frequency of P among non-protected mice samples. The strength of association was then measured by the size of the gap: X(P) - Y(P).

2.3.13. Mapping of protection-associated peptides onto amino acid sequences of selected *B. burgdorferi* surface proteins

The obtained set of 761 non-redundant peptides was analyzed across samples, to identify those that were present only in the sera from protected mice, resulting in a list of

400 peptides. These 400 peptides were then mapped to the amino acid sequences of 1391 proteins from the complete reference genome of *B. burgdorferi* B31 (Fraser et al., 1997b) (GenBank accession: GCF_000008685.2; https://www.ncbi.nlm.nih.gov/genome/738?genome_assembly_id=168382) using BLASTP (Altschul et al., 1997; Camacho et al., 2009). Only hits that had at least 4 exact amino acid matches (i.e., identity threshold) were considered, for a total of 1516 hits. To focus on longer matches, hits of 5 or more amino acids in length without gaps were examined, resulting in 318 hits to 254 proteins (see lists A and B in Table 2-S1). However, some peptides in this subset were shared by multiple proteins, thus, such peptide hits were further filtered out. In other words, only the peptides with at least 5 identical amino acids in an aligned portion that also uniquely aligned to a single protein (to avoid a possibility to cross-matching of the same peptide to multiple proteins) were kept in the last step of the analysis. This resulted in 94 peptides matched to 85 proteins of interest (see list B in Table 2-S1).

2.3.14. Alignment of protection-associated peptides with conformational epitopes of outer surface proteins A, B, and C

Protection-associated peptides were compared with protein sequences of the genome reference of *B. burgdorferi* B31 via BLASTP (Altschul et al., 1997). BLASTP parameters were adjusted as appropriate for short (7-mer) peptide sequences, with E-value threshold 2000, substitution matrix PAM30 and word size 2, without applying composition-based statistics (Ryvkin et al., 2012). Furthermore, formation of gaps in sequence alignments was suppressed by setting the BLASTP gap-opening and -extension

penalties to their maximum possible value (32767). Gaps correspond to insertions or deletions that are likely to disrupt antibody-antigen binding if they occur within epitope sequences. Only BLASTP hits with peptide-protein sequence alignments at least four residues in length were considered for further analysis. No cutoff values were set for minimum sequence identity. The latter allowed for potential inclusion of epitope structures (e.g., helices) with residues that are at least partly oriented away from the antibody surface. This way the residues were more likely to be represented at phage-displayed sequence positions of high residue variability due to the diversity of side chains compatible with particular main-chain conformations.

The peptides were aligned with protein antigen sequences that contained known epitopes and pertinent epitope-related sequences of *B. burgdorferi*, identified mainly via the Immune Epitope Database (IEDB) 3.0 (Vita et al., 2015). IEDB searches were conducted from 6 to 8 October 2017 using the B Cell Assay Details interface (http://www.iedb.org/bcelldetails_v3.php) with "Epitope Source Organism" set to "*Borreliella burgdorferi* (Lyme disease spirochete)" (including *B. burgdorferi* B31 and other strains). Conformational epitopes were identified by setting "Epitope Structure Type" to "Discontinuous Epitopes". Additionally, sequences that elicit antipeptide antibodies with biological activity against *B. burgdorferi* were identified by setting "Epitope Structure Type" to "Linear Epitopes", "1st Immunogen Epitope Relation" to "Epitope", and "Assay" to "biological activity". Likewise, phage-displayed sequences bound by antibodies to *B. burgdorferi* were identified by setting "Epitope Structure Type" to "Linear Epitopes" and "Assay" to "phage display". Any other epitope-related sequences

that have been only identified via ELISA and WB were excluded from consideration. These binding assays may potentially yield false positive results due to artefactually unfolded protein epitopes and also negative results due to masking of epitopes (Caoili, 2010).

2.3.15. Statistics

A two-tailed Fisher's exact test was used for comparison of mouse groups. A p value of <0.05 was considered significantly different. The statistical significance of the difference between the number of peptides associated with sera from protected mice and the number of peptides associated with sera from non-protected mice was measured using permutation test. The permutation test was used because of the comparatively small number of samples (3 and 4 serum samples). For each possible permutation, the difference between the numbers of associated peptides was found and compared with the actual difference.

2.4. Results

2.4.1. Assessment of anti-*B. burgdorferi* immune response upon repeated immunizations of mice with host-adapted ΔVlsE

Immunocompetent mice that have previously cleared infection by the VlsE-deficient clone (ΔVlsE) can only be reinfected by host-adapted wild-type *B. burgdorferi*, which seem to evade antibody responses because of a high level of VlsE expression at the time of challenge (Rogovskyy and Bankhead, 2013). Neither *in vitro*-grown nor tick-derived wild-type clone, whose VlsE expression level is significantly reduced (Liang et al., 2004b), nor ha-ΔVlsE clone are able to establish secondary infection in mice that have

developed or passively received anti-ΔVlsE antibodies (sera) (Rogovskyy et al., 2015). VlsE is, therefore, proposed to sterically shield surface epitopes (Labandeira-Rey et al., 2003; Liang et al., 2002; Palmer et al., 2016; Philipp et al., 2001; Rogovskyy and Bankhead, 2013). However, it is likely that VlsE does not mask the entire surface epitome of *B. burgdorferi*. It is possible that an inability of anti-ΔVlsE antibodies to clear ha-VlsE-competent wild type could be explained by the lack or low titers of antibodies against epitopes that are not shielded by VlsE. These exposed epitopes are supposedly subdominant in nature and as such do not require VlsE-mediated shielding for their avoidance of host antibodies.

To test the above assumptions, the mice were repeatedly immunized with ha-ΔVlsE and then challenged with host-adapted VlsE-competent wild type. The repeated immunization assay involved three groups of C3H mice (1X, 3X, and 4X; Fig. 2.1). Importantly, the assay was independently performed twice with three animals in each group each time. The data of two biological replicates were combined and presented in Table 2.2. Overall, there was no statistical difference in blood culture results between the three groups, 1X, 3X, and 4X. Most mice (15 out of 18 animals) prevented culture-detectable spirochetemia by the ha-WT clone. In contrast, prior data demonstrated that single immunization of C3H mice (4 mice) with *in vitro*-grown ΔVlsE did not block ha-WT spirochetemia in any of the four mice (Table 2.2) (Rogovskyy and Bankhead, 2013). The difference between the prior and current data (4/4 vs. 0/6; p=0.0048) may partially be explained by a more potent immune response developed upon immunizations with host-adapted spirochetes.

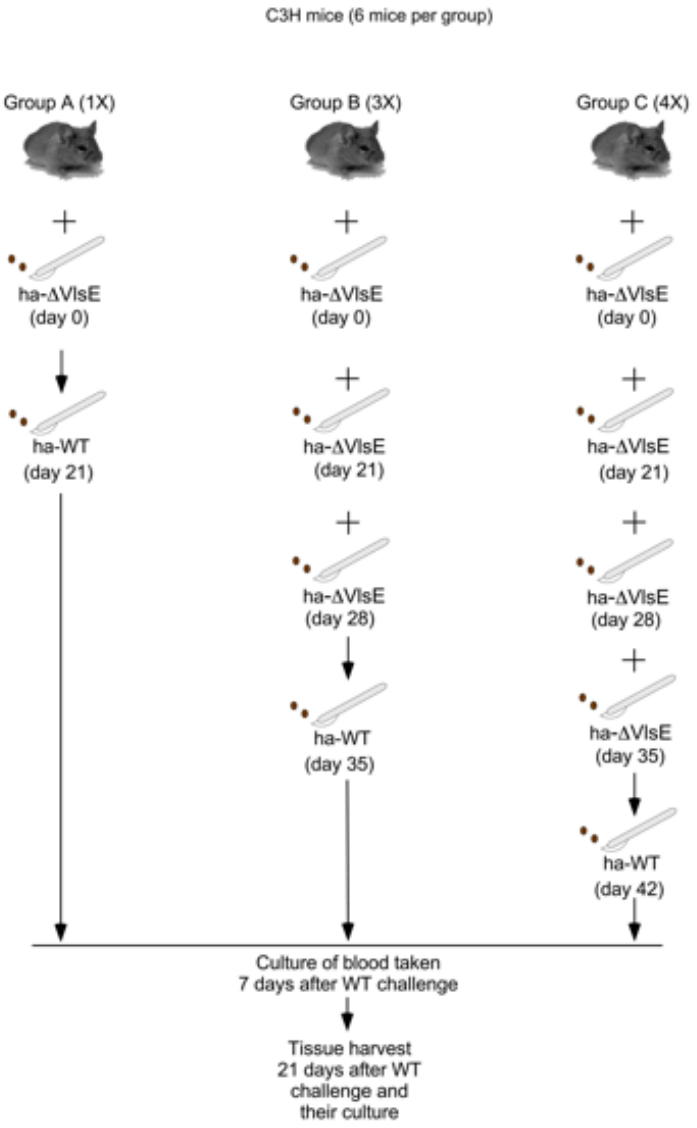

Figure 2.1 Repeated immunization assay. C3H mice of group 1X, 3X, and 4X (6 animals per group) were immunized with host-adapted (ha-)ΔVlsE. At day 21 post immunization, group 1X mice were challenged with ha-WT. Group 3X and 4X animals were also immunized with ha-ΔVlsE at day 21 and 28. At day 35, group 3X mice were challenged with ha-WT and group 4X animals were additionally immunized with ha-ΔVlsE. At day 42, the 4X mice were challenged with ha-WT. Blood and other tissues (bladder, heart, tibiotarsal joint, and ear tissues) were sampled from each animal at day 7 and 21 post WT challenge, respectively. All tissues were cultured in BSK-II for a total of 4 weeks. The cultures were checked weekly for the presence of spirochetes by dark-field microscopy.

The culture results of tissues collected from group 1X mice at day 21 demonstrated that immune response induced by single immunization with ha-ΔVlsE failed to block WT dissemination to bladder, heart, and joint tissues in all six mice (Table 2.2). In contrast, a total of two and four mice from 3X and 4X groups, respectively, were protected from ha-WT challenge. In each biological replicate experiment, 33 and 66% of 3X and 4X group mice, respectively, were consistently protected from ha-WT challenge. It seems as with the higher number of immunizations; the greater rate of protection was observed. If the latter was mainly due to an overall exposure of mice to a greater number of host-adapted spirochetes, it is well possible that the total number of immunizations could potentially be reduced by utilizing more ear biopsies per immunization. The infectivity of ha-WT clone used for challenge was verified upon completion of all the experiments. Immunologically naive C3H mice (3 control animals per group per biological replicate) showed culture-detectable spirochetemia at day 7 post challenge and the presence of wild-type spirochetes in bladder, heart, ear, and joint tissues harvested at day 21 (Table 2.3). Thus, 50% of repeatedly immunized animals were protected from highly immune-evasive VlsE-expressing spirochetes (6/12 vs. 0/10 (combined data on singly-immunized mice obtained from this and prior (Rogovskyy and Bankhead, 2013) studies; p=0.0152).

Table 2.2 Protective efficacy of immune response developed in ΔVlsE-immunized C3H mice against *in vitro*-grown and host-adapted wild-type *B. burgdorferi* B31

WT challenge of mice immunized with	No. of cultures positive/numbers tested (day of harvest post challenge)					No. of mice protected b /total
	Blood (7)	Ear (21[a])	Heart (21[a])	Bladder (21[a])	Joint (21[a])	
in vitro-grown ΔVlsE one time	4/4	4/4	4/4	4/4	4/4	0/4
host-adapted ΔVlsE one time (Group 1X)	2/6	6/6	6/6	6/6	6/6	0/6
host-adapted ΔVlsE three times (Group 3X)	0/6	4/6	3/6	3/6	3/6	2/6
host-adapted ΔVlsE four times (Group 4X)	1/6	2/6	2/6	2/6	2/6	4/6

[a] Mice singly immunized with *in vitro*-grown ΔVlsE were sacrificed at day 28 post wild type challenge (Rogovskyy and Bankhead, 2013).
[b] Mice were considered to be protected when all the tissues tested had been negative by culture.

Table 2.3 Infectivity of host-adapted wild-type *B. burgdorferi* B31 in control immunologically naïve C3H mice

Tissue (days post challenge)	Group 1X Control	Group 3X Control	Group 4X Control
Blood (7)	6/6 [a]	6/6	6/6
Ear (21)	6/6	6/6	6/6
Heart (21)	6/6	6/6	5/6
Bladder (21)	5/6	5/6	6/6
Joint (21)	6/6	6/6	6/6
Total	6/6	6/6	6/6

[a] Values listed correspond to numbers of cultures positive/numbers tested.

2.4.2. Characterization of antibody response via passive immunization assay, Western blot, and random peptide phage display libraries analyses

In order to examine whether the protection observed in the repeatedly immunized mice was due to antibody response, passive immunization assay was performed. A total

of 8 C3H mice (4 animals per biological replicate) were retro-orbitally injected with immune sera taken from quadruplely-immunized (4X) individual animals and then challenged with ha-WT. In order to obtain sufficient amount of sera, eight C3H mice were repeatedly immunized with ha-ΔVlsE four times (day 0, 21, 28, and 35) and at day 42 blood was collected via cardiac punch from each animal. Thus, these mice were never challenged and therefore it was unknown which animals had actually developed immunity that would prevent ha-WT infection.

At day 7 post ha-WT challenge, blood was collected from each passively immunized animal. The blood culture results showed that, in contrast to eleven control animals, 7 out of eight passively immunized mice successfully prevented host-adapted (highly immune-evasive) spirochetes from establishing culture-detectable spirochetemia (Table 2.4; p=0.0002). The latter demonstrates that it was anti-ΔVlsE antibodies that had been primarily responsible for prevention of ha-WT spirochetemia in the repeatedly immunized mice. However, when mouse tissues were collected at day 14 post challenge, the culture results showed that only one out of 8 animals remained culture-negative for wild-type spirochetes. Such a low protection rate could be well accounted for by limited amount of sera (only 400µl) delivered over the first few days to each mouse and, importantly, short half-lives of mouse serum immunoglobulins (Vieira and Rajewsky, 1988). Taken together, the data indicate that the protection observed in 50% of repeatedly immunized animals was likely due to the host antibody response.

Western blot (WB) analysis of 2-D gel electrophoresis performed using 3X and 4X sera indicates that the antibody response was augmented by repeated immunizations

(Fig. 2.2). Sera were collected from each mouse immediately prior to ha-WT challenge in the repeated immunization assay. Based on the culture results of mouse tissues collected after wild type challenge (Table 2.2), the samples were ultimately categorized as "protective" and "non-protective" sera. For WB analysis, the protective and non-protective sera were pooled from four quadruplely-immunized protected and three triple-immunized non-protected C3H mice, respectively. The two sera pools were then individually blotted against whole-cell lysates of *in vitro*-grown WT spirochetes. The results demonstrated that the protective sera were reactive to a number of additional antigens when compared to WB reacted with the non-protective sera (Fig. 2.2). Thus, the antibody response in the protected animals was, in general, more pronounced compared to that of non-protected mice.

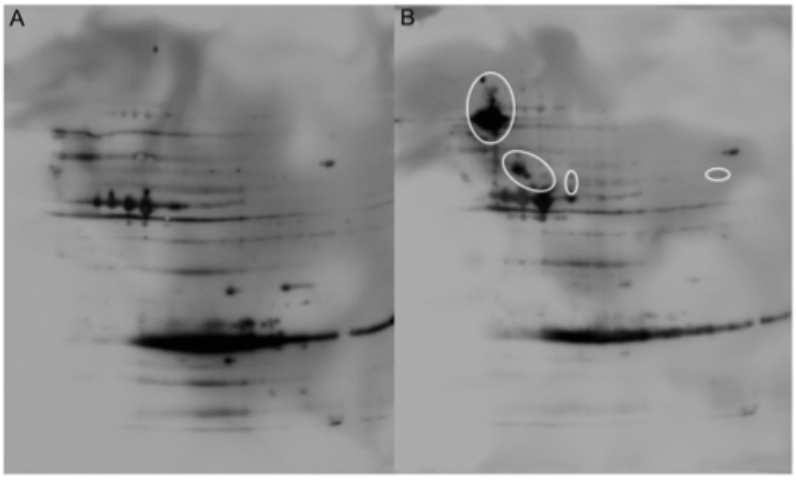

Figure 2.2 Western blots of 2-D gel electrophoresis of non-protective (A) and protective sera (B) blotted against lysate of *in-vitro* grown wild-type *B. burgdorferi* B31. The whole cell lysate of wild-type *B. burgdorferi* B31-A3 (10^6 cells per lane) was treated with non-protective (A) and protective (B) mouse sera collected prior to challenge with host-adapted wild type. The white oval shows additional reactivity of the protective sera compared to that of the non-protective sera. The blots can be compared to Coomassie Blue-stained whole-cell lysates of *B. burgdorferi* B31-A3 (see Fig. 2-S1 in the supplemental material).

To further characterize the antibody response in the protected and non-protected animals, an approach that involved RPPDL/NGS was taken. This approach was successfully applied to define anti-*Borrelia* antibody repertoires in persistently *B. burgdorferi*-infected mice (Rogovskyy et al., 2017a). Thus, in order to compare antibody repertoires in the protected and non-protected mice, four protective 4X and three non-protective 3X sera were analyzed via RPPDL/NGS. Mimotope profile was composed of approximately 1.4×10^5 distinct peptide sequences in each serum. The seven profiles were compared with each other and, as a result, 761 non-redundant peptides were found to be significantly associated with the four protective sera ($p<0.05$). Moreover, 400 of the 761 protection-associated peptides were only identified in the four protective 4X sera. These 400 peptides were missing in all non-protective 3X sera. Finally, in order to examine whether the identified difference in mimotope profiles could also be detected between protective and non-protective 4X sera, additional serum samples from two quadruplely-immunized susceptible mice were later analyzed via RPPDL/NGS. The results showed that 390 out of the 400 peptides were still uniquely present in all four protective 4X sera and absent in the three and two non-protective 3X and 4X sera, respectively. Taken together, the mice that became immune upon repeated immunizations had developed additional antibodies, whose specificities could potentially be responsible for the observed protection.

Table 2.4 Culture results of tissues from passively immunized mice challenged with host-adapted wild-type *B. burgdorferi* B31

Tissues (day of harvest)	C3H mice treated with 400 µl of 4X sera	Control C3H mice
Blood (7)	1/8 [a]	11/11 [b]
Ear (14)	4/8	11/11
Heart (14)	6/8	10/11
Bladder (14)	7/8	11/11
Joint (14)	7/8	11/11
No. of mice protected [c] /total	1/8	n/a [d]

[a] Mouse tissues were cultured in BSK-II for four weeks.
[b] Values listed correspond to numbers of cultures positive/numbers tested.
[c] Mice were considered to be protected when all the tissues tested had been negative by culture.
[d] n/a denotes non-applicable.

2.4.3. Identification of protection-associated surface proteins of *B. burgdorferi* and their respective linear epitopes

It is plausible that host antibodies whose specificities correspond to the protection-associated peptides may account for the distinct reactivity of protective sera as shown by WB analysis (Fig. 2.2). To test this possibility, the protein spots that represented distinct reactivity were excised from SDS-PAGE and subjected to sequencing. This resulted in identification of 33 *B. burgdorferi* B31-A3 proteins (Table 2-S2 in the supplemental material). Then, the 400 peptides were mapped onto these 33 proteins and, as a result, 77 unique peptide hits to the 33 *B. burgdorferi* B31-A3 proteins were identified. Each hit represented a peptide with a gapless match of at least 4 amino acid long to a single protein. To increase the stringency, however, only hits with 5 amino acid matches were further considered. Consequently, a total of 9 proteins were identified (Table 2.5), of which two, fibronectin-binding protein BBK32 and enolase are surface-exposed (Carrasco et al.,

2015; Dowdell et al., 2017; Floden et al., 2011; Kenedy et al., 2012a; Nogueira et al., 2012; Probert and Johnson, 1998; Szczepanski et al., 1990; Toledo et al., 2012).

Identification of only two surface proteins by WB is most likely due to inherent caveats of 2-D electrophoretic analysis of membrane proteins: isoelectric precipitation (Rabilloud, 2009) and substantial loss of proteins (Zhou et al., 2005). Therefore, it is well possible that surface proteins of *B. burgdorferi* that could have been recognized by the protective sera was missed in the WB analysis. To overcome this challenge, an approach involving *in silico* identification of *B. burgdorferi* protection-associated proteins was undertaken. Specifically, the 400 peptides were mapped to all the proteins (a total of 1391) of *B. burgdorferi* B31 genome (Fraser et al., 1997b). This resulted in 1516 BLASTP hits with at least 4 amino acid matches to 769 proteins (Fig. 2.3). In order to increase the stringency, any hits with gaps were further excluded from the downstream analysis and only 5 amino acid matches were considered. As a result, alignment of 318 gapless hits resulted in identification of 254 proteins, including numerous enzymes, transport proteins, and hypothetical proteins (see Table 2-S1 in the supplemental material). Out of 254 proteins, only 16 were surface-exposed (Table 2.6). A total 22 of the 400 peptides aligned to these 16 surface (lipo) proteins with at least 5 amino acid matches (Table 2.7). These peptides putatively represent 22 linear epitopes of *B. burgdorferi* surface proteins. Identification of low number of these putative epitopes may be partially explained by a possibility that there are limited number of subdominant surface epitopes that could induce protective immune response.

Table 2.5 Mapping results of 400 protection-associated peptides with 5 amino acid matches against 2D-gel proteins of *B. burgdorferi* B31

Accession #	ORF (plasmid #)	Protein name	Protein length (amino acids)
NP_045605.1	BBK32 (lp36)	Fibronectin-binding protein BBK32*	354
NP_212471.1	BB0337	Enolase*	433
NP_212674.1	BB0540	Elongation factor G	693
NP_212678.1	BB0544	Phosphoribosylpyrophosphate synthetase	406
NP_212692.1	BB0558	Phosphoenolpyruvate-protein phosphatase	573
NP_212701.1	BB0567	Chemotaxis histidine kinase	714
NP_212776.1	BB0642	Spermidine/putrescine ABC transporter ATP-binding protein	347
NP_212803.1	BB0669	Chemotaxis protein CheA	864
NP_212606.2	BB0472	UDP-N-acetylglucosamine 1-carboxyvinyltransferase	427

* The proteins are surface-exposed.

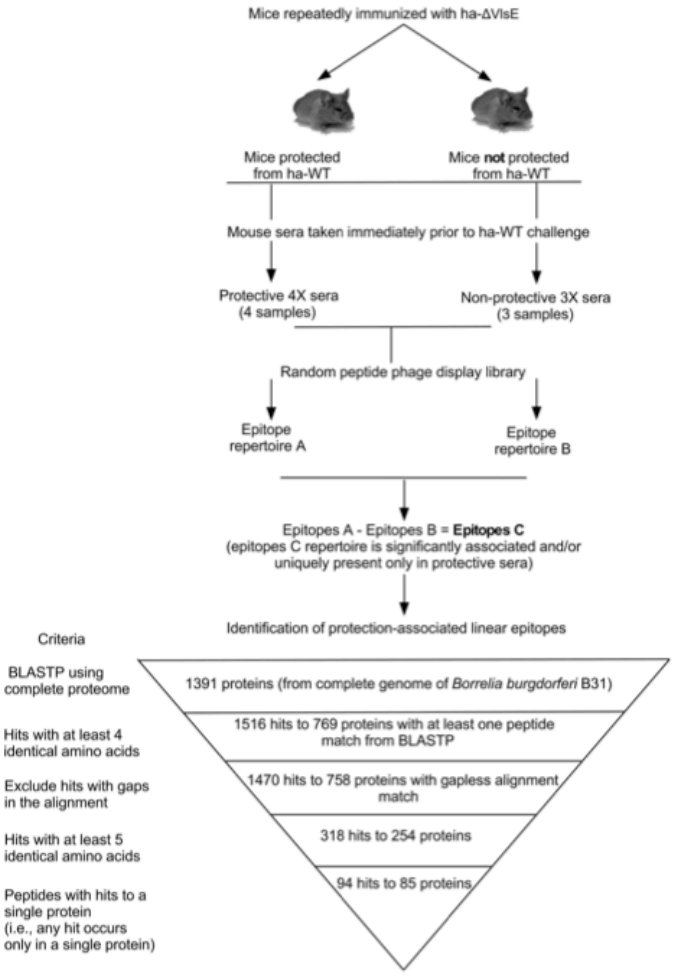

Figure 2.3 Identification of *B. burgdorferi* B31 proteins associated with protective immune response in ΔVlsE-immunized C3H mice. Mouse sera were initially collected from the repeatedly immunized animals prior to ha-WT challenge. Upon completion of repeated immunization assay, the samples were categorized as protective (4 samples) and non-protective (3 samples) based on the challenge experiment. The sera were then analyzed via random peptide phage display library in order to identify peptides (antibody) repertoires of protective (repertoire A) and non-protective sera (repertoire B). Repertoires A and B were then compared via the permutation test. As a result, 761 peptides (repertoire C) were found to be significantly associated with the protective sera. Out of 761, 400 peptides were detected in all protective sera samples and absent in the three non-protective sera. These 400 peptides were then mapped to the amino acid sequences of 1391 proteins from the complete genome of *B. burgdorferi* B31 via BLASTP. Only matches that had at least 4 exact amino acid matches were first considered, for a total of 1516 hits. Then, 318 gapless hits with at least 5 contiguous identical amino acids were only considered, resulting in identification of 254 proteins. A total of 94 peptides with hits to a single protein represented 85 out of 254 proteins.

Based on the frequency of amino acid sequence matches to non-surface proteins of *B. burgdorferi* (other proteins, hereafter), the 22 peptides were divided into four categories, A-D. Category A included any peptide that had a 5- or 6-amino acid match to a surface-exposed protein and no other 5(6)-amino acid match to any of the other 1391 *B. burgdorferi* B31 proteins. This category contained three peptides (p126, p168, and p259) that were mapped to OspE-related protein M (ErpM), protein BB0405, and surface-located membrane protein 1 (Lmp1), respectively (Table 2.7). Category B consisted of peptides that had at least one 4-amino acid match to other protein(s) of *B. burgdorferi*. Category B peptides, p60, p222, p282, p293, and p361 aligned to surface proteins BB0405, enolase, P13, P35, and *Borrelia* efflux system protein C (BesC), respectively. Category C was composed of peptides that had 4-amino acid match(es) and only one 5- or 6-amino acid match to other proteins. Lastly, category D comprised peptides that had two or more 5- and/or 6-amino acid matches to other proteins of *B. burgdorferi*. Categories C and D were equally represented by seven distinct peptides (Table 2.7).

Table 2.6 Surface-exposed proteins of *B. burgdorferi* B31 identified in silico via epitope mapping

Accession #	ORF (plasmid #)	Protein name	Protein length (amino acids)	Reference*
NP_045547.1	BBI16 (lp28-4)	Virulent strain-associated repetitive antige A (VraA)	451	(Dowdell et al., 2017; Labandeira-Rey et al., 2001)
NP_045575.1	BBK01 (lp36)	Lipoprotein BBK01	297	(Dowdell et al., 2017)
NP_045605.1	BBK32 (lp36)	Fibronectin-binding protein (Fbp) BBK32	354	(Dowdell et al., 2017; Kenedy et al., 2012a; Probert and Johnson, 1998; Szczepanski et al., 1990)
NP_045660.1	BBJ36 (lp38)	Lipoprotein BBJ36	352	(Dowdell et al., 2017)
NP_045709.2	BBA36 (lp54)	Lipoprotein BBA36	212	(Brooks et al., 2006; Dowdell et al., 2017)
NP_045739.1	BBA66 (lp54)	Lipoprotein BBA66	411	(Hughes et al., 2008)
NP_051319.1	BBM28 (cp32-6)	Multicopy lipoprotein F (MlpF)	149	(Dowdell et al., 2017)
NP_051373.1	BBO40 (cp32-7)	OspE-related protein M (ErpM)	363	(Dowdell et al., 2017; El-Hage et al., 2001)
NP_051469.1	BBA64 (lp54)	P35	250	(Brooks et al., 2006; Dowdell et al., 2017)
NP_212168.1	BB0034	P13	179	(Sadziene et al., 1995)
NP_212276.2	BB0142	Borrelia efflux system protein C (BesC)	428	(Bunikis et al., 2008)
NP_212471.1	BB0337	Enolase	433	(Carrasco et al., 2015; Floden et al., 2011; Nogueira et al., 2012; Toledo et al., 2012)
NP_212486.1	BB0352	Hypothetical protein BB0352	377	(Dowdell et al., 2017)
NP_212539.1	BB0405	Protein BB0405	203	(Brooks et al., 2006)
NP_212929.1	BB0795	β-barrel assembly machine A (BamA)	821	(Lenhart and Akins, 2010)
YP_008686569.1	BB0210	Surface-located membrane protein 1 (Lmp1)	1119	(Antonara et al., 2007)

* Listed are the studies that showed surface localization of *Borrelia burgdorferi* protein.

Table 2.7 Protection-associated peptides with 5(6)-amino acid gapless matches to surface-exposed proteins of *B. burgdorferi* B31

Peptide ID	Protein name	Alignment length	No. of identical amino acid matches	No. of amino acid mismatches	No. of 4-amino acid matches to non-surface proteins	No. of 5-amino acid matches to non-surface proteins	No. of 6-amino acid matches to non-surface proteins
Category A peptides							
p126	ErpM	6	5	1	0	0	0
p168	Protein BB0405	7	5	2	0	0	0
p259	Lmp1	6	5	1	0	0	0
Category B peptides							
p060	Protein BB0405	6	5	1	4	0	0
p222	Enolase	6	5	1	4	0	0
p282	P13	5	5	0	7	0	0
p293	P35	6	5	1	4	0	0
p361	BesC	7	5	2	1	0	0
Category C peptides							
p040	Protein BB0405	6	5	1	12	1	0
p105	Fbp BBK32	5	5	0	2	1	0
p185	Lipoprotein BBK01	6	5	1	1	1	0
p275	VraA	7	6	1	5	0	1
p285	BamA	5	5	0	0	1	0
p358	Enolase	7	5	2	3	1	0
p392	Lipoprotein BBJ36	7	5	2	20	1	0

Table 2.7 Continued

Peptide ID	Protein name	Alignment length	No. of identical amino acid matches	No. of amino acid mismatches	No. of 4-amino acid matches to non-surface proteins	No. of 5-amino acid matches to non-surface proteins	No. of 6-amino acid matches to non-surface proteins
Category D peptides							
P005	ErpM	6	5	1	4	1	1
P138	Protein BB0405	6	5	1	0	3	0
P151	Lmp1	6	5	1	11	6	0
p301	MlpF	6	5	1	2	4	0
p333	Lipoprotein BBK01	5	5	0	2	2	0
p340	Lipoprotein BBA36	5	5	0	3	2	0
P397	Lipoprotein BBA66	7	5	2	0	4	2

Table 2.8 Conservation of linear epitopes among *B. burgdorferi*, *B. afzelii*, and *B. garinii* relative to protection-associated peptide

Peptide ID	*B. burgdorferi* B31-A3 protein name (protein accession #)	No. of identical amino acid matches/alignment length (protein accession # / identity with respective *B. burgdorferi* B31 protein)	
		B. afzelii	***B. garinii***
Category A peptides			
p126	ErpM (NP_051373.1)	4/6 (WP_012579260.1/42%)	6/6 (WP_031508412.1/49%)
p168	Protein BB0405 (NP_212539.1)	5/7 (WP_004790339.1/90%)	5/7 (WP_029347955.1/94%)
p259	Lmp1 (YP_008686569.1)	3/6 (WP_048830530.1/78%)	3/6 (WP_004793842.1/82%)
Category B peptides			
p060	Protein BB0405 (NP_212539.1)	5/6 (WP_004790339.1/90%)	5/6 (WP_029347955.1/94%)
p222	Enolase (NP_212471.1)	5/6 (WP_011600962.1/97%)	5/6 (WP_015026804.1/97%)
p282	P13 (NP_212168.1)	4/5 (WP_015055259.1/85%)	4/5 (WP_014653294.1/82%)
p293	P35 (NP_051469.1)	4/6 (WP_011703839.1/53%)	4/6 (WP_032986135.1/50%)
p361	BesC (NP_212276.2)	4/7 (WP_038850757/93%)	5/7 (WP_015026657.1/91%)
Category C peptides			
p040	Protein BB0405 (NP_212539.1)	5/6 (WP_004790339.1/90%)	5/6 (WP_029347955.1/94%)
p105	Fbp BBK32 (NP_045605.1)	1/5 (WP_015945545.1/72%)	5/5 (ACR57087.1/99%)
p185	Lipoprotein BBK01 (NP_045575.1)	5/6 (WP_014486288.1/74%)	4/6 (WP_032984282.1/68%)
p275	VraA (NP_045547.1)	5/7 (WP_011703877.1/56%)	5/7 (WP_029362035.1/49%)
p285	BamA (NP_212929.1)	5/5 (WP_048830718.1/95%)	5/5 (WP_015027152.1/95%)
p358	Enolase (NP_212471.1)	5/7 (WP_011600962.1/97%)	5/7 (WP_015026804.1/97%)
p392	Lipoprotein BBJ36 (NP_045660.1)	N/A*	1/7 (WP_012621181.1/74%)

*N/A - not available. The respective protein sequence was not found via BLASTP.

As opposed to the first three categories, category D peptides were more likely to represent linear epitopes of non-surface proteins and, therefore, were excluded from the further analysis. In order to examine a degree of conservation of identified putative linear epitopes between various *Borrelia* genospecies, the eleven surface proteins of *B. burgdorferi* B31-A3 represented by all the peptides of categories A-C were aligned, via BLASTP, with the respective proteins of *Borrelia garinii* and *Borrelia afzelii*.

Also, the proteins of the three genospecies were individually aligned to the respective protection-associated peptides. As a result, most putative epitopes showed a high degree of conservation among *B. burgdorferi*, *B. garinii*, and *B. afzelii* despite the fact that some proteins had an overall very low degree of identity (Table 2.8). For example, ErpM of *B. burgdorferi* B31-A3 (NP_051373.1) had only 42 and 49% of amino acid identity, respectively, with the corresponding proteins of *B. afzelii* (WP_012579260.1) and *B. garinii* (WP_031508412.1) (Table 2.8). Yet, peptide p126 still had 4-6-amino acid matches with three putative epitopes of the *Borrelia* genospecies (Tables 2.7 and 2.8). The epitope represented by p392 was the least conserved between *B. burgdorferi* and *B. garinii*: the number of identical amino acid matches per alignment length (the conservation ratio, hereafter) was only 1/7. In contrast, the epitopes defined by p040, p060, p168, p222, and p285 were highly conserved with the conservation ratio being 5/5-5/7 for the three genospecies. Interestingly, the Fbp BKK32 epitope mapped by p105 was only conserved between *B. burgdorferi* B31-A3 (5/5) and *B. garinii* (5/5), and not *B. afzelii* (1/5). Overall, the newly identified putative epitopes had a high degree of conservation between the main

pathogenic *Borrelia* genospecies and therefore could be tested as potential vaccine candidates.

2.4.4. Comparison of RPPDL application results with known *B. burgdorferi* conformational surface epitopes and protective sequences

In addition to linear epitopes, an attempt was made to identify conformational surface epitopes associated with the observed protection in the repeated immunization assay. A total of 5 conformational epitopes within *B. burgdorferi* B31-A3 outer surface proteins A (OspA) and B (OspB) were mapped (Fig. 2.4; A1 through A4 and B1). These epitopes were previously derived from X-ray crystallography (A1 (Li et al., 1997), A3 (Ding et al., 2000) and B1 (Becker et al., 2005)), nuclear magnetic resonance (A3 (Ding et al., 2000) and A4 (Huang et al., 1998)), or mass spectrometry of immune-complex-derived proteolytic products (A2 (Legros et al., 2000)). Epitopes A3 and A4 shared two constituent residues (K231 and S250). Identified were also two 10-mer peptides whose sequences exactly matched OspA ^{247}QYDSNGTKLE^{256} (encompassing OspA ^{249}DSNGT^{253} of A3) and OspB ^{211}TLKREIEKDG^{220}. These neutralizing epitopes were previously shown to be recognized by complement-dependent and -independent monoclonal antibodies (MAbs), B3G11 (anti-OspA) and N5G5 (anti-OspB), respectively (Ma et al., 1995).

Peptides p047 (GKGKYEI) and p554 (NKLSKYL) aligned with OspA sequences that comprised Y52, a residue of epitope A1 (Fig. 2.4). Peptides p576 (VLNGYVH) and p599 (MDKTTLA) aligned with sequences that contained residues of A2 (OspA ^{145}VLKGYVLE^{152} and ^{160}TTLVVKE^{166}). Peptide p231 (YAAGSAV) aligned so as to

overlap with a constituent sequence (OspA ^{256}EGSAVE^{261}) of A4. Furthermore, p024 (ATVHLKP) partially aligned with OspB ^{211}TLKREIEKDG^{220} (bound by MAb N5G5). In contrast, the other protection-associated peptides aligned with OspA or OspB sequences without overlapping known epitope residues (Fig. 2.4).

Figure 2.4 Conformational epitopes (labeled as A1 through A4 and B1) of *B. burgdorferi* B31 outer surface proteins A (OspA) and B (OspB) with aligned protection-associated peptides. Each epitope label is followed by its cognate monoclonal-antibody (MAb) name. A1 (Li et al., 1997), A2 (Legros et al., 2000), A3 (Ding et al., 2000), and A4 (Huang et al., 1998) are on OspA while B1 (Becker et al., 2005) is on OspB. Epitope residues are underlined in the protein sequences, with representative sequence positions numbered. Peptide residues are rendered in upper case if part of a BLASTP hit alignment or lower case if otherwise. Peptide IDs are in parentheses. Residues of A3 marked with asterisks (*) are critical for LA-2 binding and complement-dependent bactericidal activity (Shandilya et al., 2017). Residues common to both A3 and A4 are marked with carets (^). A3 is topologically analogous to B1, with B1 centered around OspB residue K253 (marked '+'), which is essential for binding of OspB by H6831 (Becker et al., 2005). The other MAb B3G11 and MAb N5G5 bind 10-mer peptide analogs (sequences highlighted with magenta background) of OspA and OspB, respectively (Ma et al., 1995).

Three protective sequences (Fig. 2.5), one each from *B. burgdorferi* B31 OspA, OspB, and OspC were previously shown to elicit anti-peptide antibodies with

complement-dependent (anti-OspA and anti-OspC) or -independent (anti-OspB) bactericidal activity (Buckles et al., 2006; Izac et al., 2017; Sadziene et al., 1994). Peptide p394 (NATSTLL) aligned with the OspA (^{221}STLTITVNSKKTKDLVFTKE^{240}) and OspB (^{238}KWEDSTSTLTISADSKKTKD^{257}) protective sequences. The latter comprised residues of conformational epitopes (A3, A4, and B1 in Fig. 2.4), despite the fact that the p394-aligned protein sequences themselves (with exact matching for OspA ^{220}TSTL^{223} and OspB ^{243}TSTL^{246}) were entirely outside of the epitopes. Furthermore, peptides p223 (WKKHTDM), p387 (VSKHSDL), and p652 (LNKHTDI) all aligned within the OspC protective sequence (^{130}CSETFTNKLKEKHTDLGKEGV^{150}), with a consensus sequence exactly matching OspC ^{141}KHTD^{144} (Fig. 2.5). KHTD occurred only once in the entire *B. burgdorferi* B31 proteome and may be regarded as part of an extended consensus sequence KHTDZG. Z was a residue that had a long aliphatic nonpolar sidechain (i.e., M, L or I). KHTDZG matched OspC ^{141}KHTDLG^{146}.

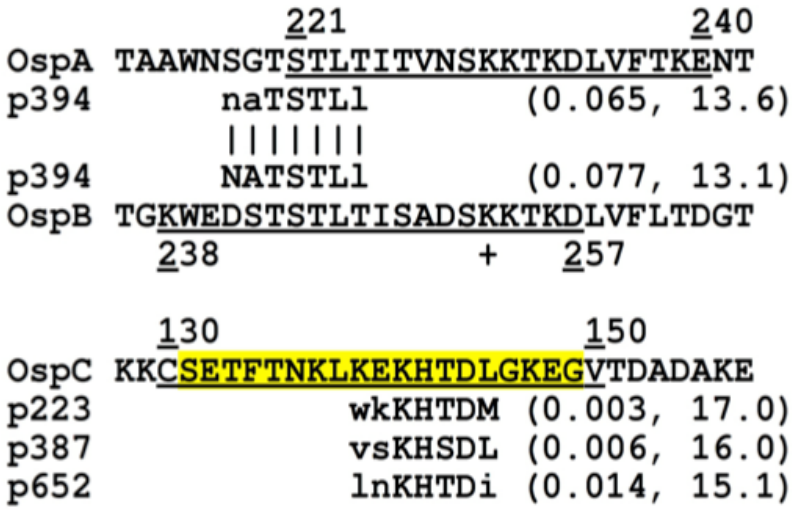

Figure 2.5 Protective sequences of *B. burgdorferi* B31 outer surface proteins A (OspA), B (OspB), and C (OspC) with aligned protection-associated peptides. Underlined sequences (with N- and C-terminal residue positions numbered) of OspA, OspB, and OspC elicit antipeptide antibodies with complement-dependent (anti-OspA and anti-OspC) and -independent (anti-OspB) bactericidal activity (Buckles et al., 2006; Izac et al., 2017; Sadziene et al., 1994). Peptide IDs are on the lines of their respective sequences, whose residues are rendered in upper case if part of a BLASTP hit alignment or lower case if otherwise. BLASTP E-values and bit scores are in parentheses. OspA and OspB sequences are aligned to emphasize their homology, with OspB residue K253 marked '+' as in Figure 4 (within conformational epitope B1). Subsequence exactly matching OspC residues 131-149 (highlighted with yellow background) forms part of a chimeric vaccinogen that elicits anti-peptide antibodies having complement-dependent bactericidal activity (Earnhart et al., 2007).

Prior study has identified six epitope sequences (Fig. 2.6; E1 through E6) of *B. burgdorferi* SKT-2 OspC via 12-mer phage-displayed peptide library (Pulzova et al., 2016). The library was selected by panning with human LD patient antibodies that was affinity-purified using the same OspC. Importantly, all epitopes except E2 were recognized by antibody in WB following SDS-PAGE, indicating that E2 comprised residues of a conformational epitope, whereas the other five were linear (Pulzova et al., 2016). Alignment of the epitopes with *B. burgdorferi* B31 OspC revealed that they were

identical (E1 and E6) or nearly so (differing only at a single residue position) to homologous regions of the reference genome of *B. burgdorferi* B31. Three protection-associated peptides, p471 (TSTGVAY), p636 (RDFSPKK), and p697 (AERGTKP) aligned with sequences overlapping E6 (PVVAES) (Fig. 2.6). Peptide p697 aligned with the OspC C-terminal heptapeptide (^{205}AESPKKP^{211}), which was part of the decapeptide (^{202}PVVAESPKKP^{211}) used in serodiagnostic tests to detect anti-OspC IgM in LD patient sera (Mathiesen et al., 1998). Peptide p057 (LPLSLAA) partially aligned with OspC ^{184}LSKAAKEM^{191}, which was homologous to E5 (LLKAAKEM) (Fig. 2.6). Peptide p521 (NTSAPDL) aligned such that its N-terminus overlapped with the C-terminus of E1 (CNNSGKDGN). p223, p387, and p652 with consensus sequence ^{141}KHTD^{144} aligned with OspC without overlapping any residues of E1 through E6. However, the three peptides aligned to the 15-mer peptide to which blocking anti-OspC MAb 16.22 was shown to bind (Fig. 2.6) (Yang et al., 2006). This complement-independent bactericidal antibody was produced by immunization with recombinant OspC (Yang et al., 2006). Peptides p521, p595 (TSTRSAQ), p631 (MTSENSF), and p710 (TSTQSAH) all aligned to exactly match OspC ^{28}TS^{29} adjacent to the C-terminus of the E1-homologous region (Fig. 2.6).

Figure 2.6 *B. burgdorferi* B31 outer surface protein C (OspC) sequence with aligned epitope sequences (labeled E1 through E6) and protection-associated peptides. Epitope sequences (with N- and C-terminal residue positions numbered) were inferred from 12-mer phage-displayed peptide sequences of *B. burgdorferi* SKT-2 OspC (Pulzova et al., 2016). Homologous sequences in *B. burgdorferi* B31 OspC are underlined. Epitope sequence differences between the two *B. burgdorferi* strains are highlighted with cyan background. Peptide residues are rendered in upper case if part of a BLASTP hit alignment or lower case if otherwise. Peptide IDs are in parentheses. Angled brackets (<>) delineate residues 130-150, which constitutes the protective sequence that contains a vaccinogen-component subsequence (highlighted with yellow background). The 15-mer peptide whose sequence exactly matches residues 133-147 (highlighted with magenta overhead band) is bound by bactericidal complement-independent MAb 16.22 (Yang et al., 2006).

2.5. Discussion

2.5.1. Is the VlsE system that omnipotent?

The study shows that repeated exposure to antigens expressed by live VlsE-deleted spirochetes can result in an antibody-mediated immunity against host-adapted wild-type *B. burgdorferi*, despite the activated VlsE system. This indicates that variable VlsE does not have the capacity to mask the entire surface epitome of *B. burgdorferi*. If VlsE sterically does shield surface antigens as proposed (Labandeira-Rey et al., 2003; Liang et

al., 2002; Palmer et al., 2016; Philipp et al., 2001; Rogovskyy and Bankhead, 2013), it is highly likely that a portion of epitopes is still exposed. These epitopes are probably subdominant by nature and as such present no risk to *B. burgdorferi*. These assumptions have been supported by a number of observations.

First, despite robust anti-*Borrelia* immune response developed by infected immunocompetent mice, mouse antibodies consistently fail to clear wild-type *B. burgdorferi*. Both laboratory and *Peromyscus* mice become persistently infected with VlsE-competent *B. burgdorferi* (Coutte et al., 2009; Labandeira-Rey et al., 2003; Liang et al., 2002; Philipp et al., 2001; Rogovskyy and Bankhead, 2013; Rogovskyy et al., 2015). Since VlsE expression is highly upregulated *in vivo* (Liang et al., 2004b), antibodies that dominate in these persistently infected animals are simply non-protective against the spirochetes that express variable VlsE. Second, the prior (Rogovskyy and Bankhead, 2013) and present data consistently show that antibodies from singly immunized mice produce anti-ΔVlsE antibodies (anti-ΔVlsE 1X antibodies, hereafter) that fail to prevent ha-WT infection. In contrast, the same antibodies efficiently block infection by *in vitro*-grown and tick-adapted WT, whose VlsE expression level is low (Crother et al., 2004; Indest et al., 2001; Liang et al., 2004b; Ohnishi et al., 2003; Rogovskyy and Bankhead, 2013; Rogovskyy et al., 2015). Thus, only the spirochetes with the activated VlsE system are able to establish a long-term infection in the face of anti-ΔVlsE 1X antibodies (Rogovskyy and Bankhead, 2013). It is therefore suggested that anti-ΔVlsE 1X antibodies primarily target dominant surface epitopes whose recognition are otherwise blocked by VlsE. Finally, the present study suggests that repeated exposure to putatively subdominant

epitopes exposed by the ΔVlsE clone may render some of these epitopes dominant. As shown herein, induced protection in the repeatedly immunized animals was significantly associated with an emergence of novel antibody repertoires (represented by the 400 peptides unique for the protected quadruplely-immunized mice).

As a summary, we propose the model that abstracts the above observations (Fig. 2.7). Specifically, the model (panels A-C) depicts how VlsE sterically shields surface epitopes of *B. burgdorferi* from host antibodies. Upon single immunization of mice with ha-ΔVlsE, antibodies are predominantly developed against dominant epitopes (purple circles) of various surface antigens (green ovals). In contrast, repeated immunizations with ha-ΔVlsE supposedly also induce antibodies against subdominant conformational and/or linear epitopes (orange circles; panel B). These putatively subdominant epitopes possibly remain exposed even in the presence of abundant VlsE molecules. When the repeatedly immunized mice are challenged with VlsE-expressing *B. burgdorferi* (ha-WT), the exposed epitopes are freely accessible to additionally-induced antibodies. Importantly, some of these antibodies may be protective. At present, studies are under way to test whether the proposed model is valid.

2.5.2. Exposed linear epitopes as potential subunit vaccine targets

The current work has attempted to identify surface epitopes that are associated with mouse protection observed in the repeatedly immunized animals. As a result, the 400 peptides unique for the protected mice were identified. Fifteen of these peptides (categories A-C) putatively represent linear epitopes of *B. burgdorferi* surface antigens.

These epitopes are likely to be subdominant yet protective and, importantly, most of them are conserved among the *Borrelia* genospecies.

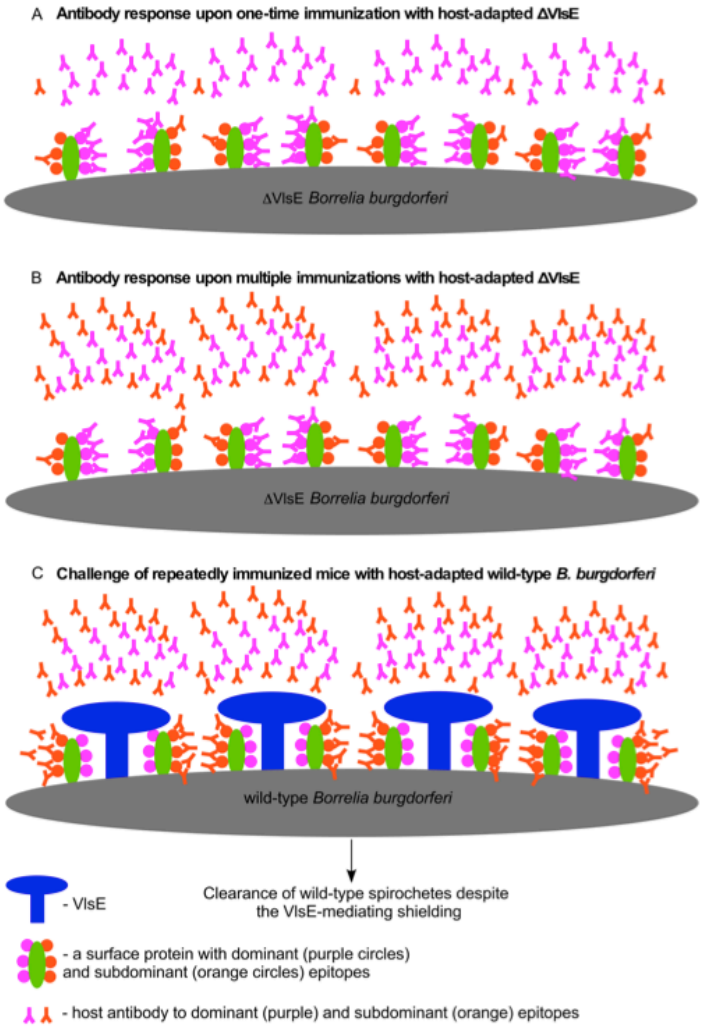

Figure 2.7 Development of protective antibody response against host-adapted *B. burgdorferi* upon repeated immunizations with ha-ΔVlsE. The diagram (panels A-C) shows how protective antibody response may have developed in mice repeatedly immunized with ha-ΔVlsE. It is plausible that VlsE sterically shields mostly dominant epitopes of *B. burgdorferi* surface from host antibodies. After a single immunization, antibodies are primarily developed against dominant epitopes (purple circles) of various surface antigens (green ovals; panel A). However, repeated immunizations with ha-ΔVlsE result in development of antibodies against previously subdominant epitopes (orange circles; panel B). Upon challenge with VlsE-expressing *B. burgdorferi* B31 (ha-WT), the subdominant epitopes are fully accessible to antibodies as VlsE does not supposedly shield them. Some of these subdominant epitopes may induce protective antibodies.

A total of 12 surface proteins of *B. burgdorferi* have been mapped by category A-C peptides. Peptides p40, p60, and p168 represent three putative linear epitopes of outer membrane protein, BB0405. BB0405 is shown to be poorly immunogenic in the mammalian host during an early stage of infection (Kung et al., 2016; Shrestha et al., 2017). In mice, anti-BB0405 antibodies do not develop for at least one month after *B. burgdorferi* infection (Kung et al., 2016). Likewise, during human infection, anti-BB0405 antibodies are not detected either. Interestingly, despite anti-BB0405 polyclonal antibodies are borreliacidal *in vitro* (Brooks et al., 2006; Shrestha et al., 2017), BB0405 immunization of mice with recombinant BB0405 does not affect any spirochetal burden in infected mice. However, this immunization still induces a long-lasting antibody response as demonstrated by WB and ELISA (Kung et al., 2016). Thus, it seems as BB0405 is subdominant antigen that, when made dominant (via immunization with the recombinant protein), may induce a detectable antibody response. The published findings directly support our observation that BB0405 may contain subdominant epitopes. Also, it has been previously suggested that, during mammalian infection, BB0405 is camouflaged by "abundant neighboring outer membrane proteins" (Kung et al., 2016). Accordingly, VlsE molecules may well fill the role of these "neighboring outer membrane proteins" and may explain why anti-BB0405 antibodies are only borreliacidal to *in vitro*-grown spirochetes (Brooks et al., 2006; Shrestha et al., 2017), whose VlsE expression is very low (Liang et al., 2004b).

In addition to having protective epitopes, BB0405 is also conserved among *B. burgdorferi* sensu lato genospecies with 78 to 90% identity between BB0405 orthologs.

Antibodies generated against *B. burgdorferi* B31-A3 recognize orthologs of different infectious *Borrelia* strains (Kung et al., 2016). Importantly, BB0405 is absolutely required for mammalian infection (Kung et al., 2016; Shrestha et al., 2017). Thus, BB0405 is a strong vaccine candidate, whose newly identified putative epitopes should be tested as potential targets of LD subunit vaccine.

Enolase (BB0337) is another surface protein of *B. burgdorferi* (Carrasco et al., 2015; Floden et al., 2011; Nogueira et al., 2012; Toledo et al., 2012), whose protection-associated epitopes have been mapped in this study. Peptides p222 and p358 define two putative antibody-binding epitopes. Enolase serves a plasminogen receptor and is highly conserved between *Borrelia* genospecies (Floden et al., 2011; Nogueira et al., 2012). Anti-enolase antibodies do not significantly reduce spirochetal burden in immunized animals despite enolase being predominantly expressed in mouse tissues during late infection. However, the same anti-enolase antibodies do interfere with pathogen persistence in ticks (Nogueira et al., 2012). Thus, the two putative linear epitopes could be tested as potential candidates for a transmission-blocking subunit vaccine.

In addition to BB0405 and enolase, the other chromosomally-encoded OMPs, BamA, BesC, P13, and Lmp1 were also mapped by the protection-associated peptides. BamA (BB0795) is part of β-barrel assembly machine (BAM), the complex that is found in all diderm bacteria (Knowles et al., 2009). BamA is involved in localization of OMPs and, as shown by depletion study, is essential in *B. burgdorferi* growth (Knowles et al., 2009; Lenhart and Akins, 2010). Peptide p285 maps the respective BamA epitope within its putative polypeptide transport-associated (POTRA) domains.

Borrelia efflux system protein C (BesC; BB0142) is a functional TolC homolog, which is part of putative export system that additionally comprises BesA and BesB (Bunikis et al., 2008). BesA/B/C are thought to form a RND-type multi-drug efflux system in *B. burgdorferi*. BesC is critical for *B. burgdorferi* to establish infection in mice (Bunikis et al., 2008).

The chromosomal P13 (BB0034) is a membrane-integrated protein with a porin activity that has four transmembrane helices and a surface immunogenic loop (Noppa et al., 2001; Ostberg et al., 2002; Pinne et al., 2004; Tusnady and Simon, 2001). Peptide p282 aligns outside the membrane-embedded P13 transmembrane helices. Antibodies to this 13-kDa surface antigen inhibits *B. burgdorferi* B313, the strain that lacks almost all the outer surface lipoproteins-encoding plasmids (Sadziene et al., 1995). In contrast, anti-P13 antibodies do not affect plasmid-competent wild-type *B. burgdorferi*, suggesting that abundant surface lipoproteins (e.g., VlsE) mask P13 epitopes (Kenedy et al., 2012a; Sadziene et al., 1995).

Lmp1 (BB0210) is a potential adhesin required for spirochetes to persist in murine tissues (Antonara et al., 2007; Yang et al., 2009). Interestingly, Lmp1 is important for *B. burgdorferi* to evade or resist an adaptive immune response (Yang et al., 2009). Lmp1 deletion results in an impaired ability of the mutant to persist in tissues of immunocompetent mice as opposed to SCIDs. Moreover, Lmp1 deficiency increases *Borrelia* susceptibility to immune sera *in vitro* (Yang et al., 2009). The 128-kDa surface protein comprises N-terminal (Lmp-N), middle (Lmp-M), and C-terminal domains (Lmp-C) (Yang et al., 2009). The immunogenic Lpm-N region is membrane-embedded and is

likely most critical for spirochete survival in the host. Lmp-N has seven unique 54-residue repeats, whereas C-terminal region is rich in tetratricopeptide (TPR3) repeats. As suggested by IFA data, the Lmp-C region is surface-exposed that probably interacts with host proteins (Yang et al., 2009). The putative protective epitope mapped by peptide p259 is found within this surface-localized Lmp-C domain.

Unlike the above-mentioned chromosomally-encoded OMPs, P35 (BBA64) is an outer surface protein, which is encoded by linear plasmid, lp54. This 35-kDa protein is highly immunogenic as consistently evidenced by its expression in *B. burgdorferi*-infected mice and humans (Barbour et al., 2008; Brooks et al., 2006; Gilmore et al., 2007; Gilmore et al., 1997; Nowalk et al., 2006). BBA64 is not expressed in replete ticks (Gilmore et al., 2001). However, *bba64* is upregulated during tick feeding (Tokarz et al., 2004) as it is absolutely required for the pathogen transfer and/or survival from the tick to the mammalian host (Gilmore et al., 2010). It is therefore suggested that BBA64 be utilized as a candidate for a tick transmission-blocking LD vaccine (Gilmore et al., 2010). Because the crystal structure of BBA64 is not entirely resolved, surface exposure of putative linear epitope mapped by p293 remains to be determined (Brangulis et al., 2013). Prior data predict that the epitope-containing region is likely to serve as a linker between the structural portion of the protein and the cell surface (Brangulis et al., 2013).

Virulent strain-associated repetitive antigen A, VraA (BBI16) is another plasmid-encoded surface protein that has been mapped by a protection-associated peptide. The *bbi16* gene is localized on lp28-4, the plasmid that is absent in non-infectious *B. burgdorferi* B31 isolates (Labandeira-Rey et al., 2001). The predicted molecular mass of

mature VraA is approximately 52 kDa. Immunization of mice with a recombinant full-length VraA shows partial protection against *in vitro*-grown *B. burgdorferi* (Labandeira-Rey et al., 2001). Importantly, the protection-associated epitope defined by p275 is localized within the carboxy-terminal region (residues 253 to 451) of VraA protein. Antibodies developed against this entire region do not react with native VraA *of B. burgdorferi* B31-A3. Likewise, these antibodies only weakly react with either a full-length or amino-terminal recombinant VraA fused to GST, most likely due to their anti-GST reactivity (Labandeira-Rey et al., 2001). Moreover, infection-derived rabbit sera do not recognize the carboxy-terminal recombinant VraA. In contrast, the rabbit antibodies are reactive with both full-length and amino-terminal recombinant VraA, indicating the immunodominant nature of only amino-terminal region (residues 18 to 260). Thus, the empirical findings clearly demonstrate that the epitope-containing carboxy-terminal region is not immunogenic (Labandeira-Rey et al., 2001) and this in turn supports our observation that the protection-associated epitope of VraA is subdominant by nature.

2.5.3. Identification of conformational surface epitopes of *B. burgdorferi* via RPPDL/NGS

Conformational epitopes are widely believed to predominate over linear epitopes among anti-protein (versus anti-peptide) antibody repertoires (Van Regenmortel, 2014). However, identification of conformational epitopes based on the current protection-associated peptide sequence data was challenging primarily due to the complexity of host immune responses to *B. burgdorferi* infection, which features expression of a wide repertoire of outer surface proteins (Pulzova et al., 2016). Whereas epitope mapping via

phage display may be tractable for a purified monoclonal antibody (Midoro-Horiuti and Goldblum, 2014), it is much less so for polyclonal antibodies. Epitope mapping with polyclonal antibodies is complicated by the possibility of multiple (e.g., overlapping) epitope sequences that occur within each identified antibody-binding protein sequence (Halperin et al., 2011). This is further confounded by the possibility of antibody-selected peptides that constitute mimotopes (Van Regenmortel, 2014). Mimotopes functionally mimic conformational epitopes even without any obvious sequence similarity between corresponding mimotopes and epitopes (Negi and Braun, 2009). Thus, conventional sequence-alignment approaches (e.g., using BLASTP) may fail to identify epitope residues. Mimotope sequences may still successfully be used to map conformational epitopes on a protein of known structure, but only if a set of phage-displayed peptides selected with monoclonal antibodies is provided (Negi and Braun, 2009). However, generalization to polyclonal antibodies against whole proteomes is difficult due to the vast number of possible mimotope-epitope combinations and also the potential of each antibody for binding different epitopes (Van Regenmortel, 2014).

2.6. Conclusions

In summary, the present study shows that VlsE-deleted *B. burgdorferi* can be used as a live attenuated strain to induce protective antibodies against surface epitopes despite the activated VlsE system. Single immunization results in complete prevention of infection by *in vitro*-grown and tick-derived wild type (Rogovskyy and Bankhead, 2013; Rogovskyy et al., 2015). Repeated immunizations protect mice against much more immune-evasive spirochetes. The study also identifies putative linear and conformational

epitopes that are strongly associated with the protection. The data suggest that, during the mammalian infection, the linear putative protection-associated epitopes remain exposed despite the VlsE presence and that their respective peptides may collectively or individually be used for development of subunit vaccine. It is expected that antibodies to these peptides will be effective during the spirochetemic phase of *Borrelia* infection, when the spirochetes have not yet invaded avascular tissues (e.g., joint) but when VlsE is already abundantly expressed. Immunization studies are currently under way to test whether the newly identified putatively epitopes are protective.

2.7. Supplementary Data

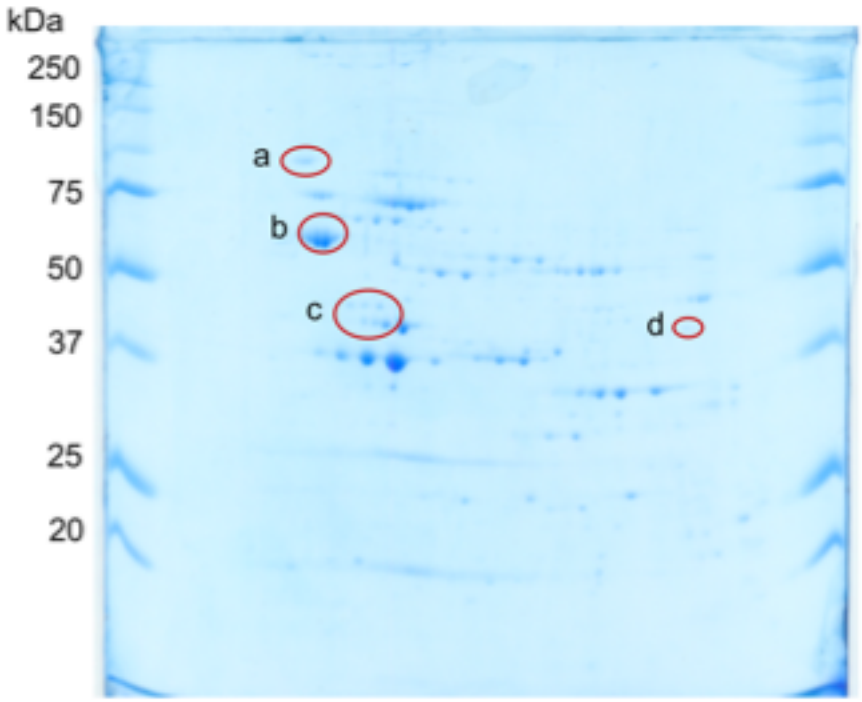

Figure 2.S1 SDS-PAGE of whole cell lysate of in vitro-grown wild-type B31 A3 strain of *B. burgdorferi*. Circles show the spots presumably containing proteins that were reactive to the protective sera and not reactive to the non-protective sera.

Table 2.S1 Sequenced proteins of *B. burgdorferi* B31 excised from sodium dodecyl sulfate slab gels

Accession #	ORF (plasmid #)	Protein name	Protein length (amino acids)
NP_045605.1	BBK32 (lp36)	Fibronectin-binding protein BBK32	354
NP_045688.1	BBA15 (lp54)	Outer surface protein A	273
NP_047003.1	BBB17 (cp26)	Inosine 5-monophosphate dehydrogenase	404
NP_212159.1	BB0025	Transcriptional regulator	243
NP_212203.1	BB0069	Aminopeptidase II	412
NP_212218.1	BB0084	Cysteine desulfurase	422
NP_212256.1	BB0122	Elongation factor Ts	279
NP_212280.1	BBO146	Glycine/betaine ABC transporter ATP-binding protein	372
NP_212281.1	BB0147	Flagellin	336
NP_212471.1	BB0337	Enolase	433
NP_212500.1	BB0366	Aminopeptidase	458
NP_212510.1	BB0376	S-adenosylmethionine synthetase	392
NP_212674.1	BB0540	Elongation factor G	693
NP_212678.1	BB0544	Phosphoribosylpyrophosphate synthetase	406
NP_212692.1	BB0558	Phosphoenolpyruvate-protein phosphatase	573
NP_212701.1	BB0567	Chemotaxis histidine kinase	714
NP_212737.1	BB0603	Integral outer membrane protein P66	618
NP_212744.1	BB0610	Trigger factor	454
NP_212776.1	BB0642	Spermidine/putrescine ABC transporter ATP-binding protein	347
NP_212783.1	BB0649	Chaperonin GroEL	545
NP_212803.1	BB0669	Chemotaxis protein CheA	864

Table 2.S1 Continued

Accession #	ORF (plasmid #)	Protein name	Protein length (amino acids)
NP_212811.1	BB0677	Sugar ABC transporter ATP-binding protein	536
NP_212825.1	BB0691	Elongation factor G	669
NP_212878.1	BB0744	P83/100 antigen	700
NP_212888.1	BB0754	ABC transporter ATP-binding protein	309
NP_212610.2	BB0476	Elongation factor Tu	394
NP_045689.2	BBA16	Outer surface protein B	296
NP_212238.2	BB0104	Periplasmic serine protease DO	474

Table 2.S2 Proteins of *B. burgdorferi* B31 identified in silico via epitope mapping (surface-exposed proteins are excluded and separately presented in Table 2.5)

Accession #	ORF (plasmid #)	Protein name	Protein length (amino acids)
List A			
NP_045426.1	BBE19 (lp25)	Hypothetical protein (PF-32)	252
NP_045475.2	BBG15 (lp28-2)	Hypothetical protein	130
NP_045530.1	BBH40 (lp28-3)	Transposase-like protein	155
NP_045597.1	BBK23 (lp36)	Borrelia ORF-A superfamily	308
NP_045614.1	BBK42 (lp36)	Hypothetical protein	72
NP_045620.1	BBK49 (lp36)	Hypothetical protein	331
NP_045655.1	BBJ31 (lp38)	Hypothetical protein	240
NP_045681.1	BBA08 (lp54)	Hypothetical protein	111
NP_045684.1	BBA11 (lp54)	Hypothetical protein	344
NP_045703.1	BBA30 (lp54)	Hypothetical protein	197
NP_045711.2	BBA38 (lp54)	Phage portal protein	408
NP_045749.1	BBA76 (lp54)	FAD-dependent thymidylate synthase	265
NP_047000.1	BBB14 (cp26)	Hypothetical protein	165
NP_051193.1	BBP32 (cp32-1)	PF-32 protein	246
NP_051245.1	BBS42 (cp32-3)	BapA protein	169
NP_051248.1	BBS45 (cp32-3)	Phage terminase large subunit	450
NP_051249.1	BBR01 (cp32-4)	Hypothetical protein	407
NP_051282.1	BBR36 (cp32-4)	BppA	441
NP_051333.1	BBM42 (cp32-6)	Phage terminase large subunit	450
NP_051377.1	BBO44 (cp32-7)	Phage terminase large subunit	450

Table 2.S2 Continued

Accession #	ORF (plasmid #)	Protein name	Protein length (amino acids)
NP_051409.1	BBL32 (cp32-8)	PF-32 protein	246
NP_051454.1	BBN43 (cp32-9)	Phage terminase large subunit	450
NP_051465.1	BBU11 (lp21)	Sua5/YciO/YrdC/YwlC family protein	330
NP_051502.1	BBQ40 (lp56)	PF-32 protein	251
NP_051505.2	BBQ43 (lp56)	Protein BppA	441
NP_051524.2	BBQ67 (lp56)	Adenine specific DNA methyltransferase	1086
NP_051542.1	BBT06 (lp56)	Sua5/YciO/YrdC/YwlC family protein	330
NP_212145.1	BB0011	Hypothetical protein	279
NP_212165.1	BB0031	Signal peptidase I	326
NP_212170.1	BB0036	DNA topoisomerase IV subunit B	599
NP_212173.1	BB0039	Hypothetical protein	500
NP_212176.1	BB0042	Phosphate-specific transport system accessory protein PhoU	233
NP_212177.1	BB0043	Hypothetical protein	346
NP_212184.1	BB0050	Hypothetical protein	224
NP_212189.1	BB0055	Triosephosphate isomerase	253
NP_212190.1	BB0056	Phosphoglycerate kinase	393
NP_212192.1	BB0058	Hypothetical protein	656
NP_212198.1	BB0064	Methionyl-tRNA formyltransferase	312
NP_212199.2	BB0065	Peptide deformylase	165
NP_212229.1	BB0095	Hypothetical protein	181
NP_212240.2	BB0106	Hypothetical protein	511

Table 2.S2 Continued

Accession #	ORF (plasmid #)	Protein name	Protein length (amino acids)
NP_212262.1	BB0128	Cytidylate kinase	221
NP_212270.1	BB0136	Penicillin-binding protein	629
NP_212279.1	BB0145	Glycine/betaine ABC transporter permease	299
NP_212288.1	BB0154	Protein translocase subunit SecA	899
NP_212298.2	BB0164	K+-dependent Na+/Ca+ exchanger-like protein	328
NP_212300.1	BB0166	4-alpha-glucanotransferase	506
NP_212308.1	BB0174	Hypothetical protein	301
NP_212312.2	BB0178	tRNA uridine 5-carboxymethylaminomethyl modification protein GidA	621
NP_212328.1	BB0194	TatD family hydrolase	269
NP_212345.1	BB0211	DNA mismatch repair protein	610
NP_212355.2	BB0221	Flagellar motor switch protein	405
NP_212362.1	BB0228	Hypothetical protein	971
NP_212364.1	BB0230	Transcription termination factor Rho	515
NP_212371.1	BB0237	Apolipoprotein N-acyltransferase	521
NP_212385.1	BB0251	Leucine-tRNA ligase	840
NP_212388.1	BB0254	Single-stranded-DNA-specific exonuclease	708
NP_212389.2	BB0255	M23 peptidase domain-containing protein	314
NP_212396.1	BB0262	M23 peptidase domain-containing protein	417
NP_212398.2	BB0264	Heat shock protein 70	489
NP_212401.1	BB0267	Hypothetical protein	634
NP_212405.1	BB0271	Flagellar biosynthesis protein FlhA	697

Table 2.S2 Continued

Accession #	ORF (plasmid #)	Protein name	Protein length (amino acids)
NP_212406.1	BB0272	Flagellar biosynthesis protein FlhB	372
NP_212409.1	BB0275	Flagellar biosynthesis protein FliP	254
NP_212427.1	BB0293	Flagellar basal body rod protein FlgC	152
NP_212429.2	BB0295	ATP-dependent protease ATPase subunit HslU	448
NP_212434.1	BB0300	Cell division protein FtsA	413
NP_212443.2	BB0309	Hypothetical protein	252
NP_212447.2	BB0313	rRNA large subunit methyltransferase	189
NP_212459.1	BB0325	Hypothetical protein	369
NP_212461.1	BB0327	Glycerol-3-phosphate O-acyltransferase	298
NP_212462.2	BB0328	Family 5 extracellular solute-binding protein (OppA1)	523
NP_212464.1	BB0330	Peptide ABC transporter substrate-binding protein (OppA3)	541
NP_212473.1	BB0339	50S ribosomal protein L13	146
NP_212475.1	BB0341	Aspartyl/glutamyl-tRNA(Asn/Gln) amidotransferase subunit B	485
NP_212476.2	BB0342	Glutamyl-tRNA(Gln) amidotransferase subunit A	481
NP_212492.1	BB0358	rRNA small subunit methyltransferase E	243
NP_212506.1	BB0372	Glutamate-tRNA ligase	490
NP_212517.1	BB0383	Basic membrane protein A (bmpA)	339
NP_212519.2	BB0385	Basic membrane protein D (bmpD)	341
NP_212532.1	BB0398	Lipoprotein	343

Table 2.S2 Continued

Accession #	ORF (plasmid #)	Protein name	Protein length (amino acids)
NP_212536.1	BB0402	Proline-tRNA ligase	488
NP_212537.2	BB0403	Hypothetical protein	201
NP_212540.1	BB0406	Hypothetical protein	203
NP_212553.1	BB0419	Response regulator	307
NP_212554.1	BB0420	Sensory transduction histidine kinase	1494
NP_212568.1	BB0434	Chromosome-partitioning protein ParB	260
NP_212570.2	BB0436	DNA gyrase subunit B	634
NP_212578.1	BB0444	Nucleotide sugar epimerase	355
NP_212602.1	BB0468	Hypothetical protein	248
NP_212618.1	BB0484	30S ribosomal protein S3	293
NP_212646.1	BB0512	Hypothetical protein	2166
NP_212652.1	BB0518	Chaperone protein DnaK	635
NP_212660.1	BB0526	Hypothetical protein	607
NP_212668.1	BB0534	Exodeoxyribonuclease III	255
NP_212674.1	BB0540	Elongation factor G	693
NP_212682.1	BB0548	DNA polymerase I	908
NP_212692.1	BB0558	Phosphoenolpyruvate-protein phosphatase	573
NP_212694.2	BB0560	Chaperone protein HtpG	616
NP_212697.2	BB0563	Hypothetical protein	172
NP_212702.1	BB0568	Chemotaxis response regulator	385
NP_212713.1	BB0579	DNA polymerase III subunit alpha	1161
NP_212714.1	BB0580	Integral membrane protein	192

Table 2.S2 Continued

Accession #	ORF (plasmid #)	Protein name	Protein length (amino acids)
NP_212715.1	BB0581	ATP-dependent DNA helicase RecG	686
NP_212721.1	BB0587	Methionine-tRNA ligase	734
NP_212727.1	BB0593	Long-chain-fatty-acid CoA ligase	645
NP_212728.2	BB0594	Arginine-tRNA ligase	585
NP_212735.1	BB0601	Serine hydroxymethyltransferase	417
NP_212741.1	BB0607	ATP-dependent DNA helicase	659
NP_212747.2	BB0613	ATP-dependent protease La	796
NP_212749.2	BB0615	30S ribosomal protein S4	208
NP_212751.1	BB0617	Hypothetical protein	122
NP_212756.2	BB0622	Acetate kinase	405
NP_212757.1	BB0623	Transcription-repair coupling factor	1125
NP_212758.1	BB0624	Hypothetical protein	320
NP_212764.1	BB0630	1-phosphofructokinase	307
NP_212766.1	BB0632	Exodeoxyribonuclease V subunit alpha	610
NP_212770.1	BB0636	Glucose-6-phosphate 1-dehydrogenase	478
NP_212772.1	BB0638	Na+/H+ antiporter	462
NP_212774.1	BB0640	Spermidine/putrescine ABC transporter permease	263
NP_212776.1	BB0642	Spermidine/putrescine ABC transporter ATP- binding protein	347
NP_212781.1	BB0647	Oxidative stress regulator BosR	176
NP_212788.1	BB0654	Hypothetical protein	380
NP_212803.1	BB0669	Chemotaxis protein CheA	864

Table 2.S2 Continued

Accession #	ORF (plasmid #)	Protein name	Protein length (amino acids)
NP_212810.1	BB0676	Phosphoglycolate phosphatase	220
NP_212843.1	BB0709	Hypothetical protein	343
NP_212846.1	BB0712	RNA polymerase sigma factor RpoD	631
NP_212848.1	BB0714	Hypothetical protein	322
NP_212850.2	BB0716	Rod shape-determining protein MreC	258
NP_212852.2	BB0718	Penicillin-binding protein	570
NP_212869.2	BB0735	Rare lipoprotein A	262
NP_212876.2	BB0742	ABC transporter ATP-binding protein	543
NP_212879.2	BB0745	Endonuclease III	211
NP_212883.2	BB0749	Hypothetical protein	424
NP_212889.1	BB0755	Ribonuclease Z	319
NP_212931.1	BB0797	DNA mismatch repair protein MutS	862
NP_212939.2	BB0805	Polyribonucleotide nucleotidyltransferase	716
NP_212950.2	BB0816	Hypothetical protein	315
NP_212952.1	BB0818	Hypothetical protein	288
NP_212961.1	BB0827	ATP-dependent helicase	823
NP_212962.1	BB0828	DNA topoisomerase I	848
NP_212963.1	BB0829	Exonuclease SbcD	413
NP_212971.1	BB0837	Excinuclease ABC subunit A	950
NP_212974.1	BB0840	Lipoprotein	538
NP_212975.1	BB0841	Arginine deiminase	410
YP_008686554.1	BB0020	Diphosphate-fructose-6-phosphate 1- phosphotransferase	555

Table 2.S2 Continued

Accession #	ORF (plasmid #)	Protein name	Protein length (amino acids)
YP_008686555.1	BB0038	Hypothetical protein	505
YP_008686561.1	BB0149	Flagellar hook-associated protein FliD	665
YP_008686563.1	BB0181	Flagellar hook-associated protein FlgK	627
YP_008686564.1	BB0182	Flagellar hook-associated protein FlgL	424
YP_008686566.1	BB0196	Peptide chain release factor 1	357
YP_008686570.1	BB0252	Hypothetical protein	767
YP_008686575.1	BB0432	Hypothetical protein	237
YP_008686580.1	BB0515	Thioredoxin reductase	326
YP_008686582.1	BB0573	ABC transporter ATP-binding protein	268
YP_008686583.1	BB0589	Phosphate acetyltransferase	352
YP_008686586.1	BB0720	Threonine-tRNA ligase	581
YP_008686590.1	BB0752	Hypothetical protein	502
List B			
NP_045458.1	BBF25(lp28-1)	Hypothetical protein	186
NP_045648.1	BBJ24 (lp38)	Hypothetical protein	260
NP_045649.2	BBJ25 (lp38)	Hypothetical protein	346
NP_045650.1	BBJ26(lp38)	ABC transporter ATP-binding protein	231
NP_045707.1	BBA34 (lp54)	Extracellular solute-binding protein, family 5	529
NP_045720.1	lp54(BBA47)	Hypothetical protein	140
NP_046989.1	cp26(BBB03)	Telomere resolvase ResT	449
NP_046990.2	cp26(BBB04)	Chitibiose transporter protein ChbC (aka Permease II C component)	440

Table 2.S2 Continued

Accession #	ORF (plasmid #)	Protein name	Protein length (amino acids)
NP_047002.1	BBB16(cp26)	Oligopeptide ABC transporter OppAIV	530
NP_051349.1	BBO16(cp32-7)	Hypothetical protein	213
NP_051512.1	BBQ50(lp56)	Phage terminase large subunit	450
NP_051521.1	BBQ62(lp56)	Hypothetical protein	124
NP_051540.1	lp5(BBT03)	Hypothetical protein	122
NP_212146.1	BB0012	tRNA pseudouridine synthase A	246
NP_212148.1	BB0014	Primosomal protein N	660
NP_212166.1	BB0032	Hypothetical protein	490
NP_212171.1	BB0037	1-acyl-sn-glycerol-3-phosphate acyltransferase	250
NP_212206.1	BB0072	Membrane protein	773
NP_212216.1	BB0082	Hypothetical protein	432
NP_212222.1	BB0088	Elongation factor EF-4	559
NP_212266.1	BB0132	Transcription elongation factor GreA	901
NP_212271.1	BB0137	Long-chain-fatty-acid CoA ligase	630
NP_212313.1	BB0179	tRNA modification GTPase	464
NP_212319.1	NP2	Glycoprotease family protein	217
NP_212350.1	BB0216	Phosphate ABC transporter permease PstC	302
NP_212359.1	BB0225	tRNA-dihydrouridine synthase A	335
NP_212368.1	BB0234	Integral membrane protein	275
NP_212369.1	BB0235	Ribosome-binding ATPase	368
NP_212374.1	BB0240	Glycerol uptake facilitator	254
NP_212375.1	BB0241	Glycerol kinase	501

Table 2.S2 Continued

Accession #	ORF (plasmid #)	Protein name	Protein length (amino acids)
NP_212379.1	BB0245	Hypothetical protein	184
NP_212457.1	BB0323	Hypothetical protein	377
NP_212460.1	BB0326	Hypothetical protein	931
NP_212485.2	BB0351	Hypothetical protein	521
NP_212497.1	BB0363	Hypothetical protein	670
NP_212504.1	BB0370	Tyrosine-tRNA ligase	405
NP_212505.1	BB0371	Glycine-tRNA ligase	445
NP_212515.1	BB0381	Hypothetical protein	475
NP_212522.1	BB0388	DNA-directed RNA polymerase subunit beta'	1377
NP_212534.1	BB0400	Hypothetical protein	516
NP_212550.1	BB0416	Pheromone shutdown protein	404
NP_212551.1	BB0417	Adenylate kinase	211
NP_212561.2	BB0427	rRNA small subunit methyltransferase	255
NP_212569.1	BB0435	DNA gyrase subunit A	810
NP_212606.2	BB0472	UDP-N-acetylglucosamine 1- carboxyvinyltransferase	427
NP_212651.1	BB0517	Chaperone protein DnaJ	364
NP_212658.1	BB0524	Inositol monophosphatase	285
NP_212669.1	BB0535	Hypothetical protein	257
NP_212678.1	BB0544	Phosphoribosylpyrophosphate synthetase	406
NP_212691.1	BB0557	Phosphocarrier protein HPr	86
NP_212701.1	BB0567	Chemotaxis histidine kinase	714
NP_212725.1	BB0591	Competence locus E	416
NP_212733.1	BB0599	Cysteine-tRNA ligase	480
NP_212778.1	BB0644	N-acetylmannosamine-6-phosphate 2-epimerase	232

Table 2.S2 Continued

Accession #	ORF (plasmid #)	Protein name	Protein length (amino acids)
NP_212790.1	BB0656	Oxygen-independent coproporphyrinogen III oxidase	377
NP_212792.2	BB0658	2,3-bisphosphoglycerate-dependent phosphoglycerate mutase	248
NP_212818.2	BB0684	Isopentenyl-diphosphate delta-isomerase	354
NP_212821.1	BB0687	Phosphomevalonate kinase	317
NP_212827.1	BB0693	Xylose operon regulatory protein	402
NP_212839.2	BB0705	Ribonuclease III	245
NP_212860.1	BB0726	ATP-binding protein	323
NP_212862.2	BB0728	CoA-disulfide reductase	443
NP_212866.1	BB0732	Penicillin-binding protein	932
NP_212872.1	BB0738	Valine-tRNA ligase	875
NP_212877.1	BB0743	Hypothetical protein	565
NP_212882.1	BB0748	Hypothetical protein	152
NP_212903.1	BB0769	tRNA N6-adenosine threonylcarbamoyltransferase	346
NP_212917.1	BB0783	Hypothetical protein	394
NP_212920.2	BB0786	50S ribosomal protein L25/general stress protein Ctc	182
NP_212925.1	BB0791	Thymidine kinase	367
NP_212948.1	BB0814	Sodium/panthothenate symporter	444
NP_212959.2	BB0825	Hypothetical protein	215
NP_212964.2	BB0830	Exonuclease SbcC	929
NP_212977.2	BB0843	Arginine-ornithine antiporter (ArcD)	474

Table 2.S2 Continued

Accession #	ORF (plasmid #)	Protein name	Protein length (amino acids)
YP_008686571.1	BB0329	ABC transporter substrate-binding protein	528
YP_008853940.1	BB0257	DNA translocase FtsK	787
YP_008853942.1	BB0553	Hypothetical protein	497

2.8. References

1. Rizzoli A, Hauffe H, Carpi G, Vourc HG, Neteler M, Rosa R. 2011. Lyme borreliosis in Europe. Euro Surveill 16.
2. Hinckley AF, Connally NP, Meek JI, Johnson BJ, Kemperman MM, Feldman KA, White JL, Mead PS. 2014. Lyme disease testing by large commercial laboratories in the United States. Clin Infect Dis 59:676-681.
3. Borchers AT, Keen CL, Huntley AC, Gershwin ME. 2015. Lyme disease: a rigorous review of diagnostic criteria and treatment. J Autoimmun 57:82-115.
4. Setubal JC, Reis M, Matsunaga J, Haake DA. 2006. Lipoprotein computational prediction in spirochaetal genomes. Microbiology 152:113-121.
5. Dowdell AS, Murphy MD, Azodi C, Swanson SK, Florens L, Chen S, Zuckert WR. 2017. Comprehensive spatial analysis of the *Borrelia burgdorferi* lipoproteome reveals a compartmentalization bias toward the bacterial surface. J Bacteriol 199.
6. Alva V, Nam SZ, Soding J, Lupas AN. 2016. The MPI bioinformatics Toolkit as an integrative platform for advanced protein sequence and structure analysis. Nucleic Acids Res 44:W410-415.
7. Kenedy MR, Lenhart TR, Akins DR. 2012. The role of *Borrelia burgdorferi* outer surface proteins. FEMS Immunol Med Microbiol doi:10.1111/j.1574-695X.2012.00980.x.
8. Fraser CM, Casjens S, Huang WM, Sutton GG, Clayton R, Lathigra R, White O, Ketchum KA, Dodson R, Hickey EK, Gwinn M, Dougherty B, Tomb JF,

Fleischmann RD, Richardson D, Peterson J, Kerlavage AR, Quackenbush J, Salzberg S, Hanson M, van Vugt R, Palmer N, Adams MD, Gocayne J, Weidman J, Utterback T, Watthey L, McDonald L, Artiach P, Bowman C, Garland S, Fujii C, Cotton MD, Horst K, Roberts K, Hatch B, Smith HO, Venter JC. 1997. Genomic sequence of a Lyme disease spirochaete, *Borrelia burgdorferi*. Nature 390:580-586.

9. Norris SJ. 2014. The *vls* antigenic variation systems of Lyme disease *Borrelia*: eluding host immunity through both random, segmental gene conversion and framework heterogeneity. Microbiol Spectr 2:doi: 10.1128/microbiolspec.MDNA1123-0038-2014.

10. Zhang JR, Hardham JM, Barbour AG, Norris SJ. 1997. Antigenic variation in Lyme disease borreliae by promiscuous recombination of VMP-like sequence cassettes. Cell 89:275-285.

11. Norris SJ. 2006. Antigenic variation with a twist - the *Borrelia* story. Mol Microbiol 60:1319-1322.

12. Purser JE, Norris SJ. 2000. Correlation between plasmid content and infectivity in *Borrelia burgdorferi*. Proc Natl Acad Sci U S A 97:13865-13870.

13. Labandeira-Rey M, Skare JT. 2001. Decreased infectivity in *Borrelia burgdorferi* strain B31 is associated with loss of linear plasmid 25 or 28-1. Infect Immun 69:446-455.

14. Labandeira-Rey M, Seshu J, Skare JT. 2003. The absence of linear plasmid 25 or 28-1 of *Borrelia burgdorferi* dramatically alters the kinetics of experimental infection via distinct mechanisms. Infect Immun 71:4608-4613.

15. Iyer R, Kalu O, Purser J, Norris S, Stevenson B, Schwartz I. 2003. Linear and circular plasmid content in *Borrelia burgdorferi* clinical isolates. Infect Immun 71:3699-3706.

16. Lawrenz MB, Wooten RM, Norris SJ. 2004. Effects of *vlsE* complementation on the infectivity of *Borrelia burgdorferi* lacking the linear plasmid lp28-1. Infect Immun 72:6577-6585.

17. Bankhead T, Chaconas G. 2007. The role of VlsE antigenic variation in the Lyme disease spirochete: persistence through a mechanism that differs from other pathogens. Mol Microbiol 65:1547-1558.

18. Rogovskyy AS, Bankhead T. 2013. Variable VlsE is critical for host reinfection by the Lyme disease spirochete. PLoS One 8:e61226.

19. Liang FT, Jacobs MB, Bowers LC, Philipp MT. 2002. An immune evasion mechanism for spirochetal persistence in Lyme borreliosis. J Exp Med 195:415-422.

20. Philipp MT, Bowers LC, Fawcett PT, Jacobs MB, Liang FT, Marques AR, Mitchell PD, Purcell JE, Ratterree MS, Straubinger RK. 2001. Antibody response to IR6, a conserved immunodominant region of the VlsE lipoprotein, wanes rapidly after antibiotic treatment of *Borrelia burgdorferi* infection in experimental animals and in humans. J Infect Dis 184:870-878.

21. Palmer GH, Bankhead T, Seifert HS. 2016. Antigenic variation in bacterial pathogens. Microbiol Spectr 4.

22. Liang FT, Alvarez AL, Gu Y, Nowling JM, Ramamoorthy R, Philipp MT. 1999. An immunodominant conserved region within the variable domain of VlsE, the variable surface antigen of *Borrelia burgdorferi*. J Immunol 163:5566-5573.

23. Elsner RA, Hastey CJ, Olsen KJ, Baumgarth N. 2015. Suppression of long-lived humoral immunity following *Borrelia burgdorferi* infection. PLoS Pathog 11:e1004976.

24. Rogovskyy AS, Gillis DC, Ionov Y, Gerasimov E, Zelikovsky A. 2017. Antibody response to Lyme disease spirochetes in the context of VlsE-mediated immune evasion. Infect Immun 85:1 e00890-00816.

25. Rogovskyy AS, Bankhead T. 2014. Bacterial heterogeneity is a requirement for host superinfection by the Lyme disease spirochete. Infect Immun 82:4542-4552.

26. Barthold SW, Fikrig E, Bockenstedt LK, Persing DH. 1995. Circumvention of outer surface protein A immunity by host-adapted *Borrelia burgdorferi*. Infect Immun 63:2255-2261.

27. Laemmli UK. 1970. Cleavage of structural proteins during the assembly of the head of bacteriophage T4. Nature 227:680-685.

28. Wessel D, Flugge UI. 1984. A method for the quantitative recovery of protein in dilute solution in the presence of detergents and lipids. Anal Biochem 138:141-143.

29. Mozdzanowski J, Hembach P, Speicher DW. 1992. High yield electroblotting onto polyvinylidene difluoride membranes from polyacrylamide gels. Electrophoresis 13:59-64.

30. Shevchenko A, Tomas H, Havlis J, Olsen JV, Mann M. 2006. In-gel digestion for mass spectrometric characterization of proteins and proteomes. Nat Protoc 1:2856-2860.

31. Craig R, Beavis RC. 2003. A method for reducing the time required to match protein sequences with tandem mass spectra. Rapid Commun Mass Spectrom 17:2310-2316.

32. Nesvizhskii AI, Keller A, Kolker E, Aebersold R. 2003. A statistical model for identifying proteins by tandem mass spectrometry. Anal Chem 75:4646-4658.

33. Searle BC, Turner M, Nesvizhskii AI. 2008. Improving sensitivity by probabilistically combining results from multiple MS/MS search methodologies. J Proteome Res 7:245-253.

34. Keller A, Nesvizhskii AI, Kolker E, Aebersold R. 2002. Empirical statistical model to estimate the accuracy of peptide identifications made by MS/MS and database search. Anal Chem 74:5383-5392.

35. Searle BC. 2010. Scaffold: a bioinformatic tool for validating MS/MS-based proteomic studies. Proteomics 10:1265-1269.

36. Liu X, Hu Q, Liu S, Tallo LJ, Sadzewicz L, Schettine CA, Nikiforov M, Klyushnenkova EN, Ionov Y. 2013. Serum antibody repertoire profiling using *in silico* antigen screen. PLoS One 8:e67181.

37. Camacho C, Coulouris G, Avagyan V, Ma N, Papadopoulos J, Bealer K, Madden TL. 2009. BLAST+: architecture and applications. BMC Bioinformatics 10:421.

38. Altschul SF, Madden TL, Schaffer AA, Zhang J, Zhang Z, Miller W, Lipman DJ. 1997. Gapped BLAST and PSI-BLAST: a new generation of protein database search programs. Nucleic Acids Res 25:3389-3402.

39. Ryvkin A, Ashkenazy H, Smelyanski L, Kaplan G, Penn O, Weiss-Ottolenghi Y, Privman E, Ngam PB, Woodward JE, May GD, Bell C, Pupko T, Gershoni JM. 2012. Deep panning: steps towards probing the IgOme. PLoS One 7:e41469.

40. Vita R, Overton JA, Greenbaum JA, Ponomarenko J, Clark JD, Cantrell JR, Wheeler DK, Gabbard JL, Hix D, Sette A, Peters B. 2015. The immune epitope database (IEDB) 3.0. Nucleic Acids Res 43:D405-412.

41. Caoili SE. 2010. Benchmarking B-cell epitope prediction for the design of peptide-based vaccines: problems and prospects. J Biomed Biotechnol 2010:910524.

42. Liang FT, Yan J, Mbow ML, Sviat SL, Gilmore RD, Mamula M, Fikrig E. 2004. *Borrelia burgdorferi* changes its surface antigenic expression in response to host immune responses. Infect Immun 72:5759-5767.

43. Rogovskyy AS, Casselli T, Tourand Y, Jones CR, Owen JP, Mason KL, Scoles GA, Bankhead T. 2015. Evaluation of the importance of VlsE antigenic variation for the enzootic cycle of *Borrelia burgdorferi*. PLoS One 10:e0124268.

44. Vieira P, Rajewsky K. 1988. The half-lives of serum immunoglobulins in adult mice. Eur J Immunol 18:313-316.

45. Probert WS, Johnson BJ. 1998. Identification of a 47 kDa fibronectin-binding protein expressed by *Borrelia burgdorferi* isolate B31. Mol Microbiol 30:1003-1015.

46. Szczepanski A, Furie M, Benach J, Lane B, Fleit H. 1990. Interaction between *Borrelia burgdorferi* and endothelium *in vitro*. J Clin Invest 85:1637-1647.

47. Toledo A, Coleman JL, Kuhlow CJ, Crowley JT, Benach JL. 2012. The enolase of *Borrelia burgdorferi* is a plasminogen receptor released in outer membrane vesicles. Infect Immun 80:359-368.

48. Floden AM, Watt JA, Brissette CA. 2011. *Borrelia burgdorferi* enolase is a surface-exposed plasminogen binding protein. PLoS One 6:e27502.

49. Nogueira SV, Smith AA, Qin JH, Pal U. 2012. A surface enolase participates in *Borrelia burgdorferi*-plasminogen interaction and contributes to pathogen survival within feeding ticks. Infect Immun 80:82-90.

50. Carrasco SE, Yang Y, Troxell B, Yang X, Pal U, Yang XF. 2015. *Borrelia burgdorferi* elongation factor EF-Tu is an immunogenic protein during Lyme borreliosis. Emerg Microbes Infect 4:e54.

51. Rabilloud T. 2009. Membrane proteins and proteomics: love is possible, but so difficult. Electrophoresis 30 Suppl 1:S174-180.

52. Zhou S, Bailey MJ, Dunn MJ, Preedy VR, Emery PW. 2005. A quantitative investigation into the losses of proteins at different stages of a two-dimensional gel electrophoresis procedure. Proteomics 5:2739-2747.

53. Li H, Dunn JJ, Luft BJ, Lawson CL. 1997. Crystal structure of Lyme disease antigen outer surface protein A complexed with an Fab. Proc Natl Acad Sci U S A 94:3584-3589.

54. Ding W, Huang X, Yang X, Dunn JJ, Luft BJ, Koide S, Lawson CL. 2000. Structural identification of a key protective B-cell epitope in Lyme disease antigen OspA. J Mol Biol 302:1153-1164.

55. Becker M, Bunikis J, Lade BD, Dunn JJ, Barbour AG, Lawson CL. 2005. Structural investigation of *Borrelia burgdorferi* OspB, a bactericidal Fab target. J Biol Chem 280:17363-17370.

56. Huang X, Yang X, Luft BJ, Koide S. 1998. NMR identification of epitopes of Lyme disease antigen OspA to monoclonal antibodies. J Mol Biol 281:61-67.

57. Legros V, Jolivet-Reynaud C, Battail-Poirot N, Saint-Pierre C, Forest E. 2000. Characterization of an anti-*Borrelia* burgdorferi OspA conformational epitope by limited proteolysis of monoclonal antibody-bound antigen and mass spectrometric peptide mapping. Protein Sci 9:1002-1010.

58. Ma J, Gingrich-Baker C, Franchi PM, Bulger P, Coughlin RT. 1995. Molecular analysis of neutralizing epitopes on outer surface proteins A and B of *Borrelia burgdorferi*. Infect Immun 63:2221-2227.

59. Izac JR, Oliver LD, Jr., Earnhart CG, Marconi RT. 2017. Identification of a defined linear epitope in the OspA protein of the Lyme disease spirochetes that elicits bactericidal antibody responses: Implications for vaccine development. Vaccine 35:3178-3185.

60. Sadziene A, Jonsson M, Bergstrom S, Bright RK, Kennedy RC, Barbour AG. 1994. A bactericidal antibody to *Borrelia burgdorferi* is directed against a variable region of the OspB protein. Infect Immun 62:2037-2045.

61. Buckles EL, Earnhart CG, Marconi RT. 2006. Analysis of antibody response in humans to the type A OspC loop 5 domain and assessment of the potential utility of the loop 5 epitope in Lyme disease vaccine development. Clin Vaccine Immunol 13:1162-1165.

62. Pulzova L, Flachbartova Z, Bencurova E, Potocnakova L, Comor L, Schreterova E, Bhide M. 2016. Identification of B-cell epitopes of *Borrelia burgdorferi* outer surface protein C by screening a phage-displayed gene fragment library. Microbiol Immunol 60:669-677.

63. Mathiesen MJ, Christiansen M, Hansen K, Holm A, Asbrink E, Theisen M. 1998. Peptide-based OspC enzyme-linked immunosorbent assay for serodiagnosis of Lyme borreliosis. J Clin Microbiol 36:3474-3479.

64. Yang X, Li Y, Dunn JJ, Luft BJ. 2006. Characterization of a unique borreliacidal epitope on the outer surface protein C of *Borrelia burgdorferi*. FEMS Immunol Med Microbiol 48:64-74.

65. Coutte L, Botkin DJ, Gao L, Norris SJ. 2009. Detailed analysis of sequence changes occurring during *vlsE* antigenic variation in the mouse model of *Borrelia burgdorferi* infection. PLoS Pathog 5:e1000293.

66. Indest KJ, Howell JK, Jacobs MB, Scholl-Meeker D, Norris SJ, Philipp MT. 2001. Analysis of *Borrelia burgdorferi vlsE* gene expression and recombination in the tick vector. Infect Immun 69:7083-7090.

67. Crother TR, Champion CI, Whitelegge JP, Aguilera R, Wu XY, Blanco DR, Miller JN, Lovett MA. 2004. Temporal analysis of the antigenic composition of *Borrelia burgdorferi* during infection in rabbit skin. Infect Immun 72:5063-5072.

68. Ohnishi J, Schneider B, Messer WB, Piesman J, de Silva AM. 2003. Genetic variation at the *vlsE* locus of *Borrelia burgdorferi* within ticks and mice over the course of a single transmission cycle. J Bacteriol 185:4432-4441.

69. Shrestha B, Kenedy MR, Akins DR. 2017. Outer membrane proteins BB0405 and BB0406 are immunogenic, but only BB0405 Is required for *Borrelia burgdorferi* infection. Infect Immun 85.

70. Kung F, Kaur S, Smith AA, Yang X, Wilder CN, Sharma K, Buyuktanir O, Pal U. 2016. A *Borrelia burgdorferi* surface-exposed transmembrane protein lacking detectable immune responses supports pathogen persistence and constitutes a vaccine target. J Infect Dis 213:1786-1795.

71. Brooks CS, Vuppala SR, Jett AM, Akins DR. 2006. Identification of *Borrelia burgdorferi* outer surface proteins. Infect Immun 74:296-304.

72. Knowles TJ, Scott-Tucker A, Overduin M, Henderson IR. 2009. Membrane protein architects: the role of the BAM complex in outer membrane protein assembly. Nat Rev Microbiol 7:206-214.

73. Lenhart TR, Akins DR. 2010. *Borrelia burgdorferi* locus BB0795 encodes a BamA orthologue required for growth and efficient localization of outer membrane proteins. Mol Microbiol 75:692-709.

74. Bunikis I, Denker K, Ostberg Y, Andersen C, Benz R, Bergstrom S. 2008. An RND-type efflux system in *Borrelia burgdorferi* is involved in virulence and resistance to antimicrobial compounds. PLoS Pathog 4:e1000009.

75. Tusnady GE, Simon I. 2001. The HMMTOP transmembrane topology prediction server. Bioinformatics 17:849-850.

76. Noppa L, Ostberg Y, Lavrinovicha M, Bergstrom S. 2001. P13, an integral membrane protein of *Borrelia burgdorferi*, is C-terminally processed and contains surface-exposed domains. Infect Immun 69:3323-3334.

77. Pinne M, Ostberg Y, Comstedt P, Bergstrom S. 2004. Molecular analysis of the channel-forming protein P13 and its paralogue family 48 from different Lyme disease *Borrelia* species. Microbiology 150:549-559.

78. Ostberg Y, Pinne M, Benz R, Rosa P, Bergstrom S. 2002. Elimination of channel-forming activity by insertional inactivation of the p13 gene in *Borrelia burgdorferi*. J Bacteriol 184:6811-6819.

79. Sadziene A, Thomas DD, Barbour AG. 1995. *Borrelia burgdorferi* mutant lacking Osp: biological and immunological characterization. Infect Immun 63:1573-1580.

80. Antonara S, Chafel RM, LaFrance M, Coburn J. 2007. *Borrelia burgdorferi* adhesins identified using *in vivo* phage display. Mol Microbiol 66:262-276.

81. Yang X, Coleman AS, Anguita J, Pal U. 2009. A chromosomally encoded virulence factor protects the Lyme disease pathogen against host-adaptive immunity. PLoS Pathog 5:e1000326.

82. Nowalk AJ, Gilmore RD, Jr., Carroll JA. 2006. Serologic proteome analysis of *Borrelia burgdorferi* membrane-associated proteins. Infect Immun 74:3864-3873.

83. Gilmore RD, Jr., Howison RR, Schmit VL, Nowalk AJ, Clifton DR, Nolder C, Hughes JL, Carroll JA. 2007. Temporal expression analysis of the *Borrelia burgdorferi* paralogous gene family 54 genes BBA64, BBA65, and BBA66 during persistent infection in mice. Infect Immun 75:2753-2764.

84. Gilmore RD, Jr., Kappel KJ, Johnson BJ. 1997. Molecular characterization of a 35-kilodalton protein of *Borrelia burgdorferi*, an antigen of diagnostic importance in early Lyme disease. J Clin Microbiol 35:86-91.

85. Barbour AG, Jasinskas A, Kayala MA, Davies DH, Steere AC, Baldi P, Felgner PL. 2008. A genome-wide proteome array reveals a limited set of immunogens in natural infections of humans and white-footed mice with *Borrelia burgdorferi*. Infect Immun 76:3374-3389.

86. Gilmore RD, Jr., Mbow ML, Stevenson B. 2001. Analysis of *Borrelia burgdorferi* gene expression during life cycle phases of the tick vector *Ixodes scapularis*. Microbes Infect 3:799-808.

87. Tokarz R, Anderton JM, Katona LI, Benach JL. 2004. Combined effects of blood and temperature shift on *Borrelia burgdorferi* gene expression as determined by whole genome DNA array. Infect Immun 72:5419-5432.

88. Gilmore RD, Jr., Howison RR, Dietrich G, Patton TG, Clifton DR, Carroll JA. 2010. The *bba64* gene of *Borrelia burgdorferi*, the Lyme disease agent, is critical for mammalian infection via tick bite transmission. Proc Natl Acad Sci U S A 107:7515-7520.

89. Brangulis K, Tars K, Petrovskis I, Kazaks A, Ranka R, Baumanis V. 2013. Structure of an outer surface lipoprotein BBA64 from the Lyme disease agent *Borrelia burgdorferi* which is critical to ensure infection after a tick bite. Acta Crystallogr D Biol Crystallogr 69:1099-1107.

90. Labandeira-Rey M, Baker EA, Skare JT. 2001. VraA (BBI16) protein of *Borrelia burgdorferi* is a surface-exposed antigen with a repetitive motif that confers partial protection against experimental Lyme borreliosis. Infect Immun 69:1409-1419.

91. Van Regenmortel MH. 2014. Specificity, polyspecificity, and heterospecificity of antibody-antigen recognition. J Mol Recognit 27:627-639.

92. Midoro-Horiuti T, Goldblum RM. 2014. Epitope mapping with random phage display library. Methods Mol Biol 1131:477-484.

93. Halperin RF, Stafford P, Johnston SA. 2011. Exploring antibody recognition of sequence space through random-sequence peptide microarrays. Mol Cell Proteomics 10:M110 000786.

94. Negi SS, Braun W. 2009. Automated detection of conformational epitopes using phage display peptide sequences. Bioinform Biol Insights 3:71-81.

95. Hughes JL, Nolder CL, Nowalk AJ, Clifton DR, Howison RR, Schmit VL, Gilmore RD, Jr., Carroll JA. 2008. *Borrelia burgdorferi* surface-localized proteins expressed during persistent murine infection are conserved among diverse *Borrelia* spp. Infect Immun 76:2498-2511.

96. El-Hage N, Babb K, Carroll JA, Lindstrom N, Fischer ER, Miller JC, Gilmore RD, Jr., Mbow ML, Stevenson B. 2001. Surface exposure and protease insensitivity of *Borrelia burgdorferi* Erp (OspEF-related) lipoproteins. Microbiology 147:821-830.

97. Shandilya S, Kurt Yilmaz N, Sadowski A, Monir E, Schiller ZA, Thomas WD, Jr., Klempner MS, Schiffer CA, Wang Y. 2017. Structural and molecular analysis of a protective epitope of Lyme disease antigen OspA and antibody interactions. J Mol Recognit 30.

98. Earnhart CG, Buckles EL, Marconi RT. 2007. Development of an OspC-based tetravalent, recombinant, chimeric vaccinogen that elicits bactericidal antibody against diverse Lyme disease spirochete strains. Vaccine 25:466-480.

3. NEW ZEALAND WHITE RABBITS EFFECTIVELY CLEAR *BORRELIA BURGDORFERI* B31 DESPITE THE BACTERIA'S FUNCTIONAL *VLSE* ANTIGENIC VARIATION SYSTEM[2*]

Maliha Batool[1], Andrew E Hillouse[2], Yurij Ionov[5], Kelli J Kochan[2], Fatemeh Mohebbi[4], George Stoica[1], David W Threadgill[1 2 5], Alex Zelikovsky[4 6], Suryakant D Waghela[1], Dominique J Wiener[1], Artem S Rogovskyy[1]

1. Department of Veterinary Pathobiology, College of Veterinary Medicine and Biomedical Sciences, Texas A&M University, College Station, Texas, USA.
2. Texas A&M Institute for Genomics Sciences and Society, Texas A&M University, College Station, Texas, USA.
3. Department of Cancer Genetics, Roswell Park Cancer Institute, Buffalo, New York, USA.
4. Department of Computer Science, Georgia State University, Atlanta, Georgia, USA.
5. Department of Molecular and Cellular Medicine, Texas A&M University, College Station, Texas, USA.

---

[2]*Reprinted with permission from "New Zealand White rabbits effectively clear *Borrelia burgdorferi* B31 despite the bacterium's functional *vlsE* antigenic variation system" by Batool M., Hillhouse A.E., Ionov Y., Kochan K.J., Mohebbi F., Stoica G., Threadgill D.W., Zelikovsky A., Waghela S.D., Wiener D.J., Rogovskyy A.S., 2019. *Infection Immunity*, 87, e00164-19, Copyright [2019] by ASM Journals.

6. Laboratory of Bioinformatics, I. M. Sechenov First Moscow State Medical University, Moscow, Russia.

3.1. Overview

B. burgdorferi is a tick-borne bacterium responsible for approximately 300,000 annual cases of LD in the USA with increasing incidents in other parts of the world. The debilitating nature of LD is mainly attributed to the ability of *B. burgdorferi* to persist in patients for many years despite strong anti-*Borrelia* antibody responses. Antimicrobial treatment of persistent infection is challenging. Similar to humans, *B. burgdorferi* establishes long-term infection in various experimental animal models except in New Zealand White (NZW) rabbits, which clear the spirochete within 4-12 weeks. LD spirochetes have a highly evolved antigenic variation *vls* system, on the lp28-1 plasmid, where gene conversion results in surface expression of antigenically variable VlsE protein. VlsE is required for *B. burgdorferi* to establish persistent infection by continually evading otherwise potent antibody. Since the clearance of *B. burgdorferi* is mediated by humoral immunity in NZW rabbits, the previously published results that LD spirochetes lose lp28-1 during the rabbit infection could potentially explain the failure of *B. burgdorferi* to persist. However, the present study unequivocally disproves that prior finding by demonstrating that LD spirochetes retain the *vls* system. Yet, despite the *vls* system being fully functional, the spirochete fails to evade anti-*Borrelia* antibody of the NZW rabbit. In addition to being protective against homologous and heterologous challenge, the rabbit antibody significantly ameliorates LD-induced arthritis in persistently infected mice. Overall, the current data indicate that NZW rabbits develop a protective antibody repertoire, whose specificities once defined will identify potential candidates for a much-anticipated LD vaccine.

3.2. Introduction

A variety of pathogenic organisms are equipped with highly evolved antigenic variation mechanisms that constantly allow the microbial invaders to escape otherwise efficacious antibody response in the infected host (Deitsch et al., 2009; Dzikowski and Deitsch, 2009; Gargantini et al., 2016; Hagblom et al., 1985; McCulloch et al., 2015; Noormohammadi et al., 2000; Norris, 2014; Obergfell and Seifert, 2015; Palmer et al., 2016; van der Woude and Baumler, 2004; Wahlgren et al., 2017). *B. burgdorferi*, a causative agent of LD is no exception. This extracellular bacterium is responsible for 30,000 confirmed cases of human LD each year in the United States alone, though the actual incidence is thought to be 10 times higher (Hinckley et al., 2014). Climate change is implicated in the spread of the vector of LD spirochete with increasing incidence rate of the disease (Brownstein et al., 2005; Ostfeld and Brunner, 2015). The debilitating nature of this multisystemic disease is substantially attributable to the ability of *B. burgdorferi* spirochetes to establish a persistent state of infection. If an early diagnosis is missed, mainly due to transient flu-like symptoms, chronic disease follows with a variety of symptoms including fatigue, musculoskeletal pain, arthritis, carditis, peripheral neuropathy, meningitis, encephalitis, cranial neuritis, and/or cognitive dysfunction (Cameron et al., 2014). Unfortunately, the antimicrobial treatment of persistent (chronic) infection is challenging and more importantly, to date, no vaccine for humans is available (Arvikar and Steere, 2015; Borchers et al., 2015; Lantos, 2015; Marques, 2010; Melia et al., 2015; Wormser et al., 2006).

In the mammalian host, the long-term survival of *B. burgdorferi*, despite robust antibody responses, is mainly attributed to the variable major protein (VMP)-like sequence (*vls*) locus (Zhang et al., 1997). The *vls* locus, which is well characterized in *B. burgdorferi* B31 strain, is located near the right telomere end of 28-kilobase linear plasmid (lp28-1) and composed of the *vlsE* gene and non-coding 15 *vls* cassettes (474-594 bp in length). The *vlsE* gene contains two constant regions that flank one central highly variable region. Because this *vlsE* central region shares 90.0-96.1% nucleotide with each silent cassette (Norris, 2014), unprogrammed events of gene conversion take place between each cassette and the *vlsE* cassette-like region. Importantly, *vlsE* recombination events are identified in mice as early as four days postinfection, while they are undetectable *in vitro* or in ticks (Bykowski et al., 2006; Indest et al., 2001; Norris, 2006b; Ohnishi et al., 2003; Verhey et al., 2018; Zhang et al., 1997; Zhang and Norris, 1998b). The end product of *vls* locus is expression, on the spirochetal surface, of highly antigenically variable protein, VlsE. This variable VlsE is absolutely required for *B. burgdorferi* to continually evade adaptive antibody responses in order for spirochetes to establish a long-term (life-long) infection in humans or other mammalian hosts (e.g., mice) (Bankhead and Chaconas, 2007; Coutte et al., 2009; Iyer et al., 2003; Labandeira-Rey et al., 2003; Labandeira-Rey and Skare, 2001; Lawrenz et al., 2004; McDowell et al., 2002; Purser and Norris, 2000; Rogovskyy and Bankhead, 2013; Rogovskyy et al., 2015). It has been consistently demonstrated that *B. burgdorferi* strains lacking the *vls* locus is rapidly cleared by mouse anti-*Borrelia* antibody (Bankhead and Chaconas, 2007; Rogovskyy and Bankhead, 2013; Rogovskyy et al., 2015).

In contrast to humans (Hudson et al., 1998; Kash et al., 2011; Logigian et al., 1990; Middelveen et al., 2018; Oksi et al., 1999; Stanek et al., 1990) and numerous animal models (Appel et al., 1993; Barthold et al., 1990; Barthold et al., 1988; Burgess, 1986; Chang et al., 2005; Chang et al., 2000; Goodman et al., 1991; Greene et al., 1988; Hodzic et al., 2008; Johnson et al., 1984; Philipp et al., 1993; Preac Mursic et al., 1990; Roberts et al., 1995; Sonnesyn et al., 1993; Straubinger, 2000; Straubinger et al., 1997), *B. burgdorferi* fails to establish a life-long infection in New Zealand White (NZW) rabbits. NZW rabbits are able to completely clear an active infection by wild-type B31 strain on average within 4-8 weeks (Embers et al., 2007b; Foley et al., 1995). The possibility that, in NZW rabbits, the clearance is due to a failure of *vls* locus to undergo recombination has been discarded by prior work (Embers et al., 2007b). It has been demonstrated that *vlsE* recombination could be detected as early as 2 weeks postinfection and that the average number of *vlsE* sequence changes in NZW rabbits was comparable to or even higher than those in mice at week 4 postinfection (Embers et al., 2007b). However, that study also showed that 50% of wild-type spirochetes recovered from rabbit skin were devoid of the *vls* locus-carrying plasmid, suggesting that it was the spontaneous loss of *vls* locus that accounted for the failure of *B. burgdorferi* to establish a long-term infection in NZW rabbits (Embers et al., 2007b). Yet, the fact that the other 50% of skin isolates retained the plasmid but were still cleared has led us to re-examine this prior finding by directly testing the retention rate of lp28-1 by skin isolates via colony PCR. The results demonstrated that all the examined rabbit skin isolates of *B. burgdorferi* uniformly retained the lp28-1 plasmid, indicating that the clearance of *B. burgdorferi* by NZW rabbits is not due to loss

of lp28-1. With this new finding, we set to define a role of VlsE for *B. burgdorferi* in NZW rabbits, the subject of this study.

The new data show that, despite the *vlsE* upregulation in NZW rabbits, *B. burgdorferi* only establishes a transient infection. The results demonstrate that host-adapted *B. burgdorferi* spirochetes, which are otherwise highly immune-evasive in the mouse host (Batool et al., 2018; Rogovskyy and Bankhead, 2013), are susceptible to anti-*B. burgdorferi* antibody of NZW rabbits (referred to here as the rabbit antibody). In passively immunized mice, the rabbit antibody completely abrogates establishment of infection by highly immune-evasive (host-adapted) wild type. Additionally, the rabbit antibody protects mice from *in vitro*-grown heterologous strain of *B. burgdorferi*. The data also show that the protective efficacy of rabbit antibody is predominantly complement-dependent. Lastly, the study demonstrates that the rabbit antibody passively transferred to the mice with an ongoing infection significantly reduce pathology of *B. burgdorferi*-induced arthritis.

3.3. Materials and Methods

3.3.1. Ethics statement

The animals were maintained at Texas A&M University in an animal facility accredited by the AAALAC. The experimental practices involving animals were approved by the Institutional Animal Care and Use Committee of Texas A&M University (IACUC 2017-0390) and were carried out in accordance with Public Health Service (PHS) Policy on Humane Care and Use of Laboratory Animals (2002), Guide for the Care and Use of

Agricultural Animals in Research and Teaching (2010), and Guide for the Care and Use of Laboratory Animals (2011).

3.3.2. *B. burgdorferi* clones and culture conditions

Wild-type strains of *B. burgdorferi*, B31-A3 (B31), B31-A3/lp28-1::*kan* Δ*vls* (ΔVlsE), and 297 were generous gifts from Dr. Troy Bankhead (Bankhead and Chaconas, 2007; Elias et al., 2002) (*SI Appendix*, Table 3-S1)**.** The *B. burgdorferi* clones were cultivated in liquid BSK-II medium with 6% rabbit serum (Gemini Bio-Products, USA; referred to here as BSK-II) and incubated at 35°C under 2% CO_2. The ΔVlsE clone was grown in BSK-II supplemented with 200 μg/ml kanamycin or 50 μg/ml streptomycin, respectively**.**

3.3.3. Infection of rabbits with *B. burgdorferi*

A total of 11 female New Zealand White (NZW) rabbits of 12-14 weeks of age (Charles River Laboratories, USA) were inoculated intradermally at six sites along the spine with B31, ΔVlsE, or 297 at 10^6 spirochetes per site as described (Embers et al., 2007b). The B31- and ΔVlsE-inoculated rabbits were bled via the marginal ear vein and skin biopsies (3 mm in diameter; Integra™ Miltex, USA) were taken around each inoculation site at weeks 1, 2, 3 and 4 postchallenge. Similarly, blood and skin biopsies were weekly sampled from the 297-inoculated NZW rabbits from week 1 through 8. The blood was kept at 4°C overnight and then centrifuged at 5,000 x g for 10 minutes to collect sera. The samples were then stored at -80°C until used. Skin biopsies that represented the six inoculation sites of each rabbit were cultured in 5 ml of BSK-II that contained antibiotic cocktail at 35°C under 2% CO_2 and also preserved in Invitrogen™ RNA*later*™

Stabilization Solution (ThermoFisher Scientific, USA) at -80°C until use. All the skin cultures were weekly examined via dark-field microscopy for up to 6 weeks for the presence of spirochetes. The B31- and ΔVlsE-inoculated rabbits were humanely sacrificed at week 4 postchallenge; 297-challenged rabbits were sacrificed at week 8. Blood was obtained from each rabbit via cardiac puncture at the time of sacrifice.

3.3.4. Identification of retention rates of the lp28-1 plasmid for rabbit skin isolates of *B. burgdorferi*

Individual *B. burgdorferi* clones from positive cultures of skin biopsies from B31-rabbits were isolated by limiting dilution. A total of 200 B31 isolates were PCR screened for the presence of lp28-1 plasmid. Each B31 isolate was directly screened via colony PCR upon limiting dilution to avoid any loss of lp28-1. For all the isolates PCR reaction mixture was prepared in 50 µL of the following reaction mixture: 10 µM of each primer (1 µL each), 200 µM of each dNTP (New England BioLabs, USA), 1.25 U of Taq DNA polymerase (New England BioLabs) with 10X standard Taq polymerase buffer (New England BioLabs) and 50-200 ng of DNA or 2 µL of culture. B31 isolates were individually screened by using published primers: 5'-ACACCGCACTAACATCGGGTTC-3' and 5'-GATACACCTCCTAGTTTGGGTCCTC-3' (Bunikis et al., 2011). PCR program was carried out as follows: denaturation at 95°C for 10 min followed by 25 cycles of 30 s at 95°C, 30 s at 54.4°C, and 45 s at 72°C with final extension step 6 min at 72°C.

3.3.5. qRT-PCR

To examine levels of *vlsE* transcripts, quantitative reverse transcription-PCR (qRT-PCR) was performed. Skin biopsies from four B31-infected rabbits were weekly collected into RNA*later*™ Stabilization Solution (ThermoFisher Scientific) for four weeks and stored at -80°C. Aurum™ Total RNA Fatty and Fibrous Tissue kit (Bio-Rad Laboratories, USA) was utilized to extract RNA from skin tissues collected at day 0, 3, 7, 14, 21, and 28 (two rabbits only) postinfection. DNA samples from days 0 (prior to infection) postinfection were used as a negative control. Then, 1 µg of RNA from each time point sample was used to prepare cDNA via Invitrogen™ SuperScript™ II Reverse Transcriptase kit (ThermoFisher Scientific) following the manufacturer's instructions. To normalize the *vlsE* expression, the *flaB* gene of *B. burgdorferi* B31 was used. qRT-PCR was performed by using our newly developed primers and probe for *vlsE* (5'-CGA TCT TAA TAG TTT GCC TAA GGA-3' and 5'-TCA ACG GCA GTT CCA ACA-3'; and 5'-CCC GTC GTA CTA CTT ATA TCG CTT-3', respectively), previously developed primers and probe for *flaB* (5'-TGT TGC AAA TCT TTT CTC TGG TGA-3' and 5'-CCT TCC TGT TGA ACA CCC TCT T-3'; and 5'-TCA AAC TGC TCA GGC TGC ACC GG-3', respectively) (Crother et al., 2004), SsoAdvanced™ Universal Probe Supermix (Bio-Rad) on CFX 96 Touch™ real-time PCR detection system (Bio-Rad). cDNA samples and no-template controls were analyzed in triplicate. The amplification program included: (i) heating at 95°C for 3 min for polymerase activation and DNA denaturation and (ii) amplification for 39 cycles with denaturation at 95°C for 15 s and extension and annealing

at 60°C for 45 s. The comparative C_T method (the $2^{-\Delta\Delta C_T}$) was used to assess the relative gene expression (Schmittgen and Livak, 2008).

3.3.6. Generation of host-adapted *B. burgdorferi* clones

Host-adapted *B. burgdorferi* spirochetes were generated as detailed (Barthold, 1993; Batool et al., 2018; Rogovskyy and Bankhead, 2013, 2014). In short, male SCID mice (The Jackson Laboratory, USA) at 4-6 weeks of age were subcutaneously inoculated with *in-vitro* grown B31, ΔVlsE, or 297 at 10^4 cells per mouse. Infection of each animal was confirmed by positive culture of blood samples (50 µl) and ear skin biopsies (~3 mm in diameter) taken at days 7 and 21 postinoculation and immediately cultivated in 3 and 1 ml of BSK-II with the antibiotic cocktail at 35°C under 2% CO_2, respectively. Ear skin tissues harvested at day 21 were stored at -80°C until use.

3.3.7. Passive immunization of mice at the time of challenge

Passive immunization assays involved male C3H/HeN (C3H) or SCID mice at 5-6 weeks of age (The Jackson Laboratory, USA). In the experiments involving the heat-inactivated sera, the C3H or SCID mice were also used. Although these mice produce their own complement, its contribution to any potential rabbit antibody-mediated killing is insignificant for the following reasons. First, the classical complement pathway was consistenty demonstrated to have a near zero activity (Bergman et al., 2000; Ratelade and Verkman, 2014). Second, mouse sera are known to contain inhibitor(s) of classical complement activation (Ratelade and Verkman, 2014). Finally, in addition to very low levels of complement proteins in mouse sera, the complement C4 protein lacks classical pathway C5 convertase subunit activity (Ebanks and Isenman, 1996).

Mice were challenged with *in vitro*-grown *B. burgdorferi* via subcutaneous inoculation of 10^4 spirochetes per mouse or host-adapted (ha-) *B. burgdorferi* at day 0. The ear skin tissues from infected SCID mice (~3 mm in diameter) were transplanted into dorsal lumbar region (one piece per mouse). The animals were retro-orbitally injected with 150 or 200 µl of preimmune or immune sera obtained from *B. burgdorferi* B31- or ΔVlsE-infected rabbits at day 28 postchallenge. Heat-inactivation of complement was performed at 56°C for 45 min (Soltis et al., 1979). Additionally, some mice were individually retro-orbitally inoculated with 150 µl of immune sera at day 2, 4, 6, and 8 postchallenge. Control mice were similarly challenged with *in vitro*-grown or ha-*B. burgdorferi* and treated with respective amounts of saline or preimmune sera to ensure that *B. burgdorferi* clones were infectious at the time of challenge. At day 7, 50 µl of blood from each mouse was cultured in 3 ml of BSK-II with the antibiotic cocktail. At day 14 or 21, bladder, ear pinnae, heart, and tibiotarsal joint tissues harvested from each animal were individually cultured in 1 ml (heart tissue in 3 ml) of BSK-II with the antibiotic cocktail. Dark-field microscopy was used to examine cultures for the presence of viable spirochetes.

3.3.8. Western blot

WB was performed as described (Rogovskyy et al., 2017a). In short, B31 spirochetes were grown in BSK-II, harvested by centrifugation, and then washed two times with ice-cold PBS followed by resuspension with SDS-PAGE sample buffer. About 1 x 10^6 spirochetes were loaded to each lane on 15% acrylamide gel (the SDS-PAGE). Resolved proteins were transferred to a PVDF membrane with a pore size of 0.45 µm (Bio-Rad). After blocking with 5% nonfat dry milk**,** the membrane was incubated in the

milk containing 1:500 diluted rabbit anti-B31 or -ΔVlsE immune or preimmune sera overnight at 4°C. To generate anti-B31 or -ΔVlsE immune sera, NZW rabbits (3 animals per group) were infected with B31 or ΔVlsE as described above. Blood was collected at day 7, 14, 21, and 28 postinfection and equal amounts of immune sera from each animal of the same group per time point were pooled. The preimmune sera was used as a negative control. The membrane was washed with TBST and the primary antibodies were detected by using goat anti-rabbit HRP-conjugated secondary antibody (Bio-Rad). The blots were developed via enhanced chemiluminescence.

3.3.9. ELISA

To quantify total levels of IgG in the B31- and ΔVlsE-infected rabbits, sera obtained from the respective rabbits at days 7, 14, 21, and 28 postinfection were individually analyzed by ELISA according to the manufacturer's instructions (Life Diagnostics, USA). The samples were diluted to 1:100,000 or 1:1,000,000 and analyzed in duplicate. Pre-immune sera was used as a negative control.

3.3.10. Passive immunization of mice with an established *B. burgdorferi* infection

A total of 9 C3H and 12 SCID mice at 5-6 weeks of age (The Jackson Laboratory, USA) were subcutaneously inoculated in the scapular region with *in-vitro* grown B31 at 10^4 cells per mouse. Infection was confirmed via culture of blood drawn from each mouse at day 7 postchallenge. At days 14, 18, 22, and 26, individually, 4 C3H and 6 SCID mice were retro-orbitally injected with 200 µl of non-treated (intact complement) immune sera. The pooled sera were originated from three B31-infected rabbits at day 28 postinfection. The other 5 C3H and 6 SCID mice were left untreated (controls). At day 45 postchallenge,

the mice were sacrificed. Bladder, ear skin, heart, and tibiotarsal joint tissues were harvested and cultured in BSK-II with the antibiotic cocktail. Tibiotarsal joints and heart tissues were subjected to histopathological analysis.

3.3.11. Histopathology

Tibiotarsal joints and hearts were fixed in 10% neutral buffered formalin, processed, and stained with hematoxylin and eosin. Scoring was performed blindly and independently by two pathologists. The following criteria were used to evaluate the joints: synovial hyperplasia (0, no change; 1, mild; 2, moderate; 3, severe; 4, severe with papilliform growth), exudate within joint and/or tendon sheath (0, no change; 1, <10 inflammatory cells (neutrophils, macrophages, and lymphocytes); 2, 10-49 inflammatory cells; 3, 50-100 inflammatory cells; 4, >100 inflammatory cells), superficial inflammation/resorption of bone (0, no change; 1, mild; 2, moderate; 3, moderate to severe; 4, severe), and overall inflammation (0, no change; 1, 1-24% of inflammatory cells (neutrophils, macrophages, and lymphocytes); 2, 25-40%; 3, 41-60%; 4, 61-100%). The overall scores were defined as follows: 0, no change (no synovial hyperplasia, no exudate within joints and/or tendon sheaths, no superficial bone inflammation/resorption, no overall inflammation); 1, mild changes (mild synovial hyperplasia, < 10 inflammatory cells within exudate in joints and/or tendon sheaths, mild superficial bone inflammation/resorption, 1-24% overall inflammation); 2, moderate changes (moderate synovial hyperplasia, moderate superficial bone inflammation/resorption, >10, >50 inflammatory cells within exudate in joints and/or tendon sheaths, 25-40% overall inflammation); 3, moderate to severe changes (severe synovial hyperplasia, moderate to

severe superficial bone inflammation/resorption, >50, <100 cells within exudate in joints and/or tendon sheaths, 41-60% overall inflammation); and 4, severe changes (severe synovial hyperplasia with papilliform growth, severe superficial bone inflammation/resorption, >100 cells within exudate in joints and/or tendon sheaths, 61-100% overall inflammation). The histologic sections of heart tissues were scored as defined: 0, no changes (no inflammation); 1, minimal changes (minimal inflammation of lymphocytes and neutrophils (single inflammatory cells) and edema); 2, mild changes (mild inflammation of lymphocytes and neutrophils (clusters of inflammatory cells) and edema); 3, mild to moderate changes (mild clusters of lymphocytes and neutrophils and edema with arteritis); and 4, moderate to severe changes (moderate to severe inflammation of lymphocytes and neutrophils (larger foci of inflammation) and edema).

3.3.12. qPCR analysis

Left tibiotarsal joint and ear skin tissues were collected from each of the 12 SCID mice sacrificed at day 45 postchallenge and stored at -80ºC. DNA was extracted via DNeasy Blood & Tissue kit (Qiagen) following the manufacturer's instructions. Quantitative PCR (qPCR) assays were performed with CFX 96 Touch™ real-time PCR detection system by utilizing SsoAdvanced™ Universal SYBR Green Supermix (Bio-Rad). The following forward and reverse primers were used for qPCR of the *actB* gene: 5'-AGA GGG AAA TCG TGC GTG AC-3' and 5'-CAA TAG TGA TGA CCT GGC CGT-3', respectively (Li et al., 2006); and the *recA* gene: 5'-GTG GAT CTA TTG TAT TAG ATG AGG CTC TCG-3' and 5'-GCC AAA GTT CTG CAA CAT TAA CAC CTA AAG-3', respectively (Morrison et al., 1999). The amplification was performed in 20-µL

reaction with 300 nM of each primer and 100 ng of DNA. The cycling parameters - (i) 95°C for 10 s and (ii) 39 cycles of 95°C for 30 s and 60°C for 1 min – were optimized from SsoAdvanced™ Supermix manufacturer's protocol. To generate absolute standards, 138-bp and 222-bp DNA fragments of *actB* and *recA* were amplified from C3H mouse and B31 DNAs, respectively. The amplification was performed in 50-µL reaction that contained 0.2 µM of each primer, 200 µM of dNTP, 1.25 U of Taq DNA polymerase (New England Biolabs), and 100 ng of DNA. The following PCR program was used: denaturation at 95°C for 10 min followed by 25 cycles of 30 s at 95°C, 30 s at 60°C (50°C for *recA*), and 45 s at 72°C with final extension step 6 min at 72°C. The PCR products were purified via PCR purification kit (Qiagen). All standard dilutions and DNA samples were amplified in triplicate. The number of spirochetes was calculated as the ratio of *recA* DNA copies per copy of *actB* gene.

3.3.13. Phage display (Ph.D.) library

A mix of 50 µl or 20 µl, respectively, of each mouse or rabbit sera sample and 10 µl of random peptide library Ph.D.-7 (NEB, USA) were incubated at 25°C for 18 hr. Antibody-bound phages were then isolated and then eluted as previously detailed (Liu et al., 2013; Rogovskyy et al., 2017a). After amplification, the phages were subjected to two rounds of biopanning and then isolated via protein G-agarose beads. DNA was extracted by phenol-chloroform extraction and ethanol precipitation. The multiplex PCR-amplified DNA library was generated as described (Rogovskyy et al., 2017a) and sequenced via Illumina HiSeq 2500 platform (University at Buffalo Genomics and Bioinformatics Core, New York State Center of Excellence Bioinformatics & Life Sciences, Buffalo, New

York). The sequencing generated approximately 1.79 x10^8 DNA reads, which were de-multiplexed based on the unique bar codes as detailed (Rogovskyy et al., 2017a). The obtained data were analyzed via Python (https://www.python.org).

3.3.14. Prediction of anti-B31 antibody reactivity to VlsE

For each serum sample, all peptides were mapped to VlsE of *B. burgdorferi* B31 strain (AAC45733.1, B31VlsE, thereafter) utilizing BLASTP with the identity threshold 4: alignments with 4 or more exact amino acid matches were considered. For each VlsE position X, a peptide with the amino acid matched to the position X and with K different VlsE matches contributed its frequency divided by K to the coverage of X. The coverage of X, C(X), was computed as the sum of contributions of all peptides matched to X.

3.3.15. Statistical analysis

A two-tailed Fisher's exact test was used for comparison of mouse groups. One-way analysis of variances (ANOVA) (GraphPad Prism Software) was applied to compare the levels of *vlsE* transcription. Histopathological scores were analyzed by paired t-test or unpaired t-test corrected for multiple comparisons using the Holm-Sidak method. Differences were considered significant at the *P* value of <0.05.

3.4. Results

3.4.1. VlsE capacitates *B. burgdorferi* to establish only a transient infection in NZW rabbits

To verify the previous finding that a portion of *B. burgdorferi* population spontaneously loses the *vls* locus-carrying plasmid, lp28-1 and to examine the role of VlsE for the rabbit infection (Embers et al., 2007b), groups A and B (4 animals per group) of

NZW rabbits were challenged with *in vitro*-grown *B. burgdorferi* B31-A3 strain (referred to here as B31) and B31-A3/lp28-1::*kan* Δ*vls* (ΔVlsE), respectively (Table 3-S1). At weeks 1, 2, 3, and 4 postinoculation, skin biopsies sampled around the inoculation sites were cultured in liquid BSK-II medium with 6% rabbit serum and incubated at 35°C under 2% CO_2. The culture results revealed that B31 strain was consistently detected at weeks 1, 2, and 3 in all the challenged rabbits (Table 3.1). By week 4, however, skin biopsies from 2 out of four B31-infected rabbits were culture-negative, indicating the beginning of clearance of wild-type infection in NZW rabbits. This finding was consistent with the prior data, which demonstrated that, by this time point, 3 out of eight NZW rabbits cleared B31-induced infection (Embers et al., 2007b). Thus, the wild-type B31 strain was able to establish an active infection that, by week 4 postinoculation, was cleared by 50% of the NZW rabbits.

Table 3.1 Culture results for skin biopsies weekly sampled from NZW rabbits challenged with *in vitro*-grown B31 or ΔVlsE

Rabbit group	Challenged with:	No. of culture positive/total no. tested			
		Weeks postchallenge			
		1	2	3	4
A	*in vitro*-grown B31	4/4	4/4	4/4	2/4
B	*in vitro*-grown ΔVlsE	2/4[a]	0/3	0/3	0/3

[a]One rabbit was sacrificed at day 7 postchallenge.

As opposed to B31, already by week 1, skin biopsies of 2 (animals B3 and B4) out of four rabbits were culture-negative for ΔVlsE spirochetes, indicating a very early clearance by 50% of the ΔVlsE-inoculated rabbits. Thus, the presence of ΔVlsE infection at week 1 was directly confirmed, via culture, only in rabbits B1 and B2. However, despite

being culture-negative at week 1, rabbits B3 and B4 were still able to develop pronounced erythrema migrans (as did rabbits B1 and B2) around each inoculation site at week 1 postchallenge, indicating that the ΔVlsE clone had actively infected these two rabbits as well (Foley et al., 1995; Kornblatt et al., 1984) (Fig. 3-S1). Prior study showed that, when NZW rabbits were inoculated with avirulent *B. burgdorferi* B31 strain, no erythrema migrans were developed (Foley et al., 1995). Importantly, the infectivity of ΔVlsE inoculum was verified on 5 SCID mice, whose blood and ear skin tissues collected at days 7 and 21 postchallenge, respectively, were uniformly culture-positive for the ΔVlsE clone (data not shown). Since rabbit B4 was added to the group later and, therefore, the inoculation was performed separately, the successful infection of this rabbit with the ΔVlsE clone was also verified by culture-positive results of skin biopsies taken at day 3 postinoculation (data not shown). All the subsequent skin biopsies sampled at weeks 2, 3, and 4 from rabbits B1, B2, and B3 (rabbit B4 was sacrificed at day 7) were culture-negative, which demonstrated an earlier clearance of the VlsE-deficient clone compared to its isogenic wild-type counterpart (Table 3.1; $P<0.05$). Together, the results indicated that, in NZW rabbits, the lack of *vls* locus resulted in a very early clearance of *B. burgdorferi*.

To verify the previously reported loss of lp28-1 by wild type, a total of 200 B31 isolates were individually PCR-screened for the presence of lp28-1. The results showed that, in contrast to the prior finding, where 25 out of fifty isolates recovered from skin of B31-infected rabbits were PCR-negative for lp28-1 (Embers et al., 2007b); every single isolate of B31 contained the plasmid (Table 3.2). The discrepancy between the prior and

current findings could well be accounted by different approaches taken. In the previous work, prior to the PCR screen, the fifty B31 isolates were first expanded in BSK-II in order to obtain sufficient amount of DNA (Embers et al., 2007b). However, it was consistently shown that, during *in vitro* propagation, *B. burgdorferi* rapidly lost various plasmids including lp28-1 (Barbour, 1988; Hinnebusch and Barbour, 1992; Moody et al., 1990; Schwan et al., 1988; Simpson et al., 1990; Zhang et al., 1997). Thus, in the present study, this propagation step was purposely avoided by directly screening all the B31 isolates for the presence of lp28-1 via colony PCR. Together, the present data unequivocally demonstrated that *B. burgdorferi* does not lose the *vls*-carrying lp28-1 plasmid during the rabbit infection.

Table 3.2 Retention rates of the lp28-1 plasmid by the B31 clone isolated from infected NZW rabbits

Rabbit ID	Weeks postchallenge	No. of isolates positive for lp28-1/total no. tested
A1	1	60/60
A2	2	60/60
A3	3	60/60
A3	4	20/20

3.4.2. The rabbit antibody are potent to prevent infection by VlsE-expressing *B. burgdorferi*

Our results showed that, despite the plasmid retention, lp28-1-carrying spirochetes were still cleared in NZW rabbits. It was possible that the failure of wild-type *B. burgdorferi* to establish a long-term infection in NZW rabbits was due to the lack of VlsE expression. To examine this, quantitative reverse transcription-PCR (qRT-PCR) was used

to detect *vlsE* transcription in B31-infected rabbits at days 3, 7, 14, 21, and 28 postchallenge. The failure to detect any *vlsE* transcripts at days 3 and 28 (data not shown) was suggestive of very low numbers of spirochetes in the respective skin biopsies. The *vlsE* transcription was consistently detected at days 7, 14, and 21, indicating that *vlsE* was upregulated in NZW rabbits (Fig. 3.1).

It has been consistently demonstrated that, mainly due to the VlsE system, *B. burgdorferi* establishes a long-term infection in mice despite their strong antibody responses (Bankhead and Chaconas, 2007; Coutte et al., 2009; Iyer et al., 2003; Labandeira-Rey et al., 2003; Labandeira-Rey and Skare, 2001; Lawrenz et al., 1999; Lawrenz et al., 2004; McDowell et al., 2002; Purser and Norris, 2000; Rogovskyy and Bankhead, 2013; Rogovskyy et al., 2015; Zhang et al., 1997; Zhang and Norris, 1998b). Thus, to examine the potency of the rabbit antibody against *B. burgdorferi* in the mouse host, 5 C3H mice (group IA) were passively immunized with the anti-B31 immune sera previously collected and pooled from three B31-infected NZW rabbits at day 28 postinoculation. As a control, C3H mice of groups IB and IC (3 animals per group) received saline and preimmune sera, respectively. Immediately after the respective treatments, all the mice were challenged with the wild-type B31 clone. Since VlsE expression was previously shown to be significantly higher in the spirochetes that resided in mouse tissues (e.g., skin) compared to *in vitro*-grown *B. burgdorferi* (Crother et al., 2003; Liang et al., 2004b), host-adapted (referred to here as ha) B31 (ear skin from infected SCID mice) was used for the challenge. Thus, it was anticipated that, immediately upon challenge, spirochetes were armored with abundant VlsE on their surface to defend

themselves against the passively transferred antibody. It was previously shown that, only when in host (mouse skin)-adapted state, did wild-type *B. burgdorferi* gain the capacity to resist anti-B31 mouse antibody, which were otherwise sufficiently potent to prevent the *in vitro*-grown B31 or ha-ΔVlsE clone (Rogovskyy and Bankhead, 2013).

At days 7 and 21 postchallenge, blood and other tissues, specifically, bladder, heart, ear skin, and tibiotarsal joint (referred to here as the other tissues) were, respectively, harvested and cultured in BSK-II to evaluate the outcome of challenge. The results showed that five out of 5 mice that had received the rabbit antibody were completely protected from the VlsE-expressing wild type. In contrast, all the control mice showed culture-detectable spirochetemia at day 7 and disseminated infection at day 21 postchallenge, confirming the full infectivity of ha-B31 clone. Together, the data demonstrated that the rabbit antibody had the capacity to efficaciously clear spirochetes despite their fully functional *vls* system in the mouse (natural) host.

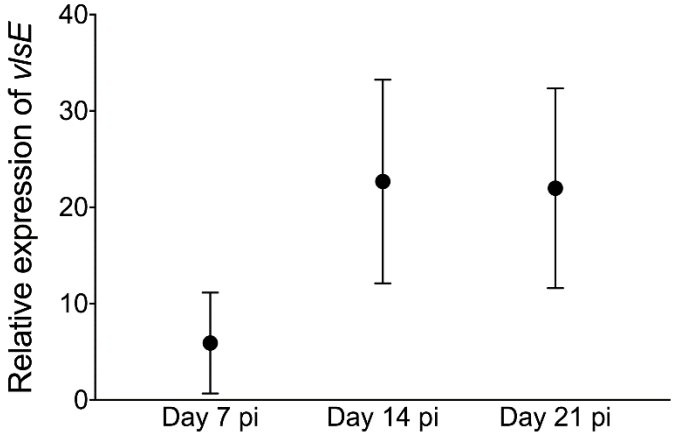

Figure 3.1 *vlsE* transcription in rabbit skin-residing *B. burgdorferi*. *vlsE* transcript levels were upregulated, as determined by qRT-PCR, in the skin of B31-infected NZW rabbits at days 7, 14, and 21 postinfection. The *flaB* gene of *B. burgdorferi* B31 served as the endogenous control to normalize the *vlsE* expression. pi denotes postinfection.

3.4.3. Protective efficacy of the rabbit antibody against *B. burgdorferi* is mainly complement-dependent

To test whether the observed protective efficacy of the rabbit antibody against *B. burgdorferi* depends on the complement, 12 C3H mice (group IIA) were treated with heat-inactivated immune sera and then immediately challenged with the ha-B31 clone. This sera was previously collected from B31-infected rabbits at day 28 postinfection. Blood and the other tissues harvested at days 7 and 21 postchallenge, respectively, were cultured in BSK-II. The results demonstrated that the heat-inactivated immune sera prevented culture-detectable spirochetemia in 12 out of twelve mice but failed to block disseminated infection in 9 out of these twelve animals (Table 3.3). Importantly, the infectivity of host-adapted wild-type spirochetes was verified by group IIB mice: three out of 3 control mice exhibited spirochetemia and disseminated infection at days 7 and 21 postchallenge, respectively. Thus, based on the results of groups IA and IIA, the complement inactivation significantly reduced the protective efficacy of the rabbit anti-B31 antibody (5/5 vs. 3/12; P=0.0090; Table 3.3), indicating that the borreliacidal function of the rabbit antibody is predominantly complement-dependent.

To further explore a role of the rabbit, complement for the potency of the rabbit anti-B31 antibody, 9 C3H mice (group IIIA) were treated with rabbit heat-inactivated anti-B31 sera and immediately challenged with *in vitro*-grown B31 clone. As a control, 3 (group IIIB) and 5 (group IIIC) C3H mice were treated with saline and preimmune sera, respectively, prior to the challenge. All the control animals exhibited culture-detectable spirochetemia and disseminated infection at days 7 and 21 postchallenge, respectively.

Thus, the control results verified the full infectivity of B31 inoculum and, importantly, demonstrated the inability of rabbit preimmune sera (intact complement, which has not been activated by infection) to block the needle *B. burgdorferi* (Table 3.3). In contrast, the culture results of blood and the other tissues collected from group IIIA at days 7 and 21 postchallenge, respectively, showed that 9 out of nine mice were completely protected from *in vitro*-grown B31 challenge ($P<0.0001$; Table 3.3). Together, the results indicated that the rabbit anti-B31 antibody were fully protective against *in vitro*-grown B31 spirochetes even in the absence of complement.

3.4.4. A potential contribution of VlsE to the *B. burgdorferi* evasion from complement-independent antibody killing in NZW rabbits

The finding that, in contrast to the needle *B. burgdorferi*, host-adapted spirochetes were more resistant to complement-independent antibody killing prompted us to examine a potential role of VlsE in this evasion. The fact, that VlsE expression was shown to be significantly higher in the mouse host than *in vitro* (Liang et al., 2004b), could explain a higher susceptibility of needle wild type to complement-independent antibody killing. To test this, 5 and 3 SCID mice were treated with heat-inactivated anti-ΔVlsE sera (group IVA) or saline (IVB; control), respectively, and then challenged with the ha-ΔVlsE clone. The anti-ΔVlsE sera was previously collected from ΔVlsE-infected rabbits at day 28 postinfection. Blood and the other tissues harvested at days 7 and 21 postchallenge, respectively, were cultured in BSK-II.

Table 3.3 Protective efficacy of the anti-*Borrelia* antibody of NZW rabbits against homologous *B. burgdorferi*

Group	Mice and treatment	Challenged with:	No. of culture positive/total no. tested (day of harvest postchallenge)		No. of mice protected[a]/total no.
			Blood (7)	Tissues (21)[a]	
IA	C3H + anti-B31 antibody (intact complement)	host-adapted B31	0/5	0/20	5/5
IB (control)	C3H + saline		3/3	11/12	0/3
IC (control)	C3H + preimmune sera		3/3	12/12	0/3
IIA	C3H + anti-B31 antibody (heat-inactivated complement)		0/12	29/48	3/12
IIB (control)	C3H + saline		3/3	12/12	0/3
IIIA	C3H + anti-B31 antibody (heat-inactivated complement)	*in vitro*-grown B31	0/9	0/36	9/9
IIIB (control)	C3H + saline		3/3	11/12	0/3
IIIC (control)	C3H + preimmune sera		5/5	19/20	0/5
IVA	SCID + anti-ΔVlsE antibody (heat-inactivated complement)	host-adapted ΔVlsE	0/5	0/20	5/5
IVB (control)	SCID + saline		3/3	11/12	0/3

[a]Mouse was considered positive when any of the tissues, specifically, ear skin, heart, bladder, or tibiotarsal joint was culture-positive. Mouse was considered protected when all four tissues were negative by culture.

As opposed to the control mice, the culture results of the experimental group showed that anti-ΔVlsE antibody completely prevented, in a complement-independent manner, both spirochetemia and disseminated infection by host-adapted VlsE-deficient *B. burgdorferi* (Table 3.3; P=0.0179). This is in contrast to the culture results of group IIA, where heat-inactivated anti-B31 sera was protective against host-adapted VlsE-expressing wild type for only 3 out of twelve mice (P=0.0090). Logically, the observed difference could potentially be accounted for by lower titers of antibody to surface antigens other than VlsE in the anti-B31 sera compared to the anti-ΔVlsE sera. However, the levels of total IgG were not significantly different between the two types of immune sera (P>0.05; Fig. 3-S2). Moreover, WB analysis of anti-B31 and anti-ΔVlsE immune sera collected, respectively, from B31-infected or ΔVlsE-infected rabbits at days 7, 14, 21, and 28 postchallenge revealed no noticeable difference in their reactivity to whole-cell lysates of B31 clone (Fig. 3-S3). Together, the data suggested that, in NZW rabbits, VlsE contributed to the evasion of *B. burgdorferi* from the complement-independent antibody killing. These results could potentially explain why, in the NZW rabbits, the VlsE-deficient clone was cleared so early compared to VlsE-competent *B. burgdorferi* B31.

3.4.5. The rabbit antibody is cross-protective against heterologous *B. burgdorferi*

To investigate whether the rabbit antibody were cross-protective against heterologous *B. burgdorferi*, C3H mice were treated with anti-B31 sera and then challenged with host-adapted (group AI) or *in vitro*-grown (group B1) 297 strain (3 mice per group). The infectivity of ha- and *in vitro*-grown 297 was confirmed by the respective saline-treated control groups (AII and BII), whose tissues were consistently culture-

positive for the 297 strain (3 animals per group; Table 3.4). The culture results of blood and the other tissues of group AI demonstrated that the rabbit anti-B31 sera did not prevent infection by ha-297 in any of the three mice. In contrast, both culture-detectable spirochetemia and disseminated infection by needle 297 were successfully blocked in 5 out of five mice ($P<0.05$). Importantly, the other 5 out of five mice treated with preimmune sera (group BIII) were successfully infected with *in vitro*-grown 297, demonstrating the inability of the rabbit complement, which has not been activated by infection, to block the needle heterologous *B. burgdorferi*. Together, the data showed that the rabbit anti-B31 antibody were cross-protective against heterologous *in vitro*-grown *B. burgdorferi*, which is consistent with previous study that demonstrated cross-protection of the rabbit antibody against *in vitro*-grown spirochetes in passively immunized hamsters (Johnson et al., 1986). To examine whether the observed cross-protection of anti-B31 antibody was dependent on the rabbit complement, 5 C3H mice (group CI) were treated with heat-inactivated anti-B31 sera and then challenged with *in vitro*-grown 297. The infectivity of the 297 inoculum was fully confirmed by culture-positive tissues of 3 control animals (group CII; Table 3.4). The culture results of blood and the other tissues from group CI mice showed that, upon complement depletion via heat-inactivation, the rabbit anti-B31 antibody were still capable of preventing heterologous infection in 3 out of five mice (Table 3.4). Thus, the data indicated that antibody-mediated killing of heterologous needle *B. burgdorferi* was partly complement-dependent.

Finally, the fact that the ha-297 clone was resistant to the rabbit anti-B31 antibody brought up a question whether, in NZW rabbits, this heterologous strain of *B. burgdorferi*

had the capacity to persist longer than the B31 clone. To test this, three NZW rabbits were challenged with *in vitro*-grown 297 at the dose and via the route identical to the B31 challenge. The three rabbits became all infected as consistently determined by culture-positive skin biopsies from weeks 1, 2, 3, and 4 postinoculation (Table 3-S2). By week 5, however, two out of 3 rabbits cleared the 297 infection. Skin biopsies from the later time points (weeks 6, 7, and 8) were culture-negative for the three rabbits, demonstrating the complete clearance of *B. burgdorferi* infection. Thus, the results were consistent with findings obtained from the B31-infected rabbits of this and prior (Embers et al., 2007b; Foley et al., 1995) studies and once again confirmed that, in NZW rabbits, *B. burgdorferi* failed to persist long-term.

3.4.6. The rabbit antibody significantly reduces pathology of *B. burgdorferi*-induced arthritis

To examine whether the rabbit antibody were sufficiently potent to exert any therapeutic effect, the experimental design involved 9 C3H mice that were infected with *in vitro*-grown B31. Infection of each mouse was confirmed by culture-positive blood sampled at day 7 postinoculation (Table 3-S3). Then, at days 14, 18, 22, and 26, four animals were retro-orbitally treated with the rabbit antibody (anti-B31 sera) and the other 5 mice were left untreated (control group). At day 45 postchallenge, bladder, ear skin, heart, and tibiotarsal joint tissues were harvested from each animal and cultured in BSK-II. The results showed that most of the tissues from all 9 mice were culture-positive for the B31 clone, indicating that the rabbit antibody did not have the capacity to abrogate the ongoing infection of *B. burgdorferi* (Table 3).

Table 3.4 Protective efficacy of the anti-*Borrelia* antibody of NZW rabbits against heterologous *B. burgdorferi*

Group	Mice and treatment	Challenged with:	No. of culture positive/total no. tested (day of harvest postchallenge)		No. of mice protected[a]/total no.
			Blood (7)	Tissues (21)[a]	
AI	C3H + anti-B31 antibody (intact complement)	host-adapted 297	3/3	12/12	0/3
AII (control)	C3H + saline		3/3	12/12	0/3
BI	C3H + anti-B31 antibody (intact complement)	*in vitro*-grown 297	0/5	0/20[b]	5/5
BII (control)	C3H + saline		3/3	12/12	0/3
BIII	C3H + preimmune sera		5/5	19/20	0/5
CI	C3H + anti-B31 antibody (heat-inactivated complement)		2/5	7/20	3/5
CII (control)	C3H + saline		3/3	11/12	0/3

[a]Mouse was considered positive when any of the tissues, ear skin, heart, bladder, or tibiotarsal joint was culture-positive. Mouse was considered protected when all four tissues were negative by culture.
[b]Mice from this group were sacrificed on day 14 postchallenge.

In order to compare infection-induced pathological changes between the two groups, heart and two tibiotarsal joints of each C3H mouse were subjected to histopathological analysis. To ensure the rigor and reproducibility, the assessment was performed blindly and independently by two board-certified pathologists. The results demonstrated that there was noticeable but statistically insignificant difference in the histopathological scores of heart tissues between the treated (1.00±1.35) and control (1.80±1.04) animals (P=0.1162; Fig. 3-S4). However, for the joints, the statistically significant difference was detected for the synovial hyperplasia and overall inflammation scores between the treated and control animals (P<0.05; Table 3.5; Fig. 3-S5). Interestingly, there were two outliers, one joint for each group, whose removal from the analysis also resulted in statistically significance difference for the exudate within joint and overall scores between the two groups (P<0.05; multiple t-test; data not shown).

Despite the reduced pathology detected in the C3H mice, it was possible that the potency of the rabbit antibody was reduced by mouse anti-rabbit immune responses in these immunocompetent animals. To overcome this potential caveat, a follow-up experiment was performed. This time, the experimental design involved 12 immunodeficient (SCID) mice that lacked adaptive immunity (Beamer et al., 1993; Blunt et al., 1995; Bosma et al., 1988; Custer et al., 1985). All the SCID mice were first infected with *in vitro*-grown B31 clone. Infection was confirmed by culture-positive blood sampled from each mouse at day 7 postchallenge. At days 14, 18, 22, and 26, six SCID mice were retro-orbitally treated with the rabbit antibody (anti-B31 immune sera) and the other six animals were left untreated (control group). Hearts and right tibiotarsal joints from the 12

SCIDs were then harvested at day 45 postchallenge and subjected to histopathological analysis. In addition, left tibiotarsal joints and ear skins from all the twelve SCID mice were analyzed by quantitative-PCR (qPCR) in order to compare spirochetal loads between the two groups.

The histopathological analysis, again performed blindly and independently by the two pathologists, demonstrated noticeable but statistically insignificant difference for the heart pathology between the treated (0.33±0.41) and control (0.92±0.38) groups (P=0.0583; Fig. 3-S6). In contrast, the joint pathology was significantly reduced in all the treated mice for the following histopathological changes: synovial hyperplasia, superficial inflammation of bone, and overall inflammation (P<0.05; Table 3.5; Fig. 3.2). The qPCR results showed that there was noticeable but statistically insignificant difference in spirochetal loads of the joint tissues between the two groups (P>0.05; Fig. 3.3). In contrast, the significant reduction in spirochetal numbers was observed between the ear skin tissues of treated and control animals (P=0.0170). Together, the results of two independent experiments demonstrated that the rabbit antibody had the capacity to significantly reduce the pathology of *B. burgdorferi*-induced arthritis.

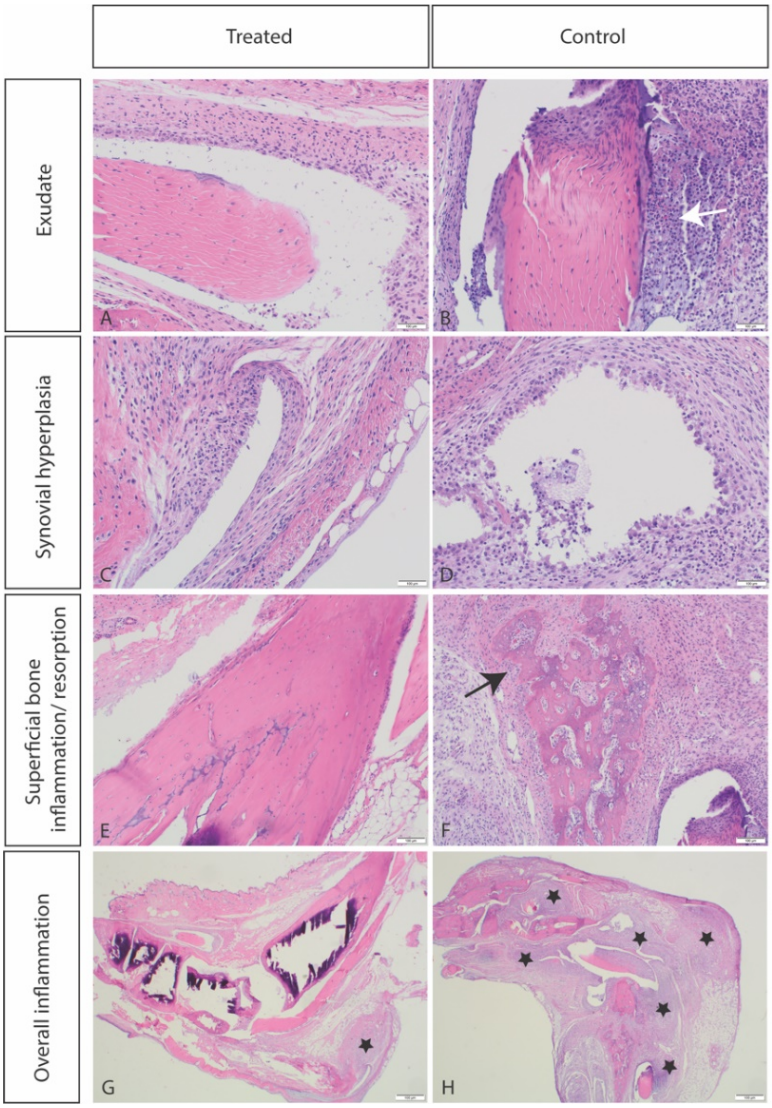

Figure 3.2 Treatment of actively *B. burgdorferi*-infected SCID mice with the rabbit anti-*Borrelia* antibody results in significant reduction of infection-induced joint pathology. Representative histologic pictures of tibiotarsal joints from treated (A, C, E, G) and control (B, D, F, H) groups. (A) Only few inflammatory cells are observed. (B) Severe inflammation is indicated with the white arrow. (C) No synovial changes are observed. (D) Moderate synovial hyperplasia is present. (E) No bone inflammation or resorption is observed. (F) Moderate to severe superficial inflammation and resorption of bone are indicated by the black arrow. (G) Inflammation (asterisks) is present in only one area. (H) Multifocal inflammation is observed. H&E staining, scale bar represents 100µm. The histopathological scores of synovial hyperplasia, superficial inflammation and/or resorption of bone, overall inflammation including the overall scores were significantly different between the two groups ($P<0.05$; see Table 3.5).

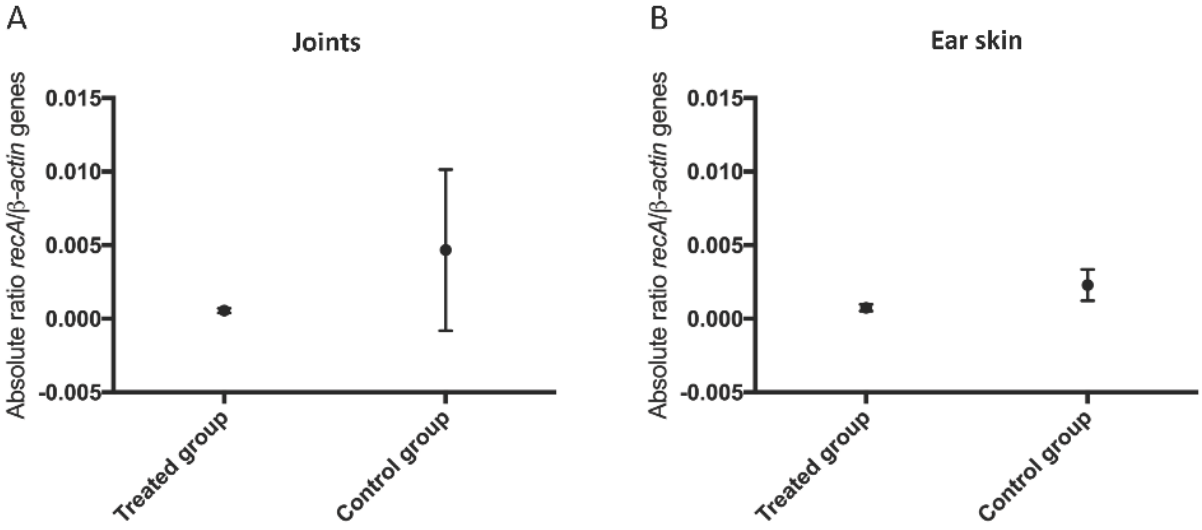

Figure 3.3 Spirochete burdens in tibiotarsal joints (A) and ear skin tissues (B) of *B. burgdorferi*-infected SCID mice that were treated with the anti-*Borrelia* antibody of NZW rabbits or remained untreated. A total of 12 SCID mice were first inoculated with the B31 clone and then, at days 14, 18, 22, and 26 postinfection, six SCID mice were treated with anti-B31 immune sera and the other six control animals remained untreated. To compare the effect of the rabbit antibody on spirochetal loads between the two groups, left tibiotarsal joint and ear skin tissues were collected from each mouse at day 45 postinfection. DNA was extracted from each sample and subjected to quantitative PCR (qPCR) assay to quantify the *actB* DNA copies relative to the *recA* gene. All standard dilutions and DNA samples were amplified in triplicate. The number of spirochetes in each DNA sample was calculated as the ratio of *recA* DNA copies per copy of *actB* gene. The significant reduction in spirochetal numbers was only observed between the ear skin tissues of treated and control animals (P=0.0170).

Table 3.5 Therapeutic effect of the anti-*Borrelia* antibody of NZW rabbits in *B. burgdorferi*-infected mice as determined by histopathology of tibiotarsal joints

Histopathological changes/criteria	Histopathological score (±SD)			
	C3H mice		SCID mice	
	Treated with rabbit antibody (4 mice)	Non-treated control (5 mice)	Treated with rabbit antibody (6 mice)	Non-treated control (6 mice)
Synovial hyperplasia	0.87±0.92[a]	1.7±0.63[a]	1.75±0.99[b]	3.17±0.26[b]
Exudate within joint and/or tendon sheath	0.25±0.38	1.15±1.05	1.83±1.12	3.42±0.74
Superficial inflammation and/or resorption of bone	0.44±0.56	0.80±0.71	1.33±0.41[b]	2.50±0.84[b]
Overall inflammation	0.94±0.78[a]	1.55±1.07[a]	2.42±0.74[b]	3.25±0.52[b]
Overall score	0.65±0.83	1.62±0.97	2.23±0.54[b]	3.35±0.48[b]

Respective histopathological scores were significantly different between the two groups of C3H[a] and SCID[b] mice as determined by paired t-test ($P<0.05$).

3.4.7. Comparison of anti-VlsE antibody repertoires developed in NZW rabbits and mice

In the attempt to identify any difference in anti-VlsE antibody repertoires between NZW rabbits and mice, the approach that involved random peptide phage display libraries coupled with next generation sequencing (RPPDL/NGS) and followed by our previously developed computational algorithms was used (Rogovskyy et al., 2017a). As a result of RPPDL/NGS application, global mimotope repertoires of the rabbit day-14 (non-protective), day-28 (protective), and mouse day-28 (non-protective) sera were identified. Then, all the repertoires were mapped, via BLASTP, to the primary structure of VlsE of *B. burgdorferi* B31 strain (referred to here as B31-VlsE). Two pooled preimmune sera taken from the same three C3H mice and three rabbits prior to their challenge, respectively, were used as two background controls. The overall results showed that there

were no major differences detected between the reactivities of rabbit and mouse sera to the primary structure of VlsE with a few noteworthy exceptions (Fig. 3.4). First, there was a pronounced reactivity of 3 rabbit day-28 and 2 out of three day-14 sera to VlsE24-31 epitope of N-terminal invariable domain. In contrast, the three mouse day-28 sera were not reactive to this epitope. Interestingly, the recognition of VlsE24-31 by the rabbit antibody was congruent with prior data derived from human sera (Chandra et al., 2011). The analyses of microarrays, which contained synthesized overlapping peptides of B31-VlsE, demonstrated that VlsE21-31 epitope was targeted by most LD patient sera (Chandra et al., 2011). Second, in contrast to the rabbit day-28 antibody, 2 out of three mouse sera intensely reacted with two epitopes: VlsE199-204 of invariant region (referred to here as IR) 3 and VlsE350-356 of C-terminal invariant domain (Fig. 3.4).

The latter reactivity was fully supported by previously observed reactivity of day-28 and day-70 antibody from C3H mice that were persistently infected with heterologous *B. burgdorferi* strain 297 (Rogovskyy et al., 2017a). Moreover, the overall reactivity to the C-terminal invariant domain was also common for LD patient sera (Chandra et al., 2011). Thus, the current data fully supports the previous conclusion that the C-terminal invariable domain of VlsE is highly immunodominant (Philipp et al., 2001). Interestingly, the previously observed reactivity of antibody from 297-infected C3H mice to 297-VlsE IR1 (Rogovskyy et al., 2017a) was not shared by any of the anti-B31 mouse or rabbit sera. The lack of reactivity to IR1 could be explained by an overall low degree of identity (46%) and similarity (53%) between B31-VlsE and 297-VlsE (Norris, 2014). Importantly, the anti-B31 rabbit and mouse antibody were also expectedly reactive to IR6, the invariant

region that was uniformly demonstrated to be highly immunogenic in humans, monkeys, and mice (Jacek et al., 2016; Liang et al., 1999; Liang and Philipp, 1999, 2000). Consistent with our prior study (Rogovskyy et al., 2017a), the present data demonstrated no or little reactivity to VlsE conserved regions, IR2 and IR4, respectively. This is in contrast to other work, where *B. burgdorferi*-infected C3H mice induced strong antibody to IR2 and IR4 (Liang and Philipp, 1999). In sum, the present study did not identify any anti-VlsE antibody reactivity that is unique to the protective rabbit sera, suggesting that any potentially protective invariant linear epitopes of VlsE are not accessible to the rabbit antibody. This is consistent with prior findings where the well-conserved regions of VlsE (e.g., IR6) were shown to be inaccessible to antibody on intact spirochetes (Embers et al., 2007a; Jacek et al., 2016; Liang et al., 1999). Overall, the present data suggest that the rabbit anti-VlsE antibody do not play a role in the sterilizing immunity of NZW rabbits to the LD pathogen.

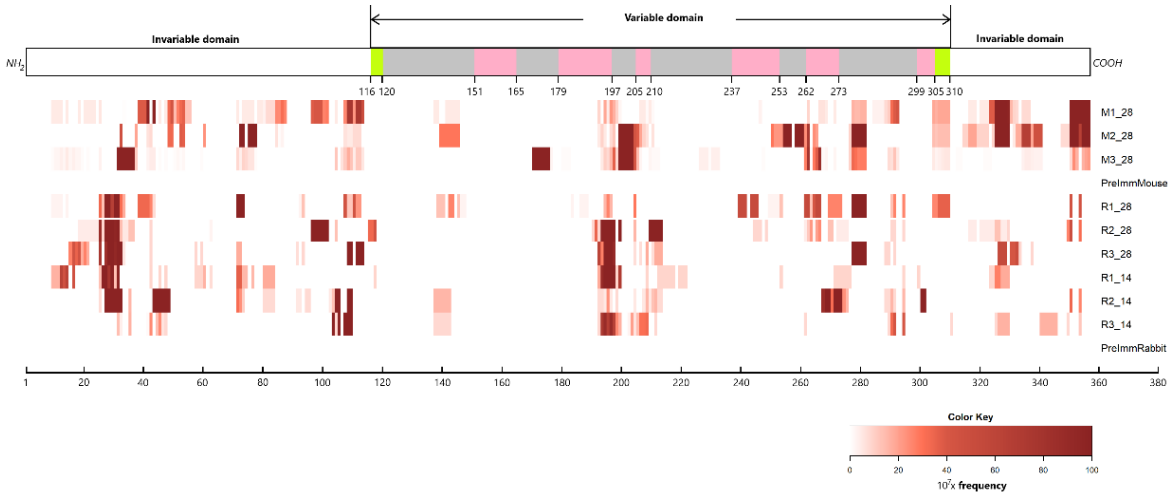

Figure 3.4 Epitope mapping of B31-VlsE. The VlsE primary structure of *B. burgdorferi* B31 strain is composed of two invariable domains and the central variable domain demarcated by two direct repeats (light green). The variable domain has six invariable (grey) and six variable (pink) regions (Eicken et al., 2002). Heat maps were generated from predicted reactivity of mouse and rabbit anti-B31 antibody to the primary structure of B31-VlsE. Immune sera were harvested from three B31-infected C3H mice at day 28 postinfection (M1_28, M2_28, M3_28) and three B31-infected rabbits at days 14 (R1_14, R2_14, R3_14) and 28 (R1_28, R2_28, R3_28) postinfection. Mouse and rabbit preimmune sera were, respectively, collected and pooled in equal amounts from the three mice (PreImmMouse) and three rabbits (PreImmRabbit) prior to the B31 challenge.

3.5. Discussion

3.5.1. An intricate role of VlsE in NZW rabbits

In humans with chronic LD, *B. burgdorferi* persists for years (Hudson et al., 1998; Kash et al., 2011; Logigian et al., 1990; Middelveen et al., 2018; Oksi et al., 1999; Stanek et al., 1990) despite a strong immune response to the infection (LaRocca and Benach, 2008; Lawrenz et al., 1999; Vaz et al., 2001; Xu et al., 2008). Numerous experimental models of various animals, such as hamster (Goodman et al., 1991; Johnson et al., 1984), dog (Appel et al., 1993; Burgess, 1986; Greene et al., 1988; Straubinger, 2000; Straubinger et al., 1997), gerbil (Preac Mursic et al., 1990), guinea pig (Sonnesyn et al., 1993), monkey

(Philipp et al., 1993; Roberts et al., 1995), mouse (Barthold et al., 1990; Hodzic et al., 2008), pony (Chang et al., 2005; Chang et al., 2000), and rat (Barthold et al., 1988) show that *B. burgdorferi* establishes persistent (chronic) infection in these mammals. The exception is NZW rabbits, which are the only known animal model, where *B. burgdorferi* fails to sustain a persistent infection (Chong-Cerrillo et al., 2000; Foley et al., 1995; Foley et al., 1997).

In the mouse model, for *B. burgdorferi* to constantly avoid mortal effect of a robust antibody response, LD spirochetes must express antigenically variable VlsE (Bankhead and Chaconas, 2007; Iyer et al., 2003; Labandeira-Rey et al., 2003; Labandeira-Rey and Skare, 2001; Lawrenz et al., 2004; McDowell et al., 2002; Purser and Norris, 2000; Rogovskyy and Bankhead, 2013; Rogovskyy et al., 2015). Since, in NZW rabbits, the clearance is mediated by humoral immunity (Chong-Cerrillo et al., 2000; Foley et al., 1997), the previously observed spontaneous loss of the *vlsE* locus-carrying plasmid by *B. burgdorferi* during the rabbit infection (Embers et al., 2007b) could potentially account for the inability of *B. burgdorferi* to persist in NZW rabbits. However, our current data unequivocally disprove this previous finding by demonstrating that LD spirochetes uniformly retain the *vls* system and yet are cleared by NZW rabbits. Thus, is the clearance of *B. burgdorferi* a result of (partially) impaired *vls* system in NZW rabbits or highly efficacious rabbit antibody response?

Numerous pieces of evidence obtained by the prior and current studies indicate that the *vls* system in rabbit-residing *B. burgdorferi* is fully functional. First, in the NZW rabbit skin, *vlsE* is highly upregulated and expressed. Our study shows that *vlsE* is

upregulated during the rabbit infection (Fig. 3.1). Consistently, by using immunoblot analysis, the prior study reveals that VlsE is the most prominent antigen expressed between day 7 and day 21 postinfection (Crother et al., 2004). Secondly, in NZW rabbits, *vlsE* recombination does occur and levels of *vlsE* gene conversion are comparable to or higher than those in mice (Embers et al., 2007b). Thirdly, the present data demonstrate that the *vls* system, which is highly efficacious for *B. burgdorferi* to constantly evade antibody in the mouse (Bankhead and Chaconas, 2007; Iyer et al., 2003; Labandeira-Rey et al., 2003; Labandeira-Rey and Skare, 2001; Lawrenz et al., 2004; McDowell et al., 2002; Purser and Norris, 2000; Rogovskyy and Bankhead, 2013; Rogovskyy et al., 2015), fails its VlsE-mediated immune-evasion function only when immunocompetent mice receive the rabbit antibody. Thus, as opposed to mice (and humans), whose antibody are ineffective against VlsE-expressing *B. burgdorferi* during the natural infection (Bankhead and Chaconas, 2007; Iyer et al., 2000; Iyer et al., 2003; Labandeira-Rey et al., 2003; Labandeira-Rey and Skare, 2001; Lawrenz et al., 2004; McDowell et al., 2002; Purser and Norris, 2000; Rogovskyy and Bankhead, 2013; Rogovskyy et al., 2015), anti-*B. burgdorferi* antibody of NZW rabbits clear the LD pathogen despite its *vls* system.

Though VlsE does not ensure a long-term infection in NZW rabbits, the current study also suggests that the presence of *vls* locus is still required for LD spirochetes to temporarily survive by presumably evading a very early immune response of NZW rabbits. The VlsE-deficient *B. burgdorferi*, which is transiently infectious in NZW rabbits, is cleared much faster than its parental VlsE-competent wild-type strain. The reason of this early clearance is not apparent. Despite our attempts to detect *vlsE* upregulation at day

3 being unsuccessful, likely due to low numbers of spirochetes; it is still possible that antigenically variable VlsE is expressed much earlier than day 7 (Crother et al., 2004). If expressed early, then it can be speculated that VlsE helps *B. burgdorferi* to avoid T-cell independent (TI) antibody, the early responders whose appearance does not require T-cell help (LaRocca and Benach, 2008). In mice, TI antibody responses are critical for the clearance of spirochetemia by Relapsing fever *Borrelia* (Alugupalli et al., 2003; Connolly and Benach, 2001). It is also plausible that VlsE is required for an early stage of spirochetal adaptation to the rabbit host independent of antibody-mediated evasion. Despite the fact that further experiments are needed to more closely examine an exact function of VlsE for the early survival in NZW rabbits, the present study concludes that, in these animals, VlsE is required for *B. burgdorferi* to establish only a very transient infection.

It is also possible that the inability of *B. burgdorferi* B31 and 297 strains to persist in NZW rabbits is due to their lack of adhesins or other bacterial factors. Prior studies showed that some wild-caught cottontail rabbits were either serologically or culture positive for *B. burgdorferi*, suggesting that cottontail rabbits may sustain a long-term infection of rabbit-adapted *B. burgdorferi* strains and therefore play a role in the enzootic cycle of LD pathogen (Anderson et al., 1989; Telford and Spielman, 1989). Regardless, in NZW rabbits, it has been consistently demonstrated that it is anti-*B. burgdorferi* immune sera that is ultimately responsible for the clearance of *B. burgdorferi* B31 (Chong-Cerrillo et al., 2000; Foley et al., 1997). NZW rabbits completely clear spirochetes from visceral organs by 8 weeks postinfection (Foley et al., 1995). Similarly, dermal infection

by wild-type B31 strain is cleared on average within 6.7 weeks postinoculation (Foley et al., 1995).

3.5.2. Potency of the rabbit antibody

The present study demonstrates that the rabbit antibody are remarkedly potent against highly immune-evasive *B. burgdorferi*. Mice treated passively with the rabbit anti-B31 antibody are completely protected not only from needle but also highly immune-evasive mouse-adapted *B. burgdorferi* B31. These results are supported by prior studies, which show that NZW rabbits with infection-derived immunity are fully protected against wild type introduced in the form of rabbit skin biopsies (rabbit-adapted spirochetes) (Shang et al., 2000; Shang et al., 2001). It should be re-emphasized that, the host-adaption prior to challenge allows wild-type spirochetes to be supremely immune-evasive, which is mainly due to abundant expression of VlsE by tissue-residing spirochetes (Liang et al., 2004b; Rogovskyy and Bankhead, 2013). In passively treated SCID mice, mouse anti-B31 antibody are avoided by wild-type *B. burgdorferi* only when spirochetes are host-adapted (Rogovskyy and Bankhead, 2013). Neither *in vitro*-grown and tick-derived wild type, whose VlsE expression is low (Crother et al., 2003; Indest et al., 2001; Liang et al., 2004b; Ohnishi et al., 2003), nor host-adapted VlsE-deficient isogenic clone has the capacity to resist mouse anti-B31 antibody (Rogovskyy and Bankhead, 2013; Rogovskyy et al., 2015).

In addition to protection against homologous challenge, the rabbit antibody can be cross-protective against heterologous infection. The present study demonstrates that anti-B31 antibody protect mice from needle *B. burgdorferi* 297, the strain that represents one

of the three major clades of *B. burgdorferi*, rDNA intergenic spacer type II (RST2) (Liveris et al., 1999; Liveris et al., 1996). However, the same rabbit antibody, when passively transferred into mice, fail to block this heterologous *B. burgdorferi* when the 297 strain is host-adapted. The overall results are consistent with prior study, which shows that B31 infection-immune NZW rabbits are susceptible to heterologous challenge with host-adapted *B. burgdorferi* N40 (RST3), Sh-2-82, or 297 (Shang et al., 2001). Together, the data indicate that, upon host-adaption, protective epitopes shared between needle *B. burgdorferi* B31 and 297 strains disappear, become subdominant, and/or become inaccessible to the rabbit antibody.

Despite that numerous previous studies showed that antibody-mediated killing of *B. burgdorferi* is complement-dependent (Kochi et al., 1993; Liang et al., 1999; Lovrich et al., 1991; Ma et al., 1995; Munson et al., 2000; Nowling and Philipp, 1999; Philipp et al., 1993), none has examined and compared a role of the rabbit complement for protection mediated by infection-induced rabbit antibody against host-adapted and *in vitro*-grown *B. burgdorferi*. As shown by the present findings, the protective efficacy of rabbit antibody predominantly depends on the presence of the rabbit complement. When the complement is destroyed, the potency of rabbit antibody against host-adapted homologous B31 strain is significantly reduced (Table 3.3). Surprisingly, the efficacy of rabbit antibody against much less immune-invasive (*in vitro*-grown) spirochetes does not depend on the complement. All the mice treated with heat-inactivated rabbit anti-B31 immune sera are uniformly protected from the needle homologous B31 strain (Table 3.3). Interestingly,

antibody-mediated killing of heterologous *in vitro*-grown *B. burgdorferi* 297 is only partially complement-dependent (Table 3.4).

Finally, in the present study, we demonstrate that, in mice with an established *B. burgdorferi* infection, the rabbit antibody have the capacity to significantly reduce pathology of LD arthritis ($P<0.05$). Amelioration of arthritis is associated with noticeable yet statistically insignificant reduction of spirochetal loads in joints of the treated mice compared to the control. This is in contrast to the ear skin tissues, where the numbers of spirochetes are significantly reduced in the treated animals. The lack of statistical significance for the spirochetal reduction in the joint tissues may be partially accounted for by a protracted timeline between the final antibody treatment and tissue harvest (19 days), short half-life of rabbit antibody (Dixon et al., 1952), and/or the limited amount of applied sera. In addition, the joints may simply be a better protective niche for *B. burgdorferi* against the rabbit antibody (Liang et al., 2004a).

Taken together, we propose a model that may explain the key difference between anti-*B. burgdorferi* antibody responses developed in mice as an animal model extensively used to study VlsE antigenic variation (or LD patients), whose antibody fail to fight off the infection and NZW rabbits, whose antibody efficiently clear LD spirochetes (Fig. 3.5). Despite the fact that, upon infection, mice and LD patients develop robust humoral responses against *B. burgdorferi* (LaRocca and Benach, 2008; Lawrenz et al., 1999; Vaz et al., 2001; Xu et al., 2008); their antibody cannot clear wild-type spirochetes due to antigenically variable VlsE (Bankhead and Chaconas, 2007; Coutte et al., 2009; Iyer et al., 2003; Labandeira-Rey et al., 2003; Labandeira-Rey and Skare, 2001; Lawrenz et al.,

2004; McDowell et al., 2002; Purser and Norris, 2000; Rogovskyy and Bankhead, 2013; Rogovskyy et al., 2015). It has been repeatedly shown that, in infected mice and LD patients, antibody are developed to various dominant protective (and non-protective) epitopes of VlsE and other surface antigens (Chandra et al., 2011; Eicken et al., 2002; Jacek et al., 2016; LaRocca and Benach, 2008; Lawrenz et al., 1999; Liang et al., 1999; Liang et al., 2001a; Liang et al., 2001b; Liang et al., 2000; Liang and Philipp, 1999, 2000; Magnarelli et al., 2002; McDowell et al., 2002; Rogovskyy et al., 2017a; Vaz et al., 2001; Xu et al., 2008). During abundant VlsE expression, any dominant protective epitopes of surface antigens become inaccessible, likely via putative VlsE-mediated shielding, to mouse (human) anti-*B. burgdorferi* antibody (Batool et al., 2018; Jacek et al., 2016; Liang et al., 2001b). At the same time, as previously proposed (Eicken et al., 2002), protective epitopes of VlsE lateral antigenically invariant surfaces are protected from mouse (human) antibody by the dense packing of VlsE molecules with each other and/or other surface proteins. As a result, only changeable protective epitopes of VlsE variable regions become a predominant target of borreliacidal anti-*B. burgdorferi* antibody (McDowell et al., 2002). However, because of ongoing VlsE-mediated antigenic variation, any newly appearing spirochetes with previously unseen VlsE variants constantly escape otherwise protective mouse (human) anti-VlsE antibody (Bankhead and Chaconas, 2007; Coutte et al., 2009; Iyer et al., 2003; Labandeira-Rey et al., 2003; Labandeira-Rey and Skare, 2001; Lawrenz et al., 2004; McDowell et al., 2002; Purser and Norris, 2000; Rogovskyy and Bankhead, 2013; Rogovskyy et al., 2015). Thus, *B. burgdorferi* establishes a life-long infection in these mammalian species. In contrast, in NZW rabbits, anti-*B. burgdorferi*

antibody are (additionally) developed against protective epitopes of surface antigens, whose antibody access is not obscured by VlsE (Fig. 3.5). Thus, as opposed to LD patients and any known LD experimental mammalian model, in NZW rabbits, development of this protective antibody repertoire results in complete clearance of LD spirochetes. Currently, as part of a larger study, we are identifying protective epitopes that are specifically recognized by the rabbit antibody and testing them as potential targets for development of a long-awaited LD subunit vaccine.

The results of the passive transfer experiment, where fully immunocompetent mice gain the capacity to prevent host-adapted *B. burgdorferi* only when they receive the rabbit antibody, indicate that, in the mouse host, protective epitopes of invariant (non-VlsE) surface antigens are still accessible to the rabbit antibody in the presence of VlsE (hence exposed protective epitopes). This, in turn, means that, in NZW rabbits, the profile of exposed protective epitopes is not (drastically) different from the respective protective epitome exposed by *B. burgdorferi* in the mouse environment. Thus, the main difference between the mouse and rabbit antibody may lie in the ability of the rabbit antibody to specifically target those protective epitopes that, despite abundant VlsE expression, remain exposed on the surface of *B. burgdorferi* - be it in the mouse or rabbit environment. It can be further speculated that the protective epitopes that are recognized by the rabbit antibody are therefore dominant and subdominant for NZW rabbit and mouse immune systems, respectively.

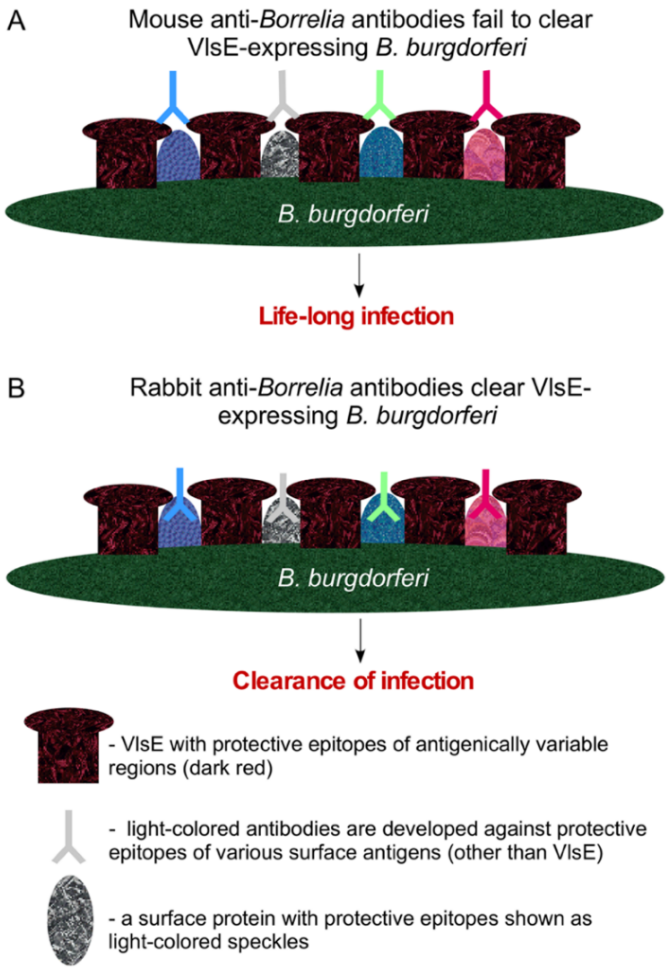

Figure 3.5 Simplified model that proposes the key difference in protective anti-*B. burgdorferi* antibody between mice and NZW rabbits. A) In infected mice, the protective antibody (light-colored "Y") are developed to various (other than VlsE) surface antigens. When VlsE is abundantly expressed in a host tissue, protective epitopes of non-VlsE surface antigens (light-colored speckles) become sterically inaccessible for the respective mouse antibody. In contrast, protective epitopes of VlsE variable regions (dark-red speckles) become a predominant target of mouse anti-VlsE antibody. However, due to antigenic variation of VlsE variable regions, newly appearing spirochetes with previously unrecognized VlsE variants will evade any already developed and otherwise protective anti-VlsE antibody. As a result, in mice, *B. burgdorferi* establishes a life-long infection. B) NZW rabbits develop (additionaly) antibody to protective epitopes of invariant surface antigens, whose antibody access is not hindered by VlsE. This results in complete clearance of LD spirochetes in NZW rabbits. Thus, the unique repertoire of NZW rabbit antibody specifically target protective epitopes of *B. burgdorferi* that are not recognized by the mouse humoral immune system.

3.6. Conclusions

To summarize, the present study provides unequivocal evidence that spirochetes retain the fully functional *vls* system during the rabbit infection. However, despite VlsE-mediated antigenic variation, *B. burgdorferi* fails to establish persistent infection in NZW rabbits. The data show that the *vls* locus is required for spirochetal survival during a very early stage of rabbit infection. Later, however, a fully developed anti-*Borrelia* antibody response clears *B. burgdorferi* despite its antigenically variable VlsE. The rabbit antibody are very potent against highly immune-evasive (mouse-adapted) *B. burgdorferi*. In addition to homologous protection, the rabbit antibody are also cross-protective against heterologous yet less immune-evasive (*in vitro*-grown) *B. burgdorferi*. Finally, the rabbit antibody have the capacity to significantly reduce arthritis pathology in mice with an established LD infection. Overall, the indication that NZW rabbits develop a unique repertoire of highly protective antibody against the LD pathogen needs to be exploited to delineate protective targets for development of the long-overdue LD vaccine.

3.7. Supplementary Data

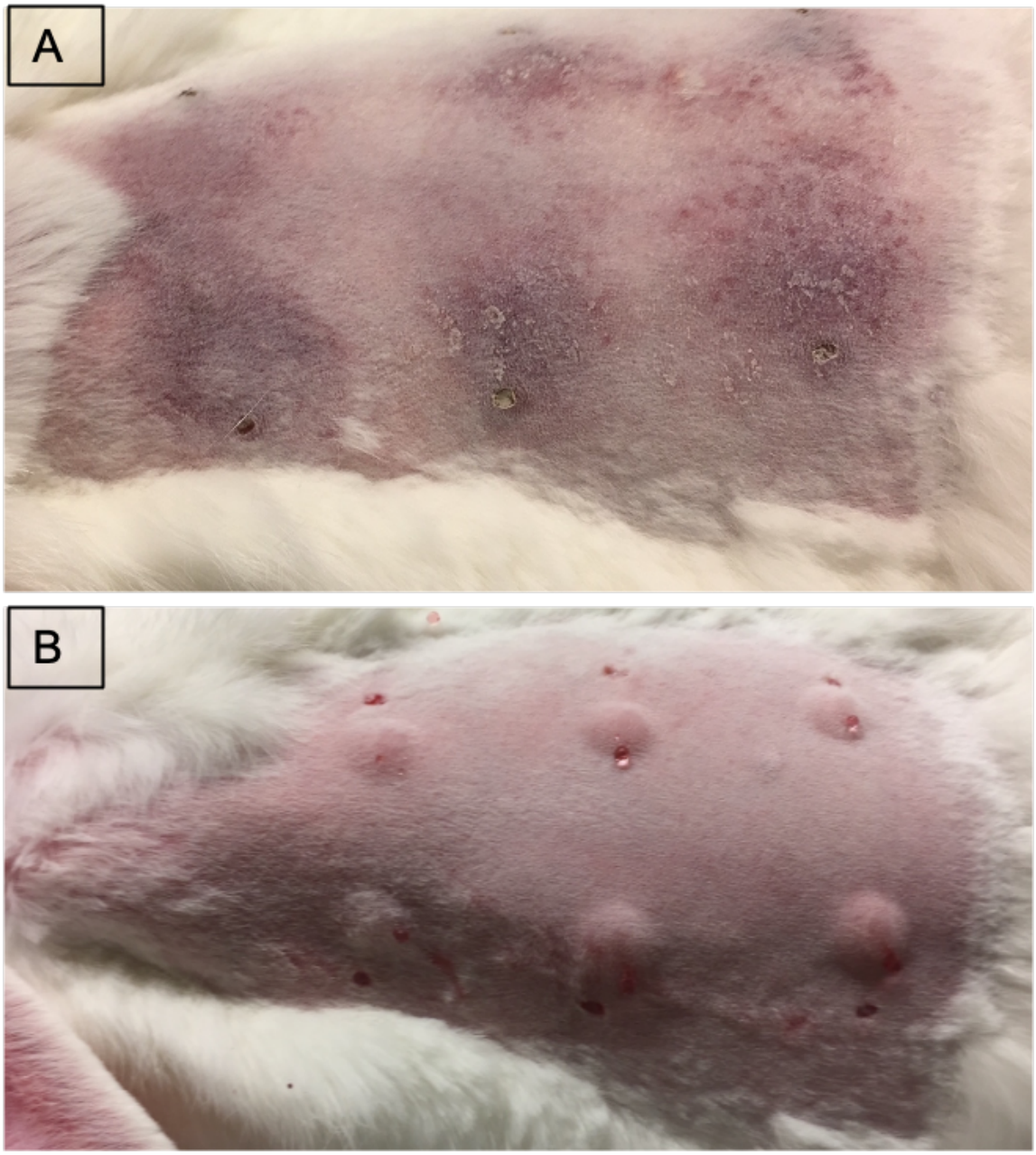

Figure 3.S1 A) Erythrema migrans developed by a ΔVlsE-infected rabbit at day 7 postchallenge. The lesions were observed around the six inoculation sites in the ΔVlsE-infected rabbit, whose skin biopsies sampled at day 7 postchallenge were culture-negative. B) The same rabbit at the time of inoculation with the ΔVlsE clone (day 0).

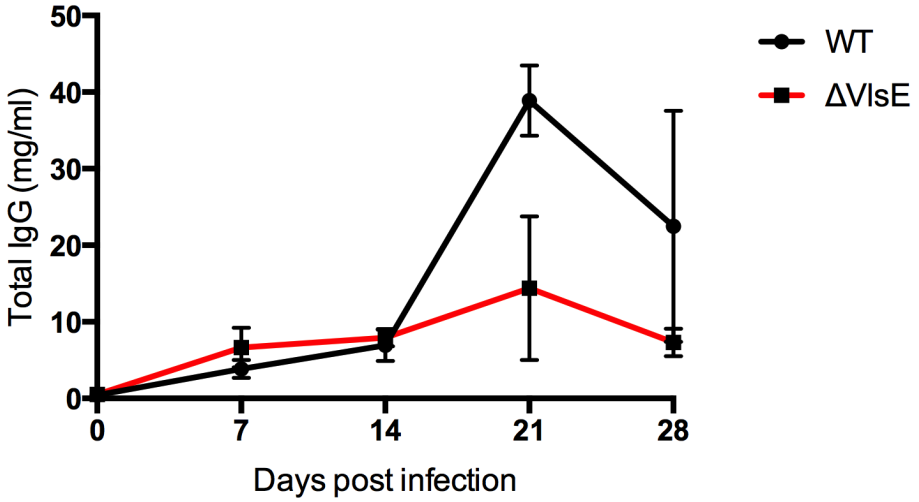

Figure 3.S2 The levels of total IgG in sera collected from B31-infected or ΔVlsE- infected New Zealand White (NZW) rabbits. Three female NZW rabbits of 12-14 weeks of age were intradermally challenged with the *B. burgdorferi* B31 or ΔVlsE clone at 1x10^6 cells per inoculation site (six sites per rabbit). Sera were weekly collected from individual rabbits and then assessed for total IgG antibody by ELISA. The levels of total IgG were not significantly different between anti-ΔVlsE sera and anti-B31 sera (P>0.05).

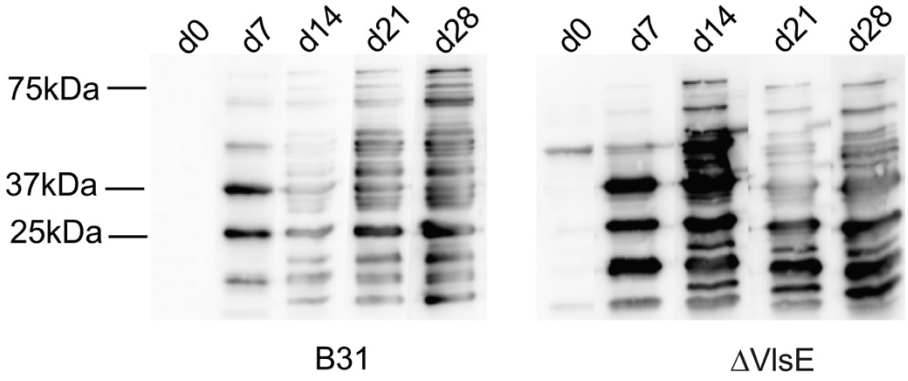

Figure 3.S3 Analysis of anti-B31 and anti-ΔVlsE immune sera by Western blotting. The whole-cell lysates of B31 clone (10^6 cells per lane) was treated with immune sera collected from B31-infected or ΔVlsE-infected rabbits at days 7, 14, 21, and 28 postchallenge. Equal amounts of immune sera from each animal of the same group per time point were pooled. The preimmune sera collected and pooled in equal volumes from three rabbits of each group prior to their challenge was used as a negative control.

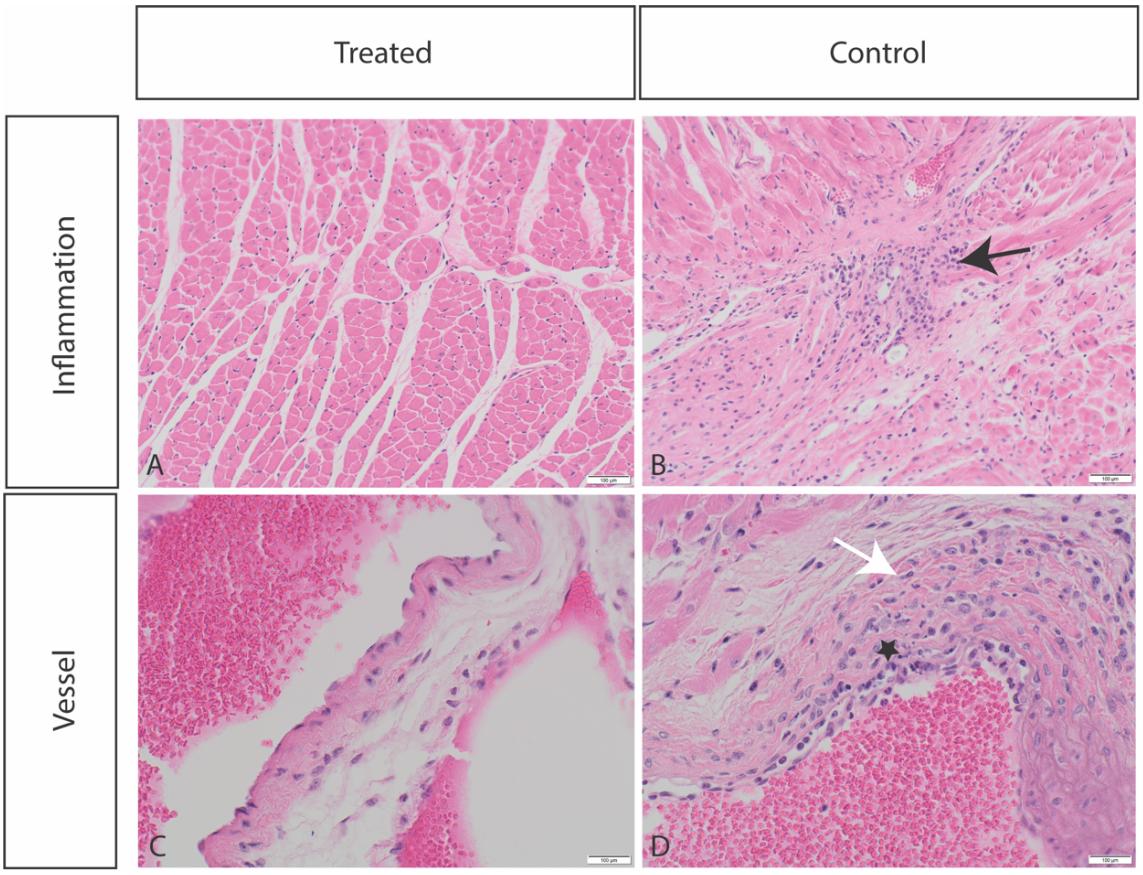

Figure 3.S4 Histopathology of heart tissues from *B. burgdorferi*-infected C3H mice that were treated with rabbit anti-*Borrelia* antibody. Representative histologic pictures of the heart from the treated and control groups of C3H mice show the absence of inflammation (A), the presence of inflammation, indicated with the black arrow (B); the absence of vessel lesions (C), and mild infiltration of vessel wall (arteritis) as indicated by the white arrow and karyorrhexis (asterisk) (D). H&E staining, scale bar represents 100μm. The histopathological scores were not significantly different between the treated (1.00±1.35) and control (1.80±1.04) groups as determined by paired t-test (P=0.1162).

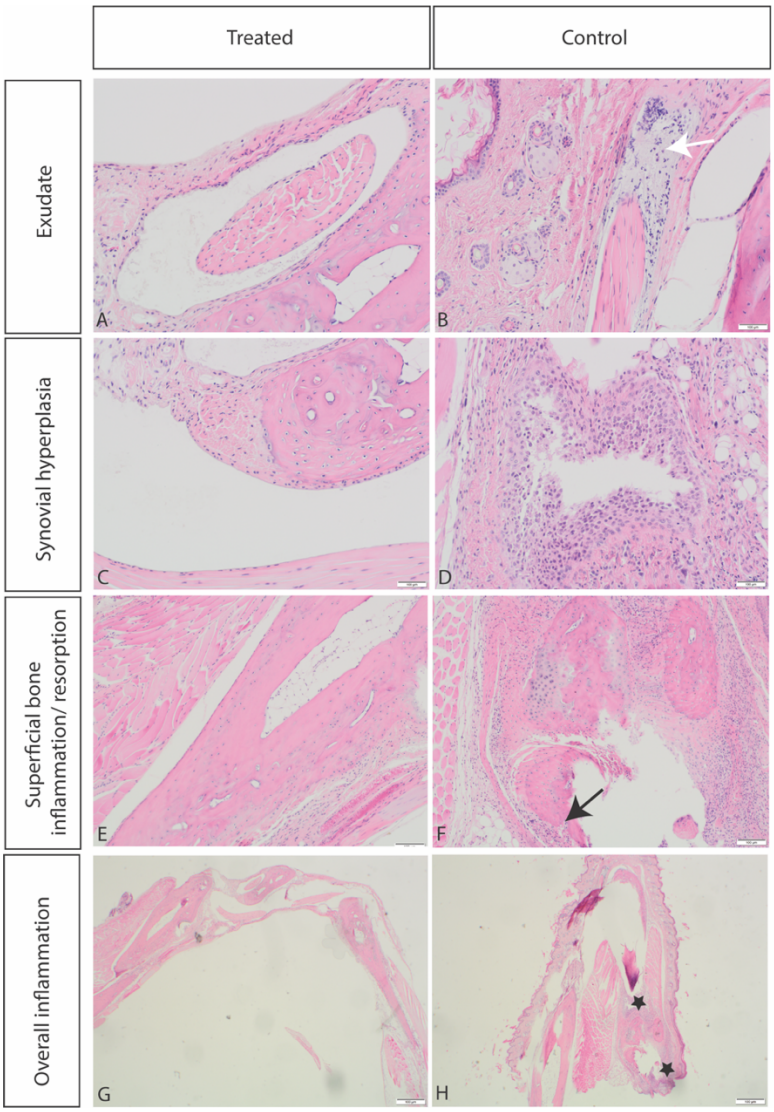

Figure 3.S5 Treatment of actively *B. burgdorferi*-infected C3H mice with rabbit anti-*Borrelia* antibody results in reduction of infection-induced joint pathology. Representative histologic pictures of tibiotarsal joints from treated (A, C, E, G) and control (B, D, F, H) groups. (A) No inflammatory cells are observed. (B) Moderate inflammation is indicated with the white arrow. (C) No synovial changes are observed. (D) Severe synovial hyperplasia is present. (E) No bone inflammation or resorption is observed. (F) Mild superficial inflammation and resorption of bone are indicated by the black arrow. (G) No inflammation is present. (H) Multifocal inflammation (asterisk) is observed. H&E staining, scale bar represents 100µm. The histopathological scores of synovial hyperplasia and overall inflammation were significantly different between the treated (0.87±0.92 and 0.94±0.78, respectively) and control (1.7±0.63 and 1.55±1.07, respectively) groups as determined by paired t-test ($P<0.05$).

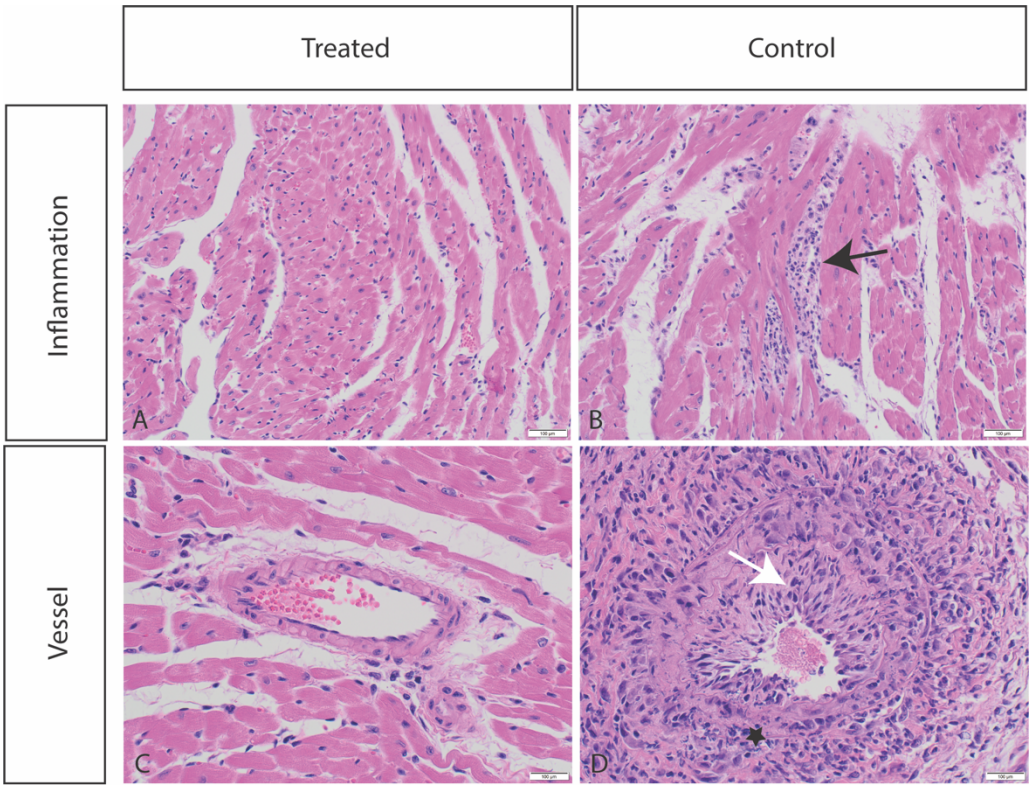

Figure 3.S6 Histopathology of heart tissues from *B. burgdorferi*-infected SCID mice that were treated with rabbit anti-*Borrelia* antibody. Representative histologic pictures of the heart from the treated and control groups of SCID mice show the absence of inflammation (A), the presence of inflammation indicated with the black arrow (B), the absence of vessel lesions (C), and infiltration of vessel wall (arteritis) as indicated by the white arrow and karyorrhexis (asterisk) (D). H&E staining, scale bar represents 100μm. The histopathological scores were not significantly different between the treated (0.33±0.41) and control (0.92±0.38) groups as determined by paired t-test (P=0.0583).

Table 3.S1 *B. burgdorferi* clones used in this study

B. burgdorferi	Presence of *vls* locus	Reference
B31-A3 (B31)	+	(Elias et al., 2002)
B31-A3/lp28-1::kan Δvls (ΔVlsE)	-	(Bankhead and Chaconas, 2007)
297	+	(Steere et al., 1983)

Table 3.S2 Culture results for skin biopsies weekly sampled from *B. burgdorferi*

Rabbit ID	Weeks postchallenge							
	1	2	3	4	5	6	7	8
1	+	+	+	+	-	-	-	-
2	+	+	+	+	+	-	-	-
3	+	+	+	*+	-	-	-	-

Table 3.S3 Culture results of tissues from *B. burgdorferi* B31-infected C3H mice that were treated with anti-*Borrelia* antibody after the infection has been established

Tissue (day of harvest postchallenge)	No. of culture positive/total no. tested	
	Treated group	Nontreated group
Blood (7)	4/4	5/5
Ear skin (45)	2/4	4/5
Heart (45)	4/4	5/5
Bladder (45)	4/4	5/5
Joint (45)	4/4	4/5

3.8. References

1. Noormohammadi AH, Markham PF, Kanci A, Whithear KG, Browning GF. 2000. A novel mechanism for control of antigenic variation in the haemagglutinin gene family of *Mycoplasma synoviae*. Mol Microbiol 35:911-923.
2. Hagblom P, Segal E, Billyard E, So M. 1985. Intragenic recombination leads to pilus antigenic variation in *Neisseria gonorrhoeae*. Nature 315:156-158.
3. Deitsch KW, Lukehart SA, Stringer JR. 2009. Common strategies for antigenic variation by bacterial, fungal and protozoan pathogens. Nat Rev Microbiol 7:493-503.
4. Dzikowski R, Deitsch KW. 2009. Genetics of antigenic variation in *Plasmodium falciparum*. Curr Genet 55:103-110.
5. Norris SJ. 2014. The *vls* antigenic variation systems of Lyme disease *Borrelia*: eluding host immunity through both random, segmental gene conversion and framework heterogeneity. Microbiol Spectr 2:doi: 10.1128/microbiolspec.MDNA1123-0038-2014.
6. McCulloch R, Morrison LJ, Hall JP. 2015. DNA recombination strategies during antigenic variation in the African Trypanosome. Microbiol Spectr 3:MDNA3-0016-2014.
7. Obergfell KP, Seifert HS. 2015. Mobile DNA in the pathogenic *Neisseria*. Microbiol Spectr 3:MDNA3-0015-2014.

8. Gargantini PR, Serradell MDC, Rios DN, Tenaglia AH, Lujan HD. 2016. Antigenic variation in the intestinal parasite *Giardia lamblia*. Curr Opin Microbiol 32:52-58.

9. Wahlgren M, Goel S, Akhouri RR. 2017. Variant surface antigens of *Plasmodium falciparum* and their roles in severe malaria. Nat Rev Microbiol 15:479-491.

10. Palmer GH, Bankhead T, Seifert HS. 2016. Antigenic variation in bacterial pathogens. Microbiol Spectr 4.

11. van der Woude MW, Baumler AJ. 2004. Phase and antigenic variation in bacteria. Clin Microbiol Rev 17:581-611.

12. Hinckley AF, Connally NP, Meek JI, Johnson BJ, Kemperman MM, Feldman KA, White JL, Mead PS. 2014. Lyme disease testing by large commercial laboratories in the United States. Clin Infect Dis 59:676-681.

13. Brownstein JS, Holford TR, Fish D. 2005. Effect of climate change on Lyme disease risk in North America. Ecohealth 2:38-46.

14. Ostfeld RS, Brunner JL. 2015. Climate change and *Ixodes* tick-borne diseases of humans. Philos Trans R Soc Lond B Biol Sci 370.

15. Cameron DJ, Johnson LB, Maloney EL. 2014. Evidence assessments and guideline recommendations in Lyme disease: the clinical management of known tick bites, erythema migrans rashes and persistent disease. Expert Rev Anti Infect Ther 12:1103-1135.

16. Arvikar SL, Steere AC. 2015. Diagnosis and treatment of Lyme arthritis. Infect Dis Clin North Am 29:269-280.

17. Lantos PM. 2015. Chronic Lyme disease. Infect Dis Clin North Am 29:325-340.

18. Melia MT, Lantos PM, Auwaerter PG. 2015. Laboratory testing for Lyme neuroborreliosis-reply. JAMA Neurol 72:126.

19. Borchers AT, Keen CL, Huntley AC, Gershwin ME. 2015. Lyme disease: a rigorous review of diagnostic criteria and treatment. J Autoimmun 57:82-115.

20. Marques AR. 2010. Lyme disease: a review. Curr Allergy Asthma Rep 10:13-20.

21. Wormser GP, Dattwyler RJ, Shapiro ED, Halperin JJ, Steere AC, Klempner MS, Krause PJ, Bakken JS, Strle F, Stanek G, Bockenstedt L, Fish D, Dumler JS, Nadelman RB. 2006. The clinical assessment, treatment, and prevention of Lyme disease, human Granulocytic Anaplasmosis, and Babesiosis: clinical practice guidelines by the Infectious Diseases Society of America. Clin Infect Dis 43:1089-1134.

22. Zhang JR, Hardham JM, Barbour AG, Norris SJ. 1997. Antigenic variation in Lyme disease borreliae by promiscuous recombination of VMP-like sequence cassettes. Cell 89:275-285.

23. Ohnishi J, Schneider B, Messer WB, Piesman J, de Silva AM. 2003. Genetic variation at the *vlsE* locus of *Borrelia burgdorferi* within ticks and mice over the course of a single transmission cycle. J Bacteriol 185:4432-4441.

24. Zhang JR, Norris SJ. 1998. Kinetics and *in vivo* induction of genetic variation of *vlsE* in *Borrelia burgdorferi*. Infect Immun 66:3689-3697.

25. Indest KJ, Howell JK, Jacobs MB, Scholl-Meeker D, Norris SJ, Philipp MT. 2001. Analysis of *Borrelia burgdorferi vlsE* gene expression and recombination in the tick vector. Infect Immun 69:7083-7090.

26. Norris SJ. 2006. The dynamic proteome of Lyme disease *Borrelia*. Genome Biol 7:209.

27. Verhey TB, Castellanos M, Chaconas G. 2018. Analysis of recombinational switching at the antigenic variation locus of the Lyme spirochete using a novel PacBio sequencing pipeline. Mol Microbiol 107:104-115.

28. Bykowski T, Babb K, von Lackum K, Riley SP, Norris SJ, Stevenson B. 2006. Transcriptional regulation of the *Borrelia burgdorferi* antigenically variable VlsE surface protein. J Bacteriol 188:4879-4889.

29. Coutte L, Botkin DJ, Gao L, Norris SJ. 2009. Detailed analysis of sequence changes occurring during *vlsE* antigenic variation in the mouse model of *Borrelia burgdorferi* infection. PLoS Pathog 5:e1000293.

30. McDowell JV, Sung SY, Hu LT, Marconi RT. 2002. Evidence that the variable regions of the central domain of VlsE are antigenic during infection with Lyme disease spirochetes. Infect Immun 70:4196-4203.

31. Purser JE, Norris SJ. 2000. Correlation between plasmid content and infectivity in *Borrelia burgdorferi*. Proc Natl Acad Sci U S A 97:13865-13870.

32. Labandeira-Rey M, Skare JT. 2001. Decreased infectivity in *Borrelia burgdorferi* strain B31 is associated with loss of linear plasmid 25 or 28-1. Infect Immun 69:446-455.

33. Labandeira-Rey M, Seshu J, Skare JT. 2003. The absence of linear plasmid 25 or 28-1 of *Borrelia burgdorferi* dramatically alters the kinetics of experimental infection via distinct mechanisms. Infect Immun 71:4608-4613.

34. Iyer R, Kalu O, Purser J, Norris S, Stevenson B, Schwartz I. 2003. Linear and circular plasmid content in *Borrelia burgdorferi* clinical isolates. Infect Immun 71:3699-3706.

35. Lawrenz MB, Wooten RM, Norris SJ. 2004. Effects of *vlsE* complementation on the infectivity of *Borrelia burgdorferi* lacking the linear plasmid lp28-1. Infect Immun 72:6577-6585.

36. Bankhead T, Chaconas G. 2007. The role of VlsE antigenic variation in the Lyme disease spirochete: persistence through a mechanism that differs from other pathogens. Mol Microbiol 65:1547-1558.

37. Rogovskyy AS, Bankhead T. 2013. Variable VlsE is critical for host reinfection by the Lyme disease spirochete. PLoS One 8:e61226.

38. Rogovskyy AS, Casselli T, Tourand Y, Jones CR, Owen JP, Mason KL, Scoles GA, Bankhead T. 2015. Evaluation of the importance of VlsE antigenic variation for the enzootic cycle of *Borrelia burgdorferi*. PLoS One 10:e0124268.

39. Hudson BJ, Stewart M, Lennox VA, Fukunaga M, Yabuki M, Macorison H, Kitchener-Smith J. 1998. Culture-positive Lyme borreliosis. Med J Aust 168:500-502.

40. Oksi J, Marjamaki M, Nikoskelainen J, Viljanen MK. 1999. *Borrelia burgdorferi* detected by culture and PCR in clinical relapse of disseminated Lyme borreliosis. Ann Med 31:225-232.

41. Kash N, Fink-Puches R, Cerroni L. 2011. Cutaneous manifestations of B-cell chronic lymphocytic leukemia associated with *Borrelia burgdorferi* infection showing a marginal zone B-cell lymphoma-like infiltrate. Am J Dermatopathol 33:712-715.

42. Middelveen MJ, Sapi E, Burke J, Filush KR, Franco A, Fesler MC, Stricker RB. 2018. Persistent *Borrelia* infection in patients with ongoing symptoms of Lyme disease. Healthcare (Basel) 6.

43. Logigian EL, Kaplan RF, Steere AC. 1990. Chronic neurologic manifestations of Lyme disease. N Engl J Med 323:1438-1444.

44. Stanek G, Klein J, Bittner R, Glogar D. 1990. Isolation of *Borrelia burgdorferi* from the myocardium of a patient with longstanding cardiomyopathy. N Engl J Med 322:249-252.

45. Johnson RC, Marek N, Kodner C. 1984. Infection of Syrian hamsters with Lyme disease spirochetes. J Clin Microbiol 20:1099-1101.

46. Goodman JL, Jurkovich P, Kodner C, Johnson RC. 1991. Persistent cardiac and urinary tract infections with *Borrelia burgdorferi* in experimentally infected Syrian hamsters. J Clin Microbiol 29:894-896.

47. Burgess EC. 1986. Experimental inoculation of dogs with *Borrelia burgdorferi*. Zentralbl Bakteriol Mikrobiol Hyg A 263:49-54.

48. Greene RT, Levine JF, Breitschwerdt EB, Walker RL, Berkhoff HA, Cullen J, Nicholson WL. 1988. Clinical and serologic evaluations of induced *Borrelia burgdorferi* infection in dogs. Am J Vet Res 49:752-757.

49. Straubinger RK, Summers BA, Chang YF, Appel MJ. 1997. Persistence of *Borrelia burgdorferi* in experimentally infected dogs after antibiotic treatment. J Clin Microbiol 35:111-116.

50. Straubinger RK. 2000. PCR-Based quantification of *Borrelia burgdorferi* organisms in canine tissues over a 500-Day postinfection period. J Clin Microbiol 38:2191-2199.

51. Appel MJ, Allan S, Jacobson RH, Lauderdale TL, Chang YF, Shin SJ, Thomford JW, Todhunter RJ, Summers BA. 1993. Experimental Lyme disease in dogs produces arthritis and persistent infection. J Infect Dis 167:651-664.

52. Preac Mursic V, Patsouris E, Wilske B, Reinhardt S, Gross B, Mehraein P. 1990. Persistence of *Borrelia burgdorferi* and histopathological alterations in experimentally infected animals. A comparison with histopathological findings in human Lyme disease. Infection 18:332-341.

53. Sonnesyn SW, Manivel JC, Johnson RC, Goodman JL. 1993. A guinea pig model for Lyme disease. Infect Immun 61:4777-4784.

54. Philipp MT, Aydintug MK, Bohm RP, Jr., Cogswell FB, Dennis VA, Lanners HN, Lowrie RC, Jr., Roberts ED, Conway MD, Karacorlu M, Peyman GA, Gubler DJ, Johnson BJ, Piesman J, Gu Y. 1993. Early and early disseminated

phases of Lyme disease in the rhesus monkey: a model for infection in humans. Infect Immun 61:3047-3059.

55. Roberts ED, Bohm RP, Jr., Cogswell FB, Lanners HN, Lowrie RC, Jr., Povinelli L, Piesman J, Philipp MT. 1995. Chronic Lyme disease in the rhesus monkey. Lab Invest 72:146-160.

56. Barthold SW, Beck DS, Hansen GM, Terwilliger GA, Moody KD. 1990. Lyme borreliosis in selected strains and ages of laboratory mice. J Infect Dis 162:133-138.

57. Hodzic E, Feng S, Holden K, Freet KJ, Barthold SW. 2008. Persistence of *Borrelia burgdorferi* following antibiotic treatment in mice. Antimicrob Agents Chemother 52:1728-1736.

58. Chang YF, Ku YW, Chang CF, Chang CD, McDonough SP, Divers T, Pough M, Torres A. 2005. Antibiotic treatment of experimentally *Borrelia burgdorferi*-infected ponies. Vet Microbiol 107:285-294.

59. Chang YF, Novosol V, McDonough SP, Chang CF, Jacobson RH, Divers T, Quimby FW, Shin S, Lein DH. 2000. Experimental infection of ponies with *Borrelia burgdorferi* by exposure to Ixodid ticks. Vet Pathol 37:68-76.

60. Barthold SW, Moody KD, Terwilliger GA, Duray PH, Jacoby RO, Steere AC. 1988. Experimental Lyme arthritis in rats infected with *Borrelia burgdorferi*. J Infect Dis 157:842-846.

61. Foley DM, Gayek RJ, Skare JT, Wagar EA, Champion CI, Blanco DR, Lovett MA, Miller JN. 1995. Rabbit model of Lyme borreliosis: erythema migrans,

infection-derived immunity, and identification of *Borrelia burgdorferi* proteins associated with virulence and protective immunity. J Clin Invest 96:965-975.

62. Embers ME, Liang FT, Howell JK, Jacobs MB, Purcell JE, Norris SJ, Johnson BJ, Philipp MT. 2007. Antigenicity and recombination of VlsE, the antigenic variation protein of *Borrelia burgdorferi*, in rabbits, a host putatively resistant to long-term infection with this spirochete. FEMS Immunol Med Microbiol 50:421-429.

63. Batool M, Caoili SEC, Dangott LJ, Gerasimov E, Ionov Y, Piontkivska H, Zelikovsky A, Waghela SD, Rogovskyy AS. 2018. Identification of surface epitopes associated with protection against highly immune-evasive VlsE-expressing Lyme disease spirochetes. Infect Immun doi:10.1128/IAI.00182-18.

64. Kornblatt AN, Steere AC, Brownstein DG. 1984. Experimental Lyme disease in rabbits: spirochetes found in erythema migrans and blood. Infect Immun 46:220-223.

65. Hinnebusch J, Barbour AG. 1992. Linear- and circular-plasmid copy numbers in *Borrelia burgdorferi*. J Bacteriol 174:5251-5257.

66. Barbour AG. 1988. Plasmid analysis of *Borrelia burgdorferi*, the Lyme disease agent. J Clin Microbiol 26:475-478.

67. Schwan TG, Burgdorfer W, Garon CF. 1988. Changes in infectivity and plasmid profile of the Lyme disease spirochete, *Borrelia burgdorferi*, as a result of *in vitro* cultivation. Infect Immun 56:1831-1836.

68. Moody KD, Barthold SW, Terwilliger GA. 1990. Lyme borreliosis in laboratory animals: effect of host species and *in vitro* passage of *Borrelia burgdorferi*. Am J Trop Med Hyg 43:87-92.

69. Simpson WJ, Garon CF, Schwan TG. 1990. Analysis of supercoiled circular plasmids in infectious and non-infectious *Borrelia burgdorferi*. Microb Pathog 8:109-118.

70. Lawrenz MB, Hardham JM, Owens RT, Nowakowski J, Steere AC, Wormser GP, Norris SJ. 1999. Human antibody responses to VlsE antigenic variation protein of *Borrelia burgdorferi*. J Clin Microbiol 37:3997-4004.

71. Crother TR, Champion CI, Wu XY, Blanco DR, Miller JN, Lovett MA. 2003. Antigenic composition of *Borrelia burgdorferi* during infection of SCID mice. Infect Immun 71:3419-3428.

72. Liang FT, Yan J, Mbow ML, Sviat SL, Gilmore RD, Mamula M, Fikrig E. 2004. *Borrelia burgdorferi* changes its surface antigenic expression in response to host immune responses. Infect Immun 72:5759-5767.

73. Johnson RC, Kodner C, Russell M. 1986. Passive immunization of hamsters against experimental infection with the Lyme disease spirochete. Infect Immun 53:713-714.

74. Blunt T, Finnie NJ, Taccioli GE, Smith GC, Demengeot J, Gottlieb TM, Mizuta R, Varghese AJ, Alt FW, Jeggo PA, Jackson SP. 1995. Defective DNA-dependent protein kinase activity is linked to V(D)J recombination and DNA repair defects associated with the murine *scid* mutation. Cell 80:813-823.

75. Beamer WG, Shultz KL, Tennent BJ, Shultz LD. 1993. Granulosa cell tumorigenesis in genetically hypogonadal-immunodeficient mice grafted with ovaries from tumor-susceptible donors. Cancer Res 53:3741-3746.

76. Custer RP, Bosma GC, Bosma MJ. 1985. Severe combined immunodeficiency (SCID) in the mouse. Pathology, reconstitution, neoplasms. Am J Pathol 120:464-477.

77. Bosma M, Schuler W, Bosma G. 1988. The scid mouse mutant. Curr Top Microbiol Immunol 137:197-202.

78. Rogovskyy AS, Gillis DC, Ionov Y, Gerasimov E, Zelikovsky A. 2017. Antibody response to Lyme disease spirochetes in the context of VlsE-mediated immune evasion. Infect Immun 85:1 e00890-00816.

79. Chandra A, Latov N, Wormser GP, Marques AR, Alaedini A. 2011. Epitope mapping of antibodies to VlsE protein of *Borrelia burgdorferi* in post-Lyme disease syndrome. Clin Immunol 141:103-110.

80. Philipp MT, Bowers LC, Fawcett PT, Jacobs MB, Liang FT, Marques AR, Mitchell PD, Purcell JE, Ratterree MS, Straubinger RK. 2001. Antibody response to IR6, a conserved immunodominant region of the VlsE lipoprotein, wanes rapidly after antibiotic treatment of *Borrelia burgdorferi* infection in experimental animals and in humans. J Infect Dis 184:870-878.

81. Liang FT, Philipp MT. 2000. Epitope mapping of the immunodominant invariable region of *Borrelia burgdorferi* VlsE in three host species. Infect Immun 68:2349-2352.

82. Liang FT, Alvarez AL, Gu Y, Nowling JM, Ramamoorthy R, Philipp MT. 1999. An immunodominant conserved region within the variable domain of VlsE, the variable surface antigen of *Borrelia burgdorferi*. J Immunol 163:5566-5573.

83. Liang FT, Philipp MT. 1999. Analysis of antibody response to invariable regions of VlsE, the variable surface antigen of *Borrelia burgdorferi*. Infect Immun 67:6702-6706.

84. Jacek E, Tang KS, Komorowski L, Ajamian M, Probst C, Stevenson B, Wormser GP, Marques AR, Alaedini A. 2016. Epitope-specific evolution of human B cell responses to *Borrelia burgdorferi* VlsE protein from early to late stages of Lyme disease. J Immunol 196:1036-1043.

85. Embers ME, Jacobs MB, Johnson BJ, Philipp MT. 2007. Dominant epitopes of the C6 diagnostic peptide of *Borrelia burgdorferi* are largely inaccessible to antibody on the parent VlsE molecule. Clin Vaccine Immunol 14:931-936.

86. Vaz A, Glickstein L, Field JA, McHugh G, Sikand VK, Damle N, Steere AC. 2001. Cellular and humoral immune responses to *Borrelia burgdorferi* antigens in patients with culture-positive early Lyme disease. Infect Immun 69:7437-7444.

87. LaRocca TJ, Benach JL. 2008. The important and diverse roles of antibodies in the host response to *Borrelia* infections. Curr Top Microbiol Immunol 319:63-103.

88. Xu Y, Bruno JF, Luft BJ. 2008. Profiling the humoral immune response to *Borrelia burgdorferi* infection with protein microarrays. Microb Pathog 45:403-407.

89. Chong-Cerrillo C, Wu X, Wang Y, Blanco DR, Lovett MA, Miller JN. 2000. Immune serum from rabbits infected with *Borrelia burgdorferi* B31 confers complete passive protection against homologous challenge. J Spiro Tick-Borne Dis:3-9.

90. Foley DM, Wang YP, Wu XY, Blanco DR, Lovett MA, Miller JN. 1997. Acquired resistance to *Borrelia burgdorferi* infection in the rabbit. Comparison between outer surface protein A vaccine- and infection-derived immunity. J Clin Invest 99:2030-2035.

91. Anderson JF, Magnarelli LA, LeFebvre RB, Andreadis TG, McAninch JB, Perng GC, Johnson RC. 1989. Antigenically variable *Borrelia burgdorferi* isolated from cottontail rabbits and Ixodes dentatus in rural and urban areas. J Clin Microbiol 27:13-20.

92. Telford SR, 3rd, Spielman A. 1989. Enzootic transmission of the agent of Lyme disease in rabbits. Am J Trop Med Hyg 41:482-490.

93. Crother TR, Champion CI, Whitelegge JP, Aguilera R, Wu XY, Blanco DR, Miller JN, Lovett MA. 2004. Temporal analysis of the antigenic composition of *Borrelia burgdorferi* during infection in rabbit skin. Infect Immun 72:5063-5072.

94. Iyer R, Hardham JM, Wormser GP, Schwartz I, Norris SJ. 2000. Conservation and heterogeneity of *vlsE* among human and tick isolates of *Borrelia burgdorferi*. Infect Immun 68:1714-1718.

95. Connolly SE, Benach JL. 2001. Cutting edge: the spirochetemia of murine relapsing fever is cleared by complement-independent bactericidal antibodies. J Immunol 167:3029-3032.

96. Alugupalli KR, Gerstein RM, Chen J, Szomolanyi-Tsuda E, Woodland RT, Leong JM. 2003. The resolution of relapsing fever borreliosis requires IgM and is concurrent with expansion of B1b lymphocytes. J Immunol 170:3819-3827.

97. Shang ES, Champion CI, Wu XY, Skare JT, Blanco DR, Miller JN, Lovett MA. 2000. Comparison of protection in rabbits against host-adapted and cultivated *Borrelia burgdorferi* following infection-derived immunity or immunization with outer membrane vesicles or outer surface protein A. Infect Immun 68:4189-4199.

98. Shang ES, Wu XY, Lovett MA, Miller JN, Blanco DR. 2001. Homologous and heterologous *Borrelia burgdorferi* challenge of infection-derived immune rabbits using host-adapted organisms. Infect Immun 69:593-598.

99. Liveris D, Varde S, Iyer R, Koenig S, Bittker S, Cooper D, McKenna D, Nowakowski J, Nadelman RB, Wormser GP, Schwartz I. 1999. Genetic diversity of *Borrelia burgdorferi* in Lyme disease patients as determined by culture versus direct PCR with clinical specimens. J Clin Microbiol 37:565-569.

100. Liveris D, Wormser GP, Nowakowski J, Nadelman R, Bittker S, Cooper D, Varde S, Moy FH, Forseter G, Pavia CS, Schwartz I. 1996. Molecular typing of

Borrelia burgdorferi from Lyme disease patients by PCR-restriction fragment length polymorphism analysis. J Clin Microbiol 34:1306-1309.

101. Nowling JM, Philipp MT. 1999. Killing of *Borrelia burgdorferi* by antibody elicited by OspA vaccine is inefficient in the absence of complement. Infect Immun 67:443-445.

102. Ma J, Gingrich-Baker C, Franchi PM, Bulger P, Coughlin RT. 1995. Molecular analysis of neutralizing epitopes on outer surface proteins A and B of *Borrelia burgdorferi*. Infect Immun 63:2221-2227.

103. Kochi SK, Johnson RC, Dalmasso AP. 1993. Facilitation of complement-dependent killing of the Lyme disease spirochete, *Borrelia burgdorferi*, by specific immunoglobulin G Fab antibody fragments. Infect Immun 61:2532-2536.

104. Lovrich SD, Callister SM, Schmitz JL, Alder JD, Schell RF. 1991. Borreliacidal activity of sera from hamsters infected with the Lyme disease spirochete. Infect Immun 59:2522-2528.

105. Munson EL, Du Chateau BK, Jobe DA, Lovrich SD, Callister SM, Schell RF. 2000. Production of borreliacidal antibody to outer surface protein A *in vitro* and modulation by interleukin-4. Infect Immun 68:5496-5501.

106. Dixon FJ, Talmage DW, Maurer PH, Deichmiller M. 1952. The half-life on homologous gamma globulin (antibody) in several species. J Exp Med 95:313-318.

107. Liang FT, Brown EL, Wang T, Iozzo RV, Fikrig E. 2004. Protective niche for *Borrelia burgdorferi* to evade humoral immunity. Am J Pathol 165:977-985.

108. Magnarelli LA, Lawrenz M, Norris SJ, Fikrig E. 2002. Comparative reactivity of human sera to recombinant VlsE and other *Borrelia burgdorferi* antigens in class-specific enzyme-linked immunosorbent assays for Lyme borreliosis. J Med Microbiol 51:649-655.

109. Eicken C, Sharma V, Klabunde T, Lawrenz MB, Hardham JM, Norris SJ, Sacchettini JC. 2002. Crystal structure of Lyme disease variable surface antigen VlsE of *Borrelia burgdorferi*. J Biol Chem 277:21691-21696.

110. Liang FT, Bowers LC, Philipp MT. 2001. C-terminal invariable domain of VlsE is immunodominant but its antigenicity is scarcely conserved among strains of Lyme disease spirochetes. Infect Immun 69:3224-3231.

111. Liang FT, Jacobs MB, Philipp MT. 2001. C-terminal invariable domain of VlsE may not serve as target for protective immune response against *Borrelia burgdorferi*. Infect Immun 69:1337-1343.

112. Liang FT, Nowling JM, Philipp MT. 2000. Cryptic and exposed invariable regions of VlsE, the variable surface antigen of *Borrelia burgdorferi* sl. J Bacteriol 182:3597-3601.

113. Elias AF, Stewart PE, Grimm D, Caimano MJ, Eggers CH, Tilly K, Bono JL, Akins DR, Radolf JD, Schwan TG, Rosa P. 2002. Clonal polymorphism of *Borrelia burgdorferi* strain B31 MI: implications for mutagenesis in an infectious strain background. Infect Immun 70:2139-2150.

114. Bunikis I, Kutschan-Bunikis S, Bonde M, Bergstrom S. 2011. Multiplex PCR as a tool for validating plasmid content of *Borrelia burgdorferi*. J Microbiol Methods 86:243-247.

115. Schmittgen TD, Livak KJ. 2008. Analyzing real-time PCR data by the comparative C(T) method. Nat Protoc 3:1101-1108.

116. Barthold SW. 1993. Antigenic stability of *Borrelia burgdorferi* during chronic infections of immunocompetent mice. Infect Immun 61:4955-4961.

117. Rogovskyy AS, Bankhead T. 2014. Bacterial heterogeneity is a requirement for host superinfection by the Lyme disease spirochete. Infect Immun 82:4542-4552.

118. Bergman I, Basse PH, Barmada MA, Griffin JA, Cheung NK. 2000. Comparison of *in vitro* antibody-targeted cytotoxicity using mouse, rat and human effectors. Cancer Immunol Immunother 49:259-266.

119. Ratelade J, Verkman AS. 2014. Inhibitor(s) of the classical complement pathway in mouse serum limit the utility of mice as experimental models of neuromyelitis optica. Mol Immunol 62:104-113.

120. Ebanks RO, Isenman DE. 1996. Mouse complement component C4 is devoid of classical pathway C5 convertase subunit activity. Mol Immunol 33:297-309.

121. Soltis RD, Hasz D, Morris MJ, Wilson ID. 1979. The effect of heat inactivation of serum on aggregation of immunoglobulins. Immunology 36:37-45.

122. Li X, Liu X, Beck DS, Kantor FS, Fikrig E. 2006. *Borrelia burgdorferi* lacking BBK32, a fibronectin-binding protein, retains full pathogenicity. Infect Immun 74:3305-3313.

123. Morrison TB, Ma Y, Weis JH, Weis JJ. 1999. Rapid and sensitive quantification of *Borrelia burgdorferi*-infected mouse tissues by continuous fluorescent monitoring of PCR. J Clin Microbiol 37:987-992.

124. Liu X, Hu Q, Liu S, Tallo LJ, Sadzewicz L, Schettine CA, Nikiforov M, Klyushnenkova EN, Ionov Y. 2013. Serum antibody repertoire profiling using *in silico* antigen screen. PLoS One 8:e67181.

125. Steere AC, Grodzicki RL, Kornblatt AN, Craft JE, Barbour AG, Burgdorfer W, Schmid GP, Johnson E, Malawista SE. 1983. The spirochetal etiology of Lyme disease. N Engl J Med 308:733-740.

4. METAGENOMIC ANALYSIS OF INDIVIDUALLY ANALYZED TICKS FROM EASTERN EUROPE DEMONSTRATES REGIONAL AND SEX-DEPENDENT DIFFERENCES IN THE MICROBIOTA OF *IXODES RICNUS* [3*]

©Ticks and tick-borne diseases

Maliha Batool[1], John C Blazier[2], Yuliya V Rogovska[1], Jiangli Wang[3], Shuling Liu[4], Igor V Nebogatkin[5], Artem S Rogovskyy[1]

1. Department of Veterinary Pathobiology, College of Veterinary Medicine and Biomedical Sciences, Texas A&M University, College Station, Texas, USA.
2. Texas A&M Institute for Genomics Sciences and Society, Texas A&M University, College Station, Texas, USA.
3. Department of Statistics and Finance, the University of Science and Technology of China, Anhui, 230026, China.
4. Statistical Collaboration Center, Department of Statistics, College of Science, Texas A&M University, College Station, Texas, USA.
5. I.I. Schmalhausen Institute of Zoology of National Academy of Sciences of Ukraine, Kyiv, 01601, Ukraine.

---

[3]*Reprinted with permission from "Metagenomic analysis of individually analyzed ticks from Eastern Europe demonstrates regional and sex-dependent differences in the microbiota of *Ixodes ricnus*" by Batool M., Blazier J.C., Rogovska Y.V., Wang J., Liu S., Nebogatkin I.V., Rogovskyy A.S., 2021. *Ticks and Tick-borne diseases*, 12, 101768, Copyright [2021] by Elsevier Journals.

4.1. Overview

Understanding the microbial ecology of disease vectors may be useful for development of novel strategies aimed at preventing transmission of vector-borne pathogens. Although *Ixodes ricinus* is one of the most important tick vectors, the microbiota of *I. ricinus* ticks has been examined for only limited parts of the globe. To date, the microbiota of *I. ricinus* ticks collected from Eastern Europe has not been defined. The objective of this study was to compare microbiota of *I. ricinus* ticks within (males vs. females) and between collection sites that represented three administrative regions of Ukraine, Dnipropetrovs'k (D), Kharkiv (K), and Poltava (P). A total of 89 questing *I. ricinus* adults were collected from region D (number of ticks, n=29; 14 males and 15 females), region K (n=30; 15 males and 15 females) and region P (n=30; 15 males and 15 females). Each tick was subjected to metagenomic analysis by targeting the V6 region of 16S rRNA gene through the Illumina 4000 Hiseq sequencing. The alpha diversity analyses demonstrated that, regardless of tick sex, patterns of bacterial diversity in ticks from regions K and P were similar, whereas the microbiota of region D ticks was quite distinct. A number of inter-regional differences were detected by most beta diversity metrics for both males and females. The inter-regional variations were also supported by the principal coordinate analysis based on the unweighted UniFrac metrics with three region-specific clusters of female ticks and one distinct cluster of region D males. Lastly, numerous region- and sex-specific differences were also identified in the relative abundance of various bacterial taxa. Collectively, the present findings demonstrate that the microbiota

of *I. ricinus* tick can exhibit a high degree of variation between tick sexes and geographical regions.

4.2. Introduction

Over the recent decades vector-borne diseases (VBDs) have represented one of serious challenges to the global health of both humans and animals (Couper and Swei, 2018; Saldana et al., 2017). It is estimated that VBDs are responsible for more than 17% of all infectious diseases, which result in ~700,000 deaths every year (WHO, 2020). Unfortunately, for most VBDs, vaccines are either not efficacious or have not been yet developed, necessitating the scientific community to explore other mitigation strategies (Couper and Swei, 2018; Saldana et al., 2017). The characterization of vector microbiota under variable environmental and experimental conditions may provide potential avenues for designing new measures to control VBDs (Couper and Swei, 2018).

Ticks are an important group of hematophagous arthropod vectors due to their ability to carry and transmit a much greater variety of pathogens than any other arthropod vectors (Clay and Fuqua, 2010). Globally, more than 900 species of ticks have been recorded and several of them are recognized as the leading vectors of diseases in animals and humans (Barker and Murrell, 2004; de la Fuente et al., 2008). Unfortunately, the case reporting and monitoring of tick-borne diseases are generally deficient, which results in poor estimation of their true incidence.

Prior to the Next Generation Sequencing (NGS) technology, identification of pathogens heavily relied on lower throughput techniques, namely: culturing, microscopy, and relatively recent molecular tools (e.g., PCR amplifications coupled with Sanger

sequencing) (Benson et al., 2004; Clay et al., 2008; Heise et al., 2010; Houpikian and Raoult, 2002; Moreno et al., 2006; Noda et al., 1997; Schabereiter-Gurtner et al., 2003; Van Overbeek et al., 2008). However, each of these methods has some inherited limitations including low sensitivity and characterization of only a fraction of microbiota (Wade, 2002). With the advent of NGS, some major limitations have been overcome, which, to date, allows host-associated, often non-culturable microbial communities to be rapidly and comprehensively identified (Carpi et al., 2011). Sequencing of 16S rRNA gene fragments results in identification of the entire microbial diversity of ticks at the genus level (Janda and Abbott, 2007; Klindworth et al., 2013; Menchaca et al., 2013; Williams-Newkirk et al., 2014).

Among medically important ticks, the sheep tick, *Ixodes ricinus* (Acari: Ixodidae), is one of the most abundant and epidemiologically important tick species in Europe (Medlock et al., 2013). In addition to being the principle vector for the Lyme disease pathogen, *Borreliella burgdorferi* sensu lato, *I. ricinus* ticks carry numerous other medically important pathogens: *Anaplasma phagocytophilum*, *Babesia divergens, Babesia microti*, *Borrelia miyamotoi, Ehrlichia phagocytophila, Rickettsia helvetica*, *Rickettsia monacensis*, Louping ill virus, and tick-borne encephalitis virus (Medlock et al., 2013; Parola and Raoult, 2001; Rizzoli et al., 2011b). Moreover, besides the tick-borne pathogens, *I. ricinus* ticks also harbor non-pathogenic microorganisms such as endosymbiotic, commensal, mutualistic, and parasitic bacteria (Hayes and Burgdorfer, 1982; Noda et al., 1997; Sacchi et al., 2004; Scoles, 2004). Although *I. ricinus* ticks are of public health significance in the Northern hemisphere, their microbiota has been defined

only for limited parts of the globe (Aivelo et al., 2019; Carpi et al., 2011; Hernandez-Jarguin et al., 2018; Kmet and Čaplová, 2019; Nakao et al., 2013; Portillo et al., 2019; Vayssier-Taussat et al., 2013). To date, microbiota of ticks from Eastern Europe has not been yet examined. Therefore, the objective of this study was to compare microbiota of *I. ricinus* ticks within (males vs. females) and between collection sites that represented three administrative regions of Ukraine (Dnipropetrovs'k, Kharkiv, and Poltava).

4.3. Materials and Methods

4.3.1. Tick collection, sample preparation, and DNA extraction

A total of 15 males and 15 females of questing *I. ricinus* ticks were collected from sites, which represented three administrative regions (also known as oblasts) of Ukraine: Dnipropetrovs'k (D; Nikopol district [47°35'07.8"N 34°22'28.9"E]), Kharkiv (K; Kharkiv [49°58'33.9"N 36°16'02.6"E] and Zmiiv [49°33'32.8"N 36°06'23.7"E] districts), and Poltava (P; Lokhvytsia [50°23'12.9"N 33°18'32.3"E], Lubny [49°59'33.2"N 33°02'00.1"E], and Orzhytsia districts [49°44'01.0"N 32°43'10.5"E]). The sampling sites were selected because tick habitats (the forest-steppe zone of Ukraine; collection distance was 3-5 km) and indices of abundance (IA) were very similar. Means of IA, which were determined as previously described (Rogovskyy et al., 2017b), were 4.80, 4.47, and 3.36 for Dnipropetrovs'k, Kharkiv, and Poltava regions, respectively. Information on the abundance of potential mammalian hosts for *I. ricinus* ticks for the sampling sites is provided in Table S1. A total of 90 ticks, which had been collected over April-May 2017 by dragging a ~100x60 cm cotton cloth across the vegetation, were identified to the species level according to their morphology at the Schmalhausen Institute of Zoology of National

Academy of Sciences of Ukraine (Filippova, 1977). Each ixodid tick was assigned its unique number based on tick location (D, K, and P), and sex (M and F denote male and female, respectively).

Prior to DNA extraction, each tick was externally (thoroughly) washed 3 times in 70% ethanol and then 3 times in ultra-pure water (Quality Biological; Gaithersburg, MD, USA) under class II type A/B3 biosafety cabinet. For each wash (approximately 20 ticks per wash), fresh ethanol or ultra-pure water was used (20 ml of ethanol or water in separate 50-ml conical tubes (6 sterile tubes were used per each wash); Quality Biological, Gaithersburg, MD, USA). Each tick was placed in a sterile 1.5-ml centrifuge tube (one tick per tube; USA Scientific, Ocala, FL, USA), then frozen in liquid nitrogen, and homogenized in a bead beater for 60 s (TissueLyser II, Qiagen, Inc.; Germantown, MD, USA). Genomic DNA was isolated with the DNeasy Minikit (Qiagen) as described (Rogovskyy et al., 2018; Rogovskyy et al., 2019). DNA was eluted in 50 µl of sterile nuclease-free water (Quality Biological). In order to monitor the contamination associated with kit reagents and steel beads, a total of 18 negative controls, which represented no-tick extractions obtained with (n=9) or without (n=9) beads, were also subjected to DNA extraction as detailed above. All the DNA samples were stored at -20°C until further analysis.

4.3.2. Bacterial 16S rRNA amplification and sequencing

The hypervariable region V6 of 16S rRNA gene was PCR amplified by using individual DNA samples. Previously published forward and reverse primers (F: 5'-CGCACAAGCGGTGGAGCAT-3', R: 5'-TCGTTGCGGGACTTAACCCAAC-3')

targeting a 16S rRNA fragment were used in this study (Carpi et al., 2011). The V6 region was chosen because, when compared to the V3 or V4 regions, it contains the maximum degree of diversity in nucleotide sequences among bacteria, and is commonly used as a target to distinguish between pathogenic and non-pathogenic bacterial taxa at the genus level (Chakravorty et al., 2007). Also, the V6 region was successfully targeted to characterize the microbiota of *I. ricinus* ticks in a previous investigation (Carpi et al., 2011; Vayssier-Taussat et al., 2013).

PCR amplification was performed in a total volume of 50-µl-reaction mixture, which consisted of 31.5 µl of nuclease-free water (Quality Biological), 10 µl of 5X HEB buffer, 1.5 µl of DMSO (Sigma-Aldrich; St. Louis, MO, USA), 0.7 µl of 10 mM dNTPs (0.14 mM; New England BioLabs; Ipswich, MA, USA), 0.5 µl of 10 µM of each primer (0.1 µM), and 0.3 µl of Phusion® High-Fidelity DNA polymerase (0.6 unit; New England BioLabs), and 5 µl of a DNA sample. PCR was carried out under the following cycling parameters: an initial denaturation at 94°C for 3 min, 32 cycles of denaturation at 94°C for 30 s, annealing at 56°C for 45 s, and extension at 72°C for 2 min, followed by 2-min extension at 72°C (Carpi et al., 2011). PCR was performed by using the C1000 Touch Thermal Cycler (Bio-Rad Laboratories, Hercules, CA, USA). The 16S rRNA amplicons were sequenced by using the Illumina 4000 HiSeq instrument for 150 cycles at Texas A&M AgriLife Genomics and Bioinformatics Service (College Station, TX, USA).

4.3.3. Sequence processing

After confirming the quality of generated raw data, data of one tick sample that did not have sufficient coverage was discarded from the analysis. The heterogeneity

spacers, which were located in the sequenced reads before the primer, were removed prior to the analysis (see the sequencing data) by using a custom-made Perl script (https://github.com/noushing/Trimming_HS_Metagenomics). Data were analyzed via QIIME 2 (version 2019.4) (Bokulich et al., 2018; Bolyen et al., 2019; Caporaso et al., 2010) at the Texas A&M Institute for Genomic Sciences and Society (TIGSS; College Station, TX, USA). For 89 tick samples, a total of 588,688,840 reads were imported, denoised, and trimmed to 135 bp using the DADA2 plugin (QIIME 2), which identified 21,210 amplicon sequence variants (ASVs).

Data for the 18 control samples were also analyzed by using QIIME 2 at the TIGSS. A total of 10,946,851 reads were imported into QIIME 2 and denoised utilizing the DADA2 plugin, with raw read counts of 409,534-881,315 per each control. Any feature that had fewer than 2 counts and was absent in at least 2 samples was filtered out and excluded from the analysis, which resulted in a total of 4,176,860 reads and 112 ASVs. Taxonomic classification was assigned to the ASVs by utilizing the naïve-Bayesian classifier that was trained on the SILVA 16S rRNA database (version 138).

4.3.4. Classification of ASVs

ASVs that were not present in at least 5 samples with ≤ 200 counts were filtered out. A threshold of 200 counts was chosen due to the large number of samples and extremely high number of reads. The filtering, which removed low-confidence and low-abundance features from 16S rRNA amplicon data sets to avoid counting sequencing errors, resulted in a total of 49,560,501 reads and 2,234 ASVs. The number of reads per sample ranged from 355,873 to 851,125 and a sampling depth of 100,000 unique

sequences per sample was used for the analysis. The sequence data were archived in the Sequence Read Archive (SRA) database under the accession numbers, PRJNA688283 (the tick data) and PRJNA688273 (the negative control data).

4.3.5. Taxonomic classification

Taxonomy was assigned to the ASVs using the naïve-Bayesian classifier based on the SILVA 16S rRNA database (version 138) (Quast et al., 2013). Additional two-dimensional PCoA plots and bar plots were generated using QIIME 2 and microbeR packages (version 3.6.1; https://github.com/jbisanz/MicrobeR).

4.3.6. Alpha and beta diversity

Alpha and beta diversity was analyzed via QIIME 2 using ASVs (bacterial richness hereafter) and the Shannon diversity index (for alpha diversity) (Hill et al., 2003), and the Jaccard index, Bray-Curtis index, weighted and unweighted UniFrac distances (for beta diversity) (Lozupone and Knight, 2005; Lozupone et al., 2007). The principal coordinate analysis (PCoA) was used to examine dissimilarities between bacterial communities based on the weighted and unweighted UniFrac distances.

4.3.7. Analysis of composition of microbiomes

The analysis of composition of microbiomes (ANCOM) (Mandal et al., 2015) was carried out to determine differences in the differential abundance of bacterial taxa across sample groups at the genus level. A pseudocount of 1 was added to remove zero counts from the feature table, and pairwise ANCOM tests were performed in QIIME 2 using the centered log-ratio (clr) transformation.

4.3.8. Statistical methods

All the statistical analyses were performed by using R software (R 3.6.2 for Windows) (Team, 2013) unless indicated otherwise. Individual data sets on bacterial relative abundance and alpha diversity were tested for normality using the Shapiro-Wilk test. The Mann-Whitney U test was used for pairwise comparison for each group (alpha diversity and bacterial relative abundance) and the Bonferroni correction was applied for multiple comparisons. Permutational multivariate analysis of variance (PERMANOVA) integrated in QIIME 2 was used to examine significant differences in beta diversity (999 permutations were used). The p value of < 0.05 was considered significant unless otherwise stated. The significant level for multiple comparisons (inter-regional comparisons of alpha diversity and beta diversity and comparisons of bacterial relative abundance) was adjusted ($p < 0.0083$) when the Bonferroni correction was applied. GraphPad Prism version 8.1.2 (227) for Mac (GraphPad Software, USA) was utilized for generating alpha diversity figures.

4.4. Results

4.4.1. 16S rRNA sequencing

A total of 90 *I. ricinus* ticks were collected from three neighboring administrative regions of Ukraine, Dnipropetrovs'k, Kharkiv, and Poltava (regions D, K, and P, respectively) that collectively represented Central (regions D and P) and Northeastern (region K) Ukraine. Individual tick samples were processed for DNA extraction and the V6 hypervariable region of mitochondrial 16S rRNA gene was targeted to explore the microbial diversity in these ticks. One of the male tick sample that did not have adequate

coverage was considered low-quality and hence was removed from the analysis. Thus, after the quality control, a total of 89 samples were retained for the downstream analysis. Since total numbers of ASVs generated per sample varied between ticks, which would have potentially introduced biases associated with the downstream analysis of bacterial taxa, the rarefaction analysis was performed (without replacement). The rarefaction analysis estimated the minimum numbers of ASVs that were required to capture the microbial diversity for individual tick samples. As a result, the sequencing depth of 100,000 unique sequences per sample was found to be sufficient for capturing the complete diversity for *I. ricinus* ticks.

The analysis results of negative controls showed that DNA extraction was associated with a minor degree of bacterial contamination (Fig. S1). Out of top 15 taxa (11 genera and 4 unclassified genera), only *Cutibacterium*, an unclassified genus of Bacillaceae, and *Staphylococcus* were by far most abundant for all the 18 negative controls. The taxa found in the negative controls were not filtered out from the tick microbiota analysis for the reasons discussed below.

4.4.2. Alpha diversity analyses

In order to detect any potential sex-specific differences in the microbiota of *I. ricinus* ticks, male and female microbiota were compared within each region. As a result, sex-associated differences were only observed for *I. ricinus* ticks from region D. The bacterial richness showed that region D females exhibited a significantly higher alpha diversity compared to the male counterparts ($p = 0.0218$ Fig. 4.1). This is in contrast to the Shannon diversity index that demonstrated the reverse: region D males had greater

alpha diversity than that of the respective females (p = 0.0073; Fig. 4.1). Both methods concordantly showed no significant inter-sex difference in alpha diversity for ticks from regions K and P.

To identify region-specific differences, tick microbiota were compared between the three regions for each tick sex. The bacterial richness and Shannon diversity index uniformly demonstrated no significant difference between region K and region P ticks (p > 0.05; Fig. 4.2). However, the bacterial richness was significantly lower for both males and females from region D when compared to those of region K and region P ticks (p < 0.05; Fig. 4.2) with one exception: the metric was similar for females from regions D and P (p > 0.0083; Fig. 4.2). Likewise, region D females had lower Shannon diversity indices compared to those of females from regions K (p = 0.0037; Fig. 4.2) and P (p = 0.0032). The Shannon diversity indices were similar for male ticks between the three regions (p > 0.05).

4.4.3. Beta diversity analyses

To assess the quantitative and qualitative aspects of beta diversity, the Jaccard index, Bray-Curtis index, unweighted and weighted UniFrac distances were measured (Lozupone and Knight, 2005; Lozupone et al., 2007). The PERMANOVA analysis of Bray-Curtis and weighted UniFrac metrics demonstrated significant inter-sex differences in the bacterial abundance for ticks from each region (p values < 0.005). Moreover, tick microbiota were significantly different between region P males and females by the four beta diversity methods (p = 0.001; Table 4.1).

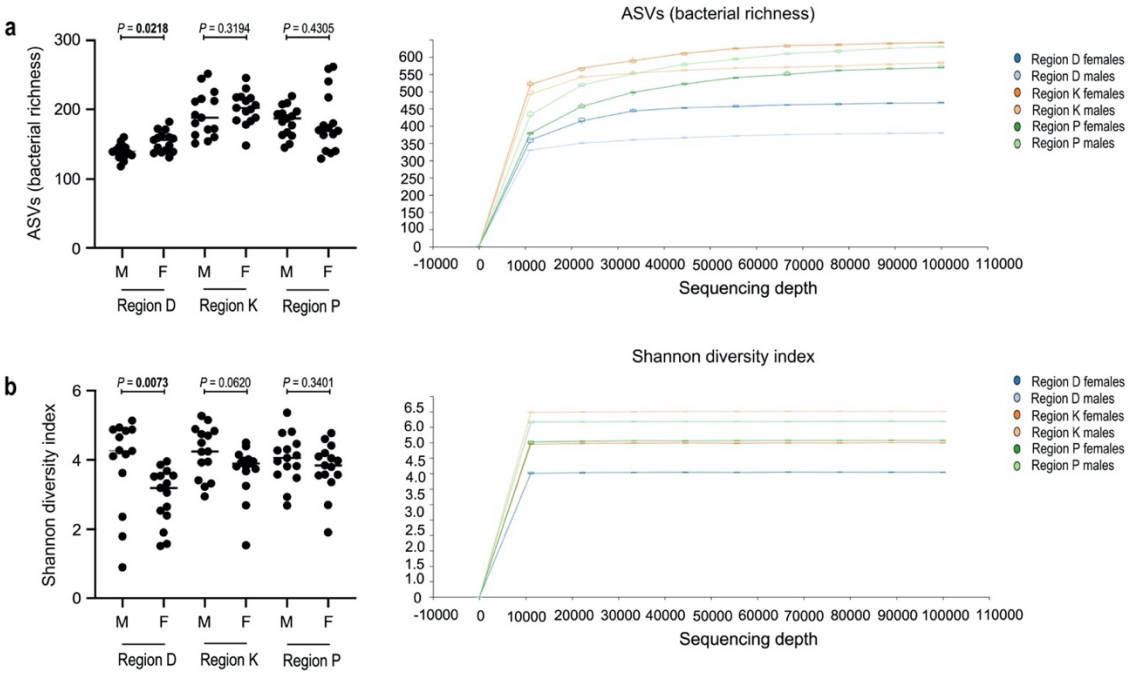

Figure 4.1 Inter-sex comparison of alpha diversity metrics for *Ixodes ricinus* ticks within each region. Alpha diversity was measured by (a) the ASVs (bacterial richness) and (b) the Shannon diversity index for the microbiota of male and female ticks and compared within each region. The respective rarefaction curves are also provided (right). D, K, and P denote Dnipropetrovs'k, Kharkiv, and Poltava regions, respectively. The significant *p* values ($p < 0.05$) are indicated in bold.

When tick microbiota were inter-regionally compared for each sex, significant differences were concordantly identified by the four methods for both males and females with some exceptions (PERMANOVA; Table 4.1). No significant difference was detected for ticks of both sexes between regions D and K and for females between regions P and K by the Bray-Curtis and weighted UniFrac metrics ($p > 0.0083$; Table 4.1). Also, the unweighted UniFrac metrics were similar for males between regions P and K. The datasets were also analyzed by PCoA, using the weighted and unweighted UniFrac metrics (Fig. 4.3). The unweighted UniFrac plots demonstrated distinct clustering of region D males

compared to male ticks from regions K and P; and three separate clusters of females by their respective origin (Fig. 4.3).

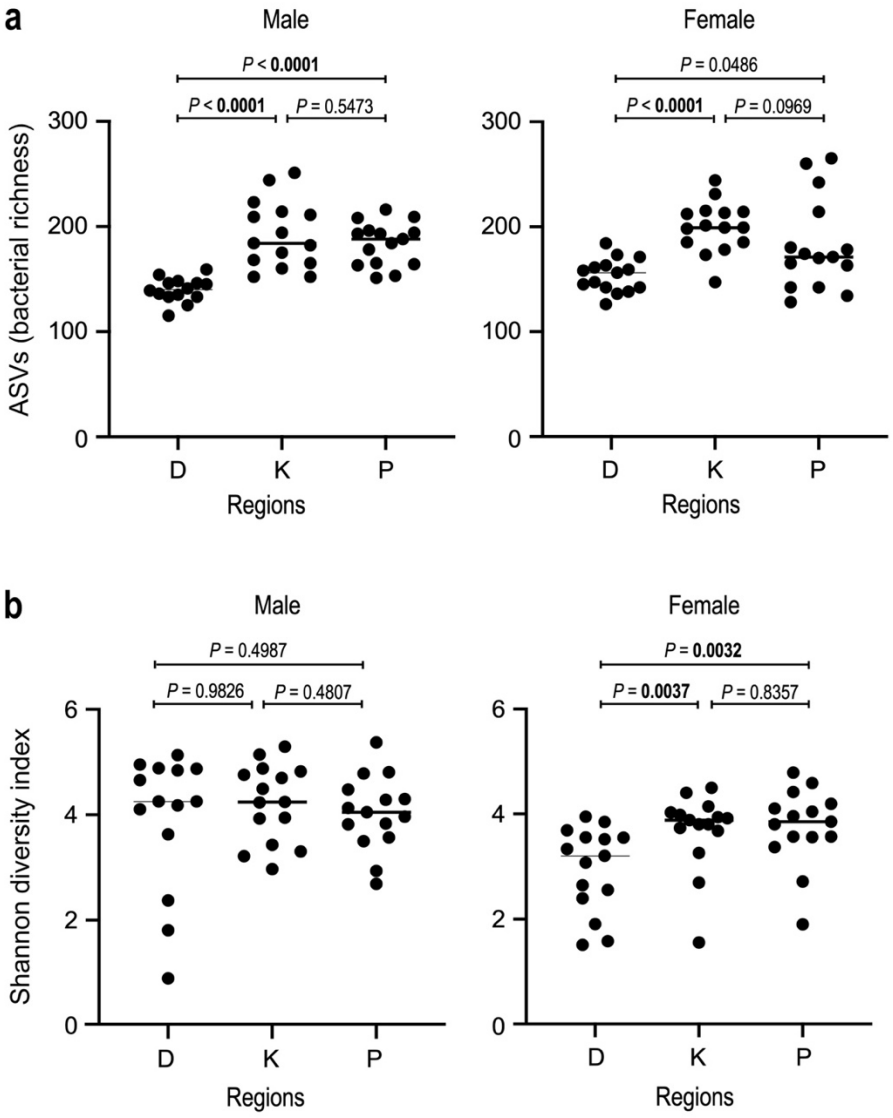

Figure 4.2 Inter-regional comparison of alpha diversity metrics for *Ixodes ricinus* ticks within each sex between the three regions. Alpha diversity was measured by (a) the ASVs (bacterial richness) and (b) the Shannon diversity index for the microbiota of male and female ticks and compared between Dnipropetrovs'k (region D), Kharkiv (region K), and Poltava (region P) regions. The significant p values ($p < 0.0083$) are indicated in bold.

Table 4.1 Inter-sex and inter-regional comparisons of beta diversity metrics
Inter-sex and inter-regional comparisons of beta diversity metrics.

Comparisons	Region	Sex	Jaccard index	Bray-Curtis index	Unweighted UniFrac distance	Weighted UniFrac distance
Within regions	D[#]	M* vs F*	0.05 (1.22)[&]	**0.002** (6.26)	0.405 (1.00)	**0.002** (10.08)
	K[#]	M vs F	0.392 (1.02)	**0.003** (4.29)	0.554 (0.88)	**0.004** (4.52)
	P[#]	M vs F	**0.001** (2.36)	**0.001** (5.93)	**0.001** (8.23)	**0.002** (9.15)
Between regions	D vs K	M	**0.001** (4.18)	0.048 (2.22)	**0.001** (3.94)	0.199 (1.40)
	D vs P		**0.001** (5.57)	**0.001** (12.56)	**0.001** (6.87)	**0.001** (9.16)
	P vs K		**0.001** (2.38)	**0.001** (6.20)	0.039 (1.82)	**0.003** (3.94)
	D vs K	F	**0.001** (4.71)	0.02 (3.12)	**0.002** (6.03)	0.02 (3.38)
	D vs P		**0.001** (3.63)	**0.001** (5.99)	**0.001** (4.37)	**0.001** (7.50)
	P vs K		**0.001** (4.12)	0.241 (1.27)	**0.001** (9.02)	0.499 (0.75)

[#]D, K, and P denote Dnipropetrovs'k, Kharkiv, and Poltava regions, respectively.
*M and F denote male and female ticks of *Ixodes ricinus,* respectively.
[&]Provided are *p* values, and pseudo-F statistic (in parantheses) generated by permutational multivariate analysis of variance (PERMANOVA). Indicated in bold are statistically significant *p* values. The significant level of $p < 0.05$ was used for inter-sex comparisons. For inter-regional comparisons the Bonferroni correction was applied and a *p* value of < 0.0083 was considered significant.

4.4.4. Inter-sex differences in the bacterial relative abundance of *I. ricinus* ticks

The analysis of bacterial relative abundance demonstrated that the microbiota of *I. ricinus* ticks comprised a total of 22 bacterial phyla. Actinobacteria and Proteobacteria were by far the most dominant phyla identified in both male and female ticks for the three regions (Fig. 4.4. and Table 4-S2). The median relative abundance of Actinobacteria and Proteobacteria ranged from 19% and 45% to 41% and 76%, respectively. Expectedly, their respective classes, Alphaproteobacteria (phylum: Proteobacteria) and Actinobacteria (phylum: Actinobacteria) were consistently most abundant in males and females across the three regions. Of note, the relative abundance of the two phyla and their respective classes significantly differed between male and female ticks for regions D and P (Table 4-S2). Although no significant differences were detected between male and female ticks for region K at the phylum level, both classes of this phylum, Alphaproteobacteria and Gammaproteobacteria, were more abundant in females ($p = 0.0344$) and less abundant in males ($p = 0.0251$). Overall, significant differences were more frequently observed for the bacterial relative abundance at the levels of phylum, class, and order for region D ticks as opposed to that of ticks from regions K and P (Table 4-S2). At the family level, region P and region D ticks had, respectively, 12 and 9 bacterial families, whose relative abundance was statistically different between males and females. This contrasts with region K ticks, which showed significant differences in the bacterial relative abundance for only 3 families (Table 4-S2). Of note, the only bacterial family, which was consistently more abundant in female ticks across the three regions ($p < 0.0001$), was Midichloriaceae

(phylum: Proteobacteria; class: Alphaproteobacteria; order: Rickettsiales) with its median relative abundance of 19-31% (vs. 0.1-0.4% in males). The sex-associated difference for each region was also noted for the family of Halomonadaceae, whose relative abundance was significantly higher in males ($p < 0.005$; Table 4-S2). Expectedly, at the genus level, the significantly higher relative abundance of *Candidatus* Midichloria ($p < 0.001$) and *Halomonas* ($p < 0.005$) was also consistently observed in females and males, respectively, across the three regions (Fig. 4.5 and Table 4-S2). Finally, regardless of the region and tick sex, *Curtobacterium, Methylobacterium, Mycobacterium, Pseudomonas,* and *Sphingomonas* were most noticeably abundant genera that were associated with the environment (Table 4-S2) (Portillo et al., 2019).

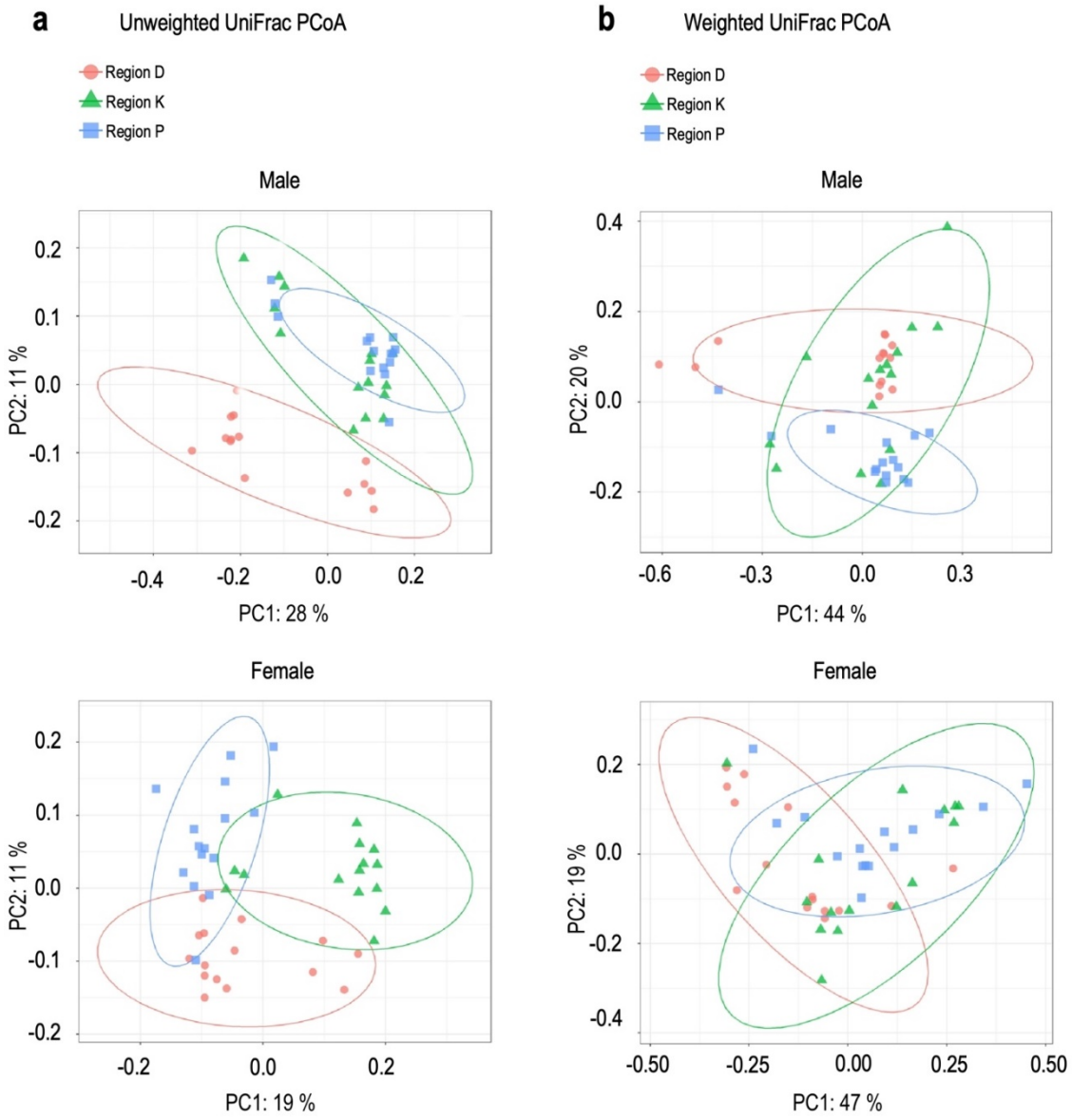

Figure 4.3 Principal coordinate analysis (PCoA) plots of beta diversity metrics in males and females of *Ixodes ricinus* ticks. Shown are PCoA plots for (a) unweighted UniFrac (b) and weighted UniFrac metrics. D, K, and P denote Dnipropetrovs'k, Kharkiv, and Poltava regions, respectively. Each symbol represents the bacterial microbiota of an individual tick. Ellipses define a 95% confidence interval.

4.4.5. Inter-regional differences in the bacterial relative abundance of *I. ricinus* ticks

To examine whether bacterial compositions of *I. ricinus* ticks varied between regions D, K, and P, microbiota were inter-regionally compared within each sex. The results demonstrated that the relative abundance of three phyla, Bacteroidetes, Firmicutes, and Proteobacteria was significantly different between the regions. Specifically, Bacteroidetes was most and least abundant in ticks of both sexes from regions P and D, respectively ($p < 0.05$; Tables 4-S3 and 4-S4). Firmicutes was least represented in both region P males and females when compared to ticks from regions D and K ($p < 0.005$; Tables 4-S3 and 4-S4). Although there was no significant variation in the relative abundance of Proteobacteria between males, significant differences were observed at the class level of this phylum between region D and region P males (Table S3). In contrast, region D females were more enriched with this phylum when compared to region K females ($p = 0.0016$; Table S4). However, the relative abundance of Alphaproteobacteria - the most abundant class of Proteobacteria phylum – was similar between females from the two regions (Table S4).

At the family level, significant inter-regional differences in the bacterial relative abundance were more frequently observed for males than female ticks. Specifically, six times as many families showed significant differences between region K and region P males as opposed to the female comparisons (12 vs. 2). Since Proteobacteria was most abundant in both males and females with its relative abundance of 45-76%, genera of this phylum were expectedly responsible for most significant differences observed between

the three regions. Similarly, genera of Actinobacteria phylum, whose relative abundance was between 19% and 41%, also showed numerous significant inter-regional variations (Tables S3 and S4).

4.4.6. Inter-sex and inter-regional differences in the differential abundance of bacterial taxa in *I. ricinus* ticks.

The ANCOM analysis was performed to identify inter-sex and inter-regional differences in the differential abundance of bacterial taxa at the genus level. Consistent with the relative abundance data, *Candidatus* Midichloria was uniformly much more abundant in female ticks than males across the three regions (Fig. 4-S3 and Table 4-S5). Reversely, *Halomonas* was significantly more abundant in region K males than the female counterparts, which is consistent with the respective relative abundance for region K ticks (Fig. 4-S3 and Table 4-S5). Compared to the other regions, a number of inter-regional differences were detected for region D ticks, where *Halomonas* and *Pseudarcicella* were more abundant in females and males, respectively; and *SWB02* and *Pedomicroboium* were more dominant in ticks of both sexes (Fig. 4-S4, Tables 4-S6 and 4-S7). *Spirosoma* was significantly more abundant in region P ticks of both sexes than region D ticks. When the differential abundance of bacterial taxa were compared between region P and region K ticks, very few significant differences were identified. *Bacillus* and *Borrelia* were, respectively, more abundant in region K ticks of both sexes; and *Actinomycetospora* was much less abundant in region K males (Fig. 4-S4, Tables 4-S6 and 4-S7).

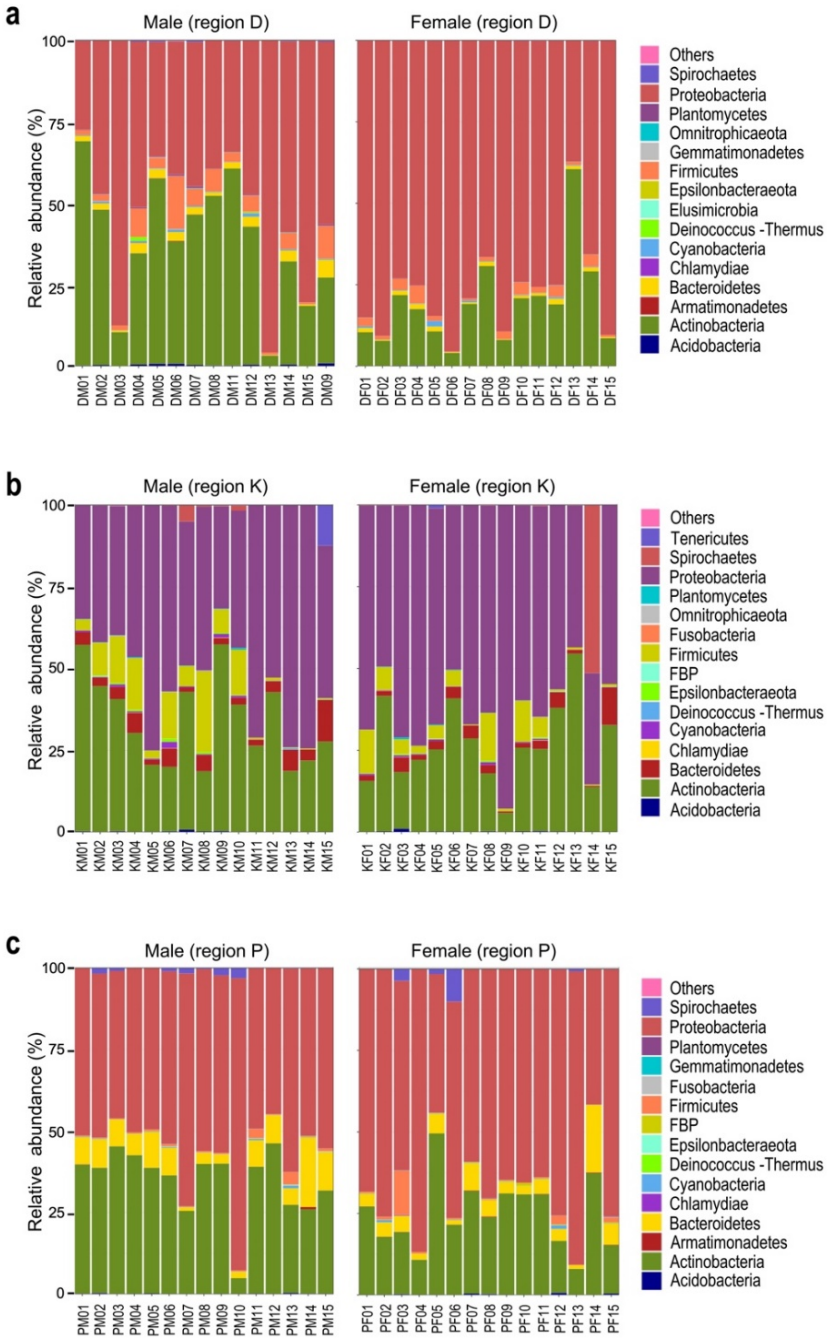

Figure 4.4 Bacterial relative abundance of top 15 phyla for *Ixodes ricinus* ticks. Each panel represents one of the three regions, where male and female ticks were collected from. D, K, and P denote (a) Dnipropetrovs'k, (b) Kharkiv, and (c) Poltava regions, respectively. Each bar reflects the bacterial relative abundance of an individual tick at the phylum level. The bacterial relative abundance of the phyla, which are not found in the top 15, are categorized as "Others"

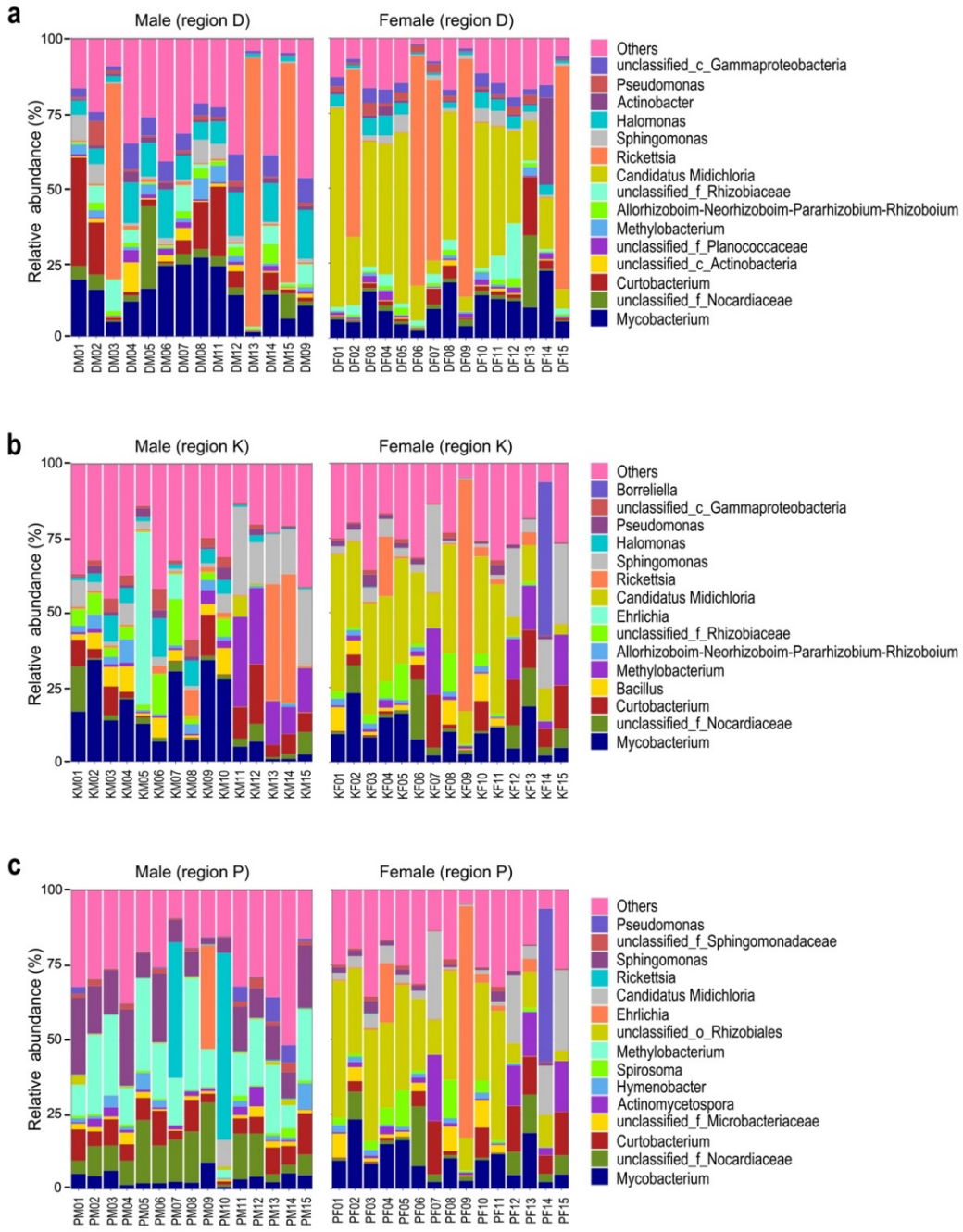

Figure 4.5 Bacterial relative abundance of top 15 genera for *Ixodes ricinus* ticks. Each panel represents one of the three regions, where male and female ticks were collected from. D, K, and P denote (a) Dnipropetrovs'k, (b) Kharkiv, and (c) Poltava regions, respectively. Each bar reflects the bacterial relative abundance of an individual tick at the genus level. The bacterial relative abundance of the genera, which are not found in the top 15, are categorized as "Others".

4.5. Discussion

The current investigation has shown that sex-dependent differences in the alpha diversity were only detected for ticks from region D. The microbiota of region D females displayed significantly higher bacterial richness but were overall less diverse when compared to that of male counterparts. Less diverse microbiota in female ticks were also previously reported for some other tick species (e.g., *Amblyomma americanum*, *Dermacentor reticulatus*, *Ixodes affinis,* and *Ixodes scapularis*) (Brinkerhoff et al., 2020; Thapa et al., 2019; Van Treuren et al., 2015; Zhang et al., 2019). In contrast, inter-sex variations were not observed for *Dermacentor marginatus* collected from Slovakia (Zhang et al., 2019). Contradictory findings in tick microbiota studies are not surprising given that numerous factors including tick species and sex, tick life stages, tick behavior and genetics, temperature, elevation, and vegetation structure may significantly shape the tick microbiota (Brinkerhoff et al., 2020; Carpi et al., 2011; Hawlena et al., 2013; Thapa et al., 2019; Van Treuren et al., 2015; Zhang et al., 2019).

Consistent with the inter-sex results of alpha diversity, the microbiota of region D males and females was quite distinct from that of *I. ricinus* ticks collected from the other two regions as demonstrated by the alpha diversity measures and ANCOM data. Moreover, the unweighted PCoA plots showed close clustering of region D males. Previous work on adults of *I. scapularis* also demonstrated separate clusters of male ticks from Texas and Massachusetts (Thapa et al., 2019).

The present study has also examined the relative abundance of bacterial taxa in *I. ricinus* ticks. Since sample processing may introduce considerable bacterial contamination

(Lejal et al., 2020), a number of negative controls were included in this study. The results demonstrated that only a minor level of contamination was associated with DNA extraction. Moreover, there was no noticeable difference in the bacterial relative abundance between the negative controls. The taxa identified in the negative controls including the three most abundant genera - *Cutibacterium*, unclassified genus of Bacillaceae, and *Staphylococcus* - were not specifically filtered out from the downstream analysis for a few reasons. First, these bacteria could well be present in ticks as part of either transient or long-term microbiota, which originates from soils and plants as shown by numerous studies (Perez-Valera et al., 2019; Portillo et al., 2019; Zarraonaindia et al., 2015). Second, the bacterial relative abundance of the "negative control" taxa was very negligible in all 89 ticks and/or under the detection threshold. For example, the median relative abundance of the two dominant "negative control" genera, *Cutibacterium* and *Staphylococcus*, was only between 0.03% and 1.19% for the analyzed ticks. Lastly, most "negative control" genera, if detected in ticks, were filtered out during the analysis as only bacterial taxon with its relative abundance of >1% was considered in this study.

The bacterial relative abundance data of this study have demonstrated that there was a total of five bacterial phyla, Proteobacteria, Actinobacteria, Bacteroidetes, Firmicutes, and Spirochaetes (listed in the increasing order of their bacterial relative abundance). The dominance of Proteobacteria phylum is well consistent with the results of earlier studies performed on questing *I. ricinus* adults and nymphs collected from Italy, Spain, and Slovakia (Carpi et al., 2011; Kmet and Čaplová, 2019; Portillo et al., 2019). Similar to the present findings, Actinobacteria was also previously reported as being the

second dominant phylum in questing *I. ricinus* ticks collected from Italy and Slovakia (Carpi et al., 2011; Kmet and Čaplová, 2019). Interestingly, Bacteroidetes, which represented one of the least abundant phyla in the current study (median range of 0.8-8%), was much more abundant (mean value of 40%) in questing nymphs and adults of *I. ricinus* collected from Spain (Portillo et al., 2019).

Consistent with the findings of previous studies, which analyzed both questing nymphs and adults of *I. ricinus*, the following genera, *Borreliella, Candidatus* Neoehrlichia*, Ehrlichia, Pseudomonas*, *Rickettsia, Rhizobium*, *Rhodococcus*, and *Spirosoma* were also identified in *I. ricinus* adults by the present study (Carpi et al., 2011; Kmet and Čaplová, 2019; Portillo et al., 2019). The significant dominance of *Candidatus* Midichloria in females from the three regions (median range of 18-31%) was in agreement with a previous study, where this bacterium was also much more abundant (mean value of 66%) in questing *I. ricinus* females collected from Spain (Portillo et al., 2019). *Candidatus* Midichloria may represent the endosymbiont of *Candidatus* Midichloria mitochondrii (CMM), whose high abundance in *I. ricinus* females is associated with its unique ability of intramitochondrial localization within tick ovaries (Sacchi et al., 2004). Because this endosymbiont is consistently detected in eggs, CMM is thought to be maternally inherited (Lo et al., 2006).

In addition to *Candidatus* Midichloria, the present study showed that *Rickettsia* was one of the least abundant genera in the examined adults. In contrast, *Rickettsia* genus was highly abundant in questing nymphs and adults of *I. ricinus* collected from Italy and Slovakia (Carpi et al., 2011; Kmet and Čaplová, 2019). The latter finding is not surprising

as the abundance of maternally-inherited symbionts were shown to greatly vary between geographical populations of various tick species (Clay et al., 2008; Duron et al., 2017; Lalzar et al., 2012). Further, contradictory results on the microbiota of *I. ricinus* ticks obtained from various studies could also be well attributed to differences in selected targets of 16S rRNA, sequencing platforms, and computational pipelines among other factors (Portillo et al., 2019; Sinha et al., 2017).

The current study also identified numerous environment-associated genera (e.g., *Curtobacterium, Methylobacterium, Mycobacterium, Pseudomonas,* and *Sphingomonas*) in *I. ricinus* adults. It is possible that some of these genera were only present on the cuticle as washing ticks with ethanol may not have efficiently eliminated external DNA contaminants. Although environmentally derived bacteria are regularly detected in ticks, it is still unclear whether they are long-term or only transient residents of the *I. ricinus* tick (Carpi et al., 2011; Greay et al., 2018; Kmet and Čaplová, 2019; Portillo et al., 2019; Zhang et al., 2019).

In addition to exoskeleton-associated contaminants, this investigation had some other limitations. First, the study did not examine any ticks for the presence of tick-borne pathogens by using pathogen-specific PCR. Second, DNA samples were obtained from whole ticks, which precluded examining tick tissue-specific microbiota. The above information could have been more informative for enhancing our understanding about the biology of ticks including their interaction with tick-borne pathogens. Lastly, the design of the study did not allow us to pinpoint parameters that have influenced extensive inter-sex and inter-regional variations in the tick microbiota.

4.6. Conclusions

The present microbiota study is the first to have assessed alpha and beta diversity of *I. ricinus* in the context of tick sex and origin. This study involved unprecedently high numbers of individually analyzed ticks. Prior to this work, the microbiota of *I. ricinus* ticks that would represent regions of Ukraine had not been defined. Collectively, the current data have demonstrated a high degree of inter-sex and inter-regional variations for questing *I. ricinus* adults. Of note, the genus *Candidatus* Midichloria exclusively dominated the microbiota of female ticks. It is plausible that the dominance of *Candidatus* Midichloria in *I. ricinus* females may affect the tick ability to acquire, maintain, and transmit tick-borne pathogens. Future experiments are warranted to directly examine how inter-sex and inter-regional variations in the *I. ricinus* microbiota can support or restrict persistence and transmission of various medically important pathogens. Furthermore, more descriptive studies are still needed to identify novel diversity patterns in the tick microbiota, the data that are crucial to elegantly rationalize designs of functional studies in the future.

4.7. Supplementary Data

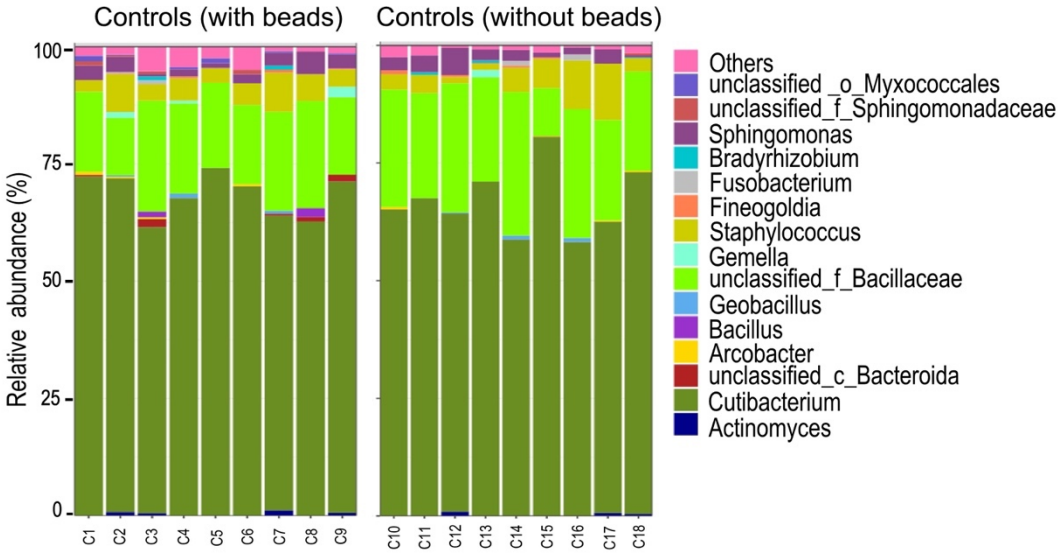

Figure 4.S1 Bacterial relative abundance of top 15 genera in the negative control samples. To identify the bacterial contamination associated with the DNA extraction step, a total of 18 negative controls, which represented no-tick extractions obtained with (n=9) or without (n=9) beads, were subjected to the microbiota analysis. The bacterial relative abundance of the genera, which are not found in the top 15, are categorized as "Others". Data for the 18 control samples were analyzed by using QIIME 2 (version 2019.4). A total of 10,946,851 reads were imported into QIIME 2 and denoised utilizing the DADA2 plugin, with raw read counts of 409,534-881,315 per each control. Any feature that had fewer than two counts and was absent in at least two samples was filtered out and excluded from the analysis, which resulted in a total of 4,176,860 reads and 112 ASVs. Taxonomic classification was assigned to the ASVs by utilizing the naïve-Bayesian classifier that was trained on the SILVA 16S rRNA database (version 138).

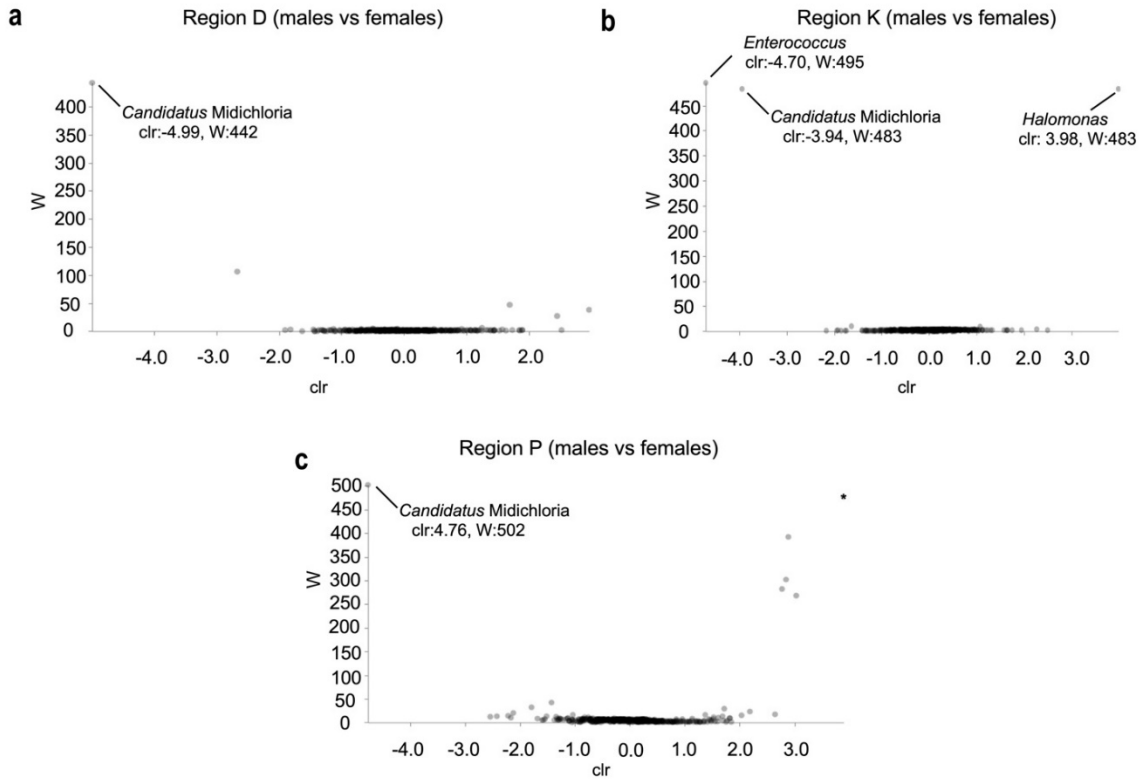

Figure 4.S2 Differentially abundant bacterial taxa based on inter-sex comparisons by ANCOM. Volcano plots of differential abundance at the genus level for male and female ticks of *Ixodes ricinus* collected from regions (a) D, (b) K, and (c) P were generated by applying the centered log-ratio transformation (clr) via ANCOM. Indicated are the bacterial taxa significantly different between males and females. *denotes unclassified taxa (see Table 4-S5 for more details).

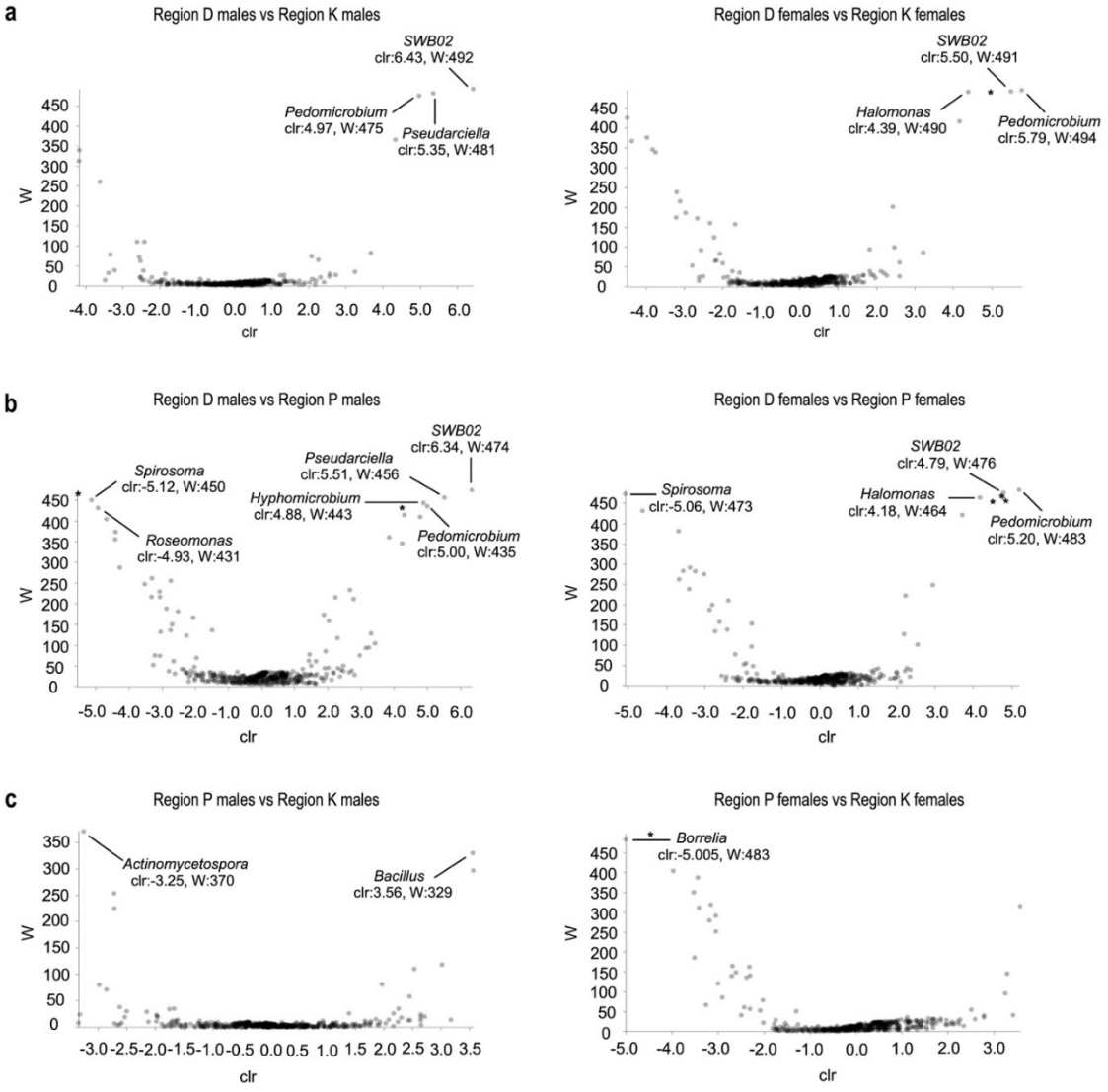

Figure 4.S3 Differentially abundant bacterial taxa based on inter-regional comparisons by ANCOM. Volcano plots of differential abundance at the genus level for male and female ticks of *Ixodes ricinus* collected from regions D, K, and P were generated by applying the centered log-ratio transformation (clr) via ANCOM. Indicated are the bacterial taxa significantly different between regions (a) D and K, (b) D and P, and (c) P and K within each tick sex. *denotes unclassified or uncultured taxa (see Tables 4-S6 and 4-S7 for more details)

Table 4.S1 The abundance of potential mammalian hosts of *Ixodes ricinus* per tick collection site

Region	Collection sites	*Apodemus agrarius* (%)	*Microtus arvalis* (%)	*Mus musculus* (%)	*Myodes glareolus* (%)	*Apodemus sylvaticus* (*A. uralensis*) (%)	*Apodemus flavicollis* (%)	*Canis lupus* (%)	*Bos taurus* (%)	*Capra hiracus* (%)	Others (%)
Region D	Nikopol district	30	0	60	0	10	0	65	8	20	7
Region K	Kharkiv District	30	0	40	0	30	0	65	8	20	7
Region K	Zmiiv District	15	15	35	5	20	10	50	30	15	5
Region P	Lokhytsia District	30	20	0	25	20	5	50	30	15	5
Region P	Lubny district	30	20	0	25	20	5	50	30	15	5
Region P	Orzhytsia district	30	20	0	25	20	5	50	30	15	5

Table 4.S2 Differences in the bacterial relative abundance between male and female ticks of *Ixodes ricinus* within each region

	Taxon[&]	Region D			Region K			Region P		
		Median RA (IQR)*		*p* value[#]	Median RA (IQR)		*p* value	Median RA (IQR)		*p* value
		Males	Females		Males	Females		Males	Females	
Phylum	Actinobacteria	40.69 (21.83)	18.58 (12.00)	**0.0083**	31.32 (20.46)	24.45 (16.02)	0.1466	36.61 (10.57)	23.35 (13.91)	**0.0114**
	Bacteroidetes	1.67 (1.28)	0.80 (0.72)	**0.0083**	2.95 (2.44)	1.87 (2.19)	0.1585	7.85 (4.38)	4.07 (2.55)	0.0745
	Firmicutes	3.65 (4.36)	1.62 (2.33)	0.0701	5.77 (13.11)	3.63 (5.74)	0.5069	0.24 (0.24)	0.27 (0.40)	0.9010
	Proteobacteria	47.65 (18.31)	75.55 (13.79)	**0.0073**	44.94 (21.18)	59.60 (16.98)	0.0971	49.16 (5.19)	64.23 (13.71)	**0.0128**
	Spirochaetes	0.09 (0.20)	0.05 (0.04)	0.0636	0.05 (0.13)	0.04 (0.07)	0.3195	0.04 (1.25)	0.02 (0.40)	0.6482
Class	Actinobacteria	39.93 (23.02)	18.36 (11.74)	**0.0083**	30.73 (20.11)	23.81 (16.55)	0.1466	36.54 (10.60)	23.06 (14.19)	**0.0128**
	Alphaproteobacteria	25.66 (14.33)	66.21 (20.85)	**0.0083**	32.82 (27.27)	57.93 (14.06)	**0.0344**	46.66 (7.28)	62.82 (8.77)	**0.0070**
	Bacilli	2.96 (4.09)	1.54 (2.33)	0.1017	5.52 (11.73)	3.24 (5.23)	0.4807	0.20 (0.14)	0.24 (0.37)	0.9339
	Bacteroidia	1.67 (1.28)	0.80 (0.72)	**0.0083**	2.95 (2.40)	1.87 (2.19)	0.1585	7.85 (4.38)	4.07 (2.55)	0.0745
	Gammaproteobacteria	18.16 (17.17)	9.31 (7.27)	**0.0471**	6.04 (11.65)	2.38 (2.83)	**0.0251**	1.57 (2.87)	1.66 (3.21)	0.6187
	Spirochaetia	0.09 (0.13)	0.03 (0.03)	**0.0219**	0.04 (0.11)	0.04 (0.07)	0.3401	0.04 (1.25)	0.02 (0.40)	0.7716
Order	Bacillales	2.40 (3.44)	1.43 (2.28)	0.1213	4.79 (9.98)	1.91 (4.70)	0.5338	0.11 (0.13)	0.16 (0.13)	0.2455
	Corynebacteriales	20.64 (12.49)	11.74 (10.34)	**0.0424**	15.75 (22.02)	11.72 (7.56)	0.3837	14.54 (7.23)	10.98 (10.26)	0.2808
	Cytophagales	0.60 (0.54)	0.30 (0.30)	**0.0195**	0.94 (1.09)	0.79 (0.83)	0.1354	3.70 (3.01)	2.94 (2.13)	0.3837
	Frankiales	0.47 (0.52)	0.18 (0.17)	**0.0246**	0.58 (1.20)	0.51 (0.56)	0.7716	2.53 (3.09)	0.58 (0.64)	**0.0011**
	Kineosporiales	0.01 (0.28)	0.01 (0.02)	0.7434	0.19 (1.73)	0.03 (0.23)	0.1466	1.04 (1.10)	0.28 (0.59)	**0.0381**
	Micrococcales	6.99 (12.14)	2.20 (1.99)	**0.0154**	5.83 (10.13)	6.66 (10.45)	1.0000	9.21 (4.80)	5.24 (5.97)	0.0680
	Oceanospirillales	8.01 (9.38)	3.66 (2.97)	**0.0028**	2.29 (4.39)	0.03 (0.04)	**<0.0001**	0.60 (0.49)	0.03 (0.02)	**<0.0001**
	Propionibacteriales	1.86 (1.60)	0.56 (0.51)	**0.0016**	1.60 (1.52)	1.38 (0.96)	**0.0381**	1.26 (0.90)	1.11 (1.04)	0.3615

[&]The same colors indicate the relatedness of the respective taxa.

*RA and IQR denote relative abundance and interquartile range, respectively.

[#]*p* values of < 0.05 were considered significant and indicated in bold.

Table 4.S2 Continued

	Taxon[&]	Region D			Region K			Region P		
		Median RA (IQR)*		*p* value[#]	Median RA (IQR)		*p* value	Median RA (IQR)		*p* value
		Males	Females		Males	Females		Males	Females	
Order	Pseudocardiales	0.28 (0.22)	0.14 (0.22)	0.0701	0.15 (0.24)	0.20 (0.24)	0.4807	1.14 (2.03)	0.39 (1.55)	0.1150
	Pseudomonadales	2.40 (1.24)	2.78 (1.69)	0.6157	1.78 (2.57)	1.48 (1.54)	0.7089	0.30 (1.52)	1.01 (1.69)	0.3837
	Rhizobiales	12.50 (9.35)	7.22 (4.86)	0.0771	16.43 (8.70)	13.97 (7.76)	0.1844	22.16 (9.41)	18.14 (9.10)	0.0971
	Rickettsiales	0.97 (1.78)	49.94 (29.99)	**0.0028**	2.51 (8.36)	36.24 (29.54)	**0.0032**	0.33 (0.26)	31.38 (22.33)	**0.0012**
	Sphingobacteriales	0.18 (0.45)	0.10 (0.26)	0.5854	0.80 (0.91)	0.48 (0.67)	0.4306	2.53 (2.87)	0.37 (1.08)	**0.0014**
	Sphingomonadales	2.09 (3.75)	2.19 (2.10)	0.7107	6.80 (11.24)	4.78 (8.88)	0.4553	12.73 (11.18)	11.77 (4.37)	0.2455
	Spirochaetales	0.09 (0.13)	0.03 (0.03)	**0.0219**	0.04 (0.11)	0.04 (0.007)	0.3401	0.04 (1.25)	0.02 (0.40)	0.7716
Family	Anaplasmataceae	0.01 (0.05)	0.01 (0.01)	0.6944	0.04 (0.09)	0.01 (0.04)	0.0776	0.01 (0.04)	0.03 (0.01)	**0.0225**
	Bacillaceae	0.22 (0.17)	0.13 (0.10)	0.0576	1.90 (6.22)	1.19 (3.78)	0.5897	0.03 (0.04)	0.04 (0.07)	0.1249
	Beijerinckiaceae	3.18 (3.34)	1.26 (2.19)	0.2301	4.86 (9.74)	2.61 (7.03)	0.2808	18.01 (11.80)	8.46 (12.41)	**0.0344**
	Geodermatophilaceae	0.05 (0.26)	0.05 (0.05)	0.5268	0.09 (0.39)	0.11 (0.09)	0.8682	0.88 (1.47)	0.26 (0.33)	**0.0003**
	Halomonadaceae	8.01 (9.38)	3.66 (2.97)	**0.0028**	2.29 (4.39)	0.03 (0.04)	**<0.0001**	0.60 (0.49)	0.03 (0.02)	**<0.0001**
	Hymenobacteraceae	0.01 (0.02)	0.01 (0.02)	0.9304	0.07 (0.67)	0.06 (0.30)	0.7089	1.59 (1.93)	0.31 (0.93)	**0.0161**
	Midichloriaceae	0.18 (0.05)	31.34 (31.63)	**<0.0001**	0.43 (0.27)	28.52 (26.03)	**<0.0001**	0.09 (0.05)	18.84 (21.66)	**<0.0001**
	Microbacteriaceae	6.56 (12.22)	1.85 (1.76)	**0.0174**	5.71 (9.72)	4.32 (10.74)	0.8357	8.62 (4.17)	5.11 (6.03)	0.0745
	Mycobacteriaceae	15.40 (11.29)	9.73 (8.32)	0.0576	12.84 (19.73)	9.53 (9.08)	0.4553	3.24 (2.65)	6.57 (6.60)	**0.0279**
	Moraxellaceae	1.07 (1.32)	0.72 (0.74)	0.2136	0.31 (0.64)	0.19 (0.33)	0.2134	0.10 (0.11)	0.05 (0.13)	**0.0310**
	Nakamurellaceae	0.12 (0.15)	0.05 (0.08)	0.3481	0.11 (0.62)	0.29 (0.21)	0.5897	0.73 (2.13)	0.13 (0.10)	**0.0144**
	Nocardiaceae	3.26 (3.58)	1.48 (1.14)	**0.0246**	2.63 (3.92)	1.67 (5.81)	0.8357	10.10 (8.30)	3.95 (6.20)	**0.0181**
	Planococcaceae	0.83 (1.15)	0.69 (1.46)	0.9826	0.06 (0.39)	0.10 (0.32)	0.5897	0.01 (0.01)	0.01 (0.01)	0.2134

[&]The same colors indicate the relatedness of the respective taxa.

*RA and IQR denote relative abundance and interquartile range, respectively.

[#]*p* values of < 0.05 were considered significant and indicated in bold.

Table 4.S2 Continued

	Taxon[&]	Region D			Region K			Region P		
		Median RA (IQR)*		*p* value[#]	Median RA (IQR)		*p* value	Median RA (IQR)		*p* value
		Males	Females		Males	Females		Males	Females	
Family	Propionibacteriaceae	1.61 (1.11)	0.34 (0.26)	**0.0003**	1.12 (1.51)	0.44 (0.65)	**0.0037**	0.94 (0.85)	0.40 (0.66)	0.1585
	Pseudonocaridiaceae	0.28 (0.22)	0.14 (0.22)	0.0701	0.15 (0.24)	0.20 (0.24)	0.4807	1.14 (2.03)	0.39 (1.55)	0.1150
	Pseudomonadaceae	0.77 (0.60)	1.57 (1.81)	0.1831	0.88 (1.96)	1.14 (1.44)	0.8682	0.21 (1.43)	0.97 (1.08)	0.1466
	Rhizobiaceae	4.83 (8.26)	2.60 (3.44)	0.7767	5.58 (8.67)	2.98 (5.49)	0.4553	1.23 (2.01)	1.10 (1.65)	0.8035
	Rickettsiaceae	0.64 (0.64)	0.33 (57.96)	0.0847	0.62 (1.43)	0.50 (2.38)	0.3615	0.18 (0.13)	1.01 (2.18)	**0.0181**
	Sphingobacteriaceae	0.07 (0.36)	0.09 (0.24)	0.6468	0.61 (0.92)	0.42 (0.70)	0.5614	2.52 (2.86)	0.37 (1.08)	**0.0014**
	Sphingomonadaceae	2.09 (3.75)	2.19 (2.10)	0.7107	6.80 (11.24)	4.78 (8.88)	0.4553	12.73 (11.81)	11.77 (4.37)	0.2455
	Staphylococcaceae	0.47 (0.64)	0.12 (0.22)	**0.0107**	0.23 (0.38)	0.11 (0.15)	0.1985	0.03 (0.05)	0.06 (0.08)	0.3615
	Spirochaetaceae	0.09 (0.13)	0.03 (0.03)	**0.0219**	0.04 (0.11)	0.04 (0.07)	0.3401	0.04 (1.25)	0.02 (0.40)	0.7716
	Spirosomaceae	0.29 (0.49)	0.11 (0.14)	**0.0424**	0.51 (0.43)	0.55 (0.46)	0.6482	1.23 (1.19)	1.69 (1.83)	0.3195
	Xanthobacteraceae	1.49 (0.83)	0.45 (0.47)	**0.0246**	0.79 (1.93)	0.74 (1.01)	0.9339	0.76 (0.71)	0.75 (0.83)	0.8035
Genus	*Actinomycetospora*	0.08 (0.12)	0.06 (0.04)	0.3947	0.04 (0.03)	0.10 (0.10)	0.0512	0.91 (1.72)	0.16 (1.35)	0.0971
	Acinetobacter	0.90 (1.31)	0.68 (0.70)	0.3051	0.13 (0.19)	0.07 (0.09)	0.1585	0.04 (0.03)	0.02 (0.03)	**0.0042**
	Allorhizobium.Neorhizobium.Pararhizobium.Rhizobium	1.33 (1.80)	0.66 (1.11)	0.1017	1.05 (1.99)	0.65 (1.53)	0.3195	0.19 (0.34)	0.22 (0.51)	0.4306
	Aureimonas	0.02 (0.32)	0.09 (0.13)	0.4715	0.43 (0.60)	0.35 (0.60)	0.7400	0.98 (1.06)	0.24 (0.47)	**0.0101**
	Bacillus	0.20 (0.18)	0.11 (0.08)	0.1213	1.84 (6.06)	1.13 (3.68)	0.5338	0.02 (0.03)	0.04 (0.07)	0.0890
	Borrelia	0.00 (0.00)	0.00 (0.00)	0.3697	0.02 (0.02)	0.02 (0.00)	0.3390	0.00 (0.00)	0.00 (0.00)	0.1644
	Borreliella	0.08 (0.08)	0.01 (0.03)	**0.0275**	0.02 (0.06)	0.01 (0.03)	0.2134	0.01 (1.24)	0.01 (0.40)	0.4807
	Bosea	0.61 (1.04)	0.67 (0.80)	0.9826	0.72 (1.20)	0.52 (0.89)	0.4553	0.09 (0.23)	0.10 (0.41)	0.6783
	Candidatus Midichloria	0.18 (0.05)	31.34 (31.63)	**<0.0001**	0.43 (0.27)	28.52 (26.03)	**<0.0001**	0.09 (0.05)	18.44 (21.66)	**<0.0001**

[&]The same colors indicate the relatedness of the respective taxa.

*RA and IQR denote relative abundance and interquartile range, respectively.

[#]*p* values of < 0.05 were considered significant and indicated in bold.

Table 4.S2 Continued

	Taxon[&]	Region D			Region K			Region P		
		Median RA (IQR)*		*p* value[#]	Median RA (IQR)		*p* value	Median RA (IQR)		*p* value
		Males	Females		Males	Females		Males	Females	
Genus	*Candidatus* Neoehrlichia	0.00 (0.00)	0.00 (0.00)	0.8684	0.01 (0.01)	0.00 (0.00)	**0.0273**	0.00 (0.01)	0.01 (0.00)	**0.0106**
	Curtobacterium	3.60 (11.72)	1.34 (1.66)	0.0847	4.07 (9.10)	3.69 (10.84)	0.9669	6.03 (3.80)	3.84 (6.32)	0.1354
	Cutibacterium	1.19 (1.35)	0.22 (0.20)	**0.0006**	0.72 (1.18)	0.24 (0.54)	0.0971	0.18 (0.14)	0.20 (0.59)	0.7716
	Ehrlichia	0.00 (0.00)	0.01 (0.01)	**0.0008**	0.02 (0.05)	0.00 (0.01)	0.0515	0.01 (0.01)	0.02 (0.01)	**0.0070**
	Geodermatophilus	0.04 (0.22)	0.02 (0.04)	0.6468	0.09 (0.39)	0.06 (0.13)	1.0000	0.88 (1.47)	0.26 (0.33)	**0.0003**
	Halomonas	8.01 (9.38)	3.66 (2.97)	**0.0028**	2.29 (4.39)	0.03 (0.04)	**<0.0001**	0.60 (0.49)	0.03 (0.02)	**<0.0001**
	Hymenobacter	0.01 (0.02)	0.01 (0.02)	0.8102	0.05 (0.64)	0.04 (0.25)	0.5338	0.97 (1.76)	0.27 (0.81)	**0.0202**
	Kineococcus	0.01 (0.28)	0.01 (0.02)	1.0000	0.17 (1.72)	0.03 (0.21)	0.2455	0.72 (1.09)	0.27 (0.58)	**0.0421**
	Methylobacterium	1.18 (2.74)	0.52 (0.46)	0.1831	1.33 (10.87)	1.66 (7.07)	0.6482	17.75 (12.27)	7.76 (12.77)	**0.0279**
	Mycobacterium	15.40 (11.29)	9.73 (8.32)	0.0576	12.84 (19.73)	9.53 (9.08)	0.4553	3.24 (2.65)	6.57 (6.60)	**0.0279**
	Nakamurella	0.12 (0.15)	0.05 (0.08)	0.3481	0.11 (0.62)	0.29 (0.21)	0.5897	0.73 (2.13)	0.13 (0.10)	**0.0144**
	Pseudomonas	0.77 (0.60)	1.57 (1.81)	0.1831	0.88 (1.96)	1.14 (1.44)	0.8682	0.21 (1.43)	0.97 (1.08)	0.1466
	Rhodococcus	0.46 (0.49)	0.22 (0.28)	0.2136	0.64 (1.26)	0.27 (0.17)	**0.0181**	0.28 (0.22)	0.19 (0.13)	0.2808
	Rickettsia	0.64 (0.64)	0.33 (57.96)	0.0929	0.62 (1.44)	0.49 (2.38)	0.3401	0.18 (0.13)	1.01 (2.18)	**0.0181**
	Sphingomonas	1.07 (3.63)	1.27 (2.13)	0.9131	6.37 (11.73)	3.79 (9.11)	0.5614	11.29 (10.19)	10.02 (6.36)	0.2455
	Staphylococcus	0.41 (0.64)	0.12 (0.19)	**0.0083**	0.21 (0.38)	0.09 (0.13)	0.1985	0.03 (0.05)	0.06 (0.08)	0.3195
	Spirosoma	0.00 (0.00)	0.01 (0.01)	0.3573	0.03 (0.04)	0.02 (0.08)	0.9339	0.65 (0.57)	0.78 (1.67)	0.4807

[&]The same colors indicate the relatedness of the respective taxa.

*RA and IQR denote relative abundance and interquartile range, respectively.

[#]*p* values of < 0.05 were considered significant and indicated in bold.

Table 4.S3 Differences in the bacterial relative abundance for male ticks of *Ixodes ricinus* between regions

Taxon[&]		Median RA (IQR)*		*p* value[#]	Median RA (IQR)		*p* value	Median RA (IQR)		*p* value
		Region D males	Region K males		Region D males	Region P males		Region P males	Region K males	
Phylum	Actinobacteria	40.69 (21.83)	31.32 (20.46)	0.3051	40.69 (21.83)	36.61 (10.57)	0.2849	36.61 (10.57)	31.32 (20.46)	0.9339
	Bacteroidetes	1.67 (1.28)	2.95 (2.44)	0.0343	1.67 (1.28)	7.85 (4.38)	**0.0003**	7.85 (4.38)	2.95 (2.44)	0.0128
	Firmicutes	3.65 (4.36)	5.77 (13.11)	0.8103	3.65 (4.36)	0.24 (0.24)	**<0.0001**	0.24 (0.24)	5.77 (13.11)	**0.0021**
	Proteobacteria	47.65 (18.31)	44.94 (21.18)	0.8103	47.65 (18.31)	49.16 (5.19)	0.3261	49.16 (5.19)	44.94 (21.18)	0.1844
	Spirochaetes	0.09 (0.20)	0.05 (0.13)	0.9131	0.09 (0.20)	0.04 (1.25)	0.6157	0.04 (1.25)	0.05 (0.13)	0.8682
Class	Actinobacteria	39.93 (23.02)	30.73 (20.11)	0.3481	39.93 (23.02)	36.54 (10.60)	0.3261	36.54 (10.60)	30.73 (20.11)	0.9010
	Alphaproteobacteria	25.66 (14.33)	32.82 (27.27)	0.1321	25.66 (14.33)	46.66 (7.28)	**0.0073**	46.66 (7.28)	32.82 (27.27)	0.0465
	Bacilli	2.96 (4.09)	5.52 (11.73)	0.8443	2.96 (4.09)	0.20 (0.14)	**<0.0001**	0.20 (0.14)	5.52 (11.73)	**0.0009**
	Bacteroidia	1.67 (1.28)	2.95 (2.40)	0.0343	1.67 (1.28)	7.85 (4.38)	**0.0003**	7.85 (4.38)	2.95 (2.40)	0.0128
	Gammaproteobacteria	18.16 (17.17)	6.04 (11.65)	0.0219	18.16 (17.17)	1.57 (2.87)	**0.0002**	1.57 (2.87)	6.04 (11.65)	0.0465
	Spirochaetia	0.09 (0.13)	0.04 (0.11)	0.8786	0.09 (0.13)	0.04 (1.25)	0.5268	0.04 (1.25)	0.04 (0.11)	0.7716
Order	Bacillales	2.40 (3.44)	4.79 (9.98)	0.8103	2.40 (3.44)	0.11 (0.13)	**<0.0001**	0.11 (0.13)	4.79 (9.98)	**0.0002**
	Corynebacteriales	20.64 (12.49)	15.75 (22.02)	0.6784	20.64 (12.49)	14.54 (7.23)	0.0636	14.54 (7.23)	15.75 (22.02)	0.5338
	Cytophagales	0.60 (0.54)	0.94 (1.09)	0.0382	0.60 (0.54)	3.70 (3.01)	**0.0004**	3.70 (3.01)	0.94 (1.09)	0.0344
	Frankiales	0.47 (0.52)	0.58 (1.20)	0.5268	0.47 (0.52)	2.53 (3.09)	**0.0003**	2.53 (3.09)	0.58 (1.20)	**0.0011**
	Kineosporiales	0.01 (0.28)	0.19 (1.73)	0.0521	0.01 (0.28)	1.04 (1.10)	**0.0008**	1.04 (1.10)	0.19 (1.73)	0.1985
	Micrococcales	6.99 (12.14)	5.83 (10.13)	0.6157	6.99 (12.14)	9.21 (4.80)	0.6784	9.21 (4.80)	5.83 (10.13)	0.4306
	Oceanospirillales	8.01 (9.38)	2.29 (4.39)	0.0107	8.01 (9.38)	0.60 (0.49)	**<0.0001**	0.60 (0.49)	2.29 (4.39)	0.0144
	Propionibacteriales	1.86 (1.60)	1.60 (1.52)	0.8443	1.86 (1.60)	1.26 (0.90)	0.2849	1.26 (0.90)	1.60 (1.52)	0.1466
	Pseudocardiales	0.28 (0.22)	0.15 (0.24)	0.1017	0.28 (0.22)	1.14 (2.03)	**0.0028**	1.14 (2.03)	0.15 (0.24)	**0.0001**
	Pseudomonadales	2.40 (1.24)	1.78 (2.57)	0.3051	2.40 (1.24)	0.30 (1.52)	0.0246	0.30 (1.52)	1.78 (2.57)	0.1985
	Rhizobiales	12.50 (9.35)	16.43 (8.70)	0.0771	12.50 (9.35)	22.16 (9.41)	**0.0043**	22.16 (9.41)	16.43 (8.70)	0.1057
	Rickettsiales	0.97 (1.78)	2.51 (8.36)	0.3710	0.97 (1.78)	0.33 (0.26)	**0.0028**	0.33 (0.26)	2.51 (8.36)	**0.0037**

[&]The same colors indicate the relatedness of the respective taxa.

*RA and IQR denote relative abundance and interquartile range, respectively.

[#]*p* values of < 0.0083 were considered significant and indicated in bold.

Table 4.S3 Continued

Taxon[&]		Median RA (IQR)*		*p* value[#]	Median RA (IQR)		*p* value	Median RA (IQR)		*p* value
		Region D males	Region K males		Region D males	Region P males		Region P males	Region K males	
Order	Sphingobacteriales	0.18 (0.45)	0.80 (0.91)	**0.0049**	0.18 (0.45)	2.53 (2.87)	**<0.0001**	2.53 (2.87)	0.80 (0.91)	**0.0070**
	Sphingomonadales	2.09 (3.75)	6.80 (11.24)	0.0083	2.09 (3.75)	12.73 (11.18)	**0.0001**	12.73 (11.18)	6.80 (11.24)	0.1057
	Spirochaetales	0.09 (0.13)	0.04 (0.11)	0.8786	0.09 (0.13)	0.04 (1.25)	0.5268	0.04 (1.25)	0.04 (0.11)	0.7716
Family	Anaplasmataceae	0.01 (0.05)	0.04 (0.09)	0.1904	0.01 (0.05)	0.01 (0.04)	0.1979	0.01 (0.04)	0.04 (0.09)	0.6783
	Bacillaceae	0.22 (0.17)	1.90 (6.22)	0.1213	0.22 (0.17)	0.03 (0.04)	**0.0002**	0.03 (0.04)	1.90 (6.22)	**0.0002**
	Beijerinckiaceae	3.18 (3.34)	4.86 (9.74)	0.1437	3.18 (3.34)	18.01 (11.80)	**<0.0001**	18.01 (11.80)	4.86 (9.74)	**0.0025**
	Geodermatophilaceae	0.05 (0.26)	0.09 (0.39)	0.6468	0.05 (0.26)	0.88 (1.47)	**0.0004**	0.88 (1.47)	0.09 (0.39)	**0.0009**
	Halomonadaceae	8.01 (9.38)	2.29 (4.39)	0.0107	8.01 (9.38)	0.60 (0.49)	**<0.0001**	0.60 (0.49)	2.29 (4.39)	0.0144
	Hymenobacteraceae	0.01 (0.02)	0.07 (0.67)	**0.0018**	0.01 (0.02)	1.59 (1.93)	**<0.0001**	1.59 (1.93)	0.07 (0.67)	**0.0032**
	Midichloriaceae	0.18 (0.05)	0.43 (0.27)	**0.0024**	0.18 (0.05)	0.09 (0.05)	**0.0010**	0.09 (0.05)	0.43 (0.27)	**<0.0001**
	Microbacteriaceae	6.56 (12.22)	5.71 (9.72)	0.6468	6.56 (12.22)	8.62 (4.17)	0.3947	8.62 (4.17)	5.71 (9.72)	0.3401
	Mycobacteriaceae	15.40 (11.29)	12.84 (19.73)	0.7107	15.40 (11.29)	3.24 (2.65)	**0.0001**	3.24 (2.65)	12.84 (19.73)	**0.0042**
	Moraxellaceae	1.07 (1.32)	0.31 (0.64)	0.0154	1.07 (1.32)	0.10 (0.11)	**0.0002**	0.10 (0.11)	0.31 (0.64)	0.0564
	Nakamurellaceae	0.12 (0.15)	0.11 (0.62)	0.3261	0.12 (0.15)	0.73 (2.13)	**0.0032**	0.73 (2.13)	0.11 (0.62)	0.0144
	Nocardiaceae	3.26 (3.58)	2.63 (3.92)	0.6784	3.26 (3.58)	10.10 (8.30)	**0.0073**	10.10 (8.30)	2.63 (3.92)	**0.0019**
	Planococcaceae	0.83 (1.15)	0.06 (0.39)	**0.0018**	0.83 (1.15)	0.01 (0.01)	**<0.0001**	0.01 (0.01)	0.06 (0.39)	**0.0002**
	Propionibacteriaceae	1.61 (1.11)	1.12 (1.51)	0.9826	1.61 (1.11)	0.94 (0.85)	0.2657	0.94 (0.85)	1.12 (1.51)	0.1585
	Pseudonocaridiaceae	0.28 (0.22)	0.15 (0.24)	0.1017	0.28 (0.22)	1.14 (2.03)	**0.0028**	1.14 (2.03)	0.15 (0.24)	**0.0001**
	Pseudomonadaceae	0.77 (0.60)	0.88 (1.96)	0.9478	0.77 (0.60)	0.21 (1.43)	0.1213	0.21 (1.43)	0.88 (1.96)	0.2998
	Rhizobiaceae	4.83 (8.26)	5.58 (8.67)	0.7434	4.83 (8.26)	1.23 (2.01)	0.0154	1.23 (2.01)	5.58 (8.67)	0.0114
	Rickettsiaceae	0.64 (0.64)	0.62 (1.43)	0.4715	0.64 (0.64)	0.18 (0.13)	**0.0004**	0.18 (0.13)	0.62 (1.43)	**0.0016**

[&]The same colors indicate the relatedness of the respective taxa.

*RA and IQR denote relative abundance and interquartile range, respectively.

[#]*p* values of < 0.0083 were considered significant and indicated in bold.

Table 4.S3 Continued

Taxon[&]		Median RA (IQR)*		*p* value[#]	Median RA (IQR)		*p* value	Median RA (IQR)		*p* value
		Region D males	Region K males		Region D males	Region P males		Region P males	Region K males	
Family	Sphingobacteriaceae	0.07 (0.36)	0.61 (0.92)	**0.0073**	0.07 (0.36)	2.52 (2.86)	**<0.0001**	2.52 (2.86)	0.61 (0.92)	**0.0032**
	Sphingomonadaceae	2.09 (3.75)	6.80 (11.24)	0.0083	2.09 (3.75)	12.73 (11.81)	**0.0001**	12.73 (11.81)	6.80 (11.24)	0.1057
	Staphylococcaceae	0.47 (0.64)	0.23 (0.38)	0.1831	0.47 (0.64)	0.03 (0.05)	**0.0002**	0.03 (0.05)	0.23 (0.38)	**0.0079**
	Spirochaetaceae	0.09 (0.13)	0.04 (0.11)	0.8786	0.09 (0.13)	0.04 (1.25)	0.5268	0.04 (1.25)	0.04 (0.11)	0.7716
	Spirosomaceae	0.29 (0.49)	0.51 (0.43)	0.1213	0.29 (0.49)	1.23 (1.19)	**0.0056**	1.23 (1.19)	0.51 (0.43)	0.0512
	Xanthobacteraceae	1.49 (0.83)	0.79 (1.93)	0.4450	1.49 (0.83)	0.76 (0.71)	0.0521	0.76 (0.71)	0.79 (1.93)	0.5897
Genus	*Actinomycetospora*	0.08 (0.12)	0.04 (0.03)	0.1112	0.08 (0.12)	0.91 (1.72)	**<0.0001**	0.91 (1.72)	0.04 (0.03)	**<0.0001**
	Acinetobacter	0.90 (1.31)	0.13 (0.19)	**0.0003**	0.90 (1.31)	0.04 (0.03)	**<0.0001**	0.04 (0.03)	0.13 (0.19)	0.0181
	Allorhizobium.Neorhizb-ium.Pararhizobium. Rhizobium	1.33 (1.80)	1.05 (1.99)	0.7767	1.33 (1.80)	0.19 (0.34)	**0.0005**	0.19 (0.34)	1.05 (1.99)	0.0181
	Aureimonas	0.02 (0.32)	0.43 (0.60)	0.0576	0.02 (0.32)	0.98 (1.06)	**0.0004**	0.98 (1.06)	0.43 (0.60)	0.0144
	Bacillus	0.20 (0.18)	1.84 (6.06)	0.0424	0.20 (0.18)	0.02 (0.03)	**0.0016**	0.02 (0.03)	1.84 (6.06)	**0.0001**
	Borrelia	0.00 (0.00)	0.02 (0.02)	**0.0003**	0.00 (0.00)	0.00 (0.00)	0.1800	0.00 (0.00)	0.02 (0.02)	**0.0053**
	Borreliella	0.08 (0.08)	0.02 (0.06)	0.3947	0.08 (0.08)	0.01 (1.24)	0.7434	0.01 (1.24)	0.02 (0.06)	0.9010
	Bosea	0.61 (1.04)	0.72 (1.20)	0.7434	0.61 (1.04)	0.09 (0.23)	0.0094	0.09 (0.23)	0.72 (1.20)	0.1249
	Candidatus Midichloria	0.18 (0.05)	0.43 (0.27)	**0.0024**	0.18 (0.05)	0.09 (0.05)	**0.0010**	0.09 (0.05)	0.43 (0.27)	**<0.0001**
	Candidatus Neoehrlichia	0.00 (0.00)	0.01 (0.01)	**0.0024**	0.00 (0.00)	0.00 (0.01)	0.0837	0.00 (0.01)	0.01 (0.01)	0.1572
	Curtobacterium	3.60 (11.72)	4.07 (9.10)	0.7107	3.60 (11.72)	6.03 (3.80)	0.3261	6.03 (3.80)	4.07 (9.10)	0.3615
	Cutibacterium	1.19 (1.35)	0.72 (1.18)	0.4715	1.19 (1.35)	0.18 (0.14)	**0.0002**	0.18 (0.14)	0.72 (1.18)	0.0181
	Ehrlichia	0.00 (0.00)	0.02 (0.05)	**0.0008**	0.00 (0.00)	0.01 (0.01)	**<0.0001**	0.01 (0.01)	0.02 (0.05)	0.9337
	Geodermatophilus	0.04 (0.22)	0.09 (0.39)	1.0000	0.04 (0.22)	0.88 (1.47)	**0.0004**	0.88 (1.47)	0.09 (0.39)	**0.0008**

[&]The same colors indicate the relatedness of the respective taxa.

*RA and IQR denote relative abundance and interquartile range, respectively.

[#]*p* values of < 0.0083 were considered significant and indicated in bold.

Table 4.S3 Continued

Taxon[&]		Median RA (IQR)* Region D males	Median RA (IQR)* Region K males	*p* value[#]	Median RA (IQR) Region D males	Median RA (IQR) Region P males	*p* value	Median RA (IQR) Region P males	Median RA (IQR) Region K males	*p* value
Genus	*Halomonas*	8.01 (9.38)	2.29 (4.39)	0.0107	8.01 (9.38)	0.60 (0.49)	**<0.0001**	0.60 (0.49)	2.29 (4.39)	0.0144
	Hymenobacter	0.01 (0.02)	0.05 (0.64)	0.0106	0.01 (0.02)	0.97 (1.76)	**<0.0001**	0.97 (1.76)	0.05 (0.64)	**0.0055**
	Kineococcus	0.01 (0.28)	0.17 (1.72)	0.0471	0.01 (0.28)	0.72 (1.09)	**0.0008**	0.72 (1.09)	0.17 (1.72)	0.2290
	Methylobacterium	1.18 (2.74)	1.33 (10.87)	0.2136	1.18 (2.74)	17.75 (12.27)	**<0.0001**	17.75 (12.27)	1.33 (10.87)	**0.0025**
	Mycobacterium	15.40 (11.29)	12.84 (19.73)	0.7107	15.40 (11.29)	3.24 (2.65)	**0.0001**	3.24 (2.65)	12.84 (19.73)	**0.0042**
	Nakamurella	0.12 (0.15)	0.11 (0.62)	0.3261	0.12 (0.15)	0.73 (2.13)	**0.0032**	0.73 (2.13)	0.11 (0.62)	0.0144
	Pseudomonas	0.77 (0.60)	0.88 (1.96)	0.9478	0.77 (0.60)	0.21 (1.43)	0.1213	0.21 (1.43)	0.88 (1.96)	0.2998
	Rhodococcus	0.46 (0.49)	0.64 (1.26)	0.1561	0.46 (0.49)	0.28 (0.22)	0.6468	0.28 (0.22)	0.64 (1.26)	0.0564
	Rickettsia	0.64 (0.64)	0.62 (1.44)	0.4987	0.64 (0.64)	0.18 (0.13)	**0.0004**	0.18 (0.13)	0.62 (1.44)	**0.0014**
	Sphingomonas	1.07 (3.63)	6.37 (11.73)	**0.0073**	1.07 (3.63)	11.29 (10.19)	**<0.0001**	11.29 (10.19)	6.37 (11.73)	0.0890
	Staphylococcus	0.41 (0.64)	0.21 (0.03)	0.1437	0.41 (0.64)	0.03 (0.05)	**0.0002**	0.03 (0.05)	0.21 (0.03)	0.0090
	Spirosoma	0.00 (0.00)	0.03 (0.04)	**<0.0001**	0.00 (0.00)	0.05 (2.85)	**<0.0001**	0.05 (2.85)	0.03 (0.04)	**0.0002**

[&]The same colors indicate the relatedness of the respective taxa.

*RA and IQR denote relative abundance and interquartile range, respectively.

[#]*p* values of < 0.0083 were considered significant and indicated in bold.

Table 4.S4 Differences in the relative abundance for female ticks of *Ixodes ricinus* between regions

	Taxon[&]	Median RA (IQR)*		*p* value[#]	Median RA (IQR)		*p* value	Median RA (IQR)		*p* value
		Region D females	Region K females		Region D females	Region P females		Region P females	Region K females	
Phylum	Actinobacteria	18.58 (12.00)	24.45 (16.02)	0.0745	18.58 (12.00)	23.35 (13.91)	0.1354	23.35 (13.91)	24.45 (16.02)	0.6783
	Bacteroidetes	0.80 (0.72)	1.87 (2.19)	**0.0016**	0.80 (0.72)	4.07 (2.55)	**<0.0001**	4.07 (2.55)	1.87 (2.19)	0.0279
	Firmicutes	1.62 (2.33)	3.63 (5.74)	0.4306	1.62 (2.33)	0.27 (0.40)	**0.0021**	0.27 (0.40)	3.63 (5.74)	**0.0048**
	Proteobacteria	75.55 (13.79)	59.60 (16.98)	**0.0016**	75.55 (13.79)	64.23 (13.71)	0.0225	64.23 (13.71)	59.60 (16.98)	0.2455
	Spirochaetes	0.05 (0.04)	0.04 (0.07)	0.5614	0.05 (0.04)	0.02 (0.40)	0.6187	0.02 (0.40)	0.04 (0.07)	0.1057
Class	Actinobacteria	18.36 (11.74)	23.81 (16.55)	0.0745	18.36 (11.74)	23.06 (14.19)	0.1354	23.06 (14.19)	23.81 (16.55)	0.7089
	Alphaproteobacteria	66.21 (20.85)	57.93 (14.06)	0.0620	66.21 (20.85)	62.82 (8.77)	0.3837	62.82 (8.77)	57.93 (14.06)	0.1711
	Bacilli	1.54 (2.33)	3.24 (5.23)	0.5614	1.54 (2.33)	0.24 (0.37)	**0.0021**	0.24 (0.37)	3.24 (5.23)	**0.0079**
	Bacteroidia	0.80 (0.72)	1.87 (2.19)	**0.0016**	0.80 (0.72)	4.07 (2.55)	**<0.0001**	4.07 (2.55)	1.87 (2.19)	0.0279
	Gammaproteobacteria	9.31 (7.27)	2.38 (2.83)	**0.0005**	9.31 (7.27)	1.66 (3.21)	**0.0004**	1.66 (3.21)	2.38 (2.83)	0.6187
	Spirochaetia	0.03 (0.03)	0.04 (0.07)	0.0620	0.03 (0.03)	0.02 (0.40)	0.4807	0.02 (0.40)	0.04 (0.07)	0.1057
Order	Bacillales	1.43 (2.28)	1.91 (4.70)	0.8357	1.43 (2.28)	0.16 (0.13)	**0.0005**	0.16 (0.13)	1.91 (4.70)	0.0161
	Corynebacteriales	11.74 (10.34)	11.72 (7.56)	0.9339	11.74 (10.34)	10.98 (10.26)	0.7716	10.98 (10.26)	11.72 (7.56)	0.5614
	Cytophagales	0.30 (0.30)	0.79 (0.83)	**0.0009**	0.30 (0.30)	2.94 (2.13)	**<0.0001**	2.94 (2.13)	0.79 (0.83)	**0.0028**
	Frankiales	0.18 (0.17)	0.51 (0.56)	**0.0025**	0.18 (0.17)	0.58 (0.64)	**0.0008**	0.58 (0.64)	0.51 (0.56)	0.6482
	Kineosporiales	0.01 (0.02)	0.03 (0.23)	0.0564	0.01 (0.02)	0.28 (0.59)	**0.0002**	0.28 (0.59)	0.03 (0.23)	0.0225
	Micrococcales	2.20 (1.99)	6.66 (10.45)	0.0620	2.20 (1.99)	5.24 (5.97)	0.0128	5.24 (5.97)	6.66 (10.45)	0.9010
	Oceanospirillales	3.66 (2.97)	0.03 (0.04)	**<0.0001**	3.66 (2.97)	0.03 (0.02)	**<0.0001**	0.03 (0.02)	0.03 (0.04)	0.8682
	Propionibacteriales	0.56 (0.51)	1.38 (0.96)	0.0202	0.56 (0.51)	1.11 (1.04)	0.0564	1.11 (1.04)	1.38 (0.96)	1.0000
	Pseudocardiales	0.14 (0.22)	0.20 (0.24)	0.1466	0.14 (0.22)	0.39 (1.55)	**0.0062**	0.39 (1.55)	0.20 (0.24)	0.1150
	Pseudomonadales	2.78 (1.69)	1.48 (1.54)	0.0310	2.78 (1.69)	1.01 (1.69)	0.0620	1.01 (1.69)	1.48 (1.54)	0.7400

[&]The same colors indicate the relatedness of the respective taxa.

*RA and IQR denote relative abundance and interquartile range, respectively.

[#]*p* values of < 0.0083 were considered significant and indicated in bold.

Table 4.S4 Continued

Taxon[&]		Median RA (IQR)*		*p* value[#]	Median RA (IQR)		*p* value	Median RA (IQR)		*p* value
		Region D females	Region K females		Region D females	Region P females		Region P females	Region K females	
Order	Rhizobiales	7.22 (4.86)	13.97 (7.76)	0.0128	7.22 (4.86)	18.14 (9.10)	**0.0037**	18.14 (9.10)	13.97 (7.76)	0.3837
	Rickettsiales	49.94 (29.99)	36.24 (29.54)	0.0144	49.94 (29.99)	31.38 (22.33)	**0.0079**	31.38 (22.33)	36.24 (29.54)	1.0000
	Sphingobacteriales	0.10 (0.26)	0.48 (0.67)	0.0128	0.10 (0.26)	0.37 (1.08)	**0.0055**	0.37 (1.08)	0.48 (0.67)	1.0000
	Sphingomonadales	2.19 (2.10)	4.78 (8.88)	0.0344	2.19 (2.10)	11.77 (4.37)	**<0.0001**	11.77 (4.37)	4.78 (8.88)	0.0815
	Spirochaetales	0.03 (0.03)	0.04 (0.007)	0.0620	0.03 (0.03)	0.02 (0.40)	0.4807	0.02 (0.40)	0.04 (0.007)	0.1057
Family	Anaplasmataceae	0.01 (0.01)	0.01 (0.04)	1.0000	0.01 (0.01)	0.03 (0.01)	**0.0004**	0.03 (0.01)	0.01 (0.04)	0.0380
	Bacillaceae	0.13 (0.10)	1.19 (3.78)	0.0620	0.13 (0.10)	0.04 (0.07)	0.0381	0.04 (0.07)	1.19 (3.78)	0.0202
	Beijerinckiaceae	1.26 (2.19)	2.61 (7.03)	0.0381	1.26 (2.19)	8.46 (12.41)	**<0.0001**	8.46 (12.41)	2.61 (7.03)	0.0090
	Geodermatophilaceae	0.05 (0.05)	0.11 (0.09)	**0.0037**	0.05 (0.05)	0.26 (0.33)	**0.0009**	0.26 (0.33)	0.11 (0.09)	0.1985
	Halomonadaceae	3.66 (2.97)	0.03 (0.04)	**<0.0001**	3.66 (2.97)	0.03 (0.02)	**<0.0001**	0.03 (0.02)	0.03 (0.04)	0.8682
	Hymenobacteraceae	0.01 (0.02)	0.06 (0.30)	**0.0021**	0.01 (0.02)	0.31 (0.93)	**<0.0001**	0.31 (0.93)	0.06 (0.30)	0.0381
	Midichloriaceae	31.34 (31.63)	28.52 (26.03)	0.4068	31.34 (31.63)	18.84 (21.66)	0.1985	18.84 (21.66)	28.52 (26.03)	0.5338
	Microbacteriaceae	1.85 (1.76)	4.32 (10.74)	0.1985	1.85 (1.76)	5.11 (6.03)	0.0128	5.11 (6.03)	4.32 (10.74)	0.8682
	Mycobacteriaceae	9.73 (8.32)	9.53 (9.08)	0.6783	9.73 (8.32)	6.57 (6.60)	0.0971	6.57 (6.60)	9.53 (9.08)	0.1466
	Moraxellaceae	0.72 (0.74)	0.19 (0.33)	**0.0021**	0.72 (0.74)	0.05 (0.13)	**<0.0001**	0.05 (0.13)	0.19 (0.33)	0.0128
	Nakamurellaceae	0.05 (0.08)	0.29 (0.21)	0.0161	0.05 (0.08)	0.13 (0.10)	0.0279	0.13 (0.10)	0.29 (0.21)	0.3195
	Nocardiaceae	1.48 (1.14)	1.67 (5.81)	0.2998	1.48 (1.14)	3.95 (6.20)	0.0815	3.95 (6.20)	1.67 (5.81)	0.8357
	Planococcaceae	0.69 (1.46)	0.10 (0.32)	**0.0006**	0.69 (1.46)	0.01 (0.01)	**<0.0001**	0.01 (0.01)	0.10 (0.32)	**0.0009**
	Propionibacteriaceae	0.34 (0.26)	0.44 (0.65)	0.0745	0.34 (0.26)	0.40 (0.66)	0.1057	0.40 (0.66)	0.44 (0.65)	0.9669
	Pseudonocardiaceae	0.14 (0.22)	0.20 (0.24)	0.1466	0.14 (0.22)	0.39 (1.55)	**0.0062**	0.39 (1.55)	0.20 (0.24)	0.1150
	Pseudomonadaceae	1.57 (1.81)	1.14 (1.44)	0.4807	1.57 (1.81)	0.97 (1.08)	0.4807	0.97 (1.08)	1.14 (1.44)	0.9010

[&]The same colors indicate the relatedness of the respective taxa.

*RA and IQR denote relative abundance and interquartile range, respectively.

[#]*p* values of < 0.0083 were considered significant and indicated in bold.

Table 4.S4 Continued

Taxon[&]		Median RA (IQR)*		*p* value[#]	Median RA (IQR)		*p* value	Median RA (IQR)		*p* value
		Region D females	Region K females		Region D females	Region P females		Region P females	Region K females	
Family	Pseudomonadaceae	1.57 (1.81)	1.14 (1.44)	0.4807	1.57 (1.81)	0.97 (1.08)	0.4807	0.97 (1.08)	1.14 (1.44)	0.9010
	Rhizobiaceae	2.60 (3.44)	2.98 (5.49)	1.0000	2.60 (3.44)	1.10 (1.65)	0.0202	1.10 (1.65)	2.98 (5.49)	0.0279
	Rickettsiaceae	0.33 (57.96)	0.50 (2.38)	0.6482	0.33 (57.96)	1.01 (2.18)	0.5897	1.01 (2.18)	0.50 (2.38)	0.4306
	Sphingobacteriaceae	0.09 (0.24)	0.42 (0.70)	0.0144	0.09 (0.24)	0.37 (1.08)	**0.0048**	0.37 (1.08)	0.42 (0.70)	0.9339
	Sphingomonadaceae	2.19 (2.10)	4.78 (8.88)	0.0344	2.19 (2.10)	11.77 (4.37)	**<0.0001**	11.77 (4.37)	4.78 (8.88)	0.0815
	Staphylococcaceae	0.12 (0.22)	0.11 (0.15)	0.6783	0.12 (0.22)	0.06 (0.08)	0.0279	0.06 (0.08)	0.11 (0.15)	0.1249
	Spirochaetaceae	0.03 (0.03)	0.04 (0.07)	0.0620	0.03 (0.03)	0.02 (0.40)	0.4807	0.02 (0.40)	0.04 (0.07)	0.1057
	Spirosomaceae	0.11 (0.14)	0.55 (0.46)	**0.0070**	0.11 (0.14)	1.69 (1.83)	**<0.0001**	1.69 (1.83)	0.55 (0.46)	**0.0037**
	Xanthobacteraceae	0.45 (0.47)	0.74 (1.01)	0.3615	0.45 (0.47)	0.75 (0.83)	0.3401	0.75 (0.83)	0.74 (1.01)	1.0000
Genus	*Actinomycetospora*	0.06 (0.04)	0.10 (0.10)	0.2998	0.06 (0.04)	0.16 (1.35)	0.0090	0.16 (1.35)	0.10 (0.10)	0.0815
	Acinetobacter	0.68 (0.70)	0.07 (0.09)	**<0.0001**	0.68 (0.70)	0.02 (0.03)	**<0.0001**	0.02 (0.03)	0.07 (0.09)	**0.0006**
	Allorhizobium.Neorhizb-ium.Pararhizobium. Rhizobium	0.66 (1.11)	0.65 (1.53)	0.7716	0.66 (1.11)	0.22 (0.51)	0.0381	0.22 (0.51)	0.65 (1.53)	0.2455
	Aureimonas	0.09 (0.13)	0.35 (0.60)	0.1150	0.09 (0.13)	0.24 (0.47)	0.0114	0.24 (0.47)	0.35 (0.60)	0.6783
	Bacillus	0.11 (0.08)	1.13 (3.68)	0.0512	0.11 (0.08)	0.04 (0.07)	0.1249	0.04 (0.07)	1.13 (3.68)	0.0161
	Borrelia	0.00 (0.00)	0.02 (0.00)	**<0.0001**	0.00 (0.00)	0.00 (0.00)	0.3506	0.00 (0.00)	0.02 (0.00)	**<0.0001**
	Borreliella	0.01 (0.03)	0.01 (0.03)	0.6482	0.01 (0.03)	0.01 (0.40)	0.4068	0.01 (0.40)	0.01 (0.03)	0.1249
	Bosea	0.67 (0.80)	0.52 (0.89)	0.3615	0.67 (0.80)	0.10 (0.41)	0.0279	0.10 (0.41)	0.52 (0.89)	0.4306
	Candidatus Midichloria	31.34 (31.63)	28.52 (26.03)	0.4068	31.34 (31.63)	18.44 (21.66)	0.1985	18.44 (21.66)	28.52 (26.03)	0.5338

[&]The same colors indicate the relatedness of the respective taxa.

*RA and IQR denote relative abundance and interquartile range, respectively.

[#]*p* values of < 0.0083 were considered significant and indicated in bold.

Table 4.S4 Continued

Taxon[&]		Median RA (IQR)*		*p* value[#]	Median RA (IQR)		*p* value	Median RA (IQR)		*p* value
		Region D females	Region K females		Region D females	Region P females		Region P females	Region K females	
Genus	*Candidatus* Neoehrlichia	0.00 (0.00)	0.01 (0.00)	0.1672	0.00 (0.00)	0.00 (0.01)	**<0.0001**	0.00 (0.01)	0.01 (0.00)	**0.0004**
	Curtobacterium	1.34 (1.66)	3.69 (10.84)	0.5338	1.34 (1.66)	3.84 (6.32)	0.0620	3.84 (6.32)	3.69 (10.84)	0.8682
	Cutibacterium	0.22 (0.20)	0.24 (0.54)	0.2808	0.22 (0.20)	0.20 (0.59)	0.9339	0.20 (0.59)	0.24 (0.54)	0.3837
	Ehrlichia	0.01 (0.01)	0.00 (0.01)	0.1009	0.01 (0.01)	0.02 (0.01)	**0.0006**	0.02 (0.01)	0.00 (0.01)	**0.0004**
	Geodermatophilus	0.02 (0.04)	0.06 (0.13)	0.0564	0.02 (0.04)	0.26 (0.33)	**0.0005**	0.26 (0.33)	0.06 (0.13)	0.0421
	Halomonas	3.66 (2.97)	0.03 (0.04)	**<0.0001**	3.66 (2.97)	0.03 (0.02)	**<0.0001**	0.03 (0.02)	0.03 (0.04)	0.8682
	Hymenobacter	0.01 (0.02)	0.04 (0.25)	**0.0062**	0.01 (0.02)	0.27 (0.81)	**<0.0001**	0.27 (0.81)	0.04 (0.25)	0.0279
	Kineococcus	0.01 (0.02)	0.03 (0.21)	0.0202	0.01 (0.02)	0.27 (0.58)	**0.0003**	0.27 (0.58)	0.03 (0.21)	0.0512
	Methylobacterium	0.52 (0.46)	1.66 (7.07)	0.0090	0.52 (0.46)	7.76 (12.77)	**<0.0001**	7.76 (12.77)	1.66 (7.07)	0.0251
	Mycobacterium	9.73 (8.32)	9.53 (9.08)	0.6783	9.73 (8.32)	6.57 (6.60)	0.0971	6.57 (6.60)	9.53 (9.08)	0.1466
	Nakamurella	0.05 (0.08)	0.29 (0.21)	0.0161	0.05 (0.08)	0.13 (0.10)	0.0279	0.13 (0.10)	0.29 (0.21)	0.3195
	Pseudomonas	1.57 (1.81)	1.14 (1.44)	0.4807	1.57 (1.81)	0.97 (1.08)	0.4807	0.97 (1.08)	1.14 (1.44)	0.9010
	Rhodococcus	0.22 (0.28)	0.27 (0.17)	0.5069	0.22 (0.28)	0.19 (0.13)	0.5338	0.19 (0.13)	0.27 (0.17)	0.1354
	Rickettsia	0.33 (57.96)	0.49 (2.38)	0.6482	0.33 (57.96)	1.01 (2.18)	0.5897	1.01 (2.18)	0.49 (2.38)	0.4068
	Sphingomonas	1.27 (2.13)	3.79 (9.11)	0.0310	1.27 (2.13)	10.02 (6.36)	**<0.0001**	10.02 (6.36)	3.79 (9.11)	0.0890
	Staphylococcus	0.12 (0.19)	0.09 (0.13)	0.6482	0.12 (0.19)	0.06 (0.08)	0.0279	0.06 (0.08)	0.09 (0.13)	0.1466
	Spirosoma	0.01 (0.01)	0.02 (0.08)	**0.0030**	0.01 (0.01)	0.78 (1.67)	**<0.0001**	0.78 (1.67)	0.02 (0.08)	**0.0002**

[&]The same colors indicate the relatedness of the respective taxa.

*RA and IQR denote relative abundance and interquartile range, respectively.

[#]*p* values of < 0.0083 were considered significant and indicated in bold.

Table 4.S5 Significantly different bacterial taxa and their percentile abundance based on inter-sex ANCOM-based comparisons for male and female ticks of *Ixodes ricinus*

	Female					Male				
Percentile	**0.0**	**25.0**	**50.0**	**75.0**	**100.0**	**0.0**	**25.0**	**50.0**	**75.0**	**100.0**
	Region D									
Candidatus Midichloria	21613.0	64762.0	156803.0	226642.0	285431.0	445.0	691.25	716.5	862.5	1257.0
	Region K									
Candidatus Midichloria	27281.0	78510.0	184629.0	250723.0	324762.0	988.0	1229.5	2419.0	2704.5	45085
Enterococcus	1.0	143.5	233.0	457.5	2785.0	1.0	1.0	1.0	1.0	1118.0
Halomonas	92.0	141.5	180.0	360.0	1826.0	1894.0	4889.0	144750.0	32604.0	82719.0
	Region P									
Candidatus Midichloria	5728.0	63740.0	119160.0	198758.5	286758.0	359.0	470.0	543.0	704.0	51484.0
Unclassified genus of Carnobacteriaceae	1.0	1.0	1.0	1.0	119.0	37.0	50.5	106.0	228.0	361.0

Table 4.S6 Significantly different bacterial taxa and their percentile abundance based on inter-regional ANCOM-based comparisons for male ticks of *Ixodes Ricinus*

Percentile	**0.0**	**25.0**	**50.0**	**75.0**	**100.0**	**0.0**	**25.0**	**50.0**	**75.0**	**100.0**
Region D vs K	**Region D**					**Region K**				
SWB02	6.0	267.0	825.5	1423.5	2183.0	1.0	1.0	1.0	1.0	12.0
Pseudarcicella	23.0	243.0	587.5	982.5	3506.0	1.0	1.0	1.0	17.5	307.0
Pedomicroboium	1.0	120.5	265.0	621.5	1692.5	1.0	1.0	1.0	1.0	36.0
Region D vs P	**Region D**					**Region P**				
SWB02	6.0	267.00	825.5	1423.50	2183.0	1.0	1.0	1.0	1.0	6.0
Unclassified genus of Hymenobacteraceae	1.0	1.00	1.0	1.00	17.0	45.0	198.0	354.0	879.0	7134.0
Pseudarcicella	23.0	243.00	587.5	982.5	3506.0	1.0	1.0	1.0	7.0	31.0
Spirosoma	1.0	11.75	20.0	30.25	45.0	282.0	1503.5	3683.0	4499.5	17833.0
Hyphomicrobium	27.0	418.00	1091.0	1963.75	3057.0	1.0	3.5	9.0	29.0	53.0
Pedomicrobium	1.0	120.50	265.0	621.50	1692.5	1.0	1.0	1.0	1.0	19.0
Roseomonas	1.0	8.50	13.0	30.00	1631.0	952.0	2035.5	3305.0	5326.5	6975.0
Unclassified genus of Planococcaceae	542.0	2019.25	3117.5	6229.75	19130.0	15.0	36.5	45.0	83.5	486.0
Region P vs K	**Region K**					**Region P**				
Actinomycetospora	67.0	154.5	221.0	362.0	1363.0	488.0	2373.5	4445.0	12550.5	35795.0
Bacillus	162.0	535.0	9664.0	37044.5	59158.0	1.0	81.5	152.0	284.0	632.0

Table 4.S7 Significantly different bacterial taxa and their percentile abundance based on inter-regional ANCOM-based comparisons for female ticks of *Ixodes ricinus*

Percentile	**0.0**	**25.0**	**50.0**	**75.0**	**100.0**	**0.0**	**25.0**	**50.0**	**75.0**	**100.0**
Region D vs K	**Region D**					**Region K**				
Pedomicroboium	45.0	78.5	208.0	372.0	776.0	1.0	1.0	1.0	1.0	1.0
SWB02	38.0	98.0	332.0	445.0	2027.0	1.0	1.0	1.0	1.0	46.0
Halomonas	2573.0	4692.0	16558.0	20331.5	34469.0	92.0	141.5	180.0	360.0	1826.0
Unclassified genus of Caulobacterales	1.0	41.0	153.0	370.0	853.0	1.0	1.0	1.0	1.0	1.0
Region D vs P	**Region D**					**Region P**				
Pedomicroboium	45.0	78.5	208.0	372.0	776.0	1.0	1.0	1.0	1.0	105.0
SWB02	38.0	98.0	332.0	445.0	2027.0	1.0	1.0	1.0	6.5	210.0
Spirosoma	1.0	19.0	30.0	46.0	190.0	293.0	1755.5	5505.0	11298.0	52997.0
Unclassified genus of Planococcaceae	252.0	2090.5	3007.0	9898.0	15809.0	1.0	27.0	42.0	54.5	766.0
Halomonas	2573.0	4692.0	16558.0	20331.5	34469.0	91.0	165.5	193.0	325.0	1229.0
Uncultured	17.0	169.0	438.0	644.0	2638.0	1.0	1.0	1.0	9.5	1115.0
Unclassified genus of Caulobacterales	1.0	41.0	153.0	370.0	853.0	1.0	1.0	1.0	1.0	17.0
Region P vs K	**Region K**					**Region P**				
Unclassified genus of Carnobacteriaceae	63.0	135.0	192.0	600.5	1274.0	1.0	1.0	1.0	1.0	119.0
Borrelia	77.0	90.0	100.0	130.5	377658.0	1.0	1.0	1.0	1.0	1.0

4.8. References

1. Saldana MA, Hegde S, Hughes GL. 2017. Microbial control of arthropod-borne disease. Mem Inst Oswaldo Cruz 112:81-93.
2. Couper L, Swei A. 2018. Tick microbiome characterization by next-generation 16S rRNA amplicon sequencing. J Vis Exp: JoVE.
3. Clay K, Fuqua C. 2010. The tick microbiome: diversity, distribution and influence of the internal microbial community for a blood-feeding disease vector. Washington, DC: Critical Needs and Gaps in Understand Prevention, Amelioration, and Resolution of Lyme and Other Tick-Borne Diseases: The Short-Term and Long-Term Outcomes.
4. Barker S, Murrell A. 2004. Systematics and evolution of ticks with a list of valid genus and species names. Parasitology 129:S15.
5. de la Fuente J, Estrada-Pena A, Venzal JM, Kocan KM, Sonenshine DE. 2008. Overview: ticks as vectors of pathogens that cause disease in humans and animals. Front Biosci 13:6938-6946.
6. Houpikian P, Raoult D. 2002. Traditional and molecular techniques for the study of emerging bacterial diseases: one laboratory's perspective. Emerg Infect Dis 8:122-31.
7. Noda H, Munderloh UG, Kurtti TJ. 1997. Endosymbionts of ticks and their relationship to Wolbachia spp. and tick-borne pathogens of humans and animals. Appl Environ Microbiol 63:3926-32.

8. Benson MJ, Gawronski JD, Eveleigh DE, Benson DR. 2004. Intracellular symbionts and other bacteria associated with deer ticks (*Ixodes scapularis*) from Nantucket and Wellfleet, Cape Cod, Massachusetts. Appl Environ Microbiol 70:616-20.

9. Moreno CX, Moy F, Daniels TJ, Godfrey HP, Cabello FC. 2006. Molecular analysis of microbial communities identified in different developmental stages of *Ixodes scapularis* ticks from Westchester and Dutchess Counties, New York. Environ Microbiol 8:761-72.

10. Clay K, Klyachko O, Grindle N, Civitello D, Oleske D, Fuqua C. 2008. Microbial communities and interactions in the lone star tick, *Amblyomma americanum*. Mol Ecol 17:4371-4381.

11. Heise SR, Elshahed M, Little S. 2010. Bacterial diversity in *Amblyomma americanum* (Acari: Ixodidae) with a focus on members of the genus Rickettsia. J Med Entomol 47:258-268.

12. Van Overbeek L, Gassner F, Van Der Plas CL, Kastelein P, Nunes–da Rocha U, Takken W. 2008. Diversity of *Ixodes ricinus* tick-associated bacterial communities from different forests. FEMS Microbiol Ecol 66:72-84.

13. Schabereiter-Gurtner C, Lubitz W, Rölleke S. 2003. Application of broad-range 16S rRNA PCR amplification and DGGE fingerprinting for detection of tick-infecting bacteria. J Microbiol Methods 52:251-260.

14. Wade W. 2002. Unculturable bacteria—the uncharacterized organisms that cause oral infections. J R Soc Med 95:81-83.

15. Carpi G, Cagnacci F, Wittekindt NE, Zhao F, Qi J, Tomsho LP, Drautz DI, Rizzoli A, Schuster SC. 2011. Metagenomic profile of the bacterial communities associated with *Ixodes ricinus* ticks. PLoS One 6:e25604.

16. Menchaca AC, Visi DK, Strey OF, Teel PD, Kalinowski K, Allen MS, Williamson PC. 2013. Preliminary assessment of microbiome changes following blood-feeding and survivorship in the *Amblyomma americanum* nymph-to-adult transition using semiconductor sequencing. PLoS One 8:e67129.

17. Williams-Newkirk AJ, Rowe LA, Mixson-Hayden TR, Dasch GA. 2014. Characterization of the bacterial communities of life stages of free living lone star ticks (*Amblyomma americanum*). PLoS One 9:e102130.

18. Klindworth A, Pruesse E, Schweer T, Peplies J, Quast C, Horn M, Glöckner FO. 2013. Evaluation of general 16S ribosomal RNA gene PCR primers for classical and next-generation sequencing-based diversity studies. Nucleic Acids Res 41:e1-e1.

19. Janda JM, Abbott SL. 2007. 16S rRNA gene sequencing for bacterial identification in the diagnostic laboratory: pluses, perils, and pitfalls. J Clin Microbiol 45:2761-2764.

20. Medlock JM, Hansford KM, Bormane A, Derdakova M, Estrada-Peña A, George J-C, Golovljova I, Jaenson TG, Jensen J-K, Jensen PM. 2013. Driving forces for changes in geographical distribution of *Ixodes ricinus* ticks in Europe. Parasit Vectors 6:1.

21. Parola P, Raoult D. 2001. Ticks and tickborne bacterial diseases in humans: an emerging infectious threat. Clin Infect Dis 32:897-928.

22. Rizzoli A, Hauffe HC, Carpi G, Vourc'h G, Neteler M, Rosa R. 2011. Lyme borreliosis in Europe. Euro Surveill 16:19906.

23. Hayes S, Burgdorfer W. 1982. Reactivation of *Rickettsia rickettsii* in *Dermacentor andersoni* ticks: an ultrastructural analysis. Infect Immun 37:779-785.

24. Sacchi L, Bigliardi E, Corona S, Beninati T, Lo N, Franceschi A. 2004. A symbiont of the tick *Ixodes ricinus* invades and consumes mitochondria in a mode similar to that of the parasitic bacterium *Bdellovibrio bacteriovorus*. Tissue Cell 36:43-53.

25. Scoles GA. 2004. Phylogenetic analysis of the Francisella-like endosymbionts of Dermacentor ticks. J Med Entomol 41:277-286.

26. Hernandez-Jarguin A, Diaz-Sanchez S, Villar M, de la Fuente J. 2018. Integrated metatranscriptomics and metaproteomics for the characterization of bacterial microbiota in unfed *Ixodes ricinus*. Ticks Tick Borne Dis 9:1241-1251.

27. Nakao R, Abe T, Nijhof AM, Yamamoto S, Jongejan F, Ikemura T, Sugimoto C. 2013. A novel approach, based on BLSOMs (Batch Learning Self-Organizing Maps), to the microbiome analysis of ticks. ISME J 7:1003-15.

28. Portillo A, Palomar AM, de Toro M, Santibanez S, Santibanez P, Oteo JA. 2019. Exploring the bacteriome in anthropophilic ticks: To investigate the vectors for diagnosis. PLoS One 14:e0213384.

29. Kmet V, Čaplová Z. 2019. AN UPDATE ON THE *IXODES RICINUS* MICROBIOME. J Microbiol Biotechnol Food Sci 8.

30. Aivelo T, Norberg A, Tschirren B. 2019. Bacterial microbiota composition of *Ixodes ricinus* ticks: the role of environmental variation, tick characteristics and microbial interactions. PeerJ 7:e8217.

31. Vayssier-Taussat M, Moutailler S, Michelet L, Devillers E, Bonnet S, Cheval J, Hebert C, Eloit M. 2013. Next generation sequencing uncovers unexpected bacterial pathogens in ticks in western Europe. PLoS One 8:e81439.

32. Rogovskyy AS, Nebogatkin IV, Scoles GA. 2017. Ixodid ticks in the megapolis of Kyiv, Ukraine. Ticks Tick Borne Dis 8:99-102.

33. Filippova N. 1977. Ixodid ticks of the subfamily Ixodinae. Fauna of the USSR, Vol. IV/4. Publishing House Nauka, Leningrad:1-396.

34. Rogovskyy A, Batool M, Gillis DC, Holman PJ, Nebogatkin IV, Rogovska YV, Rogovskyy MS. 2018. Diversity of Borrelia spirochetes and other zoonotic agents in ticks from Kyiv, Ukraine. Ticks Tick Borne Dis 9:404-409.

35. Rogovskyy AS, Threadgill DW, Akimov IA, Nebogatkin IV, Rogovska YV, Melnyk MV, Rogovskyy SP. 2019. Borrelia and other zoonotic pathogens in *Ixodes ricinus* and *Dermacentor reticulatus* ticks collected from the Chernobyl exclusion zone on the 30th anniversary of the nuclear disaster. Vector Borne Zoonotic Dis 19:466-473.

36. Chakravorty S, Helb D, Burday M, Connell N, Alland D. 2007. A detailed analysis of 16S ribosomal RNA gene segments for the diagnosis of pathogenic bacteria. J Microbiol Methods 69:330-9.

37. Caporaso JG, Kuczynski J, Stombaugh J, Bittinger K, Bushman FD, Costello EK, Fierer N, Pena AG, Goodrich JK, Gordon JI, Huttley GA, Kelley ST, Knights D, Koenig JE, Ley RE, Lozupone CA, McDonald D, Muegge BD, Pirrung M, Reeder J, Sevinsky JR, Turnbaugh PJ, Walters WA, Widmann J, Yatsunenko T, Zaneveld J, Knight R. 2010. QIIME allows analysis of high-throughput community sequencing data. Nat Methods 7:335-6.

38. Bolyen E, Rideout JR, Dillon MR, Bokulich NA, Abnet CC, Al-Ghalith GA, Alexander H, Alm EJ, Arumugam M, Asnicar F, Bai Y, Bisanz JE, Bittinger K, Brejnrod A, Brislawn CJ, Brown CT, Callahan BJ, Caraballo-Rodriguez AM, Chase J, Cope EK, Da Silva R, Diener C, Dorrestein PC, Douglas GM, Durall DM, Duvallet C, Edwardson CF, Ernst M, Estaki M, Fouquier J, Gauglitz JM, Gibbons SM, Gibson DL, Gonzalez A, Gorlick K, Guo J, Hillmann B, Holmes S, Holste H, Huttenhower C, Huttley GA, Janssen S, Jarmusch AK, Jiang L, Kaehler BD, Kang KB, Keefe CR, Keim P, Kelley ST, Knights D, et al. 2019. Author Correction: Reproducible, interactive, scalable and extensible microbiome data science using QIIME 2. Nat Biotechnol 37:1091.

39. Bokulich NA, Kaehler BD, Rideout JR, Dillon M, Bolyen E, Knight R, Huttley GA, Caporaso JG. 2018. Optimizing taxonomic classification of marker-gene

amplicon sequences with QIIME 2's q2-feature-classifier plugin. Microbiome 6:90.

40. Quast C, Pruesse E, Yilmaz P, Gerken J, Schweer T, Yarza P, Peplies J, Glockner FO. 2013. The SILVA ribosomal RNA gene database project: improved data processing and web-based tools. Nucleic Acids Res 41:D590-6.

41. Hill TC, Walsh KA, Harris JA, Moffett BF. 2003. Using ecological diversity measures with bacterial communities. FEMS Microbiol Ecol 43:1-11.

42. Lozupone C, Knight R. 2005. UniFrac: a new phylogenetic method for comparing microbial communities. Appl Environ Microbiol 71:8228-35.

43. Lozupone CA, Hamady M, Kelley ST, Knight R. 2007. Quantitative and qualitative beta diversity measures lead to different insights into factors that structure microbial communities. Appl Environ Microbiol 73:1576-85.

44. Mandal S, Van Treuren W, White RA, Eggesbo M, Knight R, Peddada SD. 2015. Analysis of composition of microbiomes: a novel method for studying microbial composition. Microb Ecol Health Dis 26:27663.

45. Team RC. 2013. R: A language and environment for statistical computing. Vienna, Austria.

46. Van Treuren W, Ponnusamy L, Brinkerhoff RJ, Gonzalez A, Parobek CM, Juliano JJ, Andreadis TG, Falco RC, Ziegler LB, Hathaway N, Keeler C, Emch M, Bailey JA, Roe RM, Apperson CS, Knight R, Meshnick SR. 2015. Variation in the Microbiota of Ixodes Ticks with Regard to Geography, Species, and Sex. Appl Environ Microbiol 81:6200-9.

47. Brinkerhoff RJ, Clark C, Ocasio K, Gauthier DT, Hynes WL. 2020. Factors affecting the microbiome of *Ixodes scapularis* and *Amblyomma americanum*. PLoS One 15:e0232398.

48. Thapa S, Zhang Y, Allen MS. 2019. Bacterial microbiomes of *Ixodes scapularis* ticks collected from Massachusetts and Texas, USA. BMC Microbiol 19:138.

49. Zhang YK, Yu ZJ, Wang D, Bronislava V, Branislav P, Liu JZ. 2019. The bacterial microbiome of field-collected *Dermacentor marginatus* and *Dermacentor reticulatus* from Slovakia. Parasit Vectors 12:325.

50. Hawlena H, Rynkiewicz E, Toh E, Alfred A, Durden LA, Hastriter MW, Nelson DE, Rong R, Munro D, Dong Q. 2013. The arthropod, but not the vertebrate host or its environment, dictates bacterial community composition of fleas and ticks. ISME J 7:221-223.

51. Lejal E, Estrada-Pena A, Marsot M, Cosson JF, Rue O, Mariadassou M, Midoux C, Vayssier-Taussat M, Pollet T. 2020. Taxon Appearance From Extraction and Amplification Steps Demonstrates the Value of Multiple Controls in Tick Microbiota Analysis. Front Microbiol 11:1093.

52. Perez-Valera E, Kyselkova M, Ahmed E, Sladecek FXJ, Goberna M, Elhottova D. 2019. Native soil microorganisms hinder the soil enrichment with antibiotic resistance genes following manure applications. Sci Rep 9:6760.

53. Zarraonaindia I, Owens SM, Weisenhorn P, West K, Hampton-Marcell J, Lax S, Bokulich NA, Mills DA, Martin G, Taghavi S, van der Lelie D, Gilbert JA. 2015. The soil microbiome influences grapevine-associated microbiota. mBio 6.

54. Lo N, Beninati T, Sassera D, Bouman EA, Santagati S, Gern L, Sambri V, Masuzawa T, Gray JS, Jaenson TG. 2006. Widespread distribution and high prevalence of an alpha-proteobacterial symbiont in the tick *Ixodes ricinus*. Environ Microbiol 8:1280-1287.

55. Duron O, Binetruy F, Noël V, Cremaschi J, McCoy KD, Arnathau C, Plantard O, Goolsby J, Pérez de León AA, Heylen DJ. 2017. Evolutionary changes in symbiont community structure in ticks. Mol Ecol 26:2905-2921.

56. Lalzar I, Harrus S, Mumcuoglu KY, Gottlieb Y. 2012. Composition and seasonal variation of *Rhipicephalus turanicus* and *Rhipicephalus sanguineus* bacterial communities. Appl Environ Microbiol 78:4110-4116.

57. Sinha R, Abu-Ali G, Vogtmann E, Fodor AA, Ren B, Amir A, Schwager E, Crabtree J, Ma S, Microbiome Quality Control Project C, Abnet CC, Knight R, White O, Huttenhower C. 2017. Assessment of variation in microbial community amplicon sequencing by the Microbiome Quality Control (MBQC) project consortium. Nat Biotechnol 35:1077-1086.

58. Greay TL, Gofton AW, Paparini A, Ryan UM, Oskam CL, Irwin PJ. 2018. Recent insights into the tick microbiome gained through next-generation sequencing. Parasit Vectors 11:12.

5. CONCLUSIONS

The antigenic variation at the *vls* locus is a key mechanism to establish persistent infection in the mammalian host by *B. burgdorferi*, a Lyme disease spirochete (Crother et al., 2004; Zhang et al., 1997). The *vls* antigenic variation continuously generates novel variants of surface antigen VlsE through unidirectional recombination of a random segment from one of several unexpressed *vls* cassettes into the central region of the *vlsE* expression site (Zhang et al., 1997). Interestingly, although there are multiple well-documented immunogenic and invariant surface antigens anchored to the outer membrane of *B. burgdorferi*, immune clearance is not affected (Radolf et al., 2012). One of the published studies has shown the VlsE-shielded mechanism, where VlsE protects surface-exposed epitopes of *B. burgdorferi* from host antibodies (Lone and Bankhead, 2020). However, it is hard to believe that VlsE can shield the entire surface-exposed proteins of *B. burgdorferi*. It is possible, that some epitopes remain exposed despite the abundant presence of VlsE. The first part of our study focused on exploring those epitopes that remain exposed in the presence of VlsE. The rationale for the work was to identify putative protection-associated peptides and use them as vaccine candidates against Lyme disease. The major conclusions are drawn from this study here as follows:

1) We now validate that VlsE does not universally shield the entire epitome of *B. burgdorferi* from host antibodies.

2) The observed protection upon repeated immunization against *B. burgdorferi* with VlsE-mutant spirochetes suggests that these peptides are subdominant in nature.
3) VlsE mutant spirochetes can be used to induce a protective immune response against subdominant surface epitopes of *B. burgdorferi* despite the presence of VlsE.
4) The present study has identified putative epitopes that are associated with protection in the mammalian host.
5) The protective potential of these putative protection-associated peptides needs to be evaluated in mouse immunization studies.

To date, the *vls* locus has not been studied in the rabbit host. However, a previously published study has shown that *B. burgdorferi* does not establish persistent infection in the rabbit host (Embers et al., 2007). We hypothesized that the clearance of *B. burgdorferi* infection in rabbits is related to the loss of *vls* locus. Furthermore, we compared anti-*Borrelia* antibody response in rabbits during the early vs late stage of LD infection. Following are the conclusions drawn from these findings:

1) This study is the first to examine the role of *vls* locus in the rabbit host.
2) Despite the functional *vls* system, *B. burgdorferi* fails to persist in the rabbit host.
3) The rabbit anti-*Borrelia* antibody response is efficacious at clearing *B. burgdorferi* spirochetes despite the presence of highly variable VlsE.
4) The rabbit anti-*Borrelia* antibodies protect mice from homologous and heterologous *B. burgdorferi* infection.

5) The rabbit anti-*Borrelia* antibodies significantly reduce Lyme arthritis in mice with an established LD infection.
6) Further studies are required to test the protective efficacy of unique repertoires of rabbit anti-*Borrelia* antibodies.

The last part of the current study focused on the microbiota of *I. ricinus* ticks from Eastern Europe, an important tick vector for LD spirochetes in Europe, which transmits pathogens of high medical and veterinary importance (Medlock et al., 2013; Parola and Raoult, 2001; Rizzoli et al., 2011). Here is the summary of our findings:

1) There is sex-specific and region-specific alpha and beta diversity of the *I. ricinus* tick microbiota.
2) There are extensive inter-sex and inter-regional differences in the microbiota of questing *I. ricinus* adults.

5.1. References

1. Crother, T.R., Champion, C.I., Whitelegge, J.P., Aguilera, R., Wu, X.Y., Blanco, D.R., Miller, J.N., Lovett, M.A., 2004. Temporal analysis of the antigenic composition of *Borrelia burgdorferi* during infection in rabbit skin. Infect Immun 72, 5063-5072.
2. Zhang, J.R., Hardham, J.M., Barbour, A.G., Norris, S.J., 1997. Antigenic variation in Lyme disease borreliae by promiscuous recombination of VMP-like sequence cassettes. Cell 89, 275-285.

3. Radolf, J.D., Caimano, M.J., Stevenson, B., Hu, L.T., 2012. Of ticks, mice, and men: understanding the dual-host lifestyle of Lyme disease spirochaetes. Nature reviews microbiology 10, 87-99.
4. Lone AG, Bankhead T. 2020. The borrelia burgdorferi VlsE lipoprotein prevents antibody binding to arthritis-related surface antigen. Cell reports 30:3663-3670.e5.
5. Embers, M.E., Liang, F.T., Howell, J.K., Jacobs, M.B., Purcell, J.E., Norris, S.J., Johnson, B.J., Philipp, M.T., 2007. Antigenicity and recombination of VlsE, the antigenic variation protein of *Borrelia burgdorferi*, in rabbits, a host putatively resistant to long-term infection with this spirochete. FEMS Immunol Med Microbiol 50, 421-429.
6. Medlock, J.M., Hansford, K.M., Bormane, A., Derdakova, M., Estrada-Peña, A., George, J.-C., Golovljova, I., Jaenson, T.G., Jensen, J.-K., Jensen, P.M., 2013. Driving forces for changes in geographical distribution of *Ixodes ricinus* ticks in Europe. Parasit. Vectors 6, 1.
7. Parola, P., Raoult, D., 2001. Ticks and tickborne bacterial diseases in humans: an emerging infectious threat. Clin. Infect. Dis. 32, 897-928.
8. Rizzoli, A., Hauffe, H.C., Carpi, G., Vourc'h, G., Neteler, M., Rosa, R., 2011. Lyme borreliosis in Europe. Euro. Surveill. 16, 19906.